Postdoctoral Working Report
Researches on Higgs and FCNC Physics

Shou Hua Zhu
Institute of Theoretical Physics, Academia Sinica, P.O.Box 2735, Beijing 100080, P.R.China

Abstract

In this report, instead to give comprehensive review on two important research fields during my first term postdoctoral working period: Higgs and FCNC physics, I will collect part of my recently works on it. Charged Higgs is the distinguished signature of new physics, in this report, I review my two works on charged Higgs associated production with top quark and W boson at hardron colliders. Our researches show that these two charged Higgs production mechanisms are important channel not only in finding charged Higgs, but also in studying the quantum structure of new physics. Flavor Changing Neutral Current (FCNC) processes are forbidden at tree level in the Standard Model (SM), so they act as the ground to test quantum structure of the SM and also very important channel in finding new physics beyond the SM. In this report, I focus on the studies on FCNC processes on linear colliders and in B-factories.

Keywords: *Higgs, FCNC, Supersymmetry, Standard Model*

Contents

I Higgs Physics 4

1 Preface 4

2 Supersymmetric Electroweak Corrections to Charged Higgs Boson Production in Association with a Top Quark at Hadron Colliders 8
- 2.1 Introduction . . . 8
- 2.2 Calculations and formulas . . . 9
- 2.3 Numerical results and conclusion . . . 12
- 2.4 Appendix A . . . 14
- 2.5 Appendix B . . . 21

3 Supersymmetric Electroweak Corrections to $W^{\pm}H^{\mp}$ Associated Production at the CERN Large Hadron Collider 31
- 3.1 Introduction . . . 31
- 3.2 Calculations and formulas . . . 33
- 3.3 Numerical results and conclusion . . . 40
- 3.4 Appendix A . . . 42
- 3.5 Appendix B . . . 43

II FCNC Physics 72

4 Preface 72

5 Top-Charm Associated Production at High Energy e^+e^- Colliders in Standard Model 73

6 SUSY-QCD Effect on Top-Charm Associated Production at Linear Collider 80

7 Bottom-Strange Associated Production at High Energy e^+e^- Colliders in Standard Model 88
- 7.1 Introduction . . . 88
- 7.2 Analytic calculations . . . 89
- 7.3 Numerical results . . . 90
- 7.4 Appendix . . . 91

8 $B \to X_s\tau^+\tau^-$ in a CP softly broken two Higgs doublet model 99
- 8.1 Introduction . . . 99
- 8.2 Model description . . . 100
- 8.3 Formula for $B \to X_s\tau^+\tau^-$ . . . 102

8.4 Numerical results 106

9 Exclusive Semileptonic Rare Decays $B \to (K, K^*)\ell^+\ell^-$ in Supersymmetric Theories **118**

9.1 Introduction 118
9.2 Effective Hamiltonian and Form Factors 120
9.3 Formula of Observables 122
9.4 Numerical analysis 128
9.5 Conclusion 138

III Acknowledgement **141**

IV Publication List **142**

Part I
Higgs Physics

At the moment, because of lack of imagination, one cannot do much more than try to calculate effects due to the Higgs system in order to make comparisons with experiments results.

–adapted from M. Veltman 1997 "Reflections on the Higgs system".

1 Preface

The standard model (SM) [1] gives an excellent theoretical description of the strong and electro-weak interaction. This theory which is based on an $SU(3) \times SU(2) \times U(1)$ gauge group, has been proven extraordinarily robust. Albeit its success, the SM still has one part untested which is the mechanism of electroweak symmetry spontaneous breaking (EWSB), through which the gauge bosons and fermions gain their masses. In the SM, EWSB is realized through one fundamental scalar field - Higgs field. After EWSB, the physical world is left with one neutral Higgs boson. The mass of Higgs boson is not predicted by the theory and can only be determined by high energy experiments.

Although the SM is robust, there are theoretical aspects of the SM, e.g. triviality [2] and naturalness [3] etc., which suggested the need for new physics. In addition, there are certain open questions within the SM, such as too many free parameters, origin of CP violation and flavor problem etc., whose answer can only be found by invoking physics beyond the SM.

Among various new physics, supersymmetry (SUSY)[4], especially minimal supersymmetrical standard model (MSSM), is the most elegant candidate. In order to preserve the SUSY and keep theory anomaly free, in the MSSM, there should be introduced two Higgs doublets to break the electroweak symmetry. After SUSY breaking and EWSB, there are five physical Higgs bosons: three neutral Higgs and two charged Higgs bosons. To find the Higgs bosons predicted by the SM and the MSSM and study theirs properties are the primary goal of present and next generation colliders for both theoretical and high energy experimental scientists.

The Higgs masses are not predicted by the SM and MSSM (in the MSSM, there is a theoretical upper limit for lightest Higgs boson $\leq$ 140 GeV), which can only be determined by experiments.The results coming from direct search for the Higgs in the process $e^+e^- \to ZH$ at LEP 200 are, for the SM Higgs boson [5]

$$m_H > 107.7 GeV \quad (95\% \text{ C.L.})$$

which is compatible with the result of the SM fit of all precision data [6]

$$M_H = \left(76^{+85}_{-47}\right) \text{ GeV}$$

or

$$M_H < 262 \text{ GeV} \quad (95\% \text{ C.L.}) \ ;$$

for MSSM CP-even Higgs boson ($\tan\beta > 1$)

$$m_H > 85.2 \quad (95\% \text{ C.L.}).$$

At upgraded Fermilab Tevatron (Run III), the mass of SM Higgs boson can be pushed up to $\sim 180 GeV$ combined subprocesses $qq' \to WH$ and $gg \to H$ [7]. And, it is commonly thought that the combination of large hadron collider (LHC) and next linear collider (NLC) will cover the mass range of the Higgs boson up to 1 TeV or so.

In the above, I have given a brief general review of this field. In the following, I shortly describe our works related to this topic:

- **The Higgs boson production in $\gamma\gamma$ collisions at NLC** [8]

  High energy $\gamma\gamma$ collision is the collision mode realized at the NLC with almost the same center-of-mass energy and luminosity, and provide more clean place to study the properties of the Higgs bosons. In the framework of the MSSM, we studied the Higgs boson production in $\gamma\gamma$ collisions at NLC. Especially, the light neutral Higgs boson pair production involves many Feynman diagrams arising both from general two-Higgs-doublet model particles and the supersymmetrical virtual particles. We found the total cross section for the Higgs boson pair production is sensitive to the model parameters, such as $\tan\beta$, triple soft breaking terms A_t, A_b and the Higgs boson masses etc.

- **Higgs boson associated production with W at hadron colliders** [9]

  Before the LHC comes to operate, to discuss the Higgs discovery potential at present collider Fermilab Tevatron is an urgent task. With the integrated luminosity $30 fb^{-1}$, through the process $P\bar{P} \to qq' \to WH$ followed by $H \to b\bar{b}$ and $W \to \ell\bar{\nu}$, Tevatron can find the mass of the Higgs boson up to $125 GeV$. In these works, we have studied the Yukawa corrections arising from the top loop as well as the leading electroweak corrections including the Higgs contributions besides the top contributions. And we found that in the SM, the corrections are small and at most few percent; however, in the MSSM, the corrections could reach tens of percent in the favorable parameters space.

- **Higgs boson discovery potential through bg channel** [10]

  For hadron colliders, especially LHC, the gluon distribution grows rapidly, it may play an important role in producing Higgs boson in particular for large $\tan\beta$ because the couplings of down-type quarks with Higgs can be enhanced in this case. We study the Higgs boson discovery potential through bg channel for both neutral and charged Higgs bosons. Indeed, we found that it is possible to find the SUSY neutral Higgs boson at Tevatron if $\tan\beta \geq 10$. For charged Higgs production, we also calculated Yukawa correction, and found the magnitude of

the radiative corrections can exceed -20% and not sensitive to the mass of charged Higgs boson, these effects could be observable in the experiments.

- **Higgs boson production at NLC** [11]

  We have also studied the Higgs production at the NLC associated with W boson or heavy quarks. The WH production is the loop-induced process, and we found that the cross section can reach 1 fb, but decease rapidly with the increment of the Higgs mass. The $t\bar{t}H$ and $b\bar{b}H$ production have been considered by many groups, we re-study this process under the framework of M-theory. Our results show that the cross sections are sensitive to the model parameters.

- **Radiative Higgs boson decay beyond the standard model** [12]

  At LHC, the decay mode $H \to \gamma\gamma$ is used in searching Higgs boson for the intermediate mass Higgs boson. However, this searching strategy is suffered by the low decay rate of this mode. In this work, we study the possibility of using $H \to f\bar{f}\gamma$ in searching intermediate mass Higgs boson where f represent light fermions. Our study shows that, at least, this channel can be used as discriminant between SM and MSSM for a wide range of parameter space.

In the first section of this part, the supersymmetric electroweak correction for $bg \to tH^-$ at hardron colliders will be presented in details; in second section, we will study the process of $b\bar{b} \to W^-H^+$ at CERN Large Hardron Collider in supersymmetrical model.

References

[1] S. L. Glashow, Nucl. Phys. **B22** (1961) 579; S. Weinberg, Phys. Rev. Lett. **19** (1967) 1264; A. Salam, in **Elementary Particle Theory**, ed. N. Svart holm (Amquist and Wiksels, Stockholm 1969).

[2] M. Aizenman, Comm. Math. Phys. **86** (1982) 1; J. Frölich, Nucl. Phys. **B200** [FS4] (1982) 281.

[3] G. 't Hooft, in **Recent Developments in Gauge Theories**, Proceedings of the Nato Advanced Study Institute, Cargese, France, 1979, eds G. 't Hoo ft *et al.* (Plenum Press, New York 1980).

[4] For an introduction see, for example, J. Wess and J. Bagger, **Supersymmetry and Supergravity** (Princeton University Press, Princeton 1992) 2$^{\rm nd}$ Edition.

[5] M.Kado, hep-ex/0005022.

[6] The fits to the SM of precision electroweak data are summarized by D. Karlen, in the Proceedings of the 29th Conference on High Energy Physics, I CHEP98,

Vancouver, Canada, July 1998, eds. A. Astbury, D. Axen and J. Robinson (World Scientific, Singapore 1999) p47.

[7] T.Han et.al., Phys.Rev.D59:105006,1999.

[8] S.H. Zhu, C.S. Li and C.S. Gao, Phys.Rev.D58, 015006 (1998); S.H. Zhu, C.S. Li and C.S. Gao, Phys.Rev.D58, 055007 (1998); S.H. Zhu, J. Phys. G24 (1998)1703; S.H. Zhu, C.S. Li and C.S. Gao, Chinese Phys. Lett.15, 89 (1998).

[9] C.S.Li and S.H. Zhu, Phys. Lett. B444,224 (1998); Q.H. Cao, C.S. Li and S.H. Zhu, hep-ph/9810458, Comm, Theor. Phys.32, 275 (2000).

[10] C.S. Huang and S.H. Zhu, Phys. Rev. D 60, 075012 (1999); L. Jin, C.S. Li, R. Oakes and S.H. Zhu, hep-ph/9907482, Eur. Phys. J. C14, 91-101 (2000).

[11] C.S. Huang, T.J. Li, W. Liao, Q.S. Yan and S.H. Zhu, Commun. Theor. Phys., **32**, 499-506 (1999); C.S. Huang, T.J. Li, W. Liao, Q.S. Yan and S.H. Zhu, hep-ph/9810412; S.H. Zhu, hep-ph/9901221.

[12] C.S. Li, C.F. Qiao and S.H. Zhu, Phys. Rev. D57,6928 (1998).

2 Supersymmetric Electroweak Corrections to Charged Higgs Boson Production in Association with a Top Quark at Hadron Colliders

ABSTRACT

We calculate the $O(\alpha_{ew} m_{t(b)}^2/m_W^2)$ and $O(\alpha_{ew} m_{t(b)}^4/m_W^4)$ supersymmetric electroweak corrections to the cross section for the charged Higgs boson production in association with a top quark at the Tevatron and the LHC. These corrections arise from the quantum effects which are induced by potentially large Yukawa couplings from the Higgs sector and the chargino-top(bottom)-sbottom(stop) couplings, neutralino-top(bottom)-stop(sbottom) couplings and charged Higgs-stop-sbottom couplings. They can decrease or increase the cross section depending on $\tan\beta$ but are not very sensitive to the mass of the charged Higgs boson for high $\tan\beta$. At low $\tan\beta(=2)$ the corrections decrease the total cross sections significantly, which exceed -12% for $m_{H^\pm}$ below $300GeV$ at both the Tevatron and the LHC, but for $m_{H^\pm} > 300GeV$ the corrections can become very small at the LHC. For high $\tan\beta(=10,30)$ these corrections can decrease or increase the total cross sections, and the magnitude of the corrections are at most a few percent at both the Tevatron and the LHC.

2.1 Introduction

There has been a great deal of interest in the charged Higgs bosons appearing in the two-Higgs-doublet models(THDM)[1], particularly the minimal supersymmetric standard model(MSSM)[2], which predicts the existence of three neutral and two charged Higgs bosons h, H, A, and $H^\pm$. When the Higgs boson of the Standard Model(SM) has a mass below 130-140 Gev and the h boson of the MSSM is in the decoupling limit (which means that $H^\pm$ is too heavy anyway to be possibly produced), the lightest neutral Higgs boson may be difficult to distinguish from the neutral Higgs boson of the standard model(SM). But charged Higgs bosons carry a distinctive signature of the Higgs sector in the MSSM. Therefore, the search for charged Higgs bosons is very important for probing the Higgs sector of the MSSM and, therefore, will be one of the prime objectives of the CERN Large Hadron Collider(LHC). At the LHC the integrated luminosity is expected to reach $L = 100fb^{-1}$ per year in the second phase. Recently, several studies of charged Higgs boson production at hadron colliders have appeared in the literature[3,4,5]. For a relatively light charged Higgs boson, $m_{H^\pm} < m_t - m_b$, the dominate production processes at the LHC are $gg \to t\bar{t}$ and $q\bar{q} \to t\bar{t}$ followed by the decay sequence $t \to bH^+ \to b\tau^+\nu_\tau$[6]. For a heavier charged Higgs boson the dominate

production process is $gb \to tH^-$[7,8,9]. Previous studies showed that the search for heavy charged Higgs bosons with $m_{H^\pm} > m_t + m_b$ at a hadron collider is seriously complicated by QCD backgrounds due to processes such as $gb \to t\bar{t}b, g\bar{b} \to t\bar{t}\bar{b}$, and $gg \to t\bar{t}b\bar{b}$, as well as others process[8]. However, recent analyses[10,11] indicate that the decay mode $H^+ \to \tau^+\nu$ provides an excellent signature for a heavy charged Higgs boson in searches at the LHC. The discovery region for $H^\pm$ is far greater than had been thought for a large range of the $(m_{H^\pm}, \tan\beta)$ parameter space, extending beyond $m_{H^\pm} \sim 1TeV$ and down to at least $\tan\beta \sim 3$, and potentially to $\tan\beta \sim 1.5$, assuming the latest results for the SM parameters and parton distribution functions as well as using kinematic selection techniques and the tau polarization analysis[11]. Of course, it is just a theoretical analysis and no experimental simulation has been performed to make the statement very reliable so far.

The one-loop radiative corrections to H^-t associated production have not been calculated, although this production process has been studied extensively at tree-level[7,8,9]. In this paper we present the calculations of the $O(\alpha_{ew}m_{t(b)}^2/m_W^2)$ supersymmetric(SUSY) electroweak corrections to this associated H^-t production process at both the Fermilab Tevatron and the LHC in the MSSM. These corrections arise from the quantum effects which are induced by potentially large Yukawa couplings from the Higgs sector and the chargino-top(bottom)-sbottom(stop) couplings, neutralino-top(bottom)-stop(sbottom) couplings and charged Higgs-stop-sbottom couplings which will contribute at the $O(\alpha_{ew}m_{t(b)}^4/m_W^4)$ to the self-energy of the charged Higgs boson. In order to get a reliable estimate this process has to be merged with the related gluon splitting contribution $gg \to H^-t\bar{b}$. This leads to a suppression by about 50% at LO[12]. However, the complete one-loop QCD corrections are probably more important, but not yet available.

2.2 Calculations and formulas

The tree-level amplitude for $gb \to tH^-$ is

$$M_0 = M_0^{(s)} + M_0^{(t)}, \tag{1}$$

where $M_0^{(s)}$ and $M_0^{(t)}$ represent the amplitudes arising from diagrams in Fig.1(a) and Fig.1(b), respectively. Explicitly,

$$\begin{aligned} M_0^{(s)} &= \frac{igg_s}{\sqrt{2}m_W(\hat{s}-m_b^2)}\overline{u}(p_t)[2m_t\cot\beta p_b^\mu P_L + 2m_b\tan\beta p_b^\mu P_R - m_t\cot\beta\gamma^\mu \not{k} P_L \\ &\quad -m_b\tan\beta\gamma^\mu \not{k} P_R]u(p_b)\varepsilon_\mu(k)T_{ij}^a, \end{aligned} \tag{2}$$

and

$$\begin{aligned} M_0^{(t)} &= \frac{igg_s}{\sqrt{2}m_W(\hat{t}-m_t^2)}\overline{u}(p_t)[2m_t\cot\beta p_t^\mu P_L + 2m_b\tan\beta p_t^\mu P_R - m_t\cot\beta\gamma^\mu \not{k} P_L \\ &\quad -m_b\tan\beta\gamma^\mu \not{k} P_R]u(p_b)\varepsilon_\mu(k)T_{ij}^a, \end{aligned} \tag{3}$$

where T^a are the $SU(3)$ color matrices and $\hat{s}$ and $\hat{t}$ are the subprocess Mandelstam variables defined by

$$\hat{s} = (p_b + k)^2 = (p_t + p_{H^-})^2,$$

and

$$\hat{t} = (p_t - k)^2 = (p_{H^-} - p_b)^2.$$

Here the Cabbibo-Kobayashi-Maskawa matrix element $V_{CKM}[bt]$ has been taken to be unity.

The SUSY electroweak corrections of order $O(\alpha_{ew} m_{t(b)}^2/m_W^2)$ and $O(\alpha_{ew} m_{t(b)}^4/m_W^4)$ to the process $gb \to H^- t$ arise from the Feynman diagrams shown in Figs.1(c)-1(v) and Fig.2. We carried out the calculation in the t'Hooft-Feynman gauge and used dimensional reduction, which preserves supersymmetry, for regularization of the ultraviolet divergences in the virtual loop corrections using the on-mass-shell renormalization scheme[13], in which the fine-structure constant α_{ew} and physical masses are chosen to be the renormalized parameters, and finite parts of the counterterms are fixed by the renormalization conditions. The coupling constant g is related to the input parameters e, m_W, and m_Z by $g^2 = e^2/s_w^2$ and $s_w^2 = 1 - m_w^2/m_Z^2$. The parameter β in the MSSM we are considering must also be renormalized. Following the analysis of ref.[14], this renormalization constant was fixed by the requirement that the on-mass-shell $H^+\bar{l}\nu_l$ coupling remain the same form as in Eq.(2) of ref.[14] to all orders of perturbation theory. Taking into account the $O(\alpha_{ew} m_{t(b)}^2/m_W^2)$ Yukawa corrections, the renormalized amplitude for the process $gb \to tH^-$ can be written as

$$\begin{aligned} M_{ren} &= M_0^{(s)} + M_0^{(t)} + \delta M^{V_1(s)} + \delta M^{V_1(t)} + \delta M^{s(s)} + \delta M^{s(t)} + \delta M^{V_2(s)} \\ &\quad + \delta M^{V_2(t)} + \delta M^{b(s)} + \delta M^{b(t)} \equiv M_0^{(s)} + M_0^{(t)} + \sum_l \delta M^l, \end{aligned} \tag{4}$$

where $\delta M^{V_1(s)}, \delta M^{V_1(t)}, \delta M^{s(s)}, \delta M^{s(t)}, \delta M^{V_2(s)}, \delta M^{V_2(t)}, \delta M^{b(s)}$, and $\delta M^{b(t)}$ represent the corrections to the tree diagrams arising, respectively, from the gbb vertex diagram Fig.1(c)-1(d), the gtt vertex diagram Fig.1(f)-1(g), the bottom quark self-energy diagram Fig.1(i), the top quark self-energy diagram Fig.1(k), the btH^- vertex diagrams Figs.1(m)-1(n) and Figs.1(p)-1(q), including their corresponding counterterms Fig.1(e), Fig.1(h), Fig.1(j), Fig.1(l), Fig.1(o), and Fig.1(r), and the box diagrams Figs.1$(s) - 1(v)$. $\sum_l \delta M^l$ then represents the sum of the contributions to the Yukawa corrections from all the diagrams in Figs.1(c)-1(v). The explicit form of δM^l can be expressed as

$$\begin{aligned} \delta M^l &= -\frac{i g^3 g_s T^a_{ij}}{4\sqrt{2} \times 16\pi^2 m_W} C^l \overline{u}(p_t) \{ f_1^l \gamma^\mu P_L + f_2^l \gamma^\mu P_R + f_3^l p_b^\mu P_L + f_4^l p_b^\mu P_R + f_5^l p_t^\mu P_L \\ &\quad + f_6^l p_t^\mu P_R + f_7^l \gamma^\mu \not{k} P_L + f_8^l \gamma^\mu \not{k} P_R + f_9^l p_b^\mu \not{k} P_L + f_{10}^l p_b^\mu \not{k} P_R + f_{11}^l p_t^\mu \not{k} P_L \\ &\quad + f_{12}^l p_t^\mu \not{k} P_R \} u(p_b) \varepsilon_\mu(k), \end{aligned} \tag{5}$$

where the C^l are coefficients that depend on $\hat{s}, \hat{t}$, and the masses, and the f_i^l are form factors; both the coefficients C^l and the form factors f_i^l are given explicitly in Appendix

A. The corresponding amplitude squared is

$$\overline{\sum}|M_{ren}|^2 = \overline{\sum}|M_0^{(s)} + M_0^{(t)}|^2 + 2Re\overline{\sum}[(\sum_l \delta M^l)(M_0^{(s)} + M_0^{(t)})^\dagger], \tag{6}$$

where

$$\begin{aligned}
\overline{\sum}|M_0^{(s)} + M_0^{(t)}|^2 &= \frac{g^2 g_s^2}{2N_C m_W^2}\{\frac{1}{(\hat{s}-m_b^2)^2}[(m_t^2\cot^2\beta + m_b^2\tan^2\beta)(p_b\cdot kp_t\cdot k \\
&- m_b^2 p_t\cdot k + 2p_b\cdot kp_b\cdot p_t - m_b^2 p_b\cdot p_t) + 2m_b^2 m_t^2(p_b\cdot k - m_b^2)] \\
&+ \frac{1}{(\hat{t}-m_t^2)^2}[(m_t^2\cot^2\beta + m_b^2\tan^2\beta)(p_b\cdot kp_t\cdot k + m_t^2 p_b\cdot k \\
&- m_t^2 p_b\cdot p_t) + 2m_b^2 m_t^2(p_t\cdot k - m_t^2)] + \frac{1}{(\hat{s}-m_b^2)(\hat{t}-m_t^2)} \\
&\times [(m_t^2\cot^2\beta + m_b^2\tan^2\beta)(2p_b\cdot kp_t\cdot k + 2p_b\cdot kp_b\cdot p_t - 2(p_b\cdot p_t)^2 \\
&- m_b^2 p_t\cdot k + m_t^2 p_b\cdot k) + 2m_b^2 m_t^2(p_t\cdot k - p_b\cdot k - 2p_b\cdot p_t)]\},
\end{aligned} \tag{7}$$

$$\overline{\sum}\delta M^l (M_0^{(s)})^\dagger = -\frac{g^4 g_s^2}{64N_C\times 16\pi^2 m_W^2(\hat{s}-m_b^2)} C^l \sum_{i=1}^{12} h_i^{(s)} f_i^l, \tag{8}$$

and

$$\overline{\sum}\delta M^l (M_0^{(t)})^\dagger = -\frac{g^4 g_s^2}{64N_C\times 16\pi^2 m_W^2(\hat{t}-m_t^2)} C^l \sum_{i=1}^{12} h_i^{(t)} f_i^l. \tag{9}$$

Here the color factor $N_C = 3$ and $h_i^{(s)}$ and $h_i^{(t)}$ are scalar functions whose explicit expressions are given in Appendix B.

The cross section for the process $gb \to tH^-$ is

$$\hat{\sigma} = \int_{\hat{t}_{min}}^{\hat{t}_{max}} \frac{1}{16\pi\hat{s}^2}\overline{\Sigma}|M_{ren}|^2 d\hat{t} \tag{10}$$

with

$$\hat{t}_{min} = \frac{m_t^2 + m_{H^-}^2 - \hat{s}}{2} - \frac{1}{2}\sqrt{(\hat{s}-(m_t+m_{H^-})^2)(\hat{s}-(m_t-m_{H^-})^2)},$$

and

$$\hat{t}_{max} = \frac{m_t^2 + m_{H^-}^2 - \hat{s}}{2} + \frac{1}{2}\sqrt{(\hat{s}-(m_t+m_{H^-})^2)(\hat{s}-(m_t-m_{H^-})^2)}.$$

The total hadronic cross section for $pp \to gb \to tH^-$ can be obtained by folding the subprocess cross section $\hat{\sigma}$ with the parton luminosity:

$$\sigma(s) = \int_{(m_t+m_{H^-})/\sqrt{s}}^{1} dz\frac{dL}{dz}\hat{\sigma}(gb \to tH^- \text{ at } \hat{s} = z^2 s). \tag{11}$$

Here $\sqrt{s}$ and $\sqrt{\hat{s}}$ are the CM energies of the pp and gb states , respectively, and dL/dz is the parton luminosity, defined as

$$\frac{dL}{dz} = 2z \int_{z^2}^{1} \frac{dx}{x} f_{b/P}(x,\mu) f_{g/P}(z^2/x,\mu), \tag{12}$$

where $f_{b/P}(x,\mu)$ and $f_{g/P}(z^2/x,\mu)$ are the bottom quark and gluon parton distribution functions.

2.3 Numerical results and conclusion

In the following we present some numerical results for charged Higgs boson production in association with a top quark at both the Tevatron and the LHC. In our numerical calculations the SM parameters were taken to be $m_W = 80.41GeV$, $m_Z = 91.187GeV$, $m_t = 176GeV$, $\alpha_s(m_Z) = 0.119$, and $\alpha_{ew}(m_Z) = \frac{1}{128.8}$[15]. And we used the running b quark mass $\approx 3GeV$ and the one-loop relations[16] from the MSSM between the Higgs boson masses $m_{h,H,A,H^\pm}$ and the parameters α and β, and chose $m_{H^\pm}$ and $\tan\beta$ as the two independent input parameters. And we used the CTEQ5M[17] parton distributions throughout the calculations. Other MSSM parameters were determined as follows:

(i) For the parameters M_1, M_2, and μ in the chargino and neutralino matrix, we put $M_2 = 300GeV$ and then used the relation $M_1 = (5/3)(g'^2/g^2)M_2 \simeq 0.5M_2$[2] to determine M_1. We also put $\mu = -100GeV$ except the numerical calculations as shown in Fig.6(b), where μ is a variable.

(ii) For the parameters $m^2_{\tilde{Q},\tilde{U},\tilde{D}}$ and $A_{t,b}$ in squark mass matrices

$$M^2_{\tilde{q}} = \begin{pmatrix} M^2_{LL} & m_q M_{LR} \\ m_q M_{RL} & M^2_{RR} \end{pmatrix} \tag{13}$$

with

$$\begin{aligned} M^2_{LL} &= m^2_{\tilde{Q}} + m^2_q + m^2_Z \cos 2\beta (I^{3L}_q - e_q \sin^2\theta_W), \\ M^2_{RR} &= m^2_{\tilde{U},\tilde{D}} + m^2_q + m^2_Z \cos 2\beta e_q \sin^2\theta_W, \\ M_{LR} = M_{RL} &= \begin{pmatrix} A_t - \mu\cot\beta & (\tilde{q} = \tilde{t}) \\ A_b - \mu\tan\beta & (\tilde{q} = \tilde{b}) \end{pmatrix}, \end{aligned} \tag{14}$$

to simplify the calculation we assumed $m^2_{\tilde{Q}} = m^2_{\tilde{U}} = m^2_{\tilde{D}}$ and $A_t = A_b$, and we put $m_{\tilde{Q}} = 500GeV$ and $A_t = 200GeV$. But in the numerical calculations of Fig.6(a) $A_t = A_b$ are the variables.

Some typical numerical calculations of the tree-level total cross sections and the $O(\alpha_{ew} m^2_{t(b)}/m^2_W)$ SUSY electroweak corrections as the functions of the charged Higgs boson mass, $A_t = A_b$ and μ, respectively, for three representative values of $\tan\beta$ are given in Figs.3-6.

Figures 3(a) and 4(a) show that the tree-level total cross sections as a function of the charged Higgs boson mass for three representative values of $\tan\beta$. For $m_{H^\pm} =$

$200GeV$ the total cross sections at the Tevatron are at most only 0.7 fb and 0.1 fb for $\tan\beta = 2, 30$ and 10, respectively, and for $m_{H^\pm} = 300GeV$ the total cross sections are smaller than 0.15 fb for all three values of $\tan\beta$. However, at the LHC the total cross sections are much larger: the order of thousands of fb for $m_{H^\pm}$ in the range 100 to $240GeV$ and $\tan\beta = 2$ and 30; and they are hundreds of fb for the intermediate value $\tan\beta = 10$. When the charged Higgs boson mass becomes heavy($<$ 500 GeV), the total cross sections still are larger than 100 fb and 10 fb for $\tan\beta = 2, 30$ and 10, respectively. For low $\tan\beta$ the top quark contribution is enhanced while for high $\tan\beta$ the bottom quark contribution becomes large. These results are smaller than ones given in ref.[8,9] because we used the running b quark mass $\approx 3GeV$ in the numerical calculations. We have confirmed that if we chose $m_b = 4.5GeV$, our results will agree with ref.[8,9].

In Figs. 3(b) and 4(b) we show the corrections to the total cross sections relative to the tree-level values as a function of $m_{H^\pm}$ for $\tan\beta = 2, 10$, and 30. For $\tan\beta = 2$ the corrections decrease the total cross sections significantly, which exceed -13% for $m_{H^\pm}$ below $300GeV$ at the both Tevatron and the LHC. But the corrections decrease as $m_{H^\pm}$ increase. For example, as shown in Fig.4(b), the corrections range between $-13\% \sim 0\%$ when $m_{H^\pm}$ increase from $300GeV$ to $1TeV$ at the LHC. For high $\tan\beta(= 10, 30)$ these corrections become smaller, which can decrease or increase the total cross sections depending on $\tan\beta$, and the magnitude of the corrections are at most a few percent for a wide range of the charged Higgs boson mass at both the Tevatron and the LHC.

In Fig.5 we present the Yukawa correction from the Higgs sector and the genuine SUSY electroweak correction from the couplings involving the genuine SUSY particles(the chargino, neutralino and squark) for $\tan\beta = 30$ at the LHC, respectively. One can see that the Yukawa correction and the genuine SUSY electroweak correction have opposite signs, and thus cancel to some extent. The former decrease the total cross sections, which can range between $-8\% \sim -4\%$ for $m_{H^\pm}$ below $300GeV$, but the latter increase the total cross sections, which range between $10\% \sim 7\%$ for $m_{H^\pm}$ in the same range. In such a case the combined effects just are about $2\% \sim 3\%$.

Figs.6(a) and 6(b) give the corrections as the functions of $A_t = A_b$ and μ for $m_{H^\pm} = 300GeV$ at the LHC, respectively, assuming $\tan\beta = 2, 10$ and 30. From Figs.6(a) and 6(b) one sees that the corrections increase or decrease slowly with increasing $A_t = A_b$ and the magnitude of μ, respectively, for $\tan\beta = 30, 10$, and the corrections are not very sensitive to both $A_t = A_b$ and μ for $\tan\beta = 2$, where the corrections are always about -12% and -13%, respectively. In general for large values of A_t and small values of $\tan\beta$ or large values of μ and $\tan\beta$, one can get much larger corrections since the charged Higgs boson-stop-sbottom couplings become stronger. For $\tan\beta = 30$, comparing Fig.4(b) with Fig.6(b), we can see that the corrections indeed become larger as the values of μ increase. But for $\tan\beta = 2$ from Fig.4(a) and Fig.6(a) we found that the corrections almost have no change when $A_t = A_b$ become larger. Obviously the effects from the stronger couplings have been suppressed by the decoupling effects because with an increase of $A_t = A_b$ all the squark masses are still heavy, which almost is same as discussed in Ref.[18].

In conclusion, we have calculated the $O(\alpha_{ew}m_{t(b)}^2/m_W^2)$ and $O(\alpha_{ew}m_{t(b)}^4/m_W^4)$ SUSY electroweak corrections to the cross section for the charged Higgs boson production in association with a top quark at the Tevatron and the LHC. These corrections decrease or increase the cross section depending on $\tan\beta$ but are not very sensitive to the mass of the charged Higgs boson for high $\tan\beta$. At low $\tan\beta(=2)$ the corrections decrease the total cross sections significantly, which exceed -12% for $m_{H^\pm}$ below $300GeV$ at both the Tevatron and the LHC, but for $m_{H^\pm} > 300GeV$ the corrections can become very small at the LHC. For high $\tan\beta(=10,30)$ these corrections can decrease or increase the total cross sections, and the magnitude of the corrections are at most a few percent at both the Tevatron and the LHC.

2.4 Appendix A

The coefficients C^l and form factors f_i^l are the following:

$$
\begin{aligned}
C^{V_1(s)} &= \frac{m_b^2}{m_W^2(\hat{s}-m_b^2)}, \quad C^{V_1(t)} = \frac{m_t^2}{m_W^2(\hat{t}-m_t^2)}, \quad C^{s(s)} = \frac{m_b^2}{m_W^2(\hat{s}-m_b^2)^2}, \\
C^{s(t)} &= \frac{m_t^2}{m_W^2(\hat{t}-m_t^2)^2}, \quad C^{V_2(s)} = \frac{m_b m_t}{m_W^2(\hat{s}-m_b^2)}, \quad C^{V_2(t)} = \frac{m_b m_t}{m_W^2(\hat{t}-m_t^2)}, \\
C^{b(s)} &= C^{b(t)} = \frac{m_t m_b}{m_W^2},
\end{aligned}
$$

$$
\begin{aligned}
f_1^{V_1(s)} &= \eta^{(1)}[m_b(g_2^{V_1(s)} - g_3^{V_1(s)}) - 2p_b\cdot k g_6^{V_1(s)}], \\
f_2^{V_1(s)} &= \eta^{(2)}[m_b(g_3^{V_1(s)} - g_2^{V_1(s)}) - 2p_b\cdot k g_7^{V_1(s)}], \\
f_3^{V_1(s)} &= \eta^{(2)}[2(g_1^{V_1(s)} + g_2^{V_1(s)}) + m_b(g_4^{V_1(s)} + g_5^{V_1(s)}) + 2p_b\cdot k g_8^{V_1(s)}], \\
f_4^{V_1(s)} &= \eta^{(1)}[2(g_1^{V_1(s)} + g_3^{V_1(s)}) + m_b(g_4^{V_1(s)} + g_5^{V_1(s)}) + 2p_b\cdot k g_9^{V_1(s)}], \\
f_7^{V_1(s)} &= \eta^{(2)}[-(g_1^{V_1(s)} + g_2^{V_1(s)}) + m_b(g_6^{V_1(s)} + g_7^{V_1(s)})], \\
f_8^{V_1(s)} &= \eta^{(1)}[-(g_1^{V_1(s)} + g_3^{V_1(s)}) + m_b(g_6^{V_1(s)} + g_7^{V_1(s)})], \\
f_9^{V_1(s)} &= \eta^{(1)}[g_4^{V_1(s)} + 2g_6^{V_1(s)} + m_b(g_8^{V_1(s)} - g_9^{V_1(s)})], \\
f_{10}^{V_1(s)} &= \eta^{(2)}[g_5^{V_1(s)} + 2g_7^{V_1(s)} + m_b(g_9^{V_1(s)} - g_8^{V_1(s)})], \\
f_1^{V_2(s)} &= 2p_b\cdot k g_3^{V_2(s)}, \qquad f_2^{V_2(s)} = 2p_b\cdot k g_4^{V_2(s)}, \\
f_3^{V_2(s)} &= 2g_1^{V_2(s)} + 2m_t\cot\beta(\delta\Lambda_L^{(1)} + \delta\Lambda_L^{(2)} + \delta\Lambda_L^{(3)}) - 2m_t g_3^{V_2(s)} + 2m_b g_4^{V_2(s)}, \\
f_4^{V_2(s)} &= 2g_2^{V_2(s)} + 2m_b\tan\beta(\delta\Lambda_R^{(1)} + \delta\Lambda_R^{(2)} + \delta\Lambda_R^{(3)}) + 2m_b g_3^{V_2(s)} - 2m_t g_4^{V_2(s)}, \\
f_7^{V_2(s)} &= -\frac{1}{2}f_3^{V_2(s)}, \qquad f_8^{V_2(s)} = -\frac{1}{2}f_4^{V_2(s)}, \\
f_1^{V_2(t)} &= 2p_t\cdot k g_3^{V_2(t)}, \qquad f_2^{V_2(t)} = 2p_t\cdot k g_4^{V_2(t)}, \\
f_5^{V_2(t)} &= 2g_1^{V_2(t)} + 2m_t\cot\beta(\delta\Lambda_L^{(1)} + \delta\Lambda_L^{(2)} + \delta\Lambda_L^{(3)}) - 2m_t g_3^{V_2(t)} + 2m_b g_4^{V_2(t)}, \\
f_6^{V_2(t)} &= 2g_2^{V_2(t)} + 2m_b\tan\beta(\delta\Lambda_R^{(1)} + \delta\Lambda_R^{(2)} + \delta\Lambda_R^{(3)}) + 2m_b g_3^{V_2(t)} - 2m_t g_4^{V_2(t)}, \\
f_7^{V_2(t)} &= -\frac{1}{2}f_5^{V_2(t)}, \qquad f_8^{V_2(t)} = -\frac{1}{2}f_6^{V_2(t)},
\end{aligned}
$$

$$\begin{aligned}
f_1^{s(s)} &= 2\eta^{(1)} p_b\cdot k[g_1^{s(s)}+m_b(g_2^{s(s)}+g_3^{s(s)})],\\
f_2^{s(s)} &= 2\eta^{(2)} p_b\cdot k[g_5^{s(s)}+m_b(g_2^{s(s)}+g_4^{s(s)})],\\
f_3^{s(s)} &= 2\eta^{(2)}[m_b(g_1^{s(s)}+g_5^{s(s)})+2(m_b^2+p_b\cdot k)g_2^{s(s)}+(m_b^2+2p_b\cdot k)g_3^{s(s)}+m_b^2g_4^{s(s)}],\\
f_4^{s(s)} &= 2\eta^{(1)}[m_b(g_1^{s(s)}+g_5^{s(s)})+2(m_b^2+p_b\cdot k)g_2^{s(s)}+m_b^2g_3^{s(s)}+(m_b^2+2p_b\cdot k)g_4^{s(s)}],\\
f_7^{s(s)} &= -\frac{1}{2}f_3^{s(s)}, \qquad\qquad f_8^{s(s)}=-\frac{1}{2}f_4^{s(s)},\\
f_1^{b(s)} &= \sum_{i=H^0,h^0,G^0,A^0}\eta_i^{(3)}\{\eta^{(2)}[2m_b(-3D_{312}+(1-\zeta_i)D_{27})+m_b^3(D_0+D_{12}-D_{22}\\
&-D_{32})-m_t^2m_b(D_{23}+2D_{39})-2m_bp_b\cdot k(2D_{36}+D_{24}+\zeta_i(D_0+D_{12}))\\
&+2m_bp_t\cdot k(D_{25}+D_{310})+2m_bp_b\cdot p_t(D_{26}+2D_{38})]+\eta^{(1)}[2m_t(-3D_{313}+(1\\
&+\zeta_i)D_{27})-m_t^3(D_{33}+(1+\zeta_i)D_{23})+m_b^2m_t(D_{13}-2D_{38}+(1+\zeta_i)(D_0\\
&-D_{22}))+2m_tp_b\cdot k(D_{13}-D_{310}-(1+\zeta_i)(D_{12}+D_{24}))+2m_tp_t\cdot k(2D_{37}\\
&+(1+\zeta_i)D_{25})+2m_tp_b\cdot p_t(2D_{39}+(1+\zeta_i)D_{26})]\}\\
&(-k,-p_b,p_t,m_b,m_b,m_i,m_t)\\
&-\frac{8\sqrt{2}m_W}{\sin 2\beta}\sum_{i,j,k}N_{k4}N_{k3}^*R_i(b)R_j(t)\sigma_{ij}D_{27}(-k,-p_b,p_t,m_{\tilde{b}_i},m_{\tilde{b}_i},m_{\tilde{\chi}_k^0},m_{\tilde{t}_j}),\\
f_2^{b(s)} &= f_1^{b(s)}(\eta^{(1)}\leftrightarrow\eta^{(2)},L_l\leftrightarrow R_l,N_{kl}\leftrightarrow N_{kl}^*),\\
f_3^{b(s)} &= \sum_{i=H^0,h^0,G^0,A^0}\eta_i^{(3)}\{\eta^{(1)}[-4D_{27}+2m_b^2(D_{22}-D_0-(1-\zeta_i)(D_{12}+D_{22}))\\
&+2m_t^2(D_{23}-(1+\zeta_i)D_{26})+4p_t\cdot k(D_{26}-D_{25})]+\eta^{(2)}2m_tm_b(1+\zeta_i)(D_{22}\\
&-D_{12}-D_{26})\}(-k,-p_b,p_t,m_b,m_b,m_i,m_t)\\
&-\frac{8\sqrt{2}m_W}{\sin 2\beta}\sum_{i,j,k}\sigma_{ij}[-m_tN_{k4}N_{k3}^*R_i(b)R_j(t)D_{26}+m_bN_{k4}^*N_{k3}L_i(b)L_j(t)(D_{12}\\
&+D_{22})+m_{\tilde{\chi}_k^0}N_{k4}^*N_{k3}^*R_i(b)L_j(t)D_{12}](-k,-p_b,p_t,m_{\tilde{b}_i},m_{\tilde{b}_i},m_{\tilde{\chi}_k^0},m_{\tilde{t}_j}),\\
f_4^{b(s)} &= f_3^{b(s)}(\eta^{(1)}\leftrightarrow\eta^{(2)},L_l\leftrightarrow R_l,N_{kl}\leftrightarrow N_{kl}^*),\\
f_5^{b(s)} &= \sum_{i=H^0,h^0,G^0,A^0}\eta_i^{(3)}\{\eta^{(1)}[12D_{313}+2m_b^2(2D_{38}-D_{13}+(1-\zeta_i)(D_{13}\\
&+D_{26}))+2m_t^2(D_{33}+(1+\zeta_i)D_{23})+4p_b\cdot k(D_{25}+D_{310})-4p_t\cdot k(D_{23}\\
&+2D_{37})-4p_t\cdot p_b(D_{23}+2D_{39})]+\eta^{(2)}2m_tm_b(1+\zeta_i)(D_{13}+D_{23}\\
&-D_{26})\}(-k,-p_b,p_t,m_b,m_b,m_i,m_t)\\
&+\frac{8\sqrt{2}m_W}{\sin 2\beta}\sum_{i,j,k}\sigma_{ij}[-m_tN_{k4}N_{k3}^*R_i(b)R_j(t)D_{23}+m_bN_{k4}^*N_{k3}L_i(b)L_j(t)(D_{13}\\
&+D_{26})+m_{\tilde{\chi}_k^0}N_{k4}^*N_{k3}^*R_i(b)L_j(t)D_{13}](-k,-p_b,p_t,m_{\tilde{b}_i},m_{\tilde{b}_i},m_{\tilde{\chi}_k^0},m_{\tilde{t}_j}),\\
f_6^{b(s)} &= f_5^{b(s)}(\eta^{(1)}\leftrightarrow\eta^{(2)},L_l\leftrightarrow R_l,N_{kl}\leftrightarrow N_{kl}^*),\\
f_7^{b(s)} &= \sum_{i=H^0,h^0,G^0,A^0}\eta_i^{(3)}\{\eta^{(1)}[6(D_{27}-D_{311})+m_b^2(D_{11}-2D_{12}-2D_{22}\\
&-2D_{36}+(1+\zeta_i)(D_0+D_{12}))-m_t^2(2D_{23}+2D_{37}+(1+\zeta_i)D_{13})-2p_b\cdot k(D_{12}
\end{aligned}$$

$$
\begin{aligned}
& +2D_{24}+2D_{34})+2p_t\cdot k(D_{13}+2D_{25}+2D_{35})+2p_t\cdot p_b(D_{13}+2D_{26} \\
& +D_{310})]+\eta^{(2)}m_t m_b(1+\zeta_i)(D_{12}-D_{13}-D_0)\}(-k,-p_b,p_t,m_b,m_b,m_i,m_t), \\
f_8^{b(s)} &= f_7^{b(s)}(\eta^{(1)}\leftrightarrow\eta^{(2)}), \\
f_9^{b(s)} &= \sum_{i=H^0,h^0,G^0,A^0}\eta_i^{(3)}\{\eta^{(1)}2m_t[-D_{13}-D_{26}+(1+\zeta_i)(D_{12}+D_{24})] \\
& +\eta^{(2)}2m_b[-D_{22}+D_{24}+\zeta_i(D_0+2D_{12}+D_{24})]\}(-k,-p_b,p_t,m_b,m_b,m_i,m_t) \\
& -\frac{8\sqrt{2}m_W}{\sin 2\beta}\sum_{i,j,k}\sigma_{ij}N_{k4}N_{k3}^*R_i(b)R_j(t)(D_{12} \\
& +D_{24})(-k,-p_b,p_t,m_{\tilde{b}_i},m_{\tilde{b}_i},m_{\tilde{\chi}_k^0},m_{\tilde{t}_j}), \\
f_{10}^{b(s)} &= f_9^{b(s)}(\eta^{(1)}\leftrightarrow\eta^{(2)},L_l\leftrightarrow R_l,N_{kl}\leftrightarrow N_{kl}^*), \\
f_{11}^{b(s)} &= \sum_{i=H^0,h^0,G^0,A^0}\eta_i^{(3)}\{\eta^{(1)}2m_t[D_{23}-(1+\zeta_i)D_{25}]-\eta^{(2)}2m_b[-D_{26}+D_{25} \\
& +\zeta_i(D_{13}+D_{25})]\}(-k,-p_b,p_t,m_b,m_b,m_i,m_t) \\
& +\frac{8\sqrt{2}m_W}{\sin 2\beta}\sum_{i,j,k}\sigma_{ij}N_{k4}N_{k3}^*R_i(b)R_j(t)(D_{13} \\
& +D_{25})(-k,-p_b,p_t,m_{\tilde{b}_i},m_{\tilde{b}_i},m_{\tilde{\chi}_k^0},m_{\tilde{t}_j}), \\
f_{12}^{b(s)} &= f_{11}^{b(s)}(\eta^{(1)}\leftrightarrow\eta^{(2)},L_l\leftrightarrow R_l,N_{kl}\leftrightarrow N_{kl}^*),
\end{aligned}
$$

where D_0, D_{ij}, D_{ijk} are the four-point Feynman integrals [19]. The explicit forms of $\delta M^{V_1(t)}, \delta M^{s(t)}, \delta M^{b(t)}$ can be respectively obtained from $\delta M^{V_1(s)}, \delta M^{s(s)}, \delta M^{b(s)}$ by the transformation U defined as

$$
\begin{gathered}
p_b\to p_t,\quad \hat{s}\to\hat{t},\quad k\to -k,\quad \xi_i^{(1)}\to\xi_i^{(2)},\quad \xi_i^{(3)}\to\xi_i^{(4)},\quad \eta_i^{(1)}\to\eta_i^{(2)}, \\
m_t\leftrightarrow m_b,\quad \eta^{(1)}\leftrightarrow\eta^{(2)},\quad \lambda_b\leftrightarrow\lambda_t,\quad m_{\tilde{t}_i}\leftrightarrow m_{\tilde{b}_i},\quad U_{i2}\leftrightarrow V_{i2}^*,\quad N_{i3}\leftrightarrow N_{i4}^*, \\
L_i(b)\leftrightarrow L_i(t),\quad R_i(b)\leftrightarrow R_i(t),\quad p_b^\mu P_{L(R)}\leftrightarrow p_t^\mu P_{R(L)},\quad \gamma^\mu \not{k}P_L\leftrightarrow\gamma^\mu \not{k}P_R.
\end{gathered}
$$

All other form factors f_i^l not listed above vanish. In the above expressions we have used the following definitions:

$$
\begin{aligned}
&\eta^{(1)}=m_b\tan\beta, \qquad \eta^{(2)}=m_t\cot\beta, \qquad \lambda_b=\frac{m_b}{\sqrt{2}m_W\cos\beta}, \qquad \lambda_t=\frac{m_t}{\sqrt{2}m_W\sin\beta} \\
&L_1(q)=\cos\theta_q, \qquad L_2(q)=-\sin\theta_q, \qquad R_1(q)=\sin\theta_q, \qquad R_2(q)=\cos\theta_q, \\
&\eta_{H^0}^{(1)}=\frac{\cos^2\alpha}{\cos^2\beta}, \qquad \eta_{h^0}^{(1)}=\frac{\sin^2\alpha}{\cos^2\beta}, \qquad \eta_{A^0}^{(1)}=\tan^2\beta, \qquad \eta_{G^0}^{(1)}=1, \\
&\eta_{H^0}^{(2)}=\frac{\sin^2\alpha}{\sin^2\beta}, \qquad \eta_{h^0}^{(2)}=\frac{\cos^2\alpha}{\sin^2\beta}, \qquad \eta_{A^0}^{(2)}=\cot^2\beta, \qquad \eta_{G^0}^{(2)}=1, \\
&\eta_{H^0}^{(3)}=-\eta_{h^0}^{(3)}=\frac{\sin\alpha\cos\alpha}{\sin\beta\cos\beta}, \qquad \eta_{G^0}^{(3)}=-\eta_{A^0}^{(3)}=1, \\
&\xi_{H^-}^{(1)}=\frac{m_t^2}{m_b^2}\cot^2\beta, \qquad \xi_{G^-}^{(1)}=\frac{m_t^2}{m_b^2}, \qquad \xi_{H^-}^{(2)}=\frac{m_b^2}{m_t^2}\tan^2\beta, \qquad \xi_{G^-}^{(2)}=\frac{m_b^2}{m_t^2}, \\
&\xi_{H^-}^{(3)}=\tan^2\beta, \qquad \xi_{G^-}^{(3)}=1, \qquad \xi_{H^-}^{(4)}=\cot^2\beta, \qquad \xi_{G^-}^{(4)}=1,
\end{aligned}
$$

$$\zeta_{H^0} = \zeta_{h^0} = \zeta_{H^-} = -\zeta_{A^0} = -\zeta_{G^0} = -\zeta_{G^-} = 1,$$

$$\begin{aligned}
\sigma_{ij} &= \frac{m_W}{\sqrt{2}}(\sin 2\beta - \frac{m_b^2\tan\beta + m_t^2\cot\beta}{m_W^2})L_i(b)L_j(t) \\
&+\frac{m_t m_b}{\sqrt{2}m_W}(\tan\beta+\cot\beta)R_i(b)R_j(t) - \frac{m_b}{\sqrt{2}m_W}(\mu - A_b\tan\beta)R_i(b)L_j(t) \\
&-\frac{m_t}{\sqrt{2}m_W}(\mu - A_t\cot\beta)L_i(b)R_j(t), \\
g_1^{V_1(s)} &= \sum_{i=H^0,h^0,G^0,A^0}\eta_i^{(1)}\{[\frac{1}{2} - 2\overline{C}_{24} + m_b^2(-2C_{11}+C_{12}-C_{21}+C_{23}) - \hat{s}(C_{12} \\
&+C_{23})](-p_b,-k,m_i,m_b,m_b) + [-F_0+F_1+2m_b^2G_1 \\
&-(1+\zeta_i)2m_b^2G_0](m_b^2,m_i,m_b)\}, \\
g_2^{V_1(s)} &= \sum_{i=H^-,G^-}2\{\xi_i^{(1)}[\frac{1}{2} - 2\overline{C}_{24} + m_t^2C_0 + m_b^2(-C_0-2C_{11}+C_{12}-C_{21}+C_{23}) \\
&-\hat{s}(C_{12}+C_{23})](-p_b,-k,m_i,m_t,m_t) + [\xi_i^{(1)}(-F_0+F_1) - 2m_t^2\zeta_iG_0 \\
&+m_b^2(\xi_i^{(1)}+\xi_i^{(3)})(G_1-\zeta_iG_0)](m_b^2,m_i,m_t)\} \\
&+\frac{4m_W^2}{m_b^2}\sum_{i,j}\{\lambda_b^2[R_j^2(b)|N_{i3}|^2(-F_0+F_1) + m_b^2|N_{i3}|^2(-G_0+G_1) - 2m_bm_{\tilde{\chi}_i^0} \\
&\times L_j(b)R_j(b)N_{i3}^{*2}G_0](m_b^2,m_{\tilde{b}_j},m_{\tilde{\chi}_i^0}) + [-2m_bm_{\tilde{\chi}_i^+}\lambda_b\lambda_tL_j(t)R_j(t)V_{i2}^{*2}U_{i2}^{*2}G_0 \\
&+\lambda_t^2R_j^2(t)|V_{i2}|^2(-F_0+F_1) + m_b^2(\lambda_t^2R_j^2(t)|V_{i2}|^2 + \lambda_b^2L_j^2(t)|U_{i2}|^2)(-G_0 \\
&+G_1)](m_b^2,m_{\tilde{t}_j},m_{\tilde{\chi}_i^+}) - 2\lambda_b^2R_j^2(b)|N_{i3}|^2\bar{C}_{24}(-p_b,-k,m_{\tilde{\chi}_i^0},m_{\tilde{b}_j},m_{\tilde{b}_j}) \\
&-2\lambda_t^2R_j^2(t)|V_{i2}|^2\bar{C}_{24}(-p_b,-k,m_{\tilde{\chi}_i^+},m_{\tilde{t}_j},m_{\tilde{t}_j})\}, \\
g_3^{V_1(s)} &= g_2^{V_1(s)}(\xi_i^{(1)}\leftrightarrow\xi_i^{(3)}, V_{i2}\leftrightarrow U_{i2}^*, N_{i3}\leftrightarrow N_{i3}^*, L_j(b)\leftrightarrow R_j(b), \lambda_bL_j(t)\leftrightarrow\lambda_tR_j(t)), \\
g_4^{V_1(s)} &= \sum_{i=H^0,h^0,G^0,A^0}\eta_i^{(1)}2m_b[C_0+2C_{11}+C_{21}+\zeta_i(C_0+C_{11})](-p_b,-k,m_i,m_b,m_b) \\
&+\sum_{i=H^-,G^-}4m_b[\xi_i^{(3)}(C_0+2C_{11}+C_{21}) + \frac{m_t^2}{m_b^2}\zeta_i(C_0+C_{11})](-p_b,-k,m_i,m_t,m_t) \\
&+\frac{8m_W^2}{m_b^2}\sum_{i,j}\{\lambda_b^2[m_{\tilde{\chi}_i^0}L_j(b)R_j(b)N_{i3}^{*2}(C_0+C_{11}) - m_bL_j^2(b)|N_{i3}|^2(C_{11} \\
&+C_{21})](-p_b,-k,m_{\tilde{\chi}_i^0},m_{\tilde{b}_j},m_{\tilde{b}_j}) \\
&+[m_{\tilde{\chi}_i^+}\lambda_b\lambda_tL_j(t)R_j(t)V_{i2}^*U_{i2}^*(C_0+C_{11}) - m_b\lambda_b^2L_j^2(t)|U_{i2}|^2(C_{11} \\
&+C_{21})](-p_b,-k,m_{\tilde{\chi}_i^+},m_{\tilde{t}_j},m_{\tilde{t}_j})\}, \\
g_5^{V_1(s)} &= g_4^{V_1(s)}(\xi_i^{(1)}\leftrightarrow\xi_i^{(3)}, V_{i2}\leftrightarrow U_{i2}^*, N_{i3}\leftrightarrow N_{i3}^*, L_j(b)\leftrightarrow R_j(b), \lambda_bL_j(t)\leftrightarrow\lambda_tR_j(t)), \\
g_6^{V_1(s)} &= -\sum_{i=H^0,h^0,G^0,A^0}\eta_i^{(1)}m_b(C_0+C_{11}+\zeta_iC_0)(-p_b,-k,m_i,m_b,m_b) \\
&-\sum_{i=H^-,G^-}2m_b[\xi_i^{(3)}(C_0+C_{11}) + \frac{m_t^2}{m_b^2}\zeta_iC_0](-p_b,-k,m_i,m_t,m_t),
\end{aligned}$$

$$
\begin{aligned}
g_7^{V_1(s)} &= g_6^{V_1(s)}(\xi_i^{(1)} \leftrightarrow \xi_i^{(3)}), \\
g_8^{V_1(s)} &= \sum_{i=H^0,h^0,G^0,A^0} 2\eta_i^{(1)}(C_{12}+C_{23})(-p_b,-k,m_i,m_b,m_b) \\
&\quad + \sum_{i=H^-,G^-} 4\xi_i^{(1)}(C_{12}+C_{24})(-p_b,-k,m_i,m_t,m_t) \\
&\quad - \frac{8m_W^2}{m_b^2}\sum_{i,j}\{\lambda_b^2 R_j^2(b)|N_{i3}|^2(C_{12}+C_{23})(-p_b,-k,m_{\tilde{\chi}_i^0},m_{\tilde{b}_j},m_{\tilde{b}_j}) \\
&\quad + \lambda_t^2 R_j^2(t)|V_{i2}|^2(C_{12}+C_{23})(-p_b,-k,m_{\tilde{\chi}_i^+},m_{\tilde{t}_j},m_{\tilde{t}_j})\}, \\
g_9^{V_1(s)} &= g_8^{V_1(s)}(\xi_i^{(1)} \leftrightarrow \xi_i^{(3)}, V_{i2} \leftrightarrow U_{i2}^*, N_{i3} \leftrightarrow N_{i3}^*, L_j(b) \leftrightarrow R_j(b), \lambda_b L_j(t) \leftrightarrow \lambda_t R_j(t)), \\
g_1^{V_2(s)} &= \sum_{i=H^0,h^0,G^0,A^0} \eta_i^{(3)}\{\eta^{(1)}[-\frac{1}{2}+4\overline{C}_{24}+m_t^2(C_0+2C_{11}+\zeta_i(C_0+C_{11}) \\
&\quad + C_{21}-C_{12}-C_{23})+m_{H^-}^2(C_{22}-C_{23})+\hat{s}(C_{12}+C_{23})]+\eta^{(2)}m_b m_t[\zeta_i C_{11} \\
&\quad + (1+\zeta_i)C_0]\}(-p_t,-p_{H^-},m_i,m_t,m_b)+\frac{4\sqrt{2}m_W}{\sin 2\beta}\sum_{i,j,k}[m_t R_i(b)R_j(t)N_{k3}^*N_{k4} \\
&\quad \times(-C_{11}+C_{12})+m_{\tilde{\chi}_k^0}L_j(t)R_i(b)N_{k3}^*N_{k4}^*C_0]\sigma_{ij}(-p_t,-p_{H^-},m_{\tilde{\chi}_k^0},m_{\tilde{b}_i},m_{\tilde{t}_j}), \\
g_2^{V_2(s)} &= g_1^{V_2(s)}(\eta^{(1)} \leftrightarrow \eta^{(2)}, L_l \leftrightarrow R_l, N_{kl} \leftrightarrow N_{kl}^*), \\
g_3^{V_2(s)} &= \sum_{i=H^0,h^0,G^0,A^0} \eta_i^{(3)}\{\eta^{(1)}m_t[C_0+C_{11}+\zeta_i(C_0+C_{12})]+\eta^{(2)}\zeta_i m_b C_{12}\} \\
&\quad (-p_t,-p_{H^-},m_i,m_t,m_b) \\
&\quad - \frac{4\sqrt{2}m_W}{\sin 2\beta}\sum_{i,j,k} R_i(b)R_j(t)N_{k3}^*N_{k4}\sigma_{ij}C_{12}(-p_t,-p_{H^-},m_{\tilde{\chi}_k^0},m_{\tilde{b}_i},m_{\tilde{t}_j}), \\
g_4^{V_2(s)} &= g_3^{V_2(s)}(\eta^{(1)} \leftrightarrow \eta^{(2)}, L_l \leftrightarrow R_l, N_{kl} \leftrightarrow N_{kl}^*), \\
g_1^{V_2(t)} &= \sum_{i=H^0,h^0,G^0,A^0} \eta_i^{(3)}\{\eta^{(1)}[-\frac{1}{2}+4\overline{C}_{24}+m_b^2(C_0+2C_{11}+\zeta_i(C_0+C_{11}) \\
&\quad + C_{21}-C_{12}-C_{23})+m_{H^-}^2(C_{22}-C_{23})+\hat{t}(C_{12}+C_{23})] \\
&\quad + \eta^{(2)}m_b m_t[C_0+\zeta_i(C_0+C_{11})]\}(-p_b,p_{H^-},m_i,m_b,m_t) \\
&\quad + \frac{4\sqrt{2}m_W}{\sin 2\beta}\sum_{i,j,k}[m_b L_i(b)L_j(t)N_{k3}^*N_{k4}(-C_{11}+C_{12}) \\
&\quad + m_{\tilde{\chi}_k^0}L_j(t)R_i(b)N_{k3}^*N_{k4}^*C_0]\sigma_{ij}(-p_b,p_{H^-},m_{\tilde{\chi}_k^0},m_{\tilde{b}_i},m_{\tilde{t}_j}), \\
g_2^{V_2(t)} &= g_1^{V_2(t)}(\eta^{(1)} \leftrightarrow \eta^{(2)}, L_l \leftrightarrow R_l, N_{kl} \leftrightarrow N_{kl}^*), \\
g_3^{V_2(t)} &= -\sum_{i=H^0,h^0,G^0,A^0} \eta_i^{(3)}\{\eta^{(1)}m_b[C_0+C_{11}+\zeta_i(C_0+C_{12})]+\eta^{(2)}\zeta_i m_t C_{12}\} \\
&\quad (-p_b,p_{H^-},m_i,m_b,m_t) \\
&\quad + \frac{4\sqrt{2}m_W}{\sin 2\beta}\sum_{i,j,k} R_i(b)R_j(t)N_{k3}^*N_{k4}\sigma_{ij}C_{12}(-p_b,p_{H^-},m_{\tilde{\chi}_k^0},m_{\tilde{b}_i},m_{\tilde{t}_j}), \\
g_4^{V_2(t)} &= g_3^{V_2(t)}(\eta^{(1)} \leftrightarrow \eta^{(2)}, L_l \leftrightarrow R_l, N_{kl} \leftrightarrow N_{kl}^*),
\end{aligned}
$$

$$
\begin{aligned}
g_1^{s(s)} &= \sum_{i=H^0,h^0,G^0,A^0} m_b\eta_i^{(1)}\{-\zeta_i F_0(p_b+k,m_i,m_b)+[\zeta_i F_0-2m_b^2(1+\zeta_i)G_0 \\
&\quad +2m_b^2G_1](m_b^2,m_i,m_b)\}+\sum_{i=H^-,G^-}2m_b\{-\frac{m_t^2}{m_b^2}\zeta_i F_0(p_b+k,m_i,m_t) \\
&\quad +[-2m_t^2\zeta_i G_0+m_b^2(\xi_i^{(1)}+\xi_i^{(3)})(G_1-\zeta_i G_0)+\zeta_i\frac{m_t^2}{m_b^2}F_0](m_b^2,m_i,m_t)\} \\
&\quad +\frac{4m_W^2}{m_b^2}\sum_{i,j}\{-m_{\tilde{\chi}_i^0}\lambda_b^2 L_j(b)R_j(b)N_{i3}^{*2}F_0(p_b+k,m_{\tilde{b}_j},m_{\tilde{\chi}_i^0}) \\
&\quad -m_{\tilde{\chi}_i^+}\lambda_b\lambda_t L_j(b)R_j(b)V_{i2}^*U_{i2}^*F_0(p_b+k,m_{\tilde{t}_j},m_{\tilde{\chi}_i^+})+[m_b^3\lambda_b^2|N_{i3}|^2(-G_0+G_1) \\
&\quad -m_{\tilde{\chi}_i^0}\lambda_b^2 L_j(b)R_j(b)N_{i3}^{*2}(2m_b^2G_0-F_0)](m_b^2,m_{\tilde{b}_j},m_{\tilde{\chi}_i^0})+[m_b^3(\lambda_b^2L_j^2(t)|U_{i2}|^2 \\
&\quad +\lambda_t^2R_j^2(t)|V_{i2}|^2)(-G_0+G_1)-m_{\tilde{\chi}_i^+}\lambda_b\lambda_t L_j(t)R_j(t)V_{i2}^*U_{i2}^*(2m_b^2G_0 \\
&\quad -F_0)](m_b^2,m_{\tilde{t}_j},m_{\tilde{\chi}_i^+})\}, \\
g_2^{s(s)} &= \sum_{i=H^0,h^0,G^0,A^0}\eta_i^{(1)}(-F_0+F_1)(p_b+k,m_i,m_b), \\
g_3^{s(s)} &= \sum_{i=H^0,h^0,G^0,A^0}\eta_i^{(1)}[F_0-F_1-2m_b^2G_1+2(1+\zeta_i)m_b^2G_0](m_b^2,m_i,m_b) \\
&\quad +\sum_{i=H^-,G^-}2\{\xi_i^{(1)}(-F_0+F_1)(p_b+k,m_i,m_t)-[\xi_i^{(1)}(-F_0+F_1) \\
&\quad -2\zeta_i m_t^2G_0+m_b^2(\xi_i^{(1)}+\xi_i^{(3)})(G_1-\zeta_i G_0)](m_b^2,m_i,m_t)\} \\
&\quad -\frac{4m_W^2}{m_b^2}\sum_{i,j}\{\lambda_b^2[R_j^2(b)|N_{i3}|^2(-F_0+F_1)+|N_{i3}|^2m_b^2(-G_0+G_1) \\
&\quad -2m_b m_{\tilde{\chi}_i^0}L_j(b)R_j(b)N_{i3}^{*2}G_0](m_b^2,m_{\tilde{b}_j},m_{\tilde{\chi}_i^0}) \\
&\quad +[\lambda_t^2R_j^2(t)|V_{i2}|^2(-F_0+F_1)+m_b^2(\lambda_t^2R_j^2(t)|V_{i2}|^2+\lambda_b^2L_j^2(t)|U_{i2}|^2)(G_1-G_0) \\
&\quad -2m_b m_{\tilde{\chi}_i^+}L_j(t)R_j(t)\lambda_b\lambda_t V_{i2}^*U_{i2}^*G_0](m_b^2,m_{\tilde{t}_j},m_{\tilde{\chi}_i^+}) \\
&\quad -\lambda_b^2R_j^2(b)|N_{i3}|^2(-F_0+F_1)(p_b+k,m_{\tilde{b}_j},m_{\tilde{\chi}_i^0}) \\
&\quad -\lambda_t^2R_j^2(t)|V_{i2}|^2(-F_0+F_1)(p_b+k,m_{\tilde{t}_j},m_{\tilde{\chi}_i^+})\}, \\
g_4^{s(s)} &= g_3^{s(s)}(\xi_i^{(1)}\leftrightarrow\xi_i^{(3)},V_{i2}\leftrightarrow U_{i2}^*,N_{i3}\leftrightarrow N_{i3}^*,L_j(b)\leftrightarrow R_j(b),\lambda_b L_j(t)\leftrightarrow\lambda_t R_j(t)), \\
g_5^{s(s)} &= g_1^{s(s)}(N_{i3}^*\to N_{i3},V_{i2}^*\to V_{i2},U_{i2}^*\to U_{i2}), \\
\delta\Lambda_L^{(1)} &= \frac{4N_c}{3m_W^2}(1-\cot^2\theta_W)[2m_t^2(\ln\frac{m_t^2}{\mu^2}-1)+m_b^2+m_t^2-\frac{5}{6}m_W^2+m_b^2F_0 \\
&\quad +(m_b^2-m_t^2-2m_W^2)F_1](m_W^2,m_b,m_t)+\frac{4N_c}{3m_W^2}\cot^2\theta_W\{-\frac{5}{6}[(g_V^b)^2+(g_A^b)^2 \\
&\quad +(g_V^t)^2+(g_A^t)^2]m_Z^2+[((g_V^t)^2+(g_A^t)^2)(2m_t^2\ln\frac{m_t^2}{\mu^2}+m_t^2F_0-2m_Z^2F_1) \\
&\quad -((g_V^t)^2-(g_A^t)^2)3m_t^2F_0](m_Z^2,m_t,m_t)+[((g_V^b)^2+(g_A^b)^2)(2m_b^2\ln\frac{m_b^2}{\mu^2}
\end{aligned}
$$

$$
\begin{aligned}
&+m_b^2F_0-2m_Z^2F_1)-((g_V^b)^2-(g_A^b)^2)3m_b^2F_0](m_Z^2,m_b,m_b)\}+\frac{4N_c}{m_W^2}[(\cot^2\beta\\
&-1)m_t^2F_0+(m_t^2-m_b^2-2m_t^2\cot^2\beta)F_1+(m_t^2\cot^2\beta+m_b^2\tan^2\beta\\
&+2m_b^2)m_t^2G_0-(m_t^2\cot^2\beta+m_b^2\tan^2\beta)m_{H^-}^2G_1](m_{H^-}^2,m_t,m_b)\\
&+\sum_{i=H^0,h^0,G^0,A^0}\frac{1}{2m_W^2}\{m_b^2\eta_i^{(1)}[F_1-F_0-2m_b^2(G_0+\zeta_iG_0-G_1)](m_b^2,m_i,m_b)\\
&-m_t^2\eta_i^{(2)}[-(1+2\zeta_i)F_0+F_1+2m_t^2(1+\zeta_i)G_0-2m_t^2G_1](m_t^2,m_i,m_t)\}\\
&+\sum_{i=H^-,G^-}\frac{1}{m_W^2}\{m_b^2[\xi_i^{(1)}(-F_0+F_1)-2m_t^2\zeta_iG_0+m_b^2(\xi_i^{(1)}+\xi_i^{(3)})\\
&\times(G_1-\zeta_iG_0)](m_b^2,m_i,m_t)-m_t^2[-\frac{2m_b^2}{m_t^2}\zeta_iF_0+\xi_i^{(2)}(-F_0+F_1)+2m_b^2\zeta_iG_0\\
&-m_t^2(\xi_i^{(2)}+\xi_i^{(4)})(G_1-\zeta_iG_0)](m_t^2,m_i,m_b)\}-2N_C\sum_{i,j}\{2\sigma_{ij}\sigma_{ij}G_0\\
&+\frac{1}{m_W^2}L_i(b)L_j(t)[L_i(b)L_j(t)(\frac{m_b^2}{\cos^2\beta}+\frac{m_t^2}{\sin^2\beta})\cos 2\beta\\
&+R_i(b)R_j(t)m_tm_b(\tan^2\beta-\cot^2\beta)]\}(m_{H^-}^2,m_{\tilde t_j},m_{\tilde b_i}),
\end{aligned}
$$

$$
\begin{aligned}
\delta\Lambda_L^{(2)} &= -2\sum_{i,j}\{\lambda_t^2[-\frac{2m_{\tilde\chi_i^0}}{m_t}L_j(t)R_j(t)N_{i4}^{*2}(F_0-m_t^2G_0)+|N_{i4}|^2(R_j^2(t)(-F_0+F_1)\\
&-m_t^2(-G_0+G_1))](m_t^2,m_{\tilde t_j},m_{\tilde\chi_i^0})+[-\frac{2m_{\tilde\chi_i^+}}{m_t}\lambda_b\lambda_tL_j(b)R_j(b)U_{i2}^*V_{i2}^*(F_0\\
&-m_t^2G_0)+\lambda_b^2R_j^2(b)|U_{i2}|^2(-F_0+F_1)-m_t^2(\lambda_t^2L_j^2(b)|V_{i2}|^2+\lambda_b^2R_j^2(b)|U_{i2}|^2)\\
&\times(-G_0+G_1)](m_t^2,m_{\tilde b_j},m_{\tilde\chi_i^+})\},\\
\delta\Lambda_L^{(3)} &= 2\sum_{i,j}\{\lambda_b^2[|Ni3|^2(R_j^2(b)(-F_0+F_1)+m_b^2(-G_0+G_1))-2m_bm_{\tilde\chi_i^0}L_j(b)R_j(b)\\
&\times N_{i3}^{*2}G_0](m_b^2,m_{\tilde b_j},m_{\tilde\chi_i^0})+[-2m_{\tilde\chi_i^+}m_b\lambda_b\lambda_tL_j(t)R_j(t)U_{i2}^*V_{i2}^*G_0\\
&+\lambda_b^2L_j^2(b)|U_{i2}|^2(-F_0+F_1)+m_b^2(\lambda_t^2R_j^2(t)|V_{i2}|^2+\lambda_b^2L_j^2(t)|U_{i2}|^2)\\
&\times(-G_0+G_1)](m_b^2,m_{\tilde t_j},m_{\tilde\chi_i^+})\},\\
\delta\Lambda_R^{(1)} &= \sum_{i=H^0,h^0,G^0,A^0}\frac{1}{2m_W^2}\{m_t^2\eta_i^{(2)}[-F_0+F_1-2m_t^2(G_0+\zeta_iG_0-G_1)](m_t^2,m_i,m_t)\\
&-m_b^2\eta_i^{(1)}[-F_0+F_1-2\zeta_iF_0+2m_b^2(1+\zeta_i)G_0-2m_b^2G_1](m_b^2,m_i,m_b)\}\\
&+\sum_{i=H^-,G^-}\frac{1}{m_W^2}\{m_t^2[\xi_i^{(2)}(-F_0+F_1)-2m_b^2\zeta_iG_0+m_t^2(\xi_i^{(2)}+\xi_i^{(4)})(G_1\\
&-\zeta_iG_0)](m_t^2,m_i,m_b)-m_b^2[-\frac{2m_t^2}{m_b^2}\zeta_iF_0+\xi_i^{(1)}(-F_0+F_1)+2m_t^2\zeta_iG_0\\
&-m_b^2(\xi_i^{(1)}+\xi_i^{(3)})(G_1-\zeta_iG_0)](m_b^2,m_i,m_t)\},\\
\delta\Lambda_R^{(2)} &= \delta\Lambda_L^{(2)}(U), \qquad \delta\Lambda_R^{(3)}=\delta\Lambda_L^{(3)}(U).
\end{aligned}
$$

Here C_0, C_{ij} are the three-point Feynman integrals[19] and $\overline{C}_{24} \equiv -\frac{1}{4}\Delta + C_{24}$, while

$$
\begin{aligned}
F_n(q, m_1, m_2) &= \int_0^1 dy y^n \ln\left[\frac{-q^2 y(1-y) + m_1^2(1-y) + m_2^2 y}{\mu^2}\right], \\
G_n(q, m_1, m_2) &= -\int_0^1 dy \frac{y^{n+1}(1-y)}{-q^2 y(1-y) + m_1^2(1-y) + m_2^2 y},
\end{aligned}
$$

and

$$
g_V^t = \frac{1}{2} - \frac{4}{3}\sin^2\theta_W, \quad g_A^t = \frac{1}{2}, \qquad g_V^b = -\frac{1}{2} + \frac{2}{3}\sin^2\theta_W, \quad g_A^b = -\frac{1}{2},
$$

which are the SM couplings of the top and bottom quarks to the Z boson. The definitions of $\theta_q, U_{ij}, V_{ij}, N_{ij}, \mu, A_q$ can be found in ref.[2].

2.5 Appendix B

$$
\begin{aligned}
h_1^{(i)} &= 4m_t\eta^{(2)}(2p_b\cdot k - p^{(i)}\cdot p_b) - 4m_b\eta^{(1)}(p^{(i)}\cdot p_t + p_t\cdot k), \\
h_2^{(i)} &= h_1^{(i)}(\eta^{(1)} \leftrightarrow \eta^{(2)}), \\
h_3^{(i)} &= 2\eta^{(2)}(2p_b\cdot kp_b\cdot p_t - m_b^2 p_t\cdot k - 2p^{(i)}\cdot p_b p_b\cdot p_t) + 2m_b m_t\eta^{(1)}(p_b\cdot k \\
&\quad -2p^{(i)}\cdot p_b), \\
h_4^{(i)} &= h_3^{(i)}(\eta^{(1)} \leftrightarrow \eta^{(2)}), \\
h_5^{(i)} &= 2\eta^{(2)}(m_t^2 p_b\cdot k - 2p^{(i)}\cdot p_t p_b\cdot p_t) + 2m_b m_t m_t\eta^{(1)}(p_t\cdot k - 2p^{(i)}\cdot p_t), \\
h_6^{(i)} &= h_5^{(i)}(\eta^{(1)} \leftrightarrow \eta^{(2)}), \\
h_7^{(i)} &= 4\eta^{(2)}(p^{(i)}\cdot p_b p_t\cdot k - p^{(i)}\cdot kp_b\cdot p_t - p_b\cdot kp^{(i)}\cdot p_t - 2p_b\cdot kp_t\cdot k) \\
&\quad -4m_b m_t\eta^{(1)}p^{(i)}\cdot k, \\
h_8^{(i)} &= h_7^{(i)}(\eta^{(1)} \leftrightarrow \eta^{(2)}), \\
h_9^{(i)} &= 4m_t\eta^{(2)}p_b\cdot k(p_b\cdot k - p^{(i)}\cdot p_b) - 4m_b\eta^{(1)}p^{(i)}\cdot p_b p_t\cdot k, \\
h_{10}^{(i)} &= h_9^{(i)}(\eta^{(1)} \leftrightarrow \eta^{(2)}), \\
h_{11}^{(i)} &= 4m_t\eta^{(2)}p_b\cdot k(p_t\cdot k - p^{(i)}\cdot p_t) - 4m_b\eta^{(1)}p_t\cdot kp^{(i)}\cdot p_t, \\
h_{12}^{(i)} &= h_{11}^{(i)}(\eta^{(1)} \leftrightarrow \eta^{(2)}),
\end{aligned}
$$

where the index i represents the two channels s and t, and $p^{(s)} = p_b$, $p^{(t)} = p_t$.

References

[1] For a review, see J.Gunion, H. Haber, G. Kane, and S.Dawson, The Higgs Hunter's Guide(Addison-Wesley, New York,1990).

[2] H.E. Haber and G.L. Kane, Phys. Rep. 117, 75(1985); J.F. Gunion and H.E. Haber, Nucl. Phys. **B272**, 1(1986).

[3] E.Eichten, I.Hinchliffe, K. Lane, and C. Quigg, Rev. Mod. Phys. 56, 579(1984); 1065(E)(1986); N.G. Deshpande, X. Tata, and D. A. Dicus, Phys. Rev. **D29**, 1527(1984); S. Willenbrock, Phys. Rev. **D35**, 173(1987); A. Krause, T.Plehn, M. Spria, and P. M. Zerwas, Nucl. Phys. **B519**, 85(1998); J.Yi, M. Wen-Gan, H.Liang, H. Meng, and Y. Zeng-Hui, J. Phys. G23, 385(1997); Erratum-ibid. G23, 1151(1997).

[4] D.A.Dicus, J.L.Hewett, C.Kao and T.G.Rizzo, Phys. Rev. **D40**, 787(1989); A.A. Barrientos Bendez*ú* and B.A. Kniehl, Phys. Rev. **D59**, 015009(1999).

[5] S. Moretti and K. Odagiri, Phys. Rev. **D59**,055008(1999).

[6] Z.Kunszt and F. Zwirner, Nucl. Phys. **B385**, 3(1992), and references cited therein.

[7] J.F. Gunion, H.E. Haber, F.E. Paige, W.-K. Tung, and S. Willenbrock, Nucl. Phys. **B294**,621(1987); R.M. Barnett, H.E. Haber, and D.E. Soper, ibid. B306, 697(1988); F.I. Olness and W.-K. Tung, ibid. **B308**, 813(1988).

[8] V. Barger, R.J.N. Phillips, and D.P. Roy, Phys. Lett. **B324**, 236(1994).

[9] C.S. Huang and S.H. Zhu, Phys. Rev. **D60**, 075012(1999).

[10] K. Odagiri, hep-ph/9901432; Phys. Lett. **B452**, 327(1999).

[11] D.P. Roy, Phys. Lett. **B459**, 607(1999).

[12] Francesca Borzumati, Jean-Loic Kneur, and Nir Polonsky, Phys. Rev. **D60**, 115011(1999).

[13] S. Sirlin, Phys. Rev. **D22**, 971 (1980); W. J. Marciano and A. Sirlin,*ibid.* **22**, 2695(1980); **31**, 213(E) (1985); A. Sirlin and W.J. Marciano, Nucl. Phys. **B189**, 442(1981); K.I. Aoki et.al., Prog. Theor. Phys. Suppl. **73**, 1(1982).

[14] A. Mendez and A. Pomarol, Phys.Lett.**B279**, 98(1992).

[15] Particle Data Group, C.Caso *et al*, Eur.Phys.J.C 3, 1(1998).

[16] J.Gunion, A.Turski, Phys. Rev. **D39**, 2701(1989); **D40**, 2333(1990); J.R.Espinosa, M.Quiros, Phys. Lett. **B266**, 389(1991); M.Carena, M.Quiros, C.E.M.Wagner, Nucl. Phys. **B461**, 407(1996).

[17] H.L. Lai, et al.(CTEQ collaboration), hep-ph/9903282.

[18 C.S.Li, R.J.Oakes, and J.M. Yang, Phys. Rev. **D55**, 5780(1997).

[19] G.Passarino and M.Veltman, Nucl. Phys. **B160**, 151(1979); A.Axelrod, *ibid.* **B209**, 349 (1982); M.Clements *et al.*, Phys. Rev. **D27**, 570 (1983).

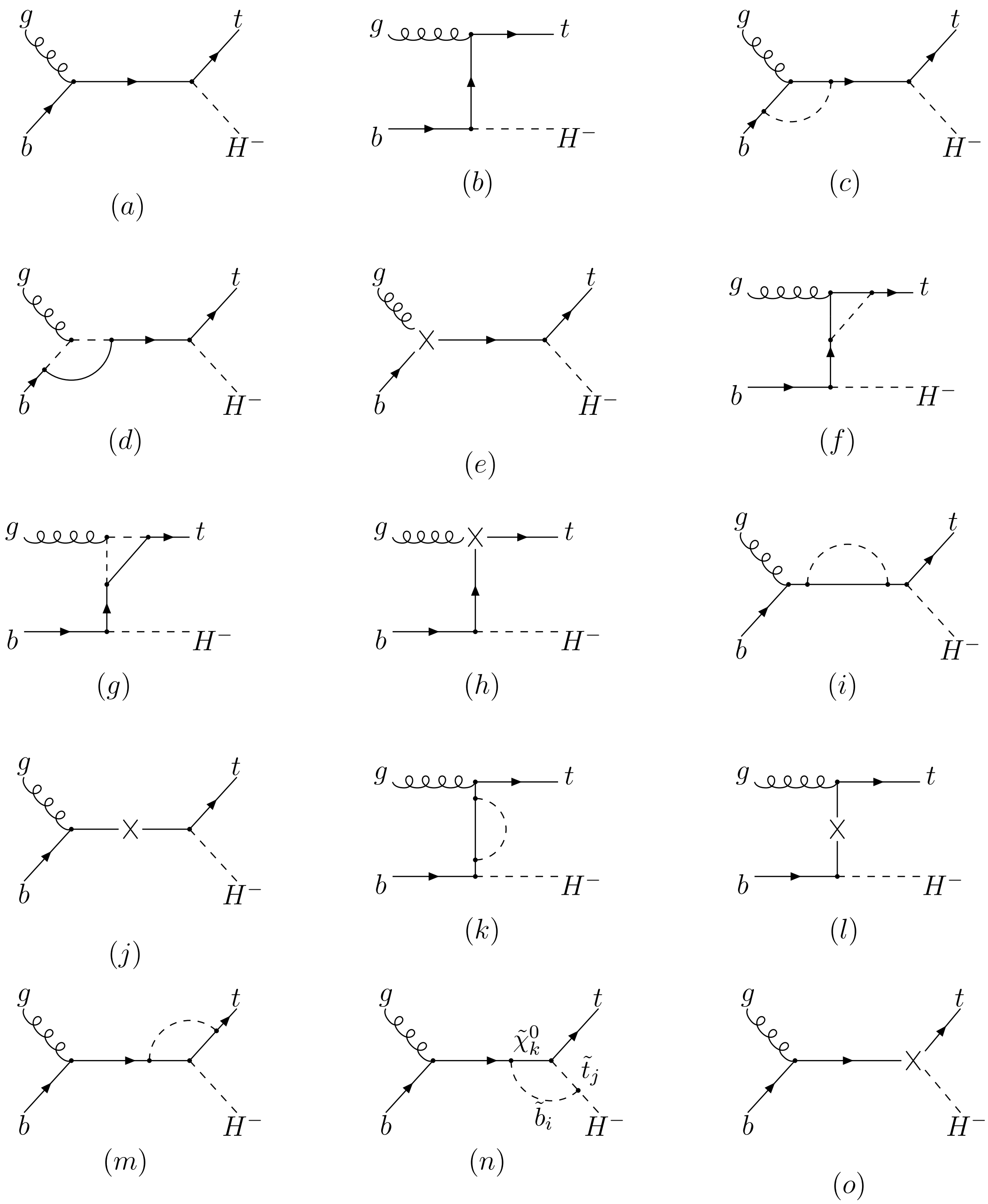
g
t
b
H^-
(a)
(b)
(c)
(d)
(e)
(f)
(g)
(h)
(i)
(j)
(k)
(l)
(m)
$\tilde{\chi}_k^0$
$\tilde{t}_j$
$\tilde{b}_i$
(n)
(o)

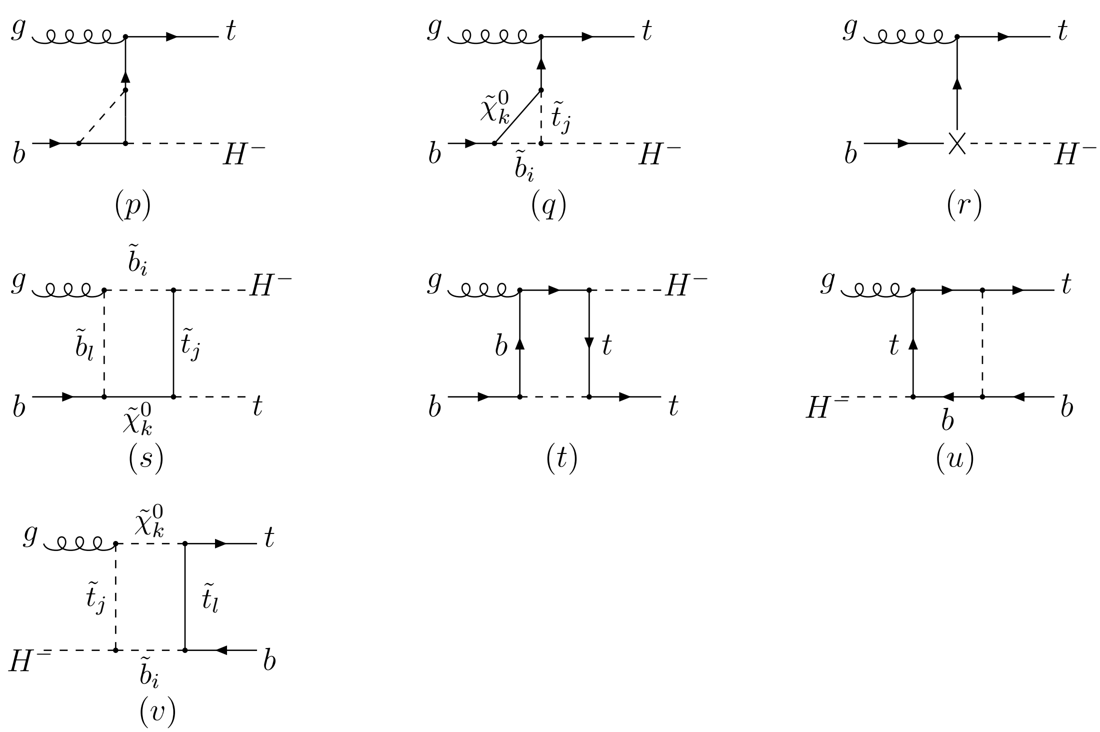

Figure 1: Feynman diagrams contributing to $O(\alpha_{ew} m_{t(b)}^2/m_W^2)$ Yukawa corrections to $gb \to tH^-$: (a) and (b) are tree level diagrams; $(c) - (v)$ are one-loop diagrams. The dashed lines represent $H, h, A, H^{\pm}, G^0$ and $G^{\pm}$ for diagrams (c) and (f); H, h, A and G^0 for diagrams $(m), (p), (t)$ and (u); $\tilde{t}, \tilde{b}, H, h, A, H^{\pm}, G^0$ and $G^{\pm}$ for (i) and (k), where the solid lines represent charginos and neutralinos if the dashed lines represent squarks. For diagrams (d) and (g), the solid lines in the loop represent $\tilde{\chi}^0$ and $\tilde{\chi}^+$ and the dashed lines represent squarks.

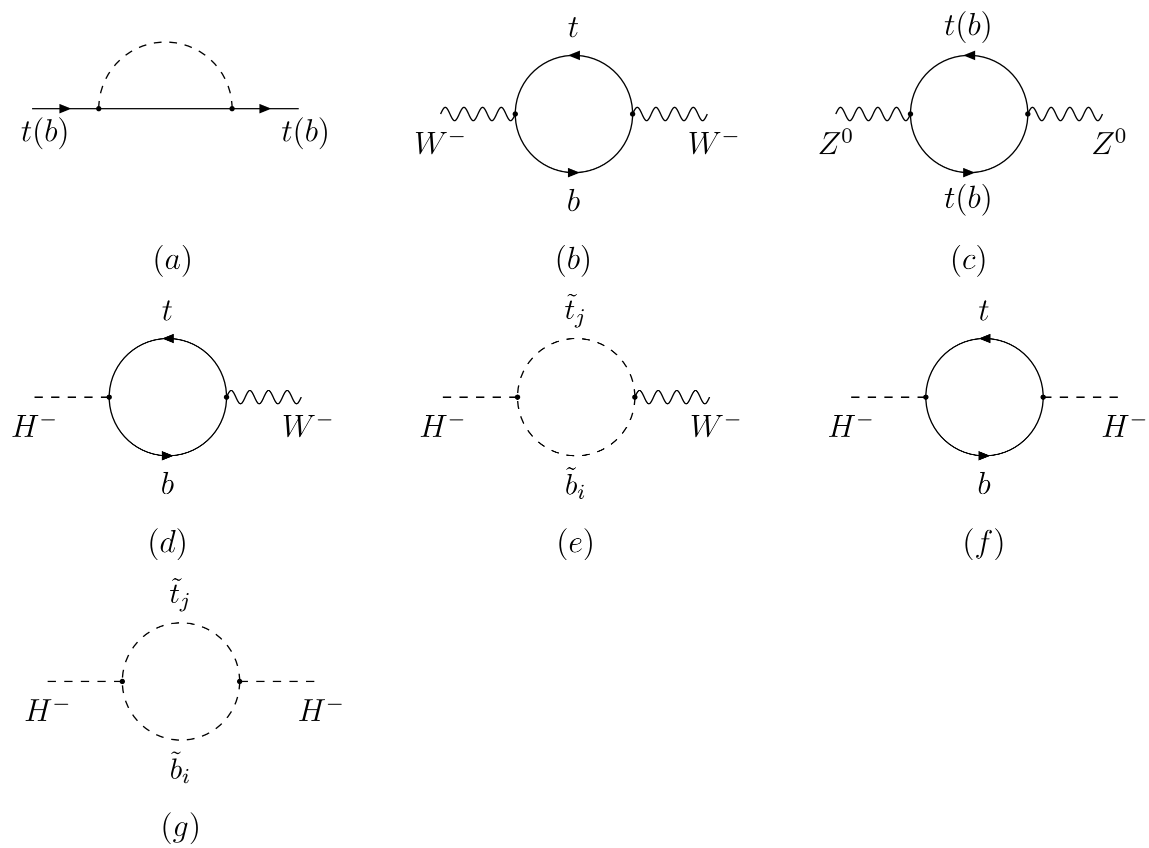

Figure 2: Self-energy Feynman diagrams contributing to renormalization constants: The dashed lines represent $\tilde{t}, \tilde{b}, H, h, A, H^{\pm}, G^0$ and $G^{\pm}$ for diagram (a), where the solid lines represent charginos and neutralinos if the dashed lines represent squarks.

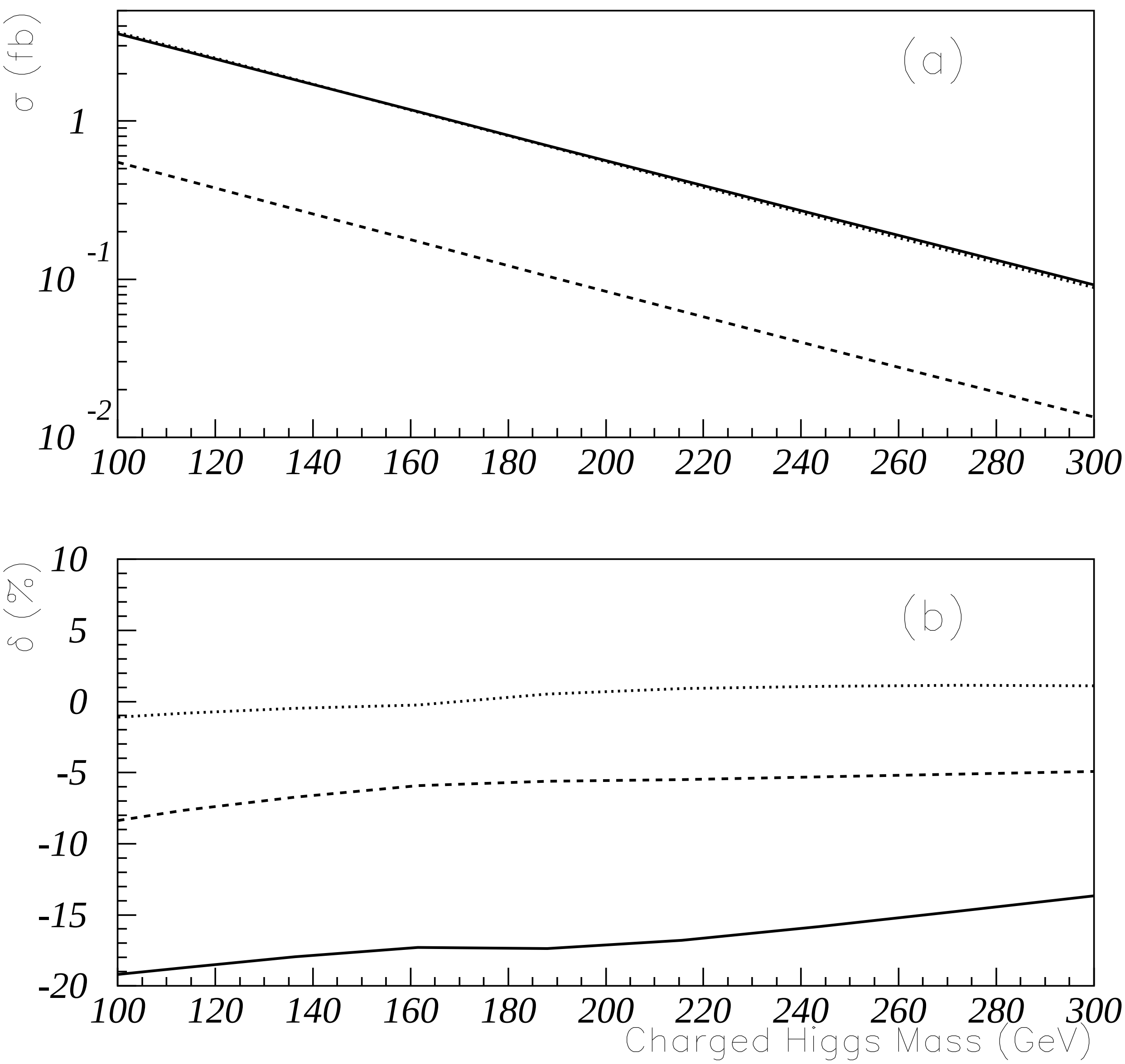

Figure 3: The tree-level total cross sections (a) and relative one-loop corrections (b) versus $m_{H^\pm}$ at the Tevatron with $\sqrt{s} = 2$ TeV. The solid, dashed and dotted lines correspond to $\tan\beta = 2, 10$ and 30, respectively.

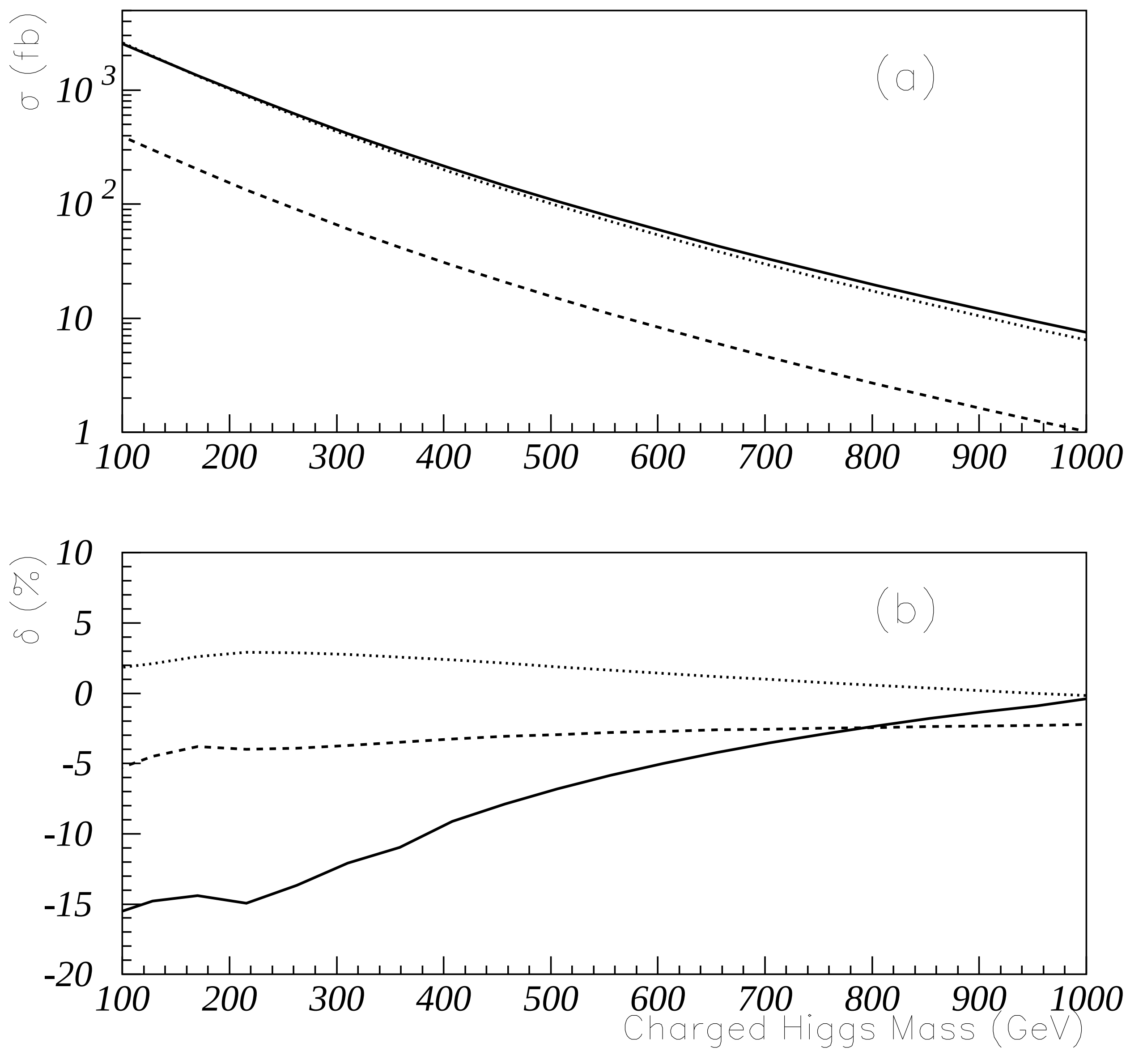

Figure 4: The tree-level total cross sections (a) and relative one-loop corrections (b) versus $m_{H^\pm}$ at the LHC with $\sqrt{s} = 14$ TeV. The solid, dashed and dotted lines correspond to $\tan\beta = 2, 10$ and 30, respectively.

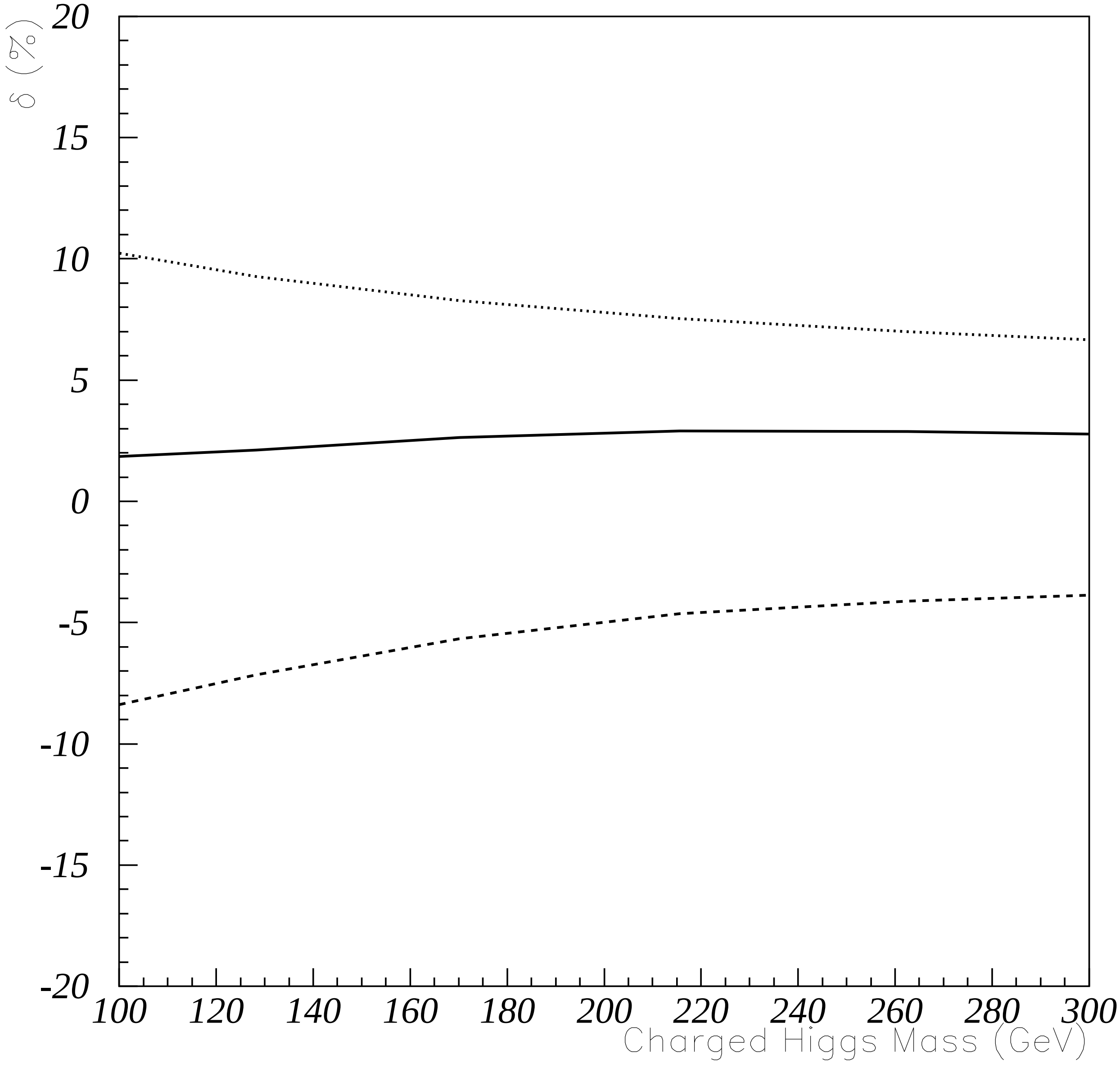

Figure 5: The radiative correction from top, bottom quarks (dashed line) and genuine SUSY particles (dotted line), as well as total contributions (solid line) when $\tan\beta = 30$ at the LHC with $\sqrt{s} = 14$ TeV.

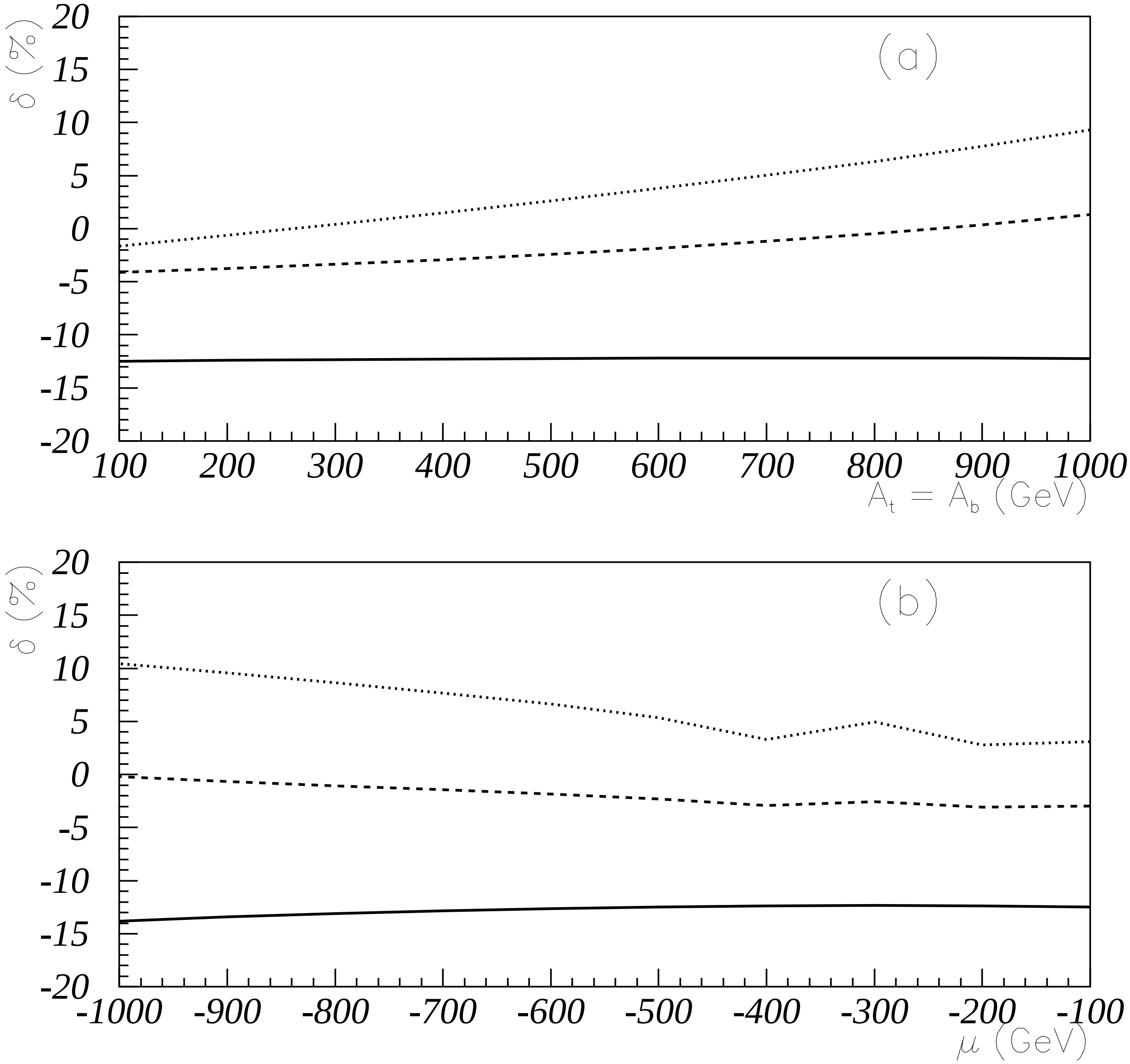

Figure 6: Relative one-loop corrections versus A_t, A_b (a) as well as μ (b) at the LHC with $\sqrt{s} = 14$ TeV, where $m_{H^\pm} = 300GeV$ and the solid, dashed and dotted lines correspond to $\tan\beta = 2, 10$ and 30, respectively. For (a), $\mu = -100GeV$, and for (b), $A_t = A_b = 200GeV$.

3 Supersymmetric Electroweak Corrections to $W^{\pm}H^{\mp}$ Associated Production at the CERN Large Hadron Collider

ABSTRACT

The $O(\alpha_{ew}m_{t(b)}^2/m_W^2)$ and $O(\alpha_{ew}m_{t(b)}^4/m_W^4)$ supersymmetric electroweak corrections to the cross section for $W^{\pm}H^{\mp}$ associated production at the LHC are calculated in the minimal supersymmetric standard model. Those corrections arise from the quantum effects which are induced by the Yukawa couplings from the Higgs sector and the chargino-top(bottom)-sbottom(stop) couplings, neutralino-top(bottom)-stop(sbottom) couplings and charged Higgs-stop-sbottom couplings. The numerical results show that the Yukawa corrections arising from the Higgs sector can decrease the total cross sections significantly for low $\tan\beta(= 1.5$ and $2)$ when $m_{H^+}(< 300)$GeV, which exceed -12%. For high $\tan\beta$ the Yukawa corrections become negligibly small. The genuine supersymmetric electroweak corrections can increase or decrease the total cross sections depending on the supersymmetric parameters, which can exceed -25% for the favorable supersymmetric parameter values. We also show that the genuine supersymmetric electroweak corrections depend strongly on the choice of $\tan\beta$, A_t, $M_{\tilde{Q}}$ and μ. For large values of A_t, or large values of μ and $\tan\beta$, one can get much larger corrections. The corrections can become very small, in contrast, for larger values of $M_{\tilde{Q}}$.

3.1 Introduction

One of the most important objectives of the CERN Large Hadron Collider (LHC) is the search for Higgs boson. In various extensions of the Higgs sector of the standard model(SM), for example, in the two-Higgs-doublet models(THDM)[1], particularly the minimal supersymmetric standard model(MSSM)[2], there are physical charged Higgs bosons, which do not belong to the spectrum of the SM and therefore their discovery would be instant evidence of new physics. In much of the parameter space preferred by the MSSM, namely $m_{H^{\pm}} > m_W$ and $1 < \tan\beta < m_t/m_b$[3,4], the LHC will provide the greatest opportunity for the discovery of charged Higgs boson. Previous studies have shown that for a relatively light charged Higgs boson, $m_{H^{\pm}} < m_t - m_b$, the dominate production processes at the LHC are $gg \to t\bar{t}$ and $q\bar{q} \to t\bar{t}$ followed by the decay sequence $t \to bH^+ \to b\tau^+\nu_\tau$[5], and for a heavier charged Higgs boson the dominate production process is $gb \to tH^-$[6,7,8]. Besides the processes mentioned above, in Ref.[9] Dicus et al. also studied the production of a charged Higgs boson in association with a W boson via $b\bar{b}$ annihilation at the tree level and gg fusion at one loop at

hadron colliders. Since the leptonic decays of W boson would serve as a spectacular trigger for the charged Higgs boson search, these processes seem attractive. But the authors of Ref.[9] only considered the case where the value of $\tan\beta$ to be in the range $0.3-2.3$. Recently Barrientos Bendezu and Kniehl[10] further studied these processes and presented theoretical predictions for the $W^{\pm}H^{\mp}$ production cross section at the LHC and Tevatron's Run II, where they generalize the analysis of Ref.[9] for arbitrary values of $\tan\beta$ and to update it. They found that the $W^{\pm}H^{\mp}$ production would have a sizeable cross section and its signal should have a significant rate at the LHC unless $m_{H^{\mp}}$ is very large.

As analyzed in Ref.[7,11], the search for heavy charged Higgs bosons with $m_{H^+} > m_t + m_b$ at a hadron collider is seriously complicated by QCD backgrounds. For example, the processes suggested in Ref.[10] suffer from the irreducible background due to top quark pair production, $q\bar{q} \to t\bar{t}$ and $gg \to t\bar{t}$ with subsequent decay through the intermediate state $b\bar{b}W^+W^-$, and heavy charged Higgs boson produced in association with $W^{\pm}$ gauge bosons cannot be resolved at the LHC, via semileptonic W^+W^- decays, for charged Higgs boson masses in the range between $2m_t$ and 600GeV at neither low nor high $\tan\beta$[11]. However, recent analyses[12,13] have shown that the decay mode $H^+ \to \tau^+\nu$, indeed dominant for light charged Higgs bosons below the top threshold for any accessible $\tan\beta$[14], provides an excellent signature for a heavy charged Higgs boson in searches at the LHC. The discover region for $H^{\pm}$ is far greater than had been thought for a large range of the $(m_{H^{\pm}}, \tan\beta)$ parameter space, extending beyond $m_{H^{\pm}} \sim 1$TeV and down to at least $\tan\beta \sim 3$, and potentially to $\tan\beta \sim 1.5$, assuming the latest results for the SM parameters and parton distribution functions as well as using kinematic selection techniques and the tau polarization analysis[13]. Of course, it is just a theoretical analysis and no experimental simulation has been performed to make the statement very reliable so far.

Since the contributions to the $W^{\pm}H^{\mp}$ production cross section due to $b\bar{b}$ annihilation at the tree level are greater than ones due to gg fusion which proceeds at one-loop, it is important to calculate the one-loop radiative corrections to the $W^{\pm}H^{\mp}$ production via $b\bar{b}$ annihilation for more accurate theoretical predictions for the cross sections. In this paper we present the calculations of the $O(\alpha_{ew}m_{t(b)}^2/m_W^2)$ and $O(\alpha_{ew}m_{t(b)}^4/m_W^4)$ supersymmetric(SUSY) electroweak(EW) corrections to this $W^{\pm}H^{\mp}$ associated production process at the LHC in the MSSM. These corrections arise from the quantum effects which are induced by potentially large Yukawa couplings from the Higgs sector and the chargino-top(bottom)-sbottom(stop) couplings, neutralino- top(bottom)-stop(sbottom) couplings and charged Higgs-stop-sbottom couplings which will contribute at the $O(\alpha_{ew}m_{t(b)}^4/m_W^4)$ to the self-energy of the charged Higgs boson. The relevant QCD corrections are expected to be larger, but not yet available.

The arrangement of this paper is as follows. In Sec.II we give the analytic results. In Sec.III we present some numerical examples and discuss the implications of our results. Some notations used in this paper and the lengthy expressions of the form factors are summarized in Appendix A, B.

3.2 Calculations and formulas

The Feynman diagrams for the charged Higgs boson production via $b(p_1)\bar{b}(p_2) \to W^{\pm}(k)H^{\mp}(p_3)$, which include the SUSY EW corrections to the process, are shown in Fig.1 and Fig.2. We carried out the calculation in the t'Hooft-Feynman gauge and used dimensional reduction, which preserves supersymmetry, for regularization of the ultraviolet divergences in the virtual loop corrections using the on-mass-shell renormalization scheme[15], in which the fine-structure constant α_{ew} and physical masses are chosen to be the renormalized parameters, and finite parts of the counterterms are fixed by the renormalization conditions. The coupling constant g is related to the input parameters e, m_W, and m_Z via $g^2 = e^2/s_w^2$ and $s_w^2 = 1 - m_W^2/m_Z^2$. As far as the parameters β and α, for the MSSM we are considering, they have to be renormalized, too. In the MSSM they are not independent. Nevertheless, we follow the approach of Mendez and Pomarol[16] in which they consider them as independent renormalized parameters and fixed the corresponding renormalization constants by a renormalization condition that the on-mass-shell $H^+\bar{l}\nu_l$ and $h\bar{l}l$ couplings keep the forms of Eq.(3) of Ref.[16] to all order of perturbation theory.

We define the Mandelstam variables as

$$
\begin{aligned}
\hat{s} &= (p_1+p_2)^2 = (k+p_3)^2, \\
\hat{t} &= (p_1-k)^2 = (p_2-p_3)^2, \\
\hat{u} &= (p_1-p_3)^2 = (p_2-k)^2.
\end{aligned}
\tag{1}
$$

The relevant renormalization constants are defined as

$$
\begin{aligned}
& m_{W0}^2 = m_W^2 + \delta m_W^2, \quad m_{Z0}^2 = m_Z^2 + \delta m_Z^2, \\
& \tan\beta_0 = (1+\delta Z_\beta)\tan\beta, \\
& \sin\alpha_0 = (1+\delta Z_\alpha)\sin\alpha, \\
& W_0^{\pm\mu} = (1+\delta Z_W)^{1/2} W^{\pm\mu} + i Z_{H^\pm W^\pm}^{1/2}\partial^\mu H^\mp, \\
& H_0^\pm = (1+\delta Z_{H^\pm})^{1/2} H^\pm, \\
& Z_0^\mu = (1+\delta Z_Z)^{1/2} Z^\mu + i Z_{ZA}^{1/2}\partial^\mu A, \\
& A_0 = (1+\delta Z_A)^{1/2} A, \\
& H_0 = (1+\delta Z_H)^{1/2} H + Z_{Hh}^{1/2} h, \\
& h_0 = (1+\delta Z_h)^{1/2} h + Z_{hH}^{1/2} H.
\end{aligned}
\tag{2}
$$

Taking into account the $O(\alpha_{ew} m_{t(b)}^2/m_W^2)$ and $O(\alpha_{ew} m_{t(b)}^4/m_W^4)$ SUSY EW corrections, the renormalized amplitude for $b\bar{b} \to W^- H^+$ can be written as

$$
\begin{aligned}
M_{ren} = {} & M_0^{(s)} + M_0^{(t)} + [\delta\hat{M}^{V_1(s)} + \delta\hat{M}^{S(s)} + \delta\hat{M}^{V_2(s)}](H_i) + [\delta\hat{M}^{V_1(s)} \\
& + \delta\hat{M}^{S(s)} + \delta\hat{M}^{V_2(s)}](A) + \delta\hat{M}^{V_1(t)} + \delta\hat{M}^{S(t)} + \delta\hat{M}^{V_2(t)} + \delta M^{box},
\end{aligned}
\tag{3}
$$

where $M_0^{(s)}$ and $M_0^{(t)}$ are the tree-level amplitudes arising from Fig.1(a) and Fig.1(b),

respectively, which are given by

$$M_0^{(s)} = -i\sum_i \frac{gh_b\alpha_{2i}\varphi_{11}}{\sqrt{2}(\hat{s}-m_{H_i}^2)}\sum_{j=1}^{4}M_j + \frac{igh_b\beta_{12}}{\sqrt{2}(\hat{s}-m_A^2)}(M_1-M_2+M_3-M_4) \quad (4)$$

and

$$M_0^{(t)} = \frac{ig}{\sqrt{2}(\hat{t}-m_t^2)}(2h_b\beta_{12}M_2 - h_bm_b\beta_{12}M_5 + h_tm_t\beta_{11}M_6 - h_b\beta_{12}M_{12}). \quad (5)$$

Here $h_b \equiv gm_b/\sqrt{2}m_W\cos\beta$ and $h_t \equiv gm_t/\sqrt{2}m_W\sin\beta$ are the Yukawa couplings from the bottom and top quarks, p_1 and p_2 denote the momentum of incoming quarks b and $\bar{b}$, respectively, while k and p_3 are used for the outgoing W^- Boson and H^+ Boson, respectively. The notations α_{ij}, β_{ij} and φ_{ij} used in the above expressions are defined in Appendix A, and H_i stands for Higgs Bosons h with $i=1$ and H with $i=2$. M_i are the standard matrix elements, which are defined by

$$\begin{aligned}
M_1 &= \bar{v}(p_2)P_Ru(p_1)p_1\cdot\varepsilon(k),\\
M_2 &= \bar{v}(p_2)P_Lu(p_1)p_1\cdot\varepsilon(k),\\
M_3 &= \bar{v}(p_2)P_Ru(p_1)p_2\cdot\varepsilon(k),\\
M_4 &= \bar{v}(p_2)P_Lu(p_1)p_2\cdot\varepsilon(k),\\
M_5 &= \bar{v}(p_2)\not{\varepsilon}(k)P_Ru(p_1),\\
M_6 &= \bar{v}(p_2)\not{\varepsilon}(k)P_Lu(p_1),\\
M_7 &= \bar{v}(p_2)\not{\varepsilon}(k)P_Ru(p_1)p_1\cdot\varepsilon(k),\\
M_8 &= \bar{v}(p_2)\not{\varepsilon}(k)P_Lu(p_1)p_1\cdot\varepsilon(k),\\
M_9 &= \bar{v}(p_2)\not{\varepsilon}(k)P_Ru(p_1)p_2\cdot\varepsilon(k),\\
M_{10} &= \bar{v}(p_2)\not{\varepsilon}(k)P_Lu(p_1)p_2\cdot\varepsilon(k),\\
M_{11} &= \bar{v}(p_2)\not{k}\not{\varepsilon}(k)P_Ru(p_1),\\
M_{12} &= \bar{v}(p_2)\not{k}\not{\varepsilon}(k)P_Lu(p_1),
\end{aligned} \quad (6)$$

where $P_{L,R} \equiv (1\mp\gamma_5)/2$. The vertex and self-energy corrections to the tree-level process are included in $\delta\hat{M}^{V,S}$, which are given by

$$\begin{aligned}
\delta\hat{M}^{V_1(s)}(H_i) = &-\frac{igh_b}{\sqrt{2}}\{\sum_{i=1,2}\frac{\alpha_{2i}\varphi_{i1}}{\hat{s}-m_{H_i}^2}[\frac{\delta h_b}{h_b}+\frac{1}{2}\delta Z_L^b+\frac{1}{2}\delta Z_R^b+\frac{1}{2}\delta Z_{H_i}]\\
&+\frac{\sin(\beta-\alpha)\sin\alpha}{\hat{s}-m_H^2}(\tan\alpha\delta Z_\alpha + Z_{hH}^{1/2}) - \frac{\cos(\beta-\alpha)}{\hat{s}-m_h^2}(\sin\alpha\delta Z_\alpha\\
&-\cos\alpha Z_{Hh}^{1/2})\}\sum_{j=1}^{4}M_j + \delta M^{V_1(s)}(H),\\
\delta\hat{M}^{V_1(s)}(A) = &-\frac{igh_b\sin\beta}{\sqrt{2}(\hat{s}-m_A^2)}[\frac{\delta h_b}{h_b}+\cos^2\beta\delta Z_\beta+\frac{1}{2}\delta Z_L^b+\frac{1}{2}\delta Z_R^b+\frac{1}{2}\delta Z_A
\end{aligned}$$

$$
\begin{aligned}
& +\frac{im_W}{\tan\beta\cos\theta_W} Z_{hH}^{1/2}](M_1 - M_2 + M_3 - M_4) + \delta M^{V_1(s)}(A), \\
\delta\hat{M}^{S(s)}(H_i) = & \frac{igh_b}{\sqrt{2}} \sum_{i=1,2} \frac{\alpha_{2i}\varphi_{i1}}{(\hat{s}-m_{H_i}^2)^2} [\delta m_{H_i}^2 - (\hat{s}-m_{H_i}^2)\delta Z_{H_i} - (\hat{s} \\
& -m_H^2) Z_{Hh}^{1/2} - (\hat{s}-m_h^2) Z_{hH}^{1/2}] \sum_{j=1}^{4} M_j + \delta M^{S(s)}(H), \\
\delta\hat{M}^{S(s)}(A) = & \frac{igh_b\sin\beta}{\sqrt{2}(\hat{s}-m_A^2)} [\delta m_A^2 - (\hat{s}-m_A^2)\delta Z_A](M_1 - M_2 + M_3 - M_4) \\
& +\delta M^{S(s)}(A), \\
\delta\hat{M}^{V_2(s)}(H_i) = & -\frac{igh_b}{\sqrt{2}} \{ \sum_{i=1,2} \frac{\alpha_{2i}\varphi_{i1}}{\hat{s}-m_{H_i}^2} (\frac{\delta g}{g} + \frac{1}{2}\delta Z_{W^-} + \frac{1}{2}\delta Z_{H^+} + \frac{1}{2} Z_{H_i}) \\
& -\frac{\cos\alpha\cos(\beta-\alpha)}{\hat{s}-m_H^2} (\sin\beta\cos\beta\delta Z_\beta - \tan\alpha\delta Z_\alpha - Z_{hH}^{1/2} \\
& +m_W Z_{HW}^{1/2}) + \frac{\sin\alpha\sin(\beta-\alpha)}{\hat{s}-m_h^2} (\sin\beta\cos\beta\delta Z_\beta \\
& -\tan\alpha\delta Z_\alpha + Z_{Hh}^{1/2} + m_W Z_{HW}^{1/2}) \} \sum_{j=1}^{4} M_j + \delta M^{V_2(s)}(H), \\
\delta\hat{M}^{V_2(s)}(A) = & -\frac{igh_b\sin\beta}{\sqrt{2}(\hat{s}-m_A^2)} [\frac{\delta g}{g} + \frac{1}{2}\delta Z^A + \frac{1}{2}\delta Z_{H^+} \\
& +\frac{1}{2}\delta Z_{W^-}](M_1 - M_2 + M_3 - M_4) + \delta M^{V_2(s)}(A), \\
\delta\hat{M}^{V_1(t)} = & \frac{ig}{\sqrt{2}(\hat{t}-m_t^2)} (2h_b\beta_{12}M_2 - h_b m_b\beta_{12}M_5 + h_t m_t\beta_{11}M_6 \\
& -h_b\beta_{12}M_{12})(\frac{\delta g}{g} + \frac{1}{2}\delta Z_L^t + \frac{1}{2}\delta Z_L^b + \frac{1}{2}\delta Z_{W^-}) + \delta M^{V_1(t)}, \\
\delta\hat{M}^{S(t)} = & \frac{ig}{\sqrt{2}(\hat{t}-m_t^2)^2} [(2m_t^2\frac{\delta m_t}{m_t} + m_t^2\delta Z_L^t - \hat{t}\delta Z_L^t)(2h_b\beta_{12}M_2 \\
& -h_b m_b\beta_{12}M_5 - h_t\beta_{12}M_{12} + \frac{1}{2}h_t m_t\beta_{11}M_6) + \frac{1}{2}(2\hat{t}\frac{\delta m_t}{m_t} \\
& +m_t^2\delta Z_R^t - \hat{t}\delta Z_R^t) h_t m_t\beta_{11}M_6] + \delta M^{S(t)}, \\
\delta\hat{M}^{V_2(t)} = & \frac{ig^2}{2m_W(\hat{t}-m_t^2)} [m_t^2\cot\beta(\frac{\delta h_t}{h_t} - \cos^2\beta\delta Z_\beta + \frac{1}{2}\delta Z_L^b + \frac{1}{2}\delta Z_R^t \\
& +\frac{1}{2}\delta Z_{H^+} + \frac{m_W}{\cot\beta} Z_{HW}^{1/2}) M_6 + m_b\tan\beta(\frac{\delta h_b}{h_b} + \sin^2\beta\delta Z_\beta + \frac{1}{2}\delta Z_L^t \\
& +\frac{1}{2}\delta Z_R^b + \frac{1}{2}\delta Z_{H^+} - \frac{m_W}{\tan\beta} Z_{HW}^{1/2})(2M_2 - M_{12} - m_b M_5)] + \delta M^{V_2(t)}, \quad (7)
\end{aligned}
$$

with

$$\begin{aligned}
\frac{\delta g}{g} &= \frac{\delta e}{e} + \frac{1}{2}\frac{\delta m_Z^2}{m_Z^2} - \frac{1}{2}\frac{\delta m_Z^2 - \delta m_W^2}{m_Z^2 - m_W^2}, \\
\frac{\delta h_b}{h_b} &= \frac{\delta g}{g} + \frac{\delta m_b}{m_b} - \frac{1}{2}\frac{\delta m_W^2}{m_W^2} + \cos^2\beta\delta Z_\beta, \\
\frac{\delta h_t}{h_t} &= \frac{\delta g}{g} + \frac{\delta m_t}{m_t} - \frac{1}{2}\frac{\delta m_W^2}{m_W^2} - \sin^2\beta\delta Z_\beta, \\
\delta Z_\beta &= -\frac{\delta g}{g} + \frac{1}{2}\frac{\delta m_W^2}{m_W^2} - \frac{1}{2}\delta Z_{H^+} - \frac{m_W}{\tan\beta} Z_{HW}^{1/2}, \\
\delta Z_\alpha &= -\frac{\delta g}{g} + \frac{1}{2}\frac{\delta m_W^2}{m_W^2} - \frac{1}{2}\delta Z_h - \cot\alpha Z_{Hh}^{1/2} - \sin^2\beta\delta Z_\beta.
\end{aligned} \tag{8}$$

The $\delta e/e$ appearing in Eq.(8) does not contain the $O(\alpha_{ew} m_{t(b)}^2/m_W^2)$ corrections and needs not be considered in our calculations. And $\delta M^{V_1(s)}(H_i)$, $\delta M^{V_1(s)}(A)$, $\delta M^{S(s)}(H_i)$, $\delta M^{S(s)}(A)$, $\delta M^{V_2(s)}(H_i)$, $\delta M^{V_2(s)}(A)$, $\delta M^{V_1(t)}$, $\delta M^{S(t)}$, $\delta M^{V_2(t)}$ and δM^{box} represent the irreducible corrections arising, respectively, from the $b\bar{b}H(h)$ vertex diagrams shown in Fig.1$(c)-1(d)$, the $b\bar{b}A$ vertex diagrams shown in Fig.1$(c)-1(d)$, the H and h boson self-energy diagrams in Fig.1$(i)-1(k)$, the A boson self-energy diagrams shown in Fig.1$(i)-1(k)$, the $H(h)W^-H^+$ vertex diagrams shown in Fig.1$(f)-1(h)$, the AW^-H^+ vertex diagrams shown in Fig.1$(f)-1(h)$, the btW^- vertex diagrams Fig.1$(l)-1(o)$, the top quark self-energy diagrams Fig.1(r), the $t\bar{b}H^+$ vertex diagrams Fig.1$(p)-1(q)$, and the box diagrams Fig.1$(s)-1(x)$. All above $\delta M^{V,S}$ and δM^{box} can be written in the form

$$\delta M^{V,S,box} = i\sum_{i=1}^{12} f_i^{V,S,box} M_i, \tag{9}$$

where the $f_i^{V,S,box}$ are form factors, which are given explicitly in Appendix B.

Calculating the self-energy diagrams in Fig.2, we can get the explicit expressions of all the renormalization constants as following:

$$\begin{aligned}
\frac{\delta m_t}{m_t} &= \sum_i \frac{-h_t^2}{32\pi^2}[\alpha_{1i}^2(-B_0^{ttH_i} + B_1^{ttH_i}) + \beta_{1i}^2(B_0^{ttA_i} + B_1^{ttA_i})] \\
&- \sum_i \frac{1}{32\pi^2 m_t}[(h_t^2 m_t \beta_{1i}^2 + h_b^2 m_b \beta_{2i}^2)B_1^{tbH_i^+} + 2h_b h_t \beta_{1i}\beta_{2i} B_0^{tbH_i^+}] \\
&+ \sum_{i,j} \frac{h_t^2}{32\pi^2 m_t}[m_t|N_{j4}|^2(B_0^{t\tilde{t}_i\tilde{\chi}_j^0} + B_1^{t\tilde{t}_i\tilde{\chi}_j^0}) + m_{\tilde{\chi}_j^0}\theta_{i1}^t\theta_{i2}^t(N_{j4}^2 + N_{j4}^{*2})B_0^{t\tilde{t}_i\tilde{\chi}_j^0}] \\
&+ \sum_{i,j} \frac{1}{32\pi^2 m_t}\{m_t[h_t^2(\theta_{i1}^b)^2|V_{j1}|^2 + h_b^2(\theta_{i2}^b)^2|U_{j2}|^2](B_0^{t\tilde{b}_i\tilde{\chi}_j^+} + B_1^{t\tilde{b}_i\tilde{\chi}_j^+}) \\
&+ h_b h_t m_{\tilde{\chi}_j^+}\theta_{i1}^b\theta_{i2}^b(U_{j2}V_{j2} + U_{j2}^* V_{j2}^*)B_0^{t\tilde{b}_i\tilde{\chi}_j^+}\},
\end{aligned}$$

$$
\begin{aligned}
\delta Z_L^t &= \sum_i \frac{h_b^2\beta_{2i}^2}{16\pi^2}B_1^{tbH_i^+} - \sum_{i,j}\frac{h_t^2(\theta_{i2}^t)^2}{16\pi^2}|N_{j4}|^2(B_0^{t\tilde{t}_i\tilde{\chi}_j^0} + B_1^{t\tilde{t}_i\tilde{\chi}_j^0}) \\
&\quad -\sum_{i,j}\frac{h_b^2(\theta_{i2}^b)^2}{16\pi^2}|U_{j2}|^2(B_0^{t\tilde{b}_i\tilde{\chi}_j^+} + B_1^{t\tilde{b}_i\tilde{\chi}_j^+}) + \delta^t, \\
\delta Z_R^t &= \sum_i \frac{h_t^2\beta_{1i}^2}{16\pi^2}B_1^{tbH_i^+} - \sum_{i,j}\frac{h_t^2(\theta_{i1}^t)^2}{16\pi^2}|N_{j4}|^2(B_0^{t\tilde{t}_i\tilde{\chi}_j^0} + B_1^{t\tilde{t}_i\tilde{\chi}_j^0}) \\
&\quad -\sum_{i,j}\frac{h_t^2(\theta_{i1}^b)^2}{16\pi^2}|V_{j2}|^2(B_0^{t\tilde{b}_i\tilde{\chi}_j^+} + B_1^{t\tilde{b}_i\tilde{\chi}_j^+}) + \delta^t, \\
\delta^t &= \sum_i \frac{h_t^2}{32\pi^2}\{\alpha_{1i}^2[B_1^{ttH_i} - 2m_t^2(B_0^{ttH_i} - B_1^{ttH_i})] + \beta_{1i}^2[B_1^{ttA_i} + 2m_t^2(B_0^{ttA_i} + B_1^{ttA_i})]\} \\
&\quad +\sum_i \frac{m_t}{16\pi^2}[m_t(h_t^2\beta_{1i}^2 + h_b^2\beta_{2i}^2)B_0^{'tbH_i^+} + 2h_bh_tm_b\beta_{1i}\beta_{2i}B_0^{'tbH_i^+}] \\
&\quad -\sum_{i,j}\frac{h_t^2m_t}{16\pi^2}[m_t|N_{j4}|^2(B_0^{'t\tilde{t}_i\tilde{\chi}_j^0} + B_1^{'t\tilde{t}_i\tilde{\chi}_j^0}) + m_{\tilde{\chi}_j^0}\theta_{i1}^t\theta_{i2}^t(N_{j4}^2 + N_{j4}^{*2})B_0^{'t\tilde{t}_i\tilde{\chi}_j^0}] \\
&\quad -\sum_{i,j}\frac{m_t}{16\pi^2}\{m_t[h_t^2(\theta_{i1}^b)^2|V_{j1}|^2 + h_b^2(\theta_{i2}^b)^2|U_{j2}|^2](B_0^{'t\tilde{b}_i\tilde{\chi}_j^+} + B_1^{'t\tilde{b}_i\tilde{\chi}_j^+}) \\
&\quad +h_bh_tm_{\tilde{\chi}_j^+}\theta_{i1}^b\theta_{i2}^b(U_{j2}V_{j2} + U_{j2}^*V_{j2}^*)B_0^{'t\tilde{b}_i\tilde{\chi}_j^+}\}, \\
\delta m_W^2 &= \frac{g^2}{16\pi^2}\{(m_b^2 - m_t^2)(1 + \frac{m_b^2 - m_t^2 - 2m_W^2}{2m_W^2}B_0^{0bt}) - 2m_t^2B_0^{0tt} \\
&\quad -\frac{1}{2m_W^2}[(m_b^2 - m_t^2)^2 + (m_b^2 + m_t^2)m_W^2]B_0^{Wbt}\}, \\
\delta Z_W &= \frac{g^2}{32\pi^2m_W^2}\{\frac{(m_b^2 - m_t^2)^2}{m_W^2}(B_0^{0bt} - B_0^{Wbt}) + [(m_b^2 - m_t^2)^2 \\
&\quad +(m_b^2 + m_t^2)m_W^2]B_0^{'Wbt}\}, \\
\delta m_Z^2 &= \frac{g^2s_W^2}{18c_W^2\pi^2}[\frac{m_b^2}{2}(3 - 2s_W^2)(B_0^{Zbb} + B_0^{0bb}) - m_t^2(3 - 4s_W^2)(B_0^{Ztt} - B_0^{0tt})] \\
&\quad +\frac{g^2}{32c_W^2\pi^2}[m_b^2(B_0^{Zbb} - 2B_0^{0bb}) - m_t^2(B_0^{Ztt} + 2B_0^{0tt})], \\
\delta Z_{H^+} &= \frac{3}{16\pi^2}[2(h_t^2\beta_{11}^2 + h_b^2\beta_{21}^2)(B_1^{H^+bt} + m_b^2B_0^{'H^+bt} + m_{H^+}^2B_1^{'H^+bt}) \\
&\quad -4h_bh_tm_bm_t\beta_{11}\beta_{21}B_0^{'H^+bt} + \sum_{i,j,i',j'}(\theta_{ii'}^b)^2(\theta_{jj'}^t)^2(h_b\Theta_{i'j'1}^5 + h_t\Theta_{i'j'1}^6)^2B_0^{'H^+\tilde{b}_i\tilde{t}_j}], \\
\delta m_{H_k}^2 &= \frac{3}{16\pi^2}\{-2h_t^2\alpha_{1k}^2[m_t^2(1 + B_0^{0tt} + 2B_0^{H_ktt}) + m_{H_k}^2B_1^{H_ktt}] - 2h_b^2\alpha_{2k}^2[m_b^2(1 \\
&\quad +B_0^{0bb} + 2B_0^{H_kbb}) + m_{H_k}^2B_1^{H_kbb}] + \sum_{i,j,i',j'}[(h_t\theta_{ii'}^t\theta_{jj'}^t\Theta_{i'j'k}^1)^2B_0^{H_k\tilde{t}_i\tilde{t}_j}
\end{aligned}
$$

$$
\begin{aligned}
&+(h_b\theta^b_{ii'}\theta^b_{jj'}\Theta^2_{i'j'k})^2B_0^{H_k\tilde{b}_i\tilde{b}_j}] + \sum_i h_b^2 m^2_{\tilde{b}_i}\alpha^2_{2k}(1+B_0^{0\tilde{b}_i\tilde{b}_i}) \\
&+\sum_i h_t^2 m^2_{\tilde{t}_i}\alpha^2_{1k}(1+B_0^{0\tilde{t}_i\tilde{t}_i})\}, \\
\delta Z_{H_k} &= \frac{3}{16\pi^2}\{2h_t^2\alpha^2_{1k}(B_1^{H_k tt}+2m_t^2 B_0^{'H_k tt}+m^2_{H_k}B_1^{'H_k tt}) + 2h_b^2\alpha^2_{2k}(B_1^{H_k bb} \\
&+2m_b^2 B_0^{'H_k bb}+m^2_{H_k}B_1^{'H_k bb}) + \sum_{i,j,i',j'}[(h_t\theta^t_{ii'}\theta^t_{jj'}\Theta^1_{i'j'k})^2 B_0^{'H_k\tilde{t}_i\tilde{t}_j} \\
&+(h_b\theta^b_{ii'}\theta^b_{jj'}\Theta^2_{i'j'k})^2B_0^{'H_k\tilde{b}_i\tilde{b}_j}]\}, \\
\delta m^2_{A_k} &= \frac{3}{16\pi^2}\{2h_t^2\beta^2_{1k}[m_t^2(1+B_0^{0tt})+m^2_{A_k}B_1^{A_k tt}] + 2h_b^2\beta^2_{2k}[m_b^2(1+B_0^{0bb}) \\
&+m^2_{A_k}B_1^{A_k bb}] - \sum_{i,j,i',j'}[(h_t\theta^t_{ii'}\theta^t_{jj'}\Theta^3_{i'j'k})^2B_0^{A_k\tilde{t}_i\tilde{t}_j} + (h_b\theta^b_{ii'}\theta^b_{jj'}\Theta^4_{i'j'k})^2B_0^{A_k\tilde{b}_i\tilde{b}_j}] \\
&+\sum_i h_b^2 m^2_{\tilde{b}_i}\beta^2_{2k}(1+B_0^{0\tilde{b}_i\tilde{b}_i}) + \sum_i h_t^2 m^2_{\tilde{t}_i}\beta^2_{1k}(1+B_0^{0\tilde{t}_i\tilde{t}_i})\}, \\
\delta Z_{A_k} &= \frac{3}{16\pi^2}\{2h_t^2\beta^2_{1k}(B_1^{A_k tt}+m^2_{A_k}B_1^{'A_k tt}) + 2h_b^2\beta^2_{2k}(B_1^{A_k bb}+m^2_{A_k}B_1^{'A_k bb}) \\
&-\sum_{i,j,i',j'}[(h_t\theta^t_{ii'}\theta^t_{jj'}\Theta^3_{i'j'k})^2B_0^{'A_k\tilde{t}_i\tilde{t}_j} + (h_b\theta^b_{ii'}\theta^b_{jj'}\Theta^4_{i'j'k})^2B_0^{'A_k\tilde{b}_i\tilde{b}_j}]\}, \\
Z_{H^+W} &= \frac{-3g}{16\sqrt{2}\pi^2 m^2_{H^+}m^2_W}[(h_t m_t\beta_{11}+h_b m_b\beta_{12})((m_b^2-m_t^2)(B_0^{0bt}-B_0^{H^+bt}) - m^2_{H^+}B_0^{H^+bt}) \\
&+\sum_{i,j,i',j'}\theta^b_{i1}\theta^b_{ii'}\theta^t_{j1}\theta^t_{jj'}(h_b\Theta^5_{i'j'1}+h_t\Theta^6_{i'j'1})(m^2_{\tilde{t}_j}-m^2_{\tilde{b}_i})(B_0^{0\tilde{b}_i\tilde{t}_j}-B_0^{H^+\tilde{b}_i\tilde{t}_j})], \\
Z_{AZ} &= \frac{-i3gc_W}{16\sqrt{2}\pi^2 m^2_W}(h_t m_t\beta_{11}B_0^{Att} - h_b m_b\beta_{12}B_0^{Abb}) \\
&+\frac{igc_W}{32\pi^2 m_A^2 m_W^2}\sum_{i,j,i',j'}\{h_b\theta^b_{ii'}\theta^b_{jj'}\Theta^4_{j'i'1}[(3-2s_W^2)\theta^b_{i1}\theta^b_{j1}-2s_W^2\theta^b_{i2}\theta^b_{j2}](m^2_{\tilde{b}_i}-m^2_{\tilde{b}_j})(B_0^{0\tilde{b}_i\tilde{b}_j} \\
&-B_0^{A\tilde{b}_i\tilde{b}_j}) - h_t\theta^t_{ii'}\theta^t_{jj'}\Theta^3_{j'i'1}[(3-4s_W^2)\theta^t_{i1}\theta^t_{j1}-4s_W^2\theta^t_{i2}\theta^t_{j2}](m^2_{\tilde{t}_i}-m^2_{\tilde{t}_j})(B_0^{0\tilde{t}_i\tilde{t}_j}-B_0^{A\tilde{t}_i\tilde{t}_j})\}, \\
Z^{1/2}_{hH} &= \frac{3\alpha_{11}\alpha_{12}}{16\pi^2(m_h^2-m_H^2)}[2m_b^2(1+B_0^{0bb}+2B_0^{Hbb}) - 2m_t^2(1+B_0^{0tt}+2B_0^{Htt}) \\
&-m_H^2(B_0^{Hbb}-B_0^{Htt})] \\
&+\frac{3}{16\pi^2(m_h^2-m_H^2)}\sum_{i,j,i',j'}[(h_b\theta^b_{ii'}\theta^b_{jj'})^2\Theta^2_{i'j'1}\Theta^2_{i'j'2}B_0^{H\tilde{b}_i\tilde{b}_j} + (h_t\theta^t_{ii'}\theta^t_{jj'})^2\Theta^1_{i'j'1}\Theta^1_{i'j'2}B_0^{H\tilde{t}_i\tilde{t}_j}] \\
&-\frac{3\alpha_{11}\alpha_{12}}{16\pi^2(m_h^2-m_H^2)}\sum_i[h_b^2 m^2_{\tilde{b}_i}(1+B_0^{0\tilde{b}_i\tilde{b}_i}) + h_t^2 m^2_{\tilde{t}_i}(1+B_0^{0\tilde{t}_i\tilde{t}_i})], \\
Z^{1/2}_{Hh} &= Z^{1/2}_{hH}|_{h\leftrightarrow H}, \qquad (10)
\end{aligned}
$$

with

$$B_n^{ijk} = (-1)^n\{\frac{\Delta}{n+1} - \int_0^1 dyy^n \ln[\frac{m_i^2 y(y-1) + m_j^2(1-y) + m_k^2 y}{\mu^2}]\}, \quad (11)$$

$$B_n^{\prime ijk} = (-1)^n \int_0^1 dy \frac{y^{n+1}(1-y)}{m_i^2 y(y-1) + m_j^2(1-y) + m_k^2 y}. \quad (12)$$

The notations θ_{ij}^t and θ_{ij}^b used in above expressions are defined in Appendix A. A_i stands for A with $i = 1$ and G^0 with $i = 2$. H_i^+ stands for H^+ with $i = 1$ and G^+ with $i = 2$. $\frac{\delta m_b}{m_b}$, δZ_L^b, δZ_R^b can be obtained, respectively, from $\frac{\delta m_t}{m_t}$, δZ_L^t, δZ_R^t by the transformation:

$$h_b \leftrightarrow h_t, m_b \leftrightarrow m_t, m_{\tilde{b}_i} \leftrightarrow m_{\tilde{t}_i}, \alpha_{1i} \leftrightarrow \alpha_{2i}, \beta_{1i} \leftrightarrow \beta_{2i}, \theta_{ij}^b \leftrightarrow \theta_{ij}^t, N_{i4} \to N_{i3}, U_{i2} \to V_{i2}.$$

The corresponding amplitude squared is

$$\overline{\sum}|M_{ren}|^2 = \overline{\sum}|M_0^{(s)} + M_0^{(t)}|^2 + 2Re\overline{\sum}[(\sum \delta M)(M_0^{(s)} + M_0^{(t)})^\dagger]. \quad (13)$$

The cross section for the process $b\bar{b} \to W^{\pm}H^{\mp}$ is

$$\hat{\sigma} = \int_{\hat{t}_-}^{\hat{t}_+} \frac{1}{16\pi\hat{s}^2} \overline{\Sigma}|M_{ren}|^2 d\hat{t} \quad (14)$$

with

$$\hat{t}_{\pm} = \frac{m_W^2 + m_{H^-}^2 - \hat{s}}{2} \pm \frac{1}{2}\sqrt{(\hat{s} - (m_W + m_{H^-})^2)(\hat{s} - (m_W - m_{H^-})^2)}. \quad (15)$$

The total hadronic cross section for $pp \to b\bar{b} \to W^{\pm}H^{\mp}$ can be obtained by folding the subprocess cross section $\hat{\sigma}$ with the parton luminosity:

$$\sigma(s) = \int_{(m_W+m_{H^-})/\sqrt{s}}^1 dz \frac{dL}{dz} \hat{\sigma}(b\bar{b} \to W^{\pm}H^{\mp} \ \text{at} \ \hat{s} = z^2 s). \quad (16)$$

Here $\sqrt{s}$ and $\sqrt{\hat{s}}$ are the CM energies of the pp and $b\bar{b}$ states , respectively, and dL/dz is the parton luminosity, defined as

$$\frac{dL}{dz} = 2z \int_{z^2}^1 \frac{dx}{x} f_{b/P}(x,\mu) f_{\bar{b}/P}(z^2/x,\mu), \quad (17)$$

where $f_{b/P}(x,\mu)$ and $f_{\bar{b}/P}(z^2/x,\mu)$ are the bottom and anti-bottom quark parton distribution functions, respectively.

3.3 Numerical results and conclusion

We now present some numerical results for the SUSY EW corrections to $W^{\pm}H^{\mp}$ associated production at the LHC. The SM input parameters in our calculations were taken to be $\alpha_{ew}(m_Z) = 1/128.8$, $m_W = 80.375$GeV and $m_Z = 91.1867$GeV[17], and $m_t = 175.6$GeV and $m_b = 4.7$GeV, which were taken according to Ref.[10] for comparison. We used the CTEQ5M parton distributions throughout the calculations[18]. The one-loop relations[19] between the Higgs boson masses $M_{h,H,A,H^{\mp}}$ and the parameters α and β in the MSSM were used, and m_{H^+} and β were chosen as the two independent input parameters. Other MSSM parameters were determined as follows:

(i) For the parameters M_1, M_2 and μ in the chargino and neutralino matrix, we take M_2 and μ as the input parameters, and then used the relation $M_1 = (5/3)(g'^2/g^2)M_2 \simeq 0.5M_2$[2] to determine M_1.

(ii) For the parameters $m^2_{\tilde{Q},\tilde{U},\tilde{D}}$ and $A_{t,b}$ in squark mass matrices

$$M^2_{\tilde{q}} = \begin{pmatrix} M^2_{LL} & m_q M_{LR} \\ m_q M_{RL} & M^2_{RR} \end{pmatrix} \tag{18}$$

with

$$\begin{aligned} M^2_{LL} &= m^2_{\tilde{Q}} + m^2_q + m^2_Z \cos 2\beta (I^{3L}_q - e_q \sin^2\theta_W), \\ M^2_{RR} &= m^2_{\tilde{U},\tilde{D}} + m^2_q + m^2_Z \cos 2\beta e_q \sin^2\theta_W, \\ M_{LR} = M_{RL} &= \begin{pmatrix} A_t - \mu\cot\beta & (\tilde{q} = \tilde{t}) \\ A_b - \mu\tan\beta & (\tilde{q} = \tilde{b}) \end{pmatrix}, \end{aligned} \tag{19}$$

to simplify the calculation we assumed $M_{\tilde{Q}} = M_{\tilde{U}} = M_{\tilde{D}}$ and $A_t = A_b$, and we used $M_{\tilde{Q}}$ and A_t as the input parameters except the numerical calculations as shown in Fig.6, where we took $m_{\tilde{t}_1}$, $m_{\tilde{b}_1}$ and $A_t = A_b$ as the input parameters.

Some typical numerical calculations of the Yukawa corrections and the genuine SUSY EW corrections are given in Fig.3-4 and Fig.5-9, respectively.

In Fig.3 we present the Yukawa corrections to the total cross sections relative to the tree-level values as a function of m_{H^+} for $\tan\beta = 1.5, 2, 6$ and 30. For $\tan\beta = 1.5$ and 2 the corrections decrease the total cross sections significantly, which exceed -6% for $m_{H^+} < 500$GeV and -12% for $m_{H^+} < 300$GeV. For $\tan\beta (= 6)$ these corrections also decrease the total cross sections, although relatively smaller, which exceed -2.5% for $m_{H^+} < 500$GeV and exceed -5% for $m_{H^+} < 250$GeV. But for high $\tan\beta (= 30)$ these corrections become positive, which increase the total cross sections slightly. Note that there are the peaks at $m_{H^+} = 180.3$GeV, which arise from the singularity of the charged Higgs boson wavefunction renormalization constant at the threshold point $m_{H^+} = m_t + m_b$.

In Fig.4 we show the Yukawa corrections as a function of $\tan\beta$ for $m_{H^+} = 100, 150, 200$ and 300GeV. For $\tan\beta < 4$ the corrections reduce the total cross sections by more than 10% with $m_{H^+} = 100, 150$ and 200GeV. With $m_{H^+} = 300$GeV the corrections are only

significant for $1 < \tan\beta < 5$. For high $\tan\beta(> 10)$ the corrections become negligibly small for all above m_{H^+} values.

Fig.5 gives the genuine SUSY EW corrections as a function of m_{H^+} for $\tan\beta = 1.5, 2, 6$ and 30, respectively, assuming $M_2 = 300$GeV, $\mu = -100$GeV, $A_t = A_b = 200$GeV, and $M_{\tilde{Q}} = M_{\tilde{U}} = M_{\tilde{D}} = 500$GeV. From this figure one sees that the corrections are very small and negligible, which is reasonable because the squark masses are now very large and also the couplings of the charged Higgs boson-squarks are small for the values of $A_{t,b}$, $M_{\tilde{Q},\tilde{U},\tilde{D}}$ and μ used in those numerical calculations. In contrast, in Fig.6 when we take the lighter sqarks masses: $m_{\tilde{t}_1} = 100$GeV and $m_{\tilde{b}_1} = 150$GeV, and put $A_t = A_b = 1$TeV, which are relatively larger, assuming $M_2 = 200$GeV, $\mu = 100$GeV and $M_{\tilde{Q}} = M_{\tilde{U}}$, the genuine SUSY EW corrections are enhanced significantly, especially for low $\tan\beta(= 1.5)$ and m_{H^+} below 250GeV, which can exceed -30%. But when $m_{H^+} > 250$GeV the corrections increase the cross sections, which can exceed 10%. For $\tan\beta = 6$ and 30 the corrections are at most 10% and become small with an increase of m_{H^+}. The sharp dips at $m_{H^+} = 250$GeV are again due to the singularity of the charged Higgs boson wavefunction renormalization constant at the threshold point $m_{H^+} = m_{\tilde{t}_1} + m_{\tilde{b}_1} = 250$GeV.

Fig.7, Fig.8 and Fig.9 give the genuine SUSY EW corrections versus $A_t = A_b$, $M_{\tilde{Q}} = M_{\tilde{U}} = M_{\tilde{D}}$ and μ, respectively, for $\tan\beta = 1.5$ and 30. In each figure we fixed $m_{H^+} = 200$GeV and $M_2 = 300$GeV.

Fig.7 shows that the corrections are negative for $\tan\beta = 1.5$ and positive for $\tan\beta = 30$, assuming $M_{\tilde{Q}} = M_{\tilde{U}} = M_{\tilde{D}} = 400$GeV and $\mu = 100$GeV. For both $\tan\beta = 1.5$ and 30 the magnitude of the corrections increases with increasing $A_t = A_b$. When $A_t = A_b = 1$TeV the corrections can reach -6% and 7.5% for $\tan\beta = 1.5$ and 30, respectively. Otherwise, when $A_t = A_b$ decrease to 100GeV, the corrections become negligibly small. This result is due to the fact that large values of $A_t = A_b$ not only enhance the couplings, but also give a large splitting between the masses of $\tilde{t}_1(\tilde{b}_1)$ and $\tilde{t}_2(\tilde{b}_2)$, and in consequence lighter $\tilde{t}_1$ and $\tilde{b}_1$.

Fig.8 also show that the corrections are negative for $\tan\beta = 1.5$ and positive for $\tan\beta = 30$, assuming $A_t = A_b = 500$GeV and $\mu = 100$GeV. When $M_{\tilde{Q},\tilde{U},\tilde{D}} = 250$GeV the corrections can reach -3.6% for $\tan\beta = 1.5$ and 7.3% for $\tan\beta = 30$. But the magnitude of the corrections drops below one percent when $M_{\tilde{Q},\tilde{U},\tilde{D}}$ increase to 750GeV. This is because for larger values of $M_{\tilde{Q},\tilde{U},\tilde{D}}$ the squarks have larger masses and their virtual effects decrease due to the decoupling effects.

In Fig.9 we present the genuine SUSY EW corrections as a function of μ, assuming $A_t = A_b = 500$GeV and $M_{\tilde{Q}} = M_{\tilde{U}} = M_{\tilde{D}} = 400$GeV. For $\tan\beta = 30$ the magnitude of the corrections increase with an increase of $|\mu|$, which varies from 0% to 5% when $|\mu|$ ranges between $0 \sim 500$GeV. For $\tan\beta = 1.5$ the corrections are relatively small and increase slowly from about 0% to 3.5% when μ ranges between -500GeV$\sim$ 500GeV. This result indicates that large values of μ and $\tan\beta$ can enhance the corrections significantly since the couplings become stronger.

In conclusion, we have calculated the $O(\alpha_{ew} m^2_{t(b)}/m^2_W)$ and $O(\alpha_{ew} m^4_{t(b)}/m^4_W)$ SUSY EW corrections to the cross sections for $W^{\pm}H^{\mp}$ associated production at the LHC in

the MSSM. The numerical results show that the Yukawa corrections arising from the Higgs sector can decrease the total cross sections significantly for low $\tan\beta(=1.5$ and 2) when $m_{H^+}(<300)$GeV, which exceed -12%. For high $\tan\beta$ the Yukawa corrections become negligibly small. The genuine SUSY EW corrections can increase or decrease the total cross sections depending on the SUSY parameters, which can exceed -25% for the favorable SUSY parameter values. We also show that the genuine SUSY EW corrections depend strongly on the choice of $\tan\beta$, A_t, $M_{\tilde{Q}}$ and μ. For large values of A_t, or large values of μ and $\tan\beta$, one can get much larger corrections. The correcan become very small, in contrast, for larger values of $M_{\tilde{Q}}$.

3.4 Appendix A

We present some notations used in this paper here. We introduce an angle $\varphi=\beta-\alpha$, and for each angle α, β, φ, θ^t or θ^b, we define

$$\alpha_{ij}=\begin{pmatrix}\cos\alpha & \sin\alpha\\ -\sin\alpha & \cos\alpha\end{pmatrix},\beta_{ij}=\begin{pmatrix}\cos\beta & \sin\beta\\ -\sin\beta & \cos\beta\end{pmatrix},\varphi_{ij}=\begin{pmatrix}\cos\varphi & \sin\varphi\\ -\sin\varphi & \cos\varphi\end{pmatrix},$$
$$\theta^t_{ij}=\begin{pmatrix}\cos\theta^t & \sin\theta^t\\ -\sin\theta^t & \cos\theta^t\end{pmatrix},\theta^b_{ij}=\begin{pmatrix}\cos\theta^b & \sin\theta^b\\ -\sin\theta^b & \cos\theta^b\end{pmatrix}$$

We define six matrix $\Theta^i_{jkl}, i=1-6$ for the couplings between squarks and Higgses:

$$\begin{aligned}
\Theta^1_{ij1}= & \frac{1}{\sqrt{2}}\begin{pmatrix}2m_t\cos\alpha & A_t\cos\alpha+\mu\sin\alpha\\ A_t\cos\alpha+\mu\sin\alpha & 2m_t\cos\alpha\end{pmatrix}\\
\Theta^1_{ij2}= & \frac{1}{\sqrt{2}}\begin{pmatrix}2m_t\sin\alpha & A_t\sin\alpha-\mu\cos\alpha\\ A_t\sin\alpha-\mu\cos\alpha & 2m_t\sin\alpha\end{pmatrix}\\
\Theta^2_{ij1}= & \frac{-1}{\sqrt{2}}\begin{pmatrix}2m_b\sin\alpha & A_b\sin\alpha+\mu\cos\alpha\\ A_b\sin\alpha+\mu\cos\alpha & 2m_b\sin\alpha\end{pmatrix}\\
\Theta^2_{ij2}= & \frac{1}{\sqrt{2}}\begin{pmatrix}2m_b\cos\alpha & A_b\cos\alpha-\mu\sin\alpha\\ A_b\cos\alpha-\mu\sin\alpha & 2m_b\cos\alpha\end{pmatrix}\\
\Theta^3_{ij1}= & \frac{1}{\sqrt{2}}\begin{pmatrix}0 & A_t\cos\beta+\mu\sin\beta\\ -A_t\cos\beta-\mu\sin\beta & 0\end{pmatrix}\\
\Theta^3_{ij2}= & \frac{1}{\sqrt{2}}\begin{pmatrix}0 & A_t\sin\beta-\mu\cos\beta\\ -A_t\sin\beta+\mu\cos\beta & 0\end{pmatrix}\\
\Theta^4_{ij1}= & \frac{1}{\sqrt{2}}\begin{pmatrix}0 & A_b\sin\beta+\mu\cos\beta\\ -A_b\sin\beta-\mu\cos\beta & 0\end{pmatrix}\\
\Theta^4_{ij2}= & \frac{1}{\sqrt{2}}\begin{pmatrix}0 & -A_b\cos\beta+\mu\sin\beta\\ A_b\cos\beta-\mu\sin\beta & 0\end{pmatrix}\\
\Theta^5_{ij1}= & \begin{pmatrix}m_b\sin\beta & 0\\ A_b\sin\beta+\mu\cos\beta & m_t\sin\beta\end{pmatrix}\\
\Theta^5_{ij2}= & \begin{pmatrix}-m_b\cos\beta & 0\\ -A_b\cos\beta+\mu\sin\beta & 0\end{pmatrix}
\end{aligned}$$

$$\Theta^6_{ij1} = \begin{pmatrix} m_t\cos\beta & A_t\cos\beta+\mu\sin\beta \\ 0 & m_b\cos\beta \end{pmatrix}$$
$$\Theta^6_{ij2} = \begin{pmatrix} m_t\sin\beta & A_t\sin\beta-\mu\cos\beta \\ 0 & 0 \end{pmatrix}$$

3.5 Appendix B

The form factors defined in Eq.(9) are the following:

$$\begin{aligned}
f_1^{V_1(s)}(H) =& \sum_{i,j}\frac{gh_b^3\alpha_{2i}^2\alpha_{2j}\varphi_{j1}}{32\sqrt{2}\pi^2(\hat{s}-m_{H_j}^2)}\{B_0^{bbH_i}+[4m_b^2C_0 \\
&+(4m_b^2+\hat{s})C_1](\hat{s},m_b^2,m_b^2,m_b^2,m_b^2,m_{H_i}^2)\} \\
&+\sum_{i,j}\frac{-gh_b^3\beta_{2i}^2\alpha_{2j}\varphi_{j1}}{32\sqrt{2}\pi^2(\hat{s}-m_{H_j}^2)}[B_0^{bbA_i}-(4m_b^2-\hat{s})C_1(\hat{s},m_b^2,m_b^2,m_b^2,m_b^2,m_{A_i}^2)] \\
&+\sum_{i,j}\frac{gh_t\alpha_{1j}\varphi_{j1}}{16\sqrt{2}\pi^2(\hat{s}-m_{H_j}^2)}\{-h_bh_t\beta_{1i}\beta_{2i}B_0^{btH_i^+}+[(h_t^2m_bm_t\beta_{1i}^2 \\
&+2h_bh_tm_t^2\beta_{1i}\beta_{2i}+h_b^2m_bm_t\beta_{2i}^2)C_0+(2h_t^2m_bm_t\beta_{1i}^2+h_bh_t\hat{s}\beta_{1i}\beta_{2i} \\
&+2h_b^2m_bm_t\beta_{2i}^2)C_1](\hat{s},m_b^2,m_b^2,m_t^2,m_t^2,m_{H_i^+}^2)\} \\
&+\sum_{i,j,k,l}\sum_{i',j'}\frac{gh_t\varphi_{l1}\theta^t_{ii'}\theta^t_{jj'}\Theta^1_{j'i'l}}{16\pi^2(\hat{s}-m_{H_l}^2)}[h_b^2m_b\theta^t_{i1}\theta^t_{j1}|U_{k2}|^2(C_0+C_1+C_2) \\
&+m_{\tilde{\chi}_k^+}h_bh_t\theta^t_{i2}\theta^t_{j1}U_{k2}V_{k2}C_0-h_t^2m_b\theta^t_{i2}\theta^t_{j2}|V_{j2}|^2C_1](\hat{s},m_b^2,m_b^2,m_{\hat{t}_i}^2,m_{\hat{t}_j}^2,m_{\tilde{\chi}_k^+}) \\
&+\sum_{i,j,k,l}\sum_{j',k'}\frac{gh_b^3\varphi_{i1}\theta^b_{jj'}\theta^b_{kk'}N_{l3}\Theta^2_{j'k'i}}{16\pi^2(\hat{s}-m_{H_i}^2)}[m_b\theta^b_{j1}\theta^b_{k1}N^*_{l3}(C_0+C_1+C_2) \\
&-m_b\theta^b_{j2}\theta^b_{k2}N^*_{l3}C_1+m_{\tilde{\chi}_l^0}\theta^b_{j1}\theta^b_{k2}N_{l3}C_0](\hat{s},m_b^2,m_b^2,m_{\hat{b}_j}^2,m_{\hat{b}_k}^2,m_{\tilde{\chi}_l^0}), \\
f_2^{V_1(s)}(H) =& f_1^{V_1(s)}(H)(h_b\theta^t_{n1}\leftrightarrow h_t\theta^t_{n2},\theta^b_{n1}\leftrightarrow\theta^b_{n2},U_{n2}\leftrightarrow V^*_{n2},N_{n3}\leftrightarrow N^*_{n3}), \\
f_3^{V_1(s)}(H) =& f_1^{V_1(s)}(H), \\
f_4^{V_1(s)}(H) =& f_2^{V_1(s)}(H); \\
f_i^{V_1(s)}(A) =& f_i^{V_1(s)}(A)_a+f_i^{V_1(s)}(A)_b,
\end{aligned}$$

where

$$\begin{aligned}
f_1^{V_1(s)}(A)_a =& \sum_{i,j,k}\sum_{i',j'}\frac{gh_t\theta^t_{ii'}\theta^t_{jj'}\Theta^3_{j'i'1}}{16\pi^2(\hat{s}-m_A^2)}[-h_b^2m_b\theta^t_{i1}\theta^t_{j1}|U_{j2}|^2(C_0+C_1+C_2) \\
&-m_{\tilde{\chi}_k^+}h_bh_t\theta^t_{i2}\theta^t_{j1}U_{k2}V_{k2}C_0+h_t^2m_b\theta^t_{i1}\theta^t_{j2}|V_{j2}|^2C_2](\hat{s},m_b^2,m_b^2,m_{\hat{t}_i}^2,m_{\hat{t}_j}^2,m_{\tilde{\chi}_k^+}) \\
&+\sum_{i,j,k}\sum_{i',j'}\frac{gh_b^3N_{k3}\theta^b_{ii'}\theta^b_{jj'}\Theta^4_{j'k'i}}{16\pi^2(\hat{s}-m_A^2)}[-m_b\theta^b_{i1}\theta^b_{j1}N^*_{k3}(C_1+C_2+C_3) \\
&+m_b\theta^b_{i2}\theta^b_{j1}N^*_{k3}C_1-m_{\tilde{\chi}_k^0}\theta^b_{j1}\theta^b_{i2}N_{k3}C_0](\hat{s},m_b^2,m_b^2,m_{\hat{b}_i}^2,m_{\hat{b}_j}^2,m_{\tilde{\chi}_k^0}), \\
f_2^{V_1(s)}(A)_a =& f_1^{V_1(s)}(A)_a(h_b\theta^t_{n1}\leftrightarrow h_t\theta^t_{n2},\theta^b_{n1}\leftrightarrow\theta^b_{n2},U_{n2}\leftrightarrow V^*_{n2},N_{n3}\leftrightarrow N^*_{n3}),
\end{aligned}$$

$$f_3^{V_1(s)}(A)_a = f_1^{V_1(s)}(A)_a,$$
$$f_4^{V_1(s)}(A)_a = f_2^{V_1(s)}(A)_a,$$
$$\begin{aligned}
f_1^{V_1(s)}(A)_b = &\sum_i \frac{g h_b^3 \alpha_{2i}^2 \beta_{21}}{32\sqrt{2}\pi^2(\hat{s}-m_A^2)}\{B_0^{bbH_i} - [4m_b^2 C_0 \\
&+(4m_b^2-\hat{s})C_1](\hat{s}, m_b^2, m_b^2, m_b^2, m_b^2, m_{H_i}^2)\} \\
&+\sum_i \frac{-g h_b^3 \beta_{2i}^2 \beta_{21}}{32\sqrt{2}\pi^2(\hat{s}-m_A^2)}[B_0^{bbA_i} - (4m_b^2-\hat{s})C_1(\hat{s}, m_b^2, m_b^2, m_b^2, m_b^2, m_{A_i}^2)] \\
&+\sum_i \frac{g h_t \beta_{11}}{16\sqrt{2}\pi^2(\hat{s}-m_A^2)}\{h_b h_t \beta_{1i}\beta_{2i} B_0^{btH_i^+} \\
&+[(h_t^2 m_b m_t \beta_{1i}^2 - 2h_b h_t m_b^2 \beta_{1i}\beta_{2i} + h_b^2 m_b m_t \beta_{2i}^2)C_0 \\
&-h_b h_t(4m_b^2-\hat{s})\beta_{1i}\beta_{2i}C_1](\hat{s}, m_b^2, m_b^2, m_t^2, m_t^2, m_{H_i^+}^2)\},
\end{aligned}$$
$$f_2^{V_1(s)}(A)_b = -f_3^{V_1(s)}(A)_b = f_4^{V_1(s)}(A)_b = -f_1^{V_1(s)}(A)_b;$$
$$\begin{aligned}
f_1^{s(s)}(H) = &\sum_{i,j} \frac{-g h_b^3 \alpha_{2i}^2 \alpha_{2j}\varphi_{j1}}{8\sqrt{2}\pi^2(\hat{s}-m_{H_i}^2)(\hat{s}-m_{H_j}^2)}[m_b^2(1+B_0^{0bb}) + (2m_b^2 B_0^{\hat{s}bb} + \hat{s}B_1^{\hat{s}bb})] \\
&+\sum_{i,j} \frac{-g h_b h_t^2 \alpha_{1i}\alpha_{1j}\alpha_{2i}\varphi_{j1}}{8\sqrt{2}\pi^2(\hat{s}-m_{H_i}^2)(\hat{s}-m_{H_j}^2)}[m_t^2(1+B_0^{0tt}) + (2m_t^2 B_0^{\hat{s}tt} + \hat{s}B_1^{\hat{s}tt})] \\
&+\sum_{i,j,k,l}\sum_{i',j'} \frac{g h_b^3 \alpha_{2k}\varphi_{l1}(\theta_{jj'}^b)^2(\theta_{ii'}^b)^2 \Theta_{i'j'k}^2 \Theta_{j'i'l}^2}{16\sqrt{2}\pi^2(\hat{s}-m_{H_l}^2)(\hat{s}-m_{H_k}^2)} B_0^{\hat{s}\tilde{b}_i\tilde{b}_j} \\
&+\sum_{i,j,k,l}\sum_{i',j'} \frac{g h_b h_t^2 \alpha_{2l}\varphi_{k1}(\theta_{jj'}^t)^2(\theta_{ii'}^t)^2 \Theta_{i'j'l}^1 \Theta_{j'i'k}^1}{16\sqrt{2}\pi^2(\hat{s}-m_{H_l}^2)(\hat{s}-m_{H_k}^2)} B_0^{\hat{s}\tilde{t}_i\tilde{t}_j} \\
&+\sum_{i,j,k} \frac{3 g h_b \alpha_{2i}\varphi_{j1}}{16\sqrt{2}\pi^2(\hat{s}-m_{H_i}^2)(\hat{s}-m_{H_j}^2)}[h_b^2 \alpha_{2i}\alpha_{2j} A_0(m_{\tilde{b}_k}^2) + h_t^2 \alpha_{1i}\alpha_{1j} A_0(m_{\tilde{t}_k}^2)],
\end{aligned}$$
$$f_2^{s(s)}(H) = f_3^{s(s)}(H) = f_4^{s(s)}(H) = f_1^{s(s)}(H);$$
$$\begin{aligned}
f_1^{s(s)}(A) = &\frac{g h_b^3 \beta_{21}^3}{8\sqrt{2}\pi^2(\hat{s}-m_A^2)^2}[m_b^2(1+B_0^{0bb}) + \hat{s}B_1^{\hat{s}bb}] \\
&+\frac{g h_b \beta_{11}^2 \beta_{21}}{8\sqrt{2}\pi^2(\hat{s}-m_A^2)^2}[m_t^2(1+B_0^{0tt}) + \hat{s}B_1^{\hat{s}tt}] \\
&-\sum_{i,j}\sum_{i',j'} \frac{g h_b^3 \beta_{21}(\theta_{jj'}^b)^2(\theta_{ii'}^b)^2(\Theta_{i'j'1}^4)^2}{16\sqrt{2}\pi^2(\hat{s}-m_A^2)^2} B_0^{\hat{s}\tilde{b}_i\tilde{b}_j} \\
&-\sum_{i,j}\sum_{i',j'} \frac{-g h_b h_t^2 \beta_{21}(\theta_{jj'}^t)^2(\theta_{ii'}^t)^2(\Theta_{i'j'l}^3)^2}{16\sqrt{2}\pi^2(\hat{s}-m_A^2)^2} B_0^{\hat{s}\tilde{t}_i\tilde{t}_j} \\
&-\sum_k \frac{3 g h_b \beta_{21}}{16\sqrt{2}\pi^2(\hat{s}-m_A^2)^2}[h_b^2 \beta_{21}^2 A_0(m_{\tilde{b}_k}^2) + h_t^2 \beta_{11}^2 A_0(m_{\tilde{t}_k}^2)],
\end{aligned}$$
$$f_2^{s(s)}(A) = -f_3^{s(s)}(A) = f_4^{s(s)}(A) = -f_1^{s(s)}(A);$$
$$f_1^{V_2(s)}(H) = \sum_i \frac{-g h_b^2 \alpha_{2i}^2}{16\sqrt{2}\pi^2(\hat{s}-m_{H_i}^2)}\{\frac{3}{2}h_b \beta_{21} B_0^{\hat{s}bb} + [(h_t m_b m_t \beta_{11}$$

$$
\begin{aligned}
&+h_b m_t^2\beta_{21})C_0 + h_b m_W^2\beta_{21}C_1 - (h_b m_b^2\beta_{21} + h_b m_t^2\beta_{21} \\
&-2h_t m_b m_t\beta_{11})C_2 - 2h_b\beta_{21}C_{00} - h_b\beta_{21}(\hat{t}+\hat{u}-2m_b^2)C_{12} \\
&-2h_b m_{H^+}^2\beta_{21}C_{22}](\hat{s}, m_{H^+}^2, m_W^2, m_b^2, m_b^2, m_t^2)\} \\
&+\sum_i \frac{g h_b h_t \alpha_{1i}\alpha_{2i}}{16\sqrt{2}\pi^2(\hat{s}-m_{H_i}^2)}\{\frac{3}{2}h_t\beta_{11}B_0^{\hat{s}tt} + [(h_t m_b^2\beta_{11} \\
&-h_b m_b m_t\beta_{21})C_0 + h_t m_W^2\beta_{11}C_1 - (h_t m_b^2\beta_{11} + h_t m_t^2\beta_{11} \\
&-2h_b m_b m_t\beta_{21})C_2 - 2h_t\beta_{11}C_{00} - h_t\beta_{11}(\hat{t}+\hat{u}-2m_b^2)C_{12} \\
&-2h_t m_{H^+}^2\beta_{11}C_{22}](\hat{s}, m_{H^+}^2, m_W^2, m_t^2, m_t^2, m_b^2)\} \\
&+\sum_{i,j,k,l}\sum_{i',j',k'} \frac{g h_b^2}{16\pi^2(\hat{s}-m_{H_l}^2)}\alpha_{2l}(\theta_{ii'}^b)^2\theta_{j1}^b\theta_{jj'}^b\theta_{k1}^t\theta_{kk'}^t\Theta_{i'j'l}^2(h_b\Theta_{i'k'1}^5 \\
&+h_t\Theta_{i'k'1}^6)C_2(\hat{s}, m_{H^+}^2, m_W^2, m_{\tilde{b}_j}^2, m_{\tilde{b}_i}^2, m_{\tilde{t}_k}^2) \\
&+\sum_{i,j,k,l}\sum_{i',j',k'} \frac{g h_b h_t}{16\pi^2(\hat{s}-m_{H_l}^2)}\alpha_{2l}(\theta_{ii'}^t)^2\theta_{j1}^t\theta_{jj'}^t\theta_{k1}^b\theta_{kk'}^b\Theta_{j'i'l}^1(h_b\Theta_{k'i'1}^5 \\
&+h_t\Theta_{k'i'1}^6)C_2(\hat{s}, m_{H^+}^2, m_W^2, m_{\tilde{t}_j}^2, m_{\tilde{t}_i}^2, m_{\tilde{b}_k}^2),
\end{aligned}
$$

$$f_2^{V_2(s)}(H) = f_3^{V_2(s)}(H) = f_4^{V_2(s)}(H) = f_1^{V_2(s)}(H);$$

$$
\begin{aligned}
f_1^{V_2(s)}(A) = &\frac{-g h_b^2\beta_{21}^2}{16\sqrt{2}\pi^2(\hat{s}-m_A^2)}\{\frac{3}{2}h_b\beta_{21}B_0^{\hat{s}bb} - [(h_t m_b m_t\beta_{11} - h_b m_t^2\beta_{21})C_0 \\
&+h_b m_W^2\beta_{21}C_1 + h_b\beta_{21}(m_b^2 - m_t^2)C_2 - 2h_b\beta_{21}C_{00} - h_b\beta_{21}(\hat{t}+\hat{u} \\
&-2m_b^2)C_{12} - 2h_b m_{H^+}^2\beta_{21}C_{22}](\hat{s}, m_{H^+}^2, m_W^2, m_b^2, m_b^2, m_t^2)\} \\
&+\frac{-g h_b h_t\beta_{11}\beta_{21}}{16\sqrt{2}\pi^2(\hat{s}-m_A^2)}\{\frac{3}{2}h_t\beta_{11}B_0^{\hat{s}tt} + [(h_t m_b^2\beta_{11} - h_b m_b m_t\beta_{21})C_0 \\
&+h_t m_W^2\beta_{11}C_1 - h_t\beta_{11}(m_b^2 - m_t^2)C_2 - 2h_t\beta_{11}C_{00} - h_t\beta_{11}(\hat{t}+\hat{u} \\
&-2m_b^2)C_{12} - 2h_t m_{H^+}^2\beta_{11}C_{22}](\hat{s}, m_{H^+}^2, m_W^2, m_t^2, m_t^2, m_b^2)\} \\
&+\sum_{i,j,k}\sum_{i',j',k'} \frac{-g h_b^2}{16\pi^2(\hat{s}-m_A^2)}\beta_{21}(\theta_{ii'}^b)^2\theta_{j1}^b\theta_{jj'}^b\theta_{k1}^t\theta_{kk'}^t\Theta_{i'j'1}^4(h_b\Theta_{i'k'1}^5 \\
&+h_t\Theta_{i'k'1}^6)C_2(\hat{s}, m_{H^+}^2, m_W^2, m_{\tilde{b}_j}^2, m_{\tilde{b}_i}^2, m_{\tilde{t}_k}^2) \\
&+\sum_{i,j,k}\sum_{i',j',k'} \frac{g h_b h_t}{16\pi^2(\hat{s}-m_{A_l}^2)}\beta_{21}(\theta_{ii'}^t)^2\theta_{j1}^t\theta_{jj'}^t\theta_{k1}^b\theta_{kk'}^b\Theta_{j'i'1}^3(h_b\Theta_{k'i'1}^5 \\
&+h_t\Theta_{k'i'1}^6)C_2(\hat{s}, m_{H^+}^2, m_W^2, m_{\tilde{t}_j}^2, m_{\tilde{t}_i}^2, m_{\tilde{b}_k}^2),
\end{aligned}
$$

$$f_2^{V_2(s)}(A) = -f_3^{V_2(s)}(A) = f_4^{V_2(s)}(A) = -f_1^{V_2(s)}(A);$$

$$
\begin{aligned}
f_1^{V_1(t)} = &\sum_i \frac{-g h_b h_t^2\alpha_{1i}\alpha_{2i}\beta_{11}}{16\sqrt{2}\pi^2(\hat{t}-m_t^2)}\{-B_0^{Wbt} + [-m_{H_i}^2C_0 + 2C_{00} + m_b^2C_{11} \\
&+(m_b^2+\hat{t})C_{12} + \hat{t}C_{22}](m_b^2, m_W^2, \hat{t}, m_{H_i}^2, m_b^2, m_t^2)\} \\
&+\sum_i \frac{-g h_b h_t^2\beta_{1i}\beta_{2i}\beta_{11}}{16\sqrt{2}\pi^2(\hat{t}-m_t^2)}\{-B_0^{Wbt} + [-m_{A_i}^2C_0 + 2C_{00} \\
&+m_b^2C_{11} + (m_b^2+\hat{t})C_{12} + \hat{t}C_{22}](m_b^2, m_W^2, \hat{t}, m_{A_i}^2, m_b^2, m_t^2)\}
\end{aligned}
$$

$$
\begin{aligned}
&+\sum_{i,j}\frac{-gh_t^2\alpha_{1i}\beta_{11}\varphi_{ij}}{16\sqrt{2}\pi^2(\hat{t}-m_t^2)}[(h_t m_b m_t\beta_{1j}-h_b m_t^2\beta_{2j})C_0+h_b\beta_{2j}(m_b^2-m_t^2)C_1\\
&+h_b\beta_{2j}(\hat{t}-m_t^2)C_2+2h_b\beta_{2j}C_{00}+(-h_t m_b m_t\beta_{1j}+h_b m_b^2\beta_{2j}+h_b\hat{t}\beta_{2j})C_{12}\\
&+(h_b\hat{t}\beta_{2j}-h_t m_b m_t\beta_{1j})C_{22}](m_b^2,m_W^2,\hat{t},m_t^2,m_{H_j^+}^2,m_{H_i}^2)\\
&+\sum_{i}\frac{gh_t^2\beta_{11}\beta_{1i}}{16\sqrt{2}\pi^2(\hat{t}-m_t^2)}[h_t m_b m_t\beta_{1i}(C_0+2C_1+2C_2+C_{11}+2C_{12}+C_{22})\\
&+2h_b\beta_{2i}C_{00}+h_b m_t^2\beta_{2i}(C_0+C_1+C_2)+h_b m_b^2\beta_{2i}(C_1+C_{11}+C_{12})\\
&+h_b\beta_{2i}\hat{t}(C_2+C_{12}+C_{22})](m_b^2,m_W^2,\hat{t},m_t^2,m_{H_i^+}^2,m_{A_i}^2)\\
&+\sum_{i,j}\frac{gh_b h_t\alpha_{2j}\beta_{11}\varphi_{ji}}{16\sqrt{2}\pi^2(\hat{t}-m_t^2)}[h_t m_b^2\beta_{1i}(C_0+C_2-C_{11}-C_{12})\\
&-2h_t\beta_{1i}C_{00}+h_b m_b m_t\beta_{2i}(-C_0+C_{11}+2C_{12}+C_{22})-h_t\beta_{1i}\hat{t}(C_2\\
&+C_{12}+C_{22})](m_b^2,m_W^2,\hat{t},m_b^2,m_{H_j}^2,m_{H_i^+}^2)\\
&+\sum_{i,j,k}\frac{-gh_b h_t^2\beta_{11}\theta_{j1}^b\theta_{i1}^t}{8\sqrt{2}\pi^2(\hat{t}-m_t^2)}\{N_{k3}N_{k4}^*\theta_{j1}^b\theta_{i1}^t[m_b^2(C_1+C_{11}+C_{12})+\hat{t}(C_2+C_{12}\\
&+C_{22})+2C_{00}]-(N_{k3}^*N_{k4}^*\theta_{j2}^b\theta_{i1}^t m_b m_{\tilde{\chi}_k^0}+N_{k3}N_{k4}\theta_{j1}^b\theta_{i2}^t m_t m_{\tilde{\chi}_k^0})(C_0\\
&+C_1+C_2)+N_{k3}^*N_{k4}m_b m_t\theta_{j1}^b\theta_{i2}^t(C_1+C_2+C_{11}+2C_{12}\\
&+C_{22})\}(m_b^2,m_W^2,\hat{t},m_{\tilde{\chi}_k^0}^2,m_{\tilde{b}_j}^2,m_{\tilde{t}_i}^2)\\
&+\sum_{i,j,k}\frac{gh_t^2\beta_{11}N_{i4}^*\theta_{k1}^t}{8\pi^2(\hat{t}-m_t^2)}\{-h_b\theta_{k1}^t O_{ji}^{R*}U_{j2}B_0^{W\tilde{\chi}_j^+\tilde{\chi}_i^0}+[h_b\theta_{k1}^t U_{j2}(m_{\tilde{\chi}_j^+}m_{\tilde{\chi}_i^0}O_{ji}^{L*}C_0\\
&+O_{ji}^{R*}(2C_{00}+m_b^2C_{11}+m_b^2C_{12}+\hat{t}C_{12}+\hat{t}C_{22}-m_{\tilde{t}_k}^2C_0))+h_t m_b O_{ji}^{L*}V_{j2}\theta_{k2}^t(C_0\\
&+C_1+C_2)](m_b^2,m_W^2,\hat{t},m_{\tilde{t}_k}^2,m_{\tilde{\chi}_j^+}^2,m_{\tilde{\chi}_i^0}^2)\}\\
&+\sum_{i,j,k}\frac{gh_t^2 m_t\beta_{11}\theta_{k2}^t O_{ji}^{L*}N_{i4}}{8\pi^2(\hat{t}-m_t^2)}[h_b m_{\tilde{\chi}_j^+}\theta_{k1}^t(C_0+C_1+C_2)+h_t m_b\theta_{k2}^t V_{j2}(C_0\\
&+2C_1+C_{11}+2C_{12}+2C_2+C_{22})](m_b^2,m_W^2,\hat{t},m_{\tilde{t}_k}^2,m_{\tilde{\chi}_j^+}^2,m_{\tilde{\chi}_i^0}^2)\\
&+\sum_{i,j,k}\frac{gh_b h_t\beta_{11}}{8\pi^2(\hat{t}-m_t^2)}\{h_t(\theta_{k1}^b)^2N_{j3}V_{i2}O_{ij}^{L*}B_0^{W\tilde{\chi}_i^+\tilde{\chi}_j^0}-[h_t(\theta_{k1}^b)^2N_{j3}V_{i2}(O_{ij}^{L*}(2C_{00}\\
&+m_b^2(C_{11}+C_{12})-m_{\tilde{b}_k}^2C_0+\hat{t}(C_{12}+C_{22}))+m_{\tilde{\chi}_i^+}m_{\tilde{\chi}_j^0}O_{ij}^{R*}C_0)\\
&+\theta_{k1}^b\theta_{k2}^b O_{ij}^{R*}(h_b m_t m_{\tilde{\chi}_j^0}N_{j3}U_{i2}+h_t m_b m_{\tilde{\chi}_i^+}N_{j3}^*V_{i2})(C_0+C_1+C_2)\\
&+h_b m_b m_t(\theta_{k2}^b)^2N_{j3}^*U_{i2}O_{ij}^{R*}(C_0+2C_1+C_{11}+2C_{12}\\
&+2C_2+C_{22})](m_b^2,m_W^2,\hat{t},m_{\tilde{b}_k}^2,m_{\tilde{\chi}_j^0}^2,m_{\tilde{\chi}_i^+}^2)\},
\end{aligned}
$$

$$
\begin{aligned}
f_2^{V_1(t)}=&\sum_{i}\frac{-gh_b^2h_t m_b m_t\alpha_{1i}\alpha_{2i}\beta_{21}}{16\sqrt{2}\pi^2(\hat{t}-m_t^2)}(4C_0+4C_1+4C_2+C_{11}+2C_{12}\\
&+C_{22})(m_b^2,m_W^2,\hat{t},m_{H_i}^2,m_b^2,m_t^2)
\end{aligned}
$$

$$
\begin{aligned}
&+\sum_i \frac{gh_b^2h_tm_bm_t\beta_{1i}\beta_{2i}\beta_{21}}{16\sqrt{2}\pi^2(\hat{t}-m_t^2)}(C_{11}+2C_{12}+C_{22})(m_b^2,m_W^2,\hat{t},m_{A_i}^2,m_b^2,m_t^2)\\
&+\sum_{i,j} \frac{-gh_bh_t\alpha_{1i}\beta_{21}\varphi_{ij}}{16\sqrt{2}\pi^2(\hat{t}-m_t^2)}[(h_bm_bm_t\beta_{2j}-h_tm_t^2\beta_{1j})C_0+h_t\beta_{1j}(m_b^2-m_t^2)C_1\\
&+h_t\beta_{1j}(\hat{t}-m_t^2)C_2+2h_t\beta_{1j}C_{00}+(-h_bm_bm_t\beta_{2j}+h_tm_b^2\beta_{1j}+h_t\hat{t}\beta_{1j})C_{12}\\
&+(h_t\hat{t}\beta_{1j}-h_bm_bm_t\beta_{2j})C_{22}](m_b^2,m_W^2,\hat{t},m_t^2,m_{H_j^+}^2,m_{H_i}^2)\\
&+\sum_i \frac{-gh_bh_t\beta_{1i}\beta_{21}}{16\sqrt{2}\pi^2(\hat{t}-m_t^2)}[h_bm_bm_t\beta_{2i}(C_0+2C_1+2C_2+C_{11}+2C_{12}+C_{22})\\
&+2h_t\beta_{1i}C_{00}+h_tm_t^2\beta_{1i}(C_0+C_1+C_2)+h_tm_b^2\beta_{1i}(C_1+C_{11}+C_{12})\\
&+h_t\beta_{1i}\hat{t}(C_2+C_{12}+C_{22})](m_b^2,m_W^2,\hat{t},m_t^2,m_{H_i^+}^2,m_{A_i}^2)\\
&+\sum_{i,j} \frac{gh_b^2\alpha_{2j}\beta_{21}\varphi_{ji}}{16\sqrt{2}\pi^2(\hat{t}-m_t^2)}[h_bm_b^2\beta_{2i}(C_0+C_2-C_{11}-C_{12})\\
&-2h_b\beta_{2i}C_{00}+h_tm_bm_t\beta_{1i}(-C_0+C_{11}+2C_{12}+C_{22})-h_b\beta_{2i}\hat{t}(C_2\\
&+C_{12}+C_{22})](m_b^2,m_W^2,\hat{t},m_b^2,m_{H_j}^2,m_{H_i^+}^2)\\
&+\sum_{i,j,k} \frac{gh_b^2h_t\beta_{21}\theta_{j1}^b\theta_{i1}^t}{8\sqrt{2}\pi^2(\hat{t}-m_t^2)}\{N_{k3}N_{k4}^*\theta_{j1}^b\theta_{i1}^tm_bm_t(C_1+C_2+C_{11}+2C_{12}+C_{22})\\
&-(N_{k3}^*N_{k4}^*\theta_{j2}^b\theta_{i1}^tm_tm_{\tilde{\chi}_k^0}+N_{k3}N_{k4}\theta_{j1}^b\theta_{i2}^tm_bm_{\tilde{\chi}_k^0})(C_0+C_1+C_2)\\
&+N_{k3}^*N_{k4}\theta_{j2}^b\theta_{i2}^t[m_b^2(C_1+C_{11}+C_{12})+\hat{t}(C_2+C_{12}+C_{22})\\
&+2C_{00}]\}(m_b^2,m_W^2,\hat{t},m_{\tilde{\chi}_k^0}^2,m_{\tilde{b}_j}^2,m_{\tilde{t}_i}^2)\\
&+\sum_{i,j,k} \frac{gh_bh_t\beta_{12}\theta_{k2}^tN_{i4}}{8\pi^2(\hat{t}-m_t^2)}\{-h_t\theta_{k2}^tO_{ji}^{L*}V_{j2}B_0^{W\tilde{\chi}_j^+\tilde{\chi}_i^0}+[h_bm_bm_{\tilde{\chi}_i^0}\theta_{k1}^tO_{ji}^{R*}U_{j2}(C_0\\
&+C_1+C_2)+h_t\theta_{k2}^tO_{ji}^{L*}V_{j2}(2C_{00}+m_b^2C_{11}+m_b^2C_{12}+\hat{t}C_{12}+\hat{t}C_{22}\\
&-m_{\tilde{t}_k}^2C_0+m_{\tilde{\chi}_i^0}m_{\tilde{\chi}_j^+}C_0)](m_b^2,m_W^2,\hat{t},m_{\tilde{t}_k}^2,m_{\tilde{\chi}_j^+}^2,m_{\tilde{\chi}_i^0}^2)\}\\
&+\sum_{i,j,k} \frac{gh_bh_tm_t\beta_{12}\theta_{k1}^tO_{ji}^{R*}N_{i4}^*}{8\pi^2(\hat{t}-m_t^2)}[h_bm_b\theta_{k1}^tU_{j2}(C_0+2C_1+C_{11}+2C_{12}+2C_2\\
&+C_{22})+h_tm_{\tilde{\chi}_j^+}\theta_{k2}^tV_{j2}(C_0+C_1+C_2)](m_b^2,m_W^2,\hat{t},m_{\tilde{t}_k}^2,m_{\tilde{\chi}_j^+}^2,m_{\tilde{\chi}_i^0}^2)\\
&-\sum_{i,j,k} \frac{gh_b^2\beta_{21}}{8\pi^2(\hat{t}-m_t^2)}\{h_b(\theta_{k2}^b)^2N_{j3}^*U_{i2}O_{ij}^{R*}B_0^{W\tilde{\chi}_i^+\tilde{\chi}_j^0}-[h_b(\theta_{k2}^b)^2N_{j3}^*U_{i2}(O_{ij}^{R*}(2C_{00}\\
&+m_b^2(C_{11}+C_{12})-m_{\tilde{b}_k}^2C_0+\hat{t}(C_{12}+C_{22}))+m_{\tilde{\chi}_i^+}m_{\tilde{\chi}_j^0}O_{ij}^{L*}C_0)\\
&+\theta_{k1}^b\theta_{k2}^bO_{ij}^{L*}(h_tm_tm_{\tilde{\chi}_j^0}N_{j3}^*V_{i2}+h_bm_bm_{\tilde{\chi}_i^+}N_{j3}U_{i2})(C_0+C_1+C_2)\\
&+h_tm_bm_t(\theta_{k1}^b)^2N_{j3}V_{i2}O_{ij}^{L*}(C_0+2C_1+C_{11}+2C_{12}\\
&+2C_2+C_{22})](m_b^2,m_W^2,\hat{t},m_{\tilde{b}_k}^2,m_{\tilde{\chi}_j^0}^2,m_{\tilde{\chi}_i^+}^2)\},
\end{aligned}
$$

$$
f_5^{V_1(t)}=\sum_i \frac{gh_b^2h_tm_t\alpha_{1i}\alpha_{2i}\beta_{21}}{32\sqrt{2}\pi^2(\hat{t}-m_t^2)}\{B_0^{Wbt}+[(4m_b^2+m_{H_i}^2)C_0+4m_b^2C_1
$$

$$
\begin{aligned}
&+2(m_b^2+\hat{t})C_2-2C_{00}](m_b^2,m_W^2,\hat{t},m_{H_i}^2,m_b^2,m_t^2)\}\\
&+\sum_i \frac{-gh_b^2h_tm_t\beta_{1i}\beta_{2i}\beta_{21}}{32\sqrt{2}\pi^2(\hat{t}-m_t^2)}[_0^{Wbt}+(m_{A_i}^2C_0-2C_{00})(m_b^2,m_W^2,\hat{t},m_{A_i}^2,m_b^2,m_t^2)]\\
&+\sum_{i,j} \frac{gh_bh_t\alpha_{1i}\beta_{21}\varphi_{ij}}{16\sqrt{2}\pi^2(\hat{t}-m_t^2)}(h_tm_b\beta_{1j}+h_bm_t\beta_{2j})C_{00}(m_b^2,m_W^2,\hat{t},m_t^2,m_{H_j^+}^2,m_{H_i}^2)\\
&+\sum_i \frac{gh_bh_t\beta_{1i}\beta_{21}}{16\sqrt{2}\pi^2(\hat{t}-m_t^2)}(h_tm_b\beta_{1i}-h_bm_t\beta_{2i})C_{00}(m_b^2,m_W^2,\hat{t},m_t^2,m_{H_i^+}^2,m_{A_i}^2)\\
&+\sum_{i,j} \frac{gh_b^2\alpha_{2j}\beta_{21}\varphi_{ji}}{16\sqrt{2}\pi^2(\hat{t}-m_t^2)}(h_tm_t\beta_{1i}+h_bm_b\beta_{2i})C_{00}(m_b^2,m_W^2,\hat{t},m_b^2,m_{H_j}^2,m_{H_i^+}^2)\\
&+\sum_{i,j,k} \frac{-gh_b^2h_t\beta_{21}\theta_{j1}^b\theta_{i1}^t}{8\sqrt{2}\pi^2(\hat{t}-m_t^2)}(m_bN_{k3}^*N_{k4}\theta_{j2}^b\theta_{i2}^t-m_tN_{k3}N_{k4}^*\theta_{j1}^b\theta_{i1}^t)C_{00}\\
&(m_b^2,m_W^2,\hat{t},m_{\tilde{\chi}_k^0}^2,m_{\tilde{b}_j}^2,m_{\tilde{t}_i}^2)\\
&+\sum_{i,j,k} \frac{gh_bh_t\beta_{12}\theta_{k2}^tN_{i4}}{16\pi^2(\hat{t}-m_t^2)}\{-h_tm_b\theta_{k2}^tO_{ji}^{L*}V_{j2}B_0^{W\tilde{\chi}_j^+\tilde{\chi}_i^0}+[-h_bm_{\tilde{\chi}_j^+}\theta_{k1}^tO_{ji}^{L*}U_{j2}(m_b^2C_1\\
&+\hat{t}C_0+\hat{t}C_2)+h_bm_{\tilde{\chi}_i^0}\theta_{k1}^tO_{ji}^{R*}U_{j2}(m_b^2C_0+m_b^2C_1+\hat{t}C_2)\\
&-h_tm_b\theta_{k2}^tO_{ji}^{L*}V_{j2}(-2C_{00}-m_b^2C_1+\hat{t}(C_0+C_1+2C_2)+m_{\tilde{t}_k}^2C_0\\
&-m_{\tilde{\chi}_i^0}m_{\tilde{\chi}_j^+}C_0)](m_b^2,m_W^2,\hat{t},m_{\tilde{t}_k}^2,m_{\tilde{\chi}_j^+}^2,m_{\tilde{\chi}_i^0}^2)\}\\
&+\sum_{i,j,k} \frac{gh_bh_tm_t\beta_{12}\theta_{k1}^tN_{i4}^*}{16\pi^2(\hat{t}-m_t^2)}\{h_b\theta_{k1}^tO_{ji}^{R*}U_{j2}B_0^{W\tilde{\chi}_j^+\tilde{\chi}_i^0}+[-h_bm_{\tilde{\chi}_i^0}m_{\tilde{\chi}_j^+}\theta_{k1}^tO_{ji}^{L*}U_{j2}C_0\\
&+h_b\theta_{k1}^tO_{ji}^{R*}U_{j2}(-2C_{00}+m_b^2C_0+2m_b^2C_1+m_b^2C_2+\hat{t}C_2+m_{\tilde{t}_k}^2C_0)\\
&+h_tm_b\theta_{k2}^tV_{j2}(m_{\tilde{\chi}_j^+}O_{ji}^{R*}-m_{\tilde{\chi}_i^0}O_{ji}^{L*})(C_0+C_1\\
&+C_2)](m_b^2,m_W^2,\hat{t},m_{\tilde{t}_k}^2,m_{\tilde{\chi}_j^+}^2,m_{\tilde{\chi}_i^0}^2)\}\\
&+\sum_{i,j,k} \frac{gh_b^2\beta_{21}}{16\pi^2(\hat{t}-m_t^2)}\{(-h_t(\theta_{k1}^b)^2N_{j3}V_{i2}O_{ij}^{L*}+h_b(\theta_{k2}^b)^2N_{j3}^*U_{i2}O_{ij}^{R*})B_0^{W\tilde{\chi}_i^+\tilde{\chi}_j^0}\\
&-[h_tm_t(\theta_{k1}^b)^2N_{j3}V_{i2}(O_{ij}^{L*}(-2C_{00}+m_b^2(C_0+2C_1+C_2)+m_{\tilde{b}_k}^2C_0+\hat{t}C_2)\\
&-m_{\tilde{\chi}_i^+}m_{\tilde{\chi}_j^0}O_{ij}^{R*}C_0)+\theta_{k1}^b\theta_{k2}^b(h_bN_{j3}U_{i2}(m_{\tilde{\chi}_i^+}O_{ij}^{L*}(m_b^2C_0+m_b^2C_1+\hat{t}C_2)\\
&-m_{\tilde{\chi}_j^0}O_{ij}^{R*}(m_b^2C_1+\hat{t}C_0+\hat{t}C_2))+h_tm_bm_tN_{j3}^*V_{i2}(m_{\tilde{\chi}_j^0}O_{ij}^{L*}(m_bm_tC_0\\
&+m_bm_tC_1+m_bm_tC_2)-m_{\tilde{\chi}_i^+}O_{ij}^{R*}(C_0+C_1+C_2)))\\
&+h_bm_b(\theta_{k2}^b)^2N_{j3}^*U_{i2}(m_{\tilde{\chi}_i^+}m_{\tilde{\chi}_j^0}O_{ij}^{L*}C_0+O_{ij}^{R*}(2C_{00}-m_b^2C_1-m_{\tilde{b}_k}^2C_0\\
&-\hat{t}(C_0+C_1+C_2)))](m_b^2,m_W^2,\hat{t},m_{\tilde{b}_k}^2,m_{\tilde{\chi}_j^0}^2,m_{\tilde{\chi}_i^+}^2)\},
\end{aligned}
$$

$$
\begin{aligned}
f_6^{V_1(t)} &= \sum_i \frac{gh_bh_t^2m_b\alpha_{1i}\alpha_{2i}\beta_{11}}{32\sqrt{2}\pi^2(\hat{t}-m_t^2)}\{B_0^{Wbt}+[2(m_t^2+\hat{t}+m_{H_i}^2)C_0\\
&+(2m_b^2+m_t^2+\hat{t})C_1+(m_t^2+3\hat{t})C_2-2C_{00}](m_b^2,m_W^2,\hat{t},m_{H_i}^2,m_b^2,m_t^2)\}
\end{aligned}
$$

$$
\begin{aligned}
&+\sum_i \frac{-gh_bh_t^2m_b\beta_{1i}\beta_{2i}\beta_{11}}{32\sqrt{2}\pi^2(\hat{t}-m_t^2)}\{B_0^{Wbt}+[m_{A_i}^2C_0-(m_t^2-\hat{t})(C_1+C_2)\\
&-2C_{00}](m_b^2,m_W^2,\hat{t},m_{A_i}^2,m_b^2,m_t^2)\}\\
&+\sum_{i,j}\frac{gh_t^2\alpha_{1i}\beta_{11}\varphi_{ij}}{16\sqrt{2}\pi^2(\hat{t}-m_t^2)}(h_tm_t\beta_{1j}+h_bm_b\beta_{2j})C_{00}(m_b^2,m_W^2,\hat{t},m_t^2,m_{H_j^+}^2,m_{H_i}^2)\\
&+\sum_i \frac{-gh_t^2\beta_{1i}\beta_{11}}{16\sqrt{2}\pi^2(\hat{t}-m_t^2)}(h_bm_b\beta_{2i}-h_tm_t\beta_{1i})C_{00}(m_b^2,m_W^2,\hat{t},m_t^2,m_{H_i^+}^2,m_{A_i}^2)\\
&+\sum_{i,j}\frac{gh_bh_t\alpha_{2j}\beta_{11}\varphi_{ji}}{16\sqrt{2}\pi^2(\hat{t}-m_t^2)}(h_tm_b\beta_{1i}+h_bm_t\beta_{2i})C_{00}(m_b^2,m_W^2,\hat{t},m_b^2,m_{H_j}^2,m_{H_i^+}^2)\\
&+\sum_{i,j,k}\frac{-gh_b^2h_t\beta_{11}\theta_{j1}^b\theta_{i1}^t}{8\sqrt{2}\pi^2(\hat{t}-m_t^2)}(m_tN_{k3}^*N_{k4}\theta_{j2}^b\theta_{i2}^t-m_bN_{k3}N_{k4}^*\theta_{j1}^b\theta_{i1}^t)C_{00}\\
&(m_b^2,m_W^2,\hat{t},m_{\tilde{\chi}_k^0}^2,m_{\tilde{b}_j}^2,m_{\tilde{t}_i}^2)\\
&+\sum_{i,j,k}\frac{gh_t^2\beta_{11}\theta_{k1}^tN_{i4}^*}{16\pi^2(\hat{t}-m_t^2)}\{h_bm_b\theta_{k1}^tO_{ji}^{R*}U_{j2}B_0^{W\tilde{\chi}_j^+\tilde{\chi}_i^0}+[-h_bm_bm_{\tilde{\chi}_i^0}m_{\tilde{\chi}_j^+}\theta_{k1}^tO_{ji}^{L*}U_{j2}C_0\\
&+h_bm_b\theta_{k1}^tO_{ji}^{R*}U_{j2}(-2C_{00}+m_b^2C_1+\hat{t}C_0+\hat{t}C_1+2\hat{t}C_2+m_{\tilde{t}_{k1}}^2C_0)\\
&-h_tm_{\tilde{\chi}_i^0}\theta_{k2}^tO_{ji}^{L*}V_{j2}(m_b^2C_0+m_b^2C_1+\hat{t}C_2)+h_tm_{\tilde{\chi}_j^+}\theta_{k2}^tO_{ji}^{R*}V_{j2}(m_b^2C_1+\hat{t}C_0\\
&+\hat{t}C_2)](m_b^2,m_W^2,\hat{t},m_{\tilde{t}_k}^2,m_{\tilde{\chi}_j^+}^2,m_{\tilde{\chi}_i^0}^2)\}\\
&+\sum_{i,j,k}\frac{gh_t^2m_t\beta_{11}\theta_{k2}^tN_{j4}}{16\pi^2(\hat{t}-m_t^2)}\{-h_t\theta_{k2}^tO_{ji}^{L*}V_{j2}B_0^{W\tilde{\chi}_j^+\tilde{\chi}_i^0}+[h_bm_b\theta_{k1}^tU_{j2}(m_{\tilde{\chi}_i^0}O_{ji}^{R*}\\
&-m_{\tilde{\chi}_j^+}O_{ji}^{L*})(C_0+C_1+C_2)-h_t\theta_{k2}^tO_{ji}^{L*}V_{j2}(2C_{00}-m_b^2C_0-2m_b^2C_1-m_b^2C_2\\
&-\hat{t}C_2-m_{\tilde{t}_k}^2C_0+m_{\tilde{\chi}_i^0}m_{\tilde{\chi}_j^+}C_0)](m_b^2,m_W^2,\hat{t},m_{\tilde{t}_k}^2,m_{\tilde{\chi}_j^+}^2,m_{\tilde{\chi}_i^0}^2)\}\\
&-\sum_{i,j,k}\frac{gh_bh_t\beta_{11}}{16\pi^2(\hat{t}-m_t^2)}\{[-h_b(\theta_{k2}^b)^2N_{j3}^*U_{i2}O_{ij}^{R*}+h_t(\theta_{k1}^b)^2N_{j3}V_{i2}O_{ij}^{L*}]B_0^{W\tilde{\chi}_i^+\tilde{\chi}_j^0}\\
&-[h_bm_t(\theta_{k2}^b)^2N_{j3}^*U_{i2}(O_{ij}^{R*}(-2C_{00}+m_b^2(C_0+2C_1+C_2)+m_{\tilde{b}_k}^2C_0+\hat{t}C_2)\\
&-m_{\tilde{\chi}_i^+}m_{\tilde{\chi}_j^0}O_{ij}^{L*}C_0)+\theta_{k1}^b\theta_{k2}^b(h_tN_{j3}^*V_{i2}(m_{\tilde{\chi}_i^+}O_{ij}^{R*}(m_b^2C_0+m_b^2C_1+\hat{t}C_2)\\
&-m_{\tilde{\chi}_j^0}O_{ij}^{L*}(m_b^2C_1+\hat{t}C_0+\hat{t}C_2))+h_bm_bm_tN_{j3}U_{i2}(m_{\tilde{\chi}_j^0}O_{ij}^{R*}(m_bm_tC_0\\
&+m_bm_tC_1+m_bm_tC_2)-m_{\tilde{\chi}_i^+}O_{ij}^{R*}(C_0+C_1+C_2)))\\
&+h_tm_b(\theta_{k1}^b)^2N_{j3}V_{i2}(m_{\tilde{\chi}_i^+}m_{\tilde{\chi}_j^0}O_{ij}^{R*}C_0+O_{ij}^{L*}(2C_{00}-m_b^2C_1-m_{\tilde{b}_k}^2C_0\\
&-\hat{t}(C_0+C_1+C_2)))](m_b^2,m_W^2,\hat{t},m_{\tilde{b}_k}^2,m_{\tilde{\chi}_j^0}^2,m_{\tilde{\chi}_i^+}^2)\},
\end{aligned}
$$

$$
\begin{aligned}
f_7^{V_1(t)}=&\sum_i \frac{-gh_b^2h_tm_t\alpha_{1i}\alpha_{2i}\beta_{21}}{32\sqrt{2}\pi^2(\hat{t}-m_t^2)}(2C_2+C_{12}+C_{22})(m_b^2,m_W^2,\hat{t},m_{H_i}^2,m_b^2,m_t^2)\\
&+\sum_i \frac{-gh_b^2h_tm_t\beta_{1i}\beta_{2i}\beta_{21}}{16\sqrt{2}\pi^2(\hat{t}-m_t^2)}(C_{12}+C_{22})(m_b^2,m_W^2,\hat{t},m_{A_i}^2,m_b^2,m_t^2)
\end{aligned}
$$

$$
\begin{aligned}
&+\sum_{i,j}\frac{gh_bh_t\alpha_{1i}\beta_{21}\varphi_{ij}}{16\sqrt{2}\pi^2(\hat{t}-m_t^2)}[h_tm_b\beta_{1j}(C_1+C_{11}+C_{12})+h_bm_t\beta_{2j}(C_0+C_1\\
&-C_{12}-C_{22})](m_b^2,m_W^2,\hat{t},m_t^2,m_{H_j^+}^2,m_{H_i}^2)\\
&+\sum_{i}\frac{gh_bh_t\beta_{1i}\beta_{21}}{16\sqrt{2}\pi^2(\hat{t}-m_t^2)}[h_tm_b\beta_{1i}(C_1+C_{11}+C_{12})+h_bm_t\beta_{2i}(C_0+C_1+2C_2\\
&+C_{12}+C_{22})](m_b^2,m_W^2,\hat{t},m_t^2,m_{H_i^+}^2,m_{A_i}^2)\\
&+\sum_{i,j}\frac{-gh_b^2\alpha_{2j}\beta_{21}\varphi_{ji}}{16\sqrt{2}\pi^2(\hat{t}-m_t^2)}[h_tm_t\beta_{1i}(C_2+C_{12}+C_{22})+h_bm_b\beta_{2i}(C_0+C_2-C_{11}\\
&-C_{12})](m_b^2,m_W^2,\hat{t},m_b^2,m_{H_j}^2,m_{H_i^+}^2)\\
&+\sum_{i,j,k}\frac{-gh_b^2h_t\beta_{21}\theta_{j1}^b\theta_{i1}^t}{8\sqrt{2}\pi^2(\hat{t}-m_t^2)}[m_bN_{k3}^*N_{k4}\theta_{j2}^b\theta_{i2}^t(C_2+C_{11}+C_{12})\\
&-N_{k3}N_{k4}\theta_{j1}^b\theta_{i2}^tm_{\tilde{\chi}_k^0}(C_0+C_1+C_2)+m_tN_{k3}N_{k4}^*\theta_{j1}^b\theta_{i1}^t(C_2+C_{12}\\
&+C_{22})](m_b^2,m_W^2,\hat{t},m_{\tilde{\chi}_k^0}^2,m_{\tilde{b}_j}^2,m_{\tilde{t}_i}^2)\\
&-\sum_{i,j,k}\frac{gh_bh_t\beta_{12}\theta_{k2}^tN_{i4}}{8\pi^2(\hat{t}-m_t^2)}[h_bm_{\tilde{\chi}_j^+}\theta_{k1}^tO_{ji}^{L*}U_{j2}C_1+h_bm_{\tilde{\chi}_i^0}\theta_{k1}^tO_{ji}^{R*}U_{j2}C_2\\
&+h_tm_b\theta_{k2}^tO_{ji}^{L*}V_{j2}(C_1+C_{11}+C_{12})](m_b^2,m_W^2,\hat{t},m_{\tilde{t}_k}^2,m_{\tilde{\chi}_j^+}^2,m_{\tilde{\chi}_i^0}^2)\\
&-\sum_{i,j,k}\frac{gh_b^2h_tm_t\beta_{12}(\theta_{k1}^t)^2}{8\pi^2(\hat{t}-m_t^2)}O_{ji}^{R*}U_{j2}N_{i4}^*(C_{12}+C_2+C_{22})(m_b^2,m_W^2,\hat{t},m_{\tilde{t}_k}^2,m_{\tilde{\chi}_j^+}^2,m_{\tilde{\chi}_i^0}^2)\\
&-\sum_{i,j,k}\frac{gh_b^2\beta_{21}}{8\pi^2(\hat{t}-m_t^2)}[h_tm_t(\theta_{k1}^b)^2N_{j3}V_{i2}O_{ij}^{L*}(C_{12}+C_2+C_{22})\\
&+h_b\theta_{k1}^b\theta_{k2}^bN_{j3}U_{i2}(m_{\tilde{\chi}_i^+}O_{ij}^{L*}C_2+m_{\tilde{\chi}_j^0}O_{ij}^{R*}C_1)\\
&+h_bm_b(\theta_{k2}^b)^2N_{j3}^*U_{i2}O_{ij}^{R*}(C_{11}+C_1+C_{12})](m_b^2,m_W^2,\hat{t},m_{\tilde{b}_k}^2,m_{\tilde{\chi}_j^0}^2,m_{\tilde{\chi}_i^+}^2),
\end{aligned}
$$

$$
\begin{aligned}
f_8^{V_1(t)}=&\sum_{i}\frac{-gh_bh_t^2m_b\alpha_{1i}\alpha_{2i}\beta_{11}}{32\sqrt{2}\pi^2(\hat{t}-m_t^2)}(2C_1+C_{11}+C_{12})(m_b^2,m_W^2,\hat{t},m_{H_i}^2,m_b^2,m_t^2)\\
&+\sum_{i}\frac{gh_bh_t^2m_b\beta_{1i}\beta_{2i}\beta_{11}}{16\sqrt{2}\pi^2(\hat{t}-m_t^2)}(C_{11}+C_{12})(m_b^2,m_W^2,\hat{t},m_{A_i}^2,m_b^2,m_t^2)\\
&+\sum_{i,j}\frac{gh_t^2\alpha_{1i}\beta_{11}\varphi_{ij}}{16\sqrt{2}\pi^2(\hat{t}-m_t^2)}[h_bm_b\beta_{2j}(C_1+C_{11}+C_{12})+h_tm_t\beta_{1j}(C_0+C_1\\
&-C_{12}-C_{22})](m_b^2,m_W^2,\hat{t},m_t^2,m_{H_j^+}^2,m_{H_i}^2)\\
&+\sum_{i}\frac{-gh_t^2\beta_{1i}\beta_{11}}{16\sqrt{2}\pi^2(\hat{t}-m_t^2)}[h_bm_b\beta_{2i}(C_1+C_{11}+C_{12})+h_tm_t\beta_{1i}(C_0+C_1+2C_2\\
&+C_{12}+C_{22})](m_b^2,m_W^2,\hat{t},m_t^2,m_{H_i^+}^2,m_{A_i}^2)\\
&+\sum_{i,j}\frac{-gh_bh_t\alpha_{2j}\beta_{11}\varphi_{ji}}{16\sqrt{2}\pi^2(\hat{t}-m_t^2)}[h_bm_t\beta_{2i}(C_2+C_{11}+C_{22})+h_tm_b\beta_{1i}(C_0+C_2-C_{11}
\end{aligned}
$$

$$
\begin{aligned}
& -C_{12})](m_b^2, m_W^2, \hat{t}, m_b^2, m_{H_j}^2, m_{H_i^+}^2) \\
& + \sum_{i,j,k} \frac{g h_b h_t^2 \beta_{11} \theta_{j1}^b \theta_{i1}^t}{8\sqrt{2}\pi^2(\hat{t} - m_t^2)} [m_t N_{k3}^* N_{k4} \theta_{j2}^b \theta_{i2}^t (C_2 + C_{12} + C_{22}) \\
& - N_{k3}^* N_{k4}^* \theta_{j2}^b \theta_{i1}^t m_{\tilde{\chi}_k^0} (C_0 + C_1 + C_2) + m_b N_{k3} N_{k4}^* \theta_{j1}^b \theta_{i1}^t (C_1 + C_{11} + C_{12})] \\
& (m_b^2, m_W^2, \hat{t}, m_{\tilde{\chi}_k^0}^2, m_{\tilde{b}_j}^2, m_{\tilde{t}_i}^2) \\
& - \sum_{i,j,k} \frac{g h_t^2 \beta_{11} \theta_{k1}^t N_{i4}^*}{8\pi^2(\hat{t} - m_t^2)} [h_t m_{\tilde{\chi}_j^+} \theta_{kw}^t O_{ji}^{R*} V_{j2} C_1 + h_t m_{\tilde{\chi}_i^0} \theta_{k2}^t O_{ji}^{L*} V_{j2} C_2 \\
& + h_b m_b \theta_{k1}^t O_{ji}^{R*} U_{j2} (C_1 + C_{11} + C_{12})](m_b^2, m_W^2, \hat{t}, m_{\tilde{t}_k}^2, m_{\tilde{\chi}_j^+}^2, m_{\tilde{\chi}_i^0}^2) \\
& - \sum_{i,j,k} \frac{g h_t^3 m_t \beta_{11} (\theta_{k2}^t)^2}{8\pi^2(\hat{t} - m_t^2)} O_{ji}^{L*} V_{j2} N_{i4}^* (C_2 + C_{12} + C_{22})(m_b^2, m_W^2, \hat{t}, m_{\tilde{t}_k}^2, m_{\tilde{\chi}_j^+}^2, m_{\tilde{\chi}_i^0}^2) \\
& + \sum_{i,j,k} \frac{g h_b h_t \beta_{11}}{8\pi^2(\hat{t} - m_t^2)} [h_b m_t (\theta_{k2}^b)^2 N_{j3}^* U_{i2} O_{ij}^{R*} (C_{12} + C_2 + C_{22}) \\
& + h_t \theta_{k1}^b \theta_{k2}^b N_{j3}^* V_{i2} (m_{\tilde{\chi}_i^+} O_{ij}^{R*} C_2 + m_{\tilde{\chi}_j^0} O_{ij}^{L*} C_1) \\
& + h_t m_b (\theta_{k1}^b)^2 N_{j3} V_{i2} O_{ij}^{L*} (C_{11} + C_1 + C_{12})](m_b^2, m_W^2, \hat{t}, m_{\tilde{b}_k}^2, m_{\tilde{\chi}_j^0}^2, m_{\tilde{\chi}_i^+}^2),
\end{aligned}
$$

$$
\begin{aligned}
f_{11}^{V_1(t)} = & \sum_i \frac{g h_b h_t^2 \alpha_{1i} \alpha_{2i} \beta_{11}}{32\sqrt{2}\pi^2(\hat{t} - m_t^2)} \{B_0^{Wbt} + [m_{H_i}^2 C_0 + 2m_b^2 C_1 + (m_t^2 + \hat{t}) C_2 \\
& - 2C_{00}](m_b^2, m_W^2, \hat{t}, m_{H_i}^2, m_b^2, m_t^2)\} \\
& + \sum_i \frac{-g h_b h_t^2 m_b \beta_{1i} \beta_{2i} \beta_{11}}{32\sqrt{2}\pi^2(\hat{t} - m_t^2)} \{B_0^{Wbt} + [m_{A_i}^2 C_0 - (m_t^2 - \hat{t}) C_2 \\
& - 2C_{00}](m_b^2, m_W^2, \hat{t}, m_{A_i}^2, m_b^2, m_t^2)\} \\
& + \sum_{i,j} \frac{g h_b h_t^2 \alpha_{1i} \beta_{11} \beta_{2j} \varphi_{ij}}{16\sqrt{2}\pi^2(\hat{t} - m_t^2)} C_{00}(m_b^2, m_W^2, \hat{t}, m_t^2, m_{H_j^+}^2, m_{H_i}^2) \\
& + \sum_i \frac{-g h_b h_t^2 \beta_{1i} \beta_{2i} \beta_{11}}{16\sqrt{2}\pi^2(\hat{t} - m_t^2)} C_{00}(m_b^2, m_W^2, \hat{t}, m_t^2, m_{H_i^+}^2, m_{A_i}^2) \\
& + \sum_{i,j} \frac{g h_b h_t^2 \alpha_{2j} \beta_{11} \beta_{1i} \varphi_{ji}}{16\sqrt{2}\pi^2(\hat{t} - m_t^2)} C_{00}(m_b^2, m_W^2, \hat{t}, m_b^2, m_{H_j}^2, m_{H_i^+}^2) \\
& + \sum_{i,j,k} \frac{g h_b h_t^2 \beta_{11} (\theta_{j1}^b)^2 (\theta_{i1}^t)^2}{8\sqrt{2}\pi^2(\hat{t} - m_t^2)} N_{k3} N_{k4}^* C_{00}(m_b^2, m_W^2, \hat{t}, m_{\tilde{\chi}_k^0}^2, m_{\tilde{b}_j}^2, m_{\tilde{t}_i}^2) \\
& + \sum_{i,j,k} \frac{g h_t^2 \beta_{11} \theta_{k1}^t N_{i4}^*}{16\pi^2(\hat{t} - m_t^2)} \{h_b \theta_{k1}^t O_{ji}^{R*} U_{j2} B_0^{Wbt} + [-h_b m_{\tilde{\chi}_i^0} m_{\tilde{\chi}_j^+} \theta_{k1}^t O_{ji}^{L*} U_{j2} C_0 \\
& + h_b \theta_{k1}^t O_{ji}^{R*} U_{j2} (-2C_{00} + m_b^2 C_1 + \hat{t} C_2 + m_{\tilde{t}_k}^2 C_0) + h_t m_b \theta_{k2}^t V_{j2} (m_{\tilde{\chi}_j^+} O_{ji}^{L*} \\
& - m_{\tilde{\chi}_i^0} O_{ji}^{R*}) C_1](m_b^2, m_W^2, \hat{t}, m_{\tilde{t}_k}^2, m_{\tilde{\chi}_j^+}^2, m_{\tilde{\chi}_i^0}^2)\} \\
& - \sum_{i,j,k} \frac{g h_t^2 \beta_{11} \theta_{k2}^t N_{i4}}{16\pi^2(\hat{t} - m_t^2)} [h_b m_{\tilde{\chi}_j^+} \theta_{k1}^t O_{ji}^{L*} U_{j2} (C_0 + C_2) - h_b m_{\tilde{\chi}_i^0} \theta_{k1}^t O_{ji}^{R*} U_{j2} C_2
\end{aligned}
$$

$$+h_t m_b \theta^t_{k2} O^{L*}_{ji} V_{j2}(C_0 + C_1 + C_2)](m_b^2, m_W^2, \hat{t}, m^2_{\tilde{t}_k}, m^2_{\tilde{\chi}^+_j}, m^2_{\tilde{\chi}^0_i})$$

$$+\sum_{i,j,k} \frac{g h_b h_t \beta_{11}}{16\pi^2(\hat{t}-m_t^2)}\{-h_t(\theta^b_{k1})^2 N_{j3} V_{i2} O^{L*}_{ij} B_0^{W\tilde{\chi}^+_i\tilde{\chi}^0_j} + [-h_t(\theta^b_{k1})^2 N_{j3} V_{i2}(m_{\tilde{\chi}^+_i} m_{\tilde{\chi}^0_j} O^{R*}_{ij} C_0$$

$$+O^{L*}_{ij}(-2C_{00} + m_b^2 C_1 + m^2_{\tilde{b}_k} C_0 + \hat{t}C_2)) - \theta^b_{k1}\theta^b_{k2}(h_b m_t N_{j3} U_{i2}(m_{\tilde{\chi}^+_i} O^{L*}_{ij} C_2$$

$$-O^{R*}_{ij}(m_{\tilde{\chi}^0_j} C_0 + m_{\tilde{\chi}^+_i} C_2)) + h_t m_b N^*_{j3} V_{i2}(m_{\tilde{\chi}^0_j} O^{L*}_{ij} C_1 - O^{R*}_{ij}(m_{\tilde{\chi}^+_i} C_0 + m_{\tilde{\chi}^0_j} C_1)))$$

$$+h_b m_b m_t (\theta^b_{k2})^2 N^*_{j3} U_{i2} O^{R*}_{ij}(C_0 + C_1 + C_2)](m_b^2, m_W^2, \hat{t}, m^2_{\tilde{b}_k}, m^2_{\tilde{\chi}^0_j}, m^2_{\tilde{\chi}^+_i})\},$$

$$f_{12}^{V_1(t)} = \sum_i \frac{-g h_b^2 h_t \alpha_{1i}\alpha_{2i}\beta_{21}}{32\sqrt{2}\pi^2(\hat{t}-m_t^2)} m_b m_t (2C_0 + C_1 + C_2)(m_b^2, m_W^2, \hat{t}, m^2_{H_i}, m_b^2, m_t^2)$$

$$+\sum_{i,j} \frac{g h_b h_t^2 \alpha_{1i}\beta_{21}\beta_{1j}\varphi_{ij}}{16\sqrt{2}\pi^2(\hat{t}-m_t^2)} C_{00}(m_b^2, m_W^2, \hat{t}, m_t^2, m^2_{H^+_j}, m^2_{H_i})$$

$$+\sum_i \frac{-g h_b h_t^2 \beta_{1i}^2 \beta_{21}}{16\sqrt{2}\pi^2(\hat{t}-m_t^2)} C_{00}(m_b^2, m_W^2, \hat{t}, m_t^2, m^2_{H^+_i}, m^2_{A_i})$$

$$+\sum_{i,j} \frac{g h_b^3 \alpha_{2j}\beta_{21}\beta_{2i}\varphi_{ji}}{16\sqrt{2}\pi^2(\hat{t}-m_t^2)} C_{00}(m_b^2, m_W^2, \hat{t}, m_b^2, m^2_{H_j}, m^2_{H^+_i})$$

$$+\sum_{i,j,k} \frac{-g h_b^2 h_t \beta_{21}\theta^b_{j1}\theta^b_{j2}\theta^t_{i1}\theta^t_{i2}}{8\sqrt{2}\pi^2(\hat{t}-m_t^2)} N^*_{k3} N_{k4} C_{00}(m_b^2, m_W^2, \hat{t}, m^2_{\tilde{\chi}^0_k}, m^2_{\tilde{b}_j}, m^2_{\tilde{t}_i})$$

$$+\sum_{i,j,k} \frac{g h_t^2 \beta_{11}\theta^t_{k1} N^*_{i4}}{16\pi^2(\hat{t}-m_t^2)}\{h_b \theta^t_{k1} O^{R*}_{ji} U_{j2} B_0^{Wbt} + [-h_b m_{\tilde{\chi}^0_i} m_{\tilde{\chi}^+_j} \theta^t_{k1} O^{L*}_{ji} U_{j2} C_0$$

$$+h_b \theta^t_{k1} O^{R*}_{ji} U_{j2}(-2C_{00} + m_b^2 C_1 + \hat{t}C_2 + m^2_{\tilde{t}_k} C_0) + h_t m_b \theta^t_{k2} V_{j2}(m_{\tilde{\chi}^+_j} O^{L*}_{ji}$$

$$-m_{\tilde{\chi}^0_i} O^{R*}_{ji})C_1](m_b^2, m_W^2, \hat{t}, m^2_{\tilde{t}_k}, m^2_{\tilde{\chi}^+_j}, m^2_{\tilde{\chi}^0_i})\}$$

$$-\sum_{i,j,k} \frac{g h_b h_t \beta_{12}\theta^t_{k1} N^*_{i4}}{16\pi^2(\hat{t}-m_t^2)}[h_t m_{\tilde{\chi}^+_j} \theta^t_{k2} O^{R*}_{ji} V_{j2}(C_0 + C_2) - h_t m_{\tilde{\chi}^0_i} \theta^t_{k2} O^{L*}_{ji} V_{j2} C_2$$

$$+h_b m_b \theta^t_{k1} O^{R*}_{ji} U_{j2}(C_0 + C_1 + C_2)](m_b^2, m_W^2, \hat{t}, m^2_{\tilde{t}_k}, m^2_{\tilde{\chi}^+_j}, m^2_{\tilde{\chi}^0_i})$$

$$-\sum_{i,j,k} \frac{g h_b^2 \beta_{21}}{16\pi^2(\hat{t}-m_t^2)}\{-h_b(\theta^b_{k2})^2 N^*_{j3} U_{i2} O^{R*}_{ij} B_0^{W\tilde{\chi}^+_i\tilde{\chi}^0_j} + [-h_b(\theta^b_{k2})^2 N^*_{j3} U_{i2}(m_{\tilde{\chi}^+_i} m_{\tilde{\chi}^0_j} O^{L*}_{ij} C_0$$

$$+O^{R*}_{ij}(-2C_{00} + m_b^2 C_1 + m^2_{\tilde{b}_k} C_0 + \hat{t}C_2)) - \theta^b_{k1}\theta^b_{k2}(h_t m_t N^*_{j3} V_{i2}(m_{\tilde{\chi}^+_i} O^{R*}_{ij} C_2$$

$$-O^{L*}_{ij}(m_{\tilde{\chi}^0_j} C_0 + m_{\tilde{\chi}^+_i} C_2)) + h_b m_b N_{j3} U_{i2}(m_{\tilde{\chi}^0_j} O^{R*}_{ij} C_1 - O^{L*}_{ij}(m_{\tilde{\chi}^+_i} C_0 + m_{\tilde{\chi}^0_j} C_1)))$$

$$+h_t m_b m_t (\theta^b_{k1})^2 N_{j3} V_{i2} O^{L*}_{ij}(C_0 + C_1 + C_2)](m_b^2, m_W^2, \hat{t}, m^2_{\tilde{b}_k}, m^2_{\tilde{\chi}^0_j}, m^2_{\tilde{\chi}^+_i})\};$$

$$f_2^{s(t)} = \sum_i \frac{-g h_b h_t^2 \alpha_{1i}^2 \beta_{21}}{16\sqrt{2}\pi^2(\hat{t}-m_t^2)^2}[2m_t^2 B_0^{\hat{t}tH_i} - (m_t^2 + \hat{t})B_1^{\hat{t}tH_i}]$$

$$+\sum_i \frac{g h_b h_t^2 \beta_{1i}^2 \beta_{21}}{16\sqrt{2}\pi^2(\hat{t}-m_t^2)^2}[2m_t^2 B_0^{\hat{t}tA_i} + (m_t^2 + \hat{t})B_1^{\hat{t}tA_i}]$$

$$+\sum_i \frac{g h_b \beta_{21}}{8\sqrt{2}\pi^2(\hat{t}-m_t^2)^2}[2h_b h_t m_b m_t \beta_{1i}\beta_{2i} B_0^{\hat{t}bH^+_i} + (h_t^2 m_t^2 \beta_{1i} + h_b^2 \hat{t}\beta_{2i})^2 B_1^{\hat{t}bH^+_i}]$$

$$
\begin{aligned}
&+\sum_{i,j}\frac{-gh_bh_t^2\beta_{21}}{8\sqrt{2}\pi^2(\hat{t}-m_t^2)^2}\{m_t\theta^t_{i1}\theta^t_{i2}(N_{j4}^2+N_{j4}^{*2})B_0^{\hat{t}\tilde{\chi}^0_j\tilde{t}_i}-[m_t^2(\theta^t_{i1})^2\\
&+\hat{t}(\theta^t_{i2})^2]|N_{j4}|^2B_1^{\hat{t}\tilde{\chi}^0_j\tilde{t}_i}\}\\
&+\sum_{i,j}\frac{-gh_b\beta_{21}}{8\sqrt{2}\pi^2(\hat{t}-m_t^2)^2}[-h_b^2m_t^2(\theta^b_{i2})^2|U_{j2}|^2B_1^{\hat{t}\tilde{\chi}^+_j\tilde{b}_i}+h_bh_tm_t\theta^b_{i1}\theta^b_{i2}(U_{j2}V_{j2}\\
&+U_{j2}^*V_{j2}^*)B_0^{\hat{t}\tilde{\chi}^+_j\tilde{b}_i}-h_t^2\hat{t}(\theta^b_{i1})^2|V_{j2}|^2B_1^{\hat{t}\tilde{\chi}^+_j\tilde{b}_i}],\\
f_5^{s(t)}&=-\frac{1}{2}m_bf_2^{s(t)},\\
f_6^{s(t)}&=\sum_i\frac{-gh_t^3m_t\alpha_{1i}^2\beta_{11}}{32\sqrt{2}\pi^2(\hat{t}-m_t^2)^2}[-(m_t^2-\hat{t})B_0^{\hat{t}tH_i}+2\hat{t}B_1^{\hat{t}tH_i}]\\
&+\sum_i\frac{-gh_t^3m_t\beta_{1i}^2\beta_{11}}{32\sqrt{2}\pi^2(\hat{t}-m_t^2)^2}[(m_t^2+\hat{t})B_0^{\hat{t}tA_i}+2\hat{t}B_1^{\hat{t}tA_i}]\\
&+\sum_i\frac{-gh_t\beta_{11}}{16\sqrt{2}\pi^2(\hat{t}-m_t^2)^2}[h_bh_tm_b\beta_{1i}\beta_{2i}(m_t^2+\hat{t})B_0^{\hat{t}bH_i^+}+(h_t^2\beta_{1i}^2+h_b^2\beta_{2i}^2)m_t\hat{t}B_1^{\hat{t}bH_i^+}]\\
&+\sum_{i,j}\frac{-gh_t^3\beta_{11}}{16\sqrt{2}\pi^2(\hat{t}-m_t^2)^2}[-\theta^t_{i1}\theta^t_{i2}(m_t^2N_{j4}^2+\hat{t}N_{j4}^{*2})B_0^{\hat{t}\tilde{\chi}^0_j\tilde{t}_i}+m_t\hat{t}|N_{j4}|^2B_1^{\hat{t}\tilde{\chi}^0_j\tilde{t}_i}]\\
&+\sum_{i,j}\frac{-gh_t\beta_{11}}{16\sqrt{2}\pi^2(\hat{t}-m_t^2)^2}[h_b^2m_t\hat{t}(\theta^b_{i2})^2|U_{j2}|^2B_1^{\hat{t}\tilde{\chi}^+_j\tilde{b}_i}-h_bh_t\theta^b_{i1}\theta^b_{i2}(m_t^2U_{j2}V_{j2}\\
&+\hat{t}U_{j2}^*V_{j2}^*)B_0^{\hat{t}\tilde{\chi}^+_j\tilde{b}_i}+h_t^2m_t\hat{t}(\theta^b_{i1})^2|V_{j2}|^2B_1^{\hat{t}\tilde{\chi}^+_j\tilde{b}_i}],\\
f_{12}^{s(t)}&=-\frac{1}{2}f_2^{s(t)};\\
f_2^{V_2(t)}&=\sum_i\frac{gh_bh_t\alpha_{1i}\alpha_{2i}}{16\sqrt{2}\pi^2(\hat{t}-m_t^2)}\{h_t\beta_{11}B_0^{H^+bt}+[h_t\beta_{11}(m_{H_i}^2C_0+2m_b^2C_1+m_t^2C_2\\
&+\hat{t}C_2)-h_bm_bm_t\beta_{21}(4C_0+2C_1+2C_2)](m_b^2,m_{H^+}^2,\hat{t},m_{H_i}^2,m_b^2,m_t^2)\}\\
&+\sum_i\frac{gh_bh_t^2\beta_{1i}\beta_{11}\beta_{2i}}{16\sqrt{2}\pi^2(\hat{t}-m_t^2)}\{B_0^{H^+bt}+[m_{A_i}^2C_0\\
&+(\hat{t}-m_t^2)C_2](m_b^2,m_{H^+}^2,\hat{t},m_{A_i}^2,m_b^2,m_t^2)\}\\
&+\sum_{i,j,k}\sum_{i',j'}\frac{-gh_bh_t\theta^b_{jj'}\theta^t_{ii'}}{8\sqrt{2}\pi^2(\hat{t}-m_t^2)}(h_b\Theta^5_{j'i'1}+h_t\Theta^6_{j'i'2})(m_tN_{k3}^*N_{k4}\theta^b_{j1}\theta^t_{i1}C_2\\
&-m_{\tilde{\chi}^0_k}N_{k3}^*N_{k4}^*\theta^b_{j1}\theta^t_{j2}C_0+m_bN_{k3}N_{k4}^*\theta^b_{j2}\theta^t_{i2}C_1)(m_b^2,m_{H^+}^2,\hat{t},m_{\tilde{\chi}^0_k}^2,m_{\tilde{b}_j}^2,m_{\tilde{t}_i}^2),\\
f_5^{V_2(t)}&=-\frac{m_b}{2}f_2^{V_2(t)},\\
f_6^{V_2(t)}&=\sum_i\frac{-gh_bh_t\alpha_{1i}\alpha_{2i}}{32\sqrt{2}\pi^2(\hat{t}-m_t^2)}\{h_bm_t\beta_{21}B_0^{H^+bt}+[h_bm_t\beta_{21}(m_{H_i}^2C_0\\
&+2\hat{t}C_2+2m_b^2C_1)-h_tm_b\beta_{11}((m_t^2+\hat{t})(2C_0+C_1)\\
&+2\hat{t}C_2)](m_b^2,m_{H^+}^2,\hat{t},m_{H_i}^2,m_b^2,m_t^2)\}
\end{aligned}
$$

$$
\begin{aligned}
&+\sum_i \frac{-gh_bh_t\beta_{1i}\beta_{2i}}{32\sqrt{2}\pi^2(\hat{t}-m_t^2)}\{h_bm_t\beta_{21}B_0^{H^+bt}+[h_bm_tm_{A_i}^2\beta_{21}C_0\\
&+h_tm_b\beta_{11}(m_t^2-\hat{t})C_1](m_b^2,m_{H^+}^2,\hat{t},m_{A_i}^2,m_b^2,m_t^2)\}\\
&+\sum_{i,j,k}\sum_{i',j'}\frac{-gh_bh_t\theta^b_{jj'}\theta^t_{ii'}}{16\sqrt{2}\pi^2(\hat{t}-m_t^2)}(h_b\Theta^5_{j'i'1}+h_t\Theta^6_{j'i'2})(m_bm_tN^*_{k3}N_{k4}\theta^b_{j1}\theta^t_{i1}C_1\\
&-m_tm_{\tilde{\chi}^0_k}N_{k3}N_{k4}\theta^b_{j2}\theta^t_{j1}C_0+\hat{t}N_{k3}N^*_{k4}\theta^b_{j2}\theta^t_{i2}C_2)(m_b^2,m_{H^+}^2,\hat{t},m^2_{\tilde{\chi}^0_k},m^2_{\tilde{b}_j},m^2_{\tilde{t}_i}),
\end{aligned}
$$

$$
f_{12}^{V_2(t)}=-\frac{1}{2}f_2^{V_2(t)};
$$

$$
\begin{aligned}
f_1^{(b)}=&\sum_i\frac{gh_b^2\alpha_{2i}^2}{16\sqrt{2}\pi^2}\{h_b\beta_{21}C_0(m_{H^+}^2,m_W^2,\hat{s},m_b^2,m_t^2,m_b^2)+[-h_tm_bm_t\beta_{11}(D_{13}\\
&+D_{23})-h_b\beta_{21}2D_{00}+h_bm_b^2\beta_{21}(2D_3-D_{11}-D_{12}+D_{13}+D_{23})\\
&+h_bm_{H^+}^2\beta_{21}(D_{13}+D_{23})-h_b\hat{t}\beta_{21}(D_{12}+D_{13}+D_{22}+D_{23})\\
&+h_bm_{H_i}^2\beta_{21}D_0](m_b^2,m_{H^+}^2,m_W^2,m_b^2,\hat{t},\hat{s},m_{H_i}^2,m_b^2,m_t^2,m_b^2)\}\\
&+\sum_i\frac{gh_b^2\beta_{2i}^2}{16\sqrt{2}\pi^2}\{-h_b\beta_{21}C_0(m_{H^+}^2,m_W^2,\hat{s},m_b^2,m_t^2,m_b^2)+[-h_tm_bm_t\beta_{11}(D_{13}\\
&+D_{23})+2h_b\beta_{21}D_{00}+h_bm_b^2\beta_{21}(D_{11}+D_{12}+D_{13}+D_{23})\\
&-h_bm_{H^+}^2\beta_{21}(D_{13}+D_{23})+h_b\hat{t}\beta_{21}(D_{12}+D_{13}+D_{22}+D_{23})\\
&-h_bm_{A_i}^2\beta_{21}D_0](m_b^2,m_{H^+}^2,m_W^2,m_b^2,\hat{t},\hat{s},m_{A_i}^2,m_b^2,m_t^2,m_b^2)\}\\
&+\sum_i\frac{gh_bm_b\beta_{2i}}{8\sqrt{2}\pi^2}[h_t^2m_b\beta_{11}\beta_{1i}(D_1+D_{11}+D_{12}+D_{13})-h_bh_tm_t\beta_{11}\beta_{2i}(D_1\\
&+D_{12}+D_{13})+h_b^2m_b\beta_{21}\beta_{2i}(D_{12}+D_{13})]\\
&(m_b^2,m_W^2,m_{H^+}^2,m_b^2,\hat{u},\hat{s},m^2_{H_i^+},m_t^2,m_b^2,m_t^2)\\
&+\sum_{i,j,k,l}\sum_{i',k'}\frac{\sqrt{2}gh_b^2}{16\pi^2}N_{l3}\theta^b_{ii'}\theta^b_{j1}\theta^t_{k1}\theta^t_{kk'}(h_b\Theta^5_{i'k'1}+h_t\Theta^6_{i'k'1})[m_b\theta^b_{i1}\theta^b_{j1}N^*_{l3}(D_3+D_{13}\\
&+D_{23})-m_{\tilde{\chi}^0_l}N_{l3}\theta^b_{i2}\theta^b_{j1}(D_0+D_1+D_2)+m_b\theta^b_{i2}\theta^b_{j2}N^*_{l3}(D_1+D_2+D_{11}\\
&+2D_{12}+D_{22})](m_b^2,m_{H^+}^2,m_W^2,m_b^2,\hat{t},\hat{s},m^2_{\tilde{\chi}^0_l},m^2_{\tilde{b}_i},m^2_{\tilde{t}_k},m^2_{\tilde{b}_j})\\
&+\sum_{i,j,k,l}\sum_{j',l'}\frac{g\theta^b_{l1}\theta^b_{ll'}\theta^t_{i1}\theta^t_{jj'}}{8\sqrt{2}\pi^2}(h_b\Theta^5_{l'j'1}+h_t\Theta^6_{l'j'1})[h_b^2m_b\theta^t_{i1}\theta^t_{j1}U^2_{k2}(D_{12}+D_{23})\\
&-h_bh_tm_{\tilde{\chi}^+_k}\theta^t_{i2}\theta^t_{j1}U_{k2}V_{k2}D_3+h_t^2m_b\theta^t_{i2}\theta^t_{j2}V^2_{k2}(D_3+D_{33})]\\
&(m_b^2,m_W^2,m_{H^+}^2,m_b^2,\hat{u},\hat{s},m^2_{\tilde{\chi}^+_k},m^2_{\tilde{t}_i},m^2_{\tilde{b}_l},m^2_{\tilde{t}_j})\\
&+\sum_{i,j}\frac{gh_b\alpha_{2i}\varphi_{ij}}{16\sqrt{2}\pi^2}\{-h_b^2\beta_{12}\beta_{2j}C_2(m_b^2,m_{H^+}^2,\hat{t},m_{H_i}^2,m_b^2,m_t^2)\\
&+[h_t^2m_b^2\beta_{11}\beta_{1j}(D_{23}+2D_3+2D_{33})-h_bh_tm_bm_t\beta_{11}\beta_{2j}(D_{23}+2D_3)\\
&+h_bh_tm_bm_t\beta_{12}\beta_{1j}D_{33}-h_b^2\beta_{12}\beta_{2j}(m_b^2(D_{23}+D_{33})+m_W^2D_{13}+\hat{u}D_{23}\\
&+m^2_{H_j^+}D_3)](m_W^2,m_b^2,m_{H^+}^2,m_b^2,\hat{u},\hat{t},m^2_{H_j^+},m^2_{H_i}m_b^2,m_t^2)\}
\end{aligned}
$$

$$
\begin{aligned}
&+\sum_i \frac{g h_b \beta_{2i}}{16\sqrt{2}\pi^2}\{h_b^2\beta_{21}\beta_{2i}(C_0+C_1+C_2)(m_{H^+}^2, m_b^2, \hat{t}, m_t^2, m_b^2, m_{A_i}^2) \\
&+[h_b^2\beta_{21}\beta_{2i}(m_b^2(D_{12}-D_{11})+m_W^2 D_{13}-\hat{u}D_{12}-m_{H_i^+}^2 D_1) \\
&+h_b h_t m_b m_t(\beta_{21}\beta_{1i}D_{11}-\beta_{11}\beta_{2i}D_{12})+h_t^2 m_b^2\beta_{11}\beta_{1i}D_{12}] \\
&(m_b^2, m_{H^+}^2, m_b^2, m_W^2, \hat{u}, \hat{t}, m_{H_i^+}^2, m_t^2, m_b^2, m_{A_i}^2)\} \\
&+\sum_{i,j,k,l}\sum_{k',l'} \frac{g h_b \theta_{kk'}^b \theta_{ll'}^t}{8\pi^2}(h_b\Theta_{k'l'1}^5+h_t\Theta_{k'l'1}^6)[h_b\theta_{k1}^b\theta_{l1}^t U_{j2}(m_b N_{i3}^* O_{ij}^{R*} D_{23} \\
&+m_{\tilde{\chi}_j^+} N_{i3} O_{ij}^{L*} D_3)+h_t m_b \theta_{k2}^b \theta_{l2}^t N_{i3} V_{j2} O_{ij}^{L*} D_{33}] \\
&(m_W^2, m_b^2, m_{H^+}^2, m_b^2, \hat{u}, \hat{t}, m_{\tilde{\chi}_j^+}^2, m_{\tilde{\chi}_i^0}^2, m_{\tilde{b}_k}^2, m_{\tilde{t}_l}^2),
\end{aligned}
$$

$$
\begin{aligned}
f_2^{(b)} &= \sum_i \frac{g h_b^2 \alpha_{2i}^2}{16\sqrt{2}\pi^2}[-h_t m_b m_t \beta_{11}(2D_1+2D_2+D_{11}+2D_{12}+D_{22}) \\
&+h_b m_b^2 \beta_{21}(4D_0+6D_1+2D_{11}+4D_{12}+D_{13}+6D_2+2D_{22} \\
&+D_{23}+2D_3)](m_b^2, m_{H^+}^2, m_W^2, m_b^2, \hat{t}, \hat{s}, m_{H_i}^2, m_b^2, m_t^2, m_b^2) \\
&+\sum_i \frac{-g h_b^2 \beta_{2i}^2}{16\sqrt{2}\pi^2}[h_t m_b m_t \beta_{11}(D_{11}+2D_{12}+D_{22}) \\
&+h_b m_b^2 \beta_{21}(D_{13}+D_{23})](m_b^2, m_{H^+}^2, m_W^2, m_b^2, \hat{t}, \hat{s}, m_{A_i}^2, m_b^2, m_t^2, m_b^2) \\
&+\sum_i \frac{g h_b \beta_{2i}}{8\sqrt{2}\pi^2}\{h_t^2\beta_{11}\beta_{1i}(C_0+C_1+C_2)(m_W^2, m_{H^+}^2, \hat{s}, m_t^2, m_b^2, m_t^2) \\
&+[-h_b h_t m_b m_t(\beta_{1i}\beta_{21}D_1+\beta_{11}\beta_{2i}D_{11})+h_b^2 m_b^2\beta_{21}\beta_{2i}^2(D_1+D_{11}) \\
&+h_t^2\beta_{11}\beta_{1i}(-m_b^2 D_{11}+m_W^2 D_{13}-\hat{u}D_{12}-\hat{u}D_{13} \\
&-m_{H_i^+}^2 D_1)](m_b^2, m_W^2, m_{H^+}^2, m_b^2, \hat{u}, \hat{s}, m_{H_i^+}^2, m_t^2, m_b^2, m_t^2)\} \\
&+\sum_{i,j,k,l}\sum_{i',k'} \frac{\sqrt{2} g h_b^2}{16\pi^2} N_{l3}^* \theta_{ii'}^b \theta_{j1}^b \theta_{k1}^t \theta_{kk'}^t (h_b\Theta_{i'k'1}^5+h_t\Theta_{i'k'1}^6)[m_b\theta_{i1}^b\theta_{j1}^b N_{l3}(D_1+D_2 \\
&+D_{11}+2D_{12}+D_{22})-m_{\tilde{\chi}_l^0} N_{l3}^* \theta_{i1}^b \theta_{j2}^b (D_0+D_1+D_2)+m_b\theta_{i2}^b\theta_{j2}^b N_{l3}(D_{13} \\
&+D_{23}+D_3)](m_b^2, m_{H^+}^2, m_W^2, m_b^2, \hat{t}, \hat{s}, m_{\tilde{\chi}_l^0}^2, m_{\tilde{b}_i}^2, m_{\tilde{t}_k}^2, m_{\tilde{b}_j}^2) \\
&+\sum_{i,j,k,l}\sum_{j',l'} \frac{g\theta_{l1}^b\theta_{ll'}^b\theta_{i1}^t\theta_{jj'}^t}{8\sqrt{2}\pi^2}(h_b\Theta_{l'j'1}^5+h_t\Theta_{l'j'1}^6)[h_b^2 m_b \theta_{i1}^t\theta_{j1}^t U_{k2}^2 D_{33} \\
&-h_b h_t m_{\tilde{\chi}_k^+}\theta_{i1}^t\theta_{j2}^t U_{k2} V_{k2} D_3+h_t^2 m_b \theta_{i2}^t\theta_{j2}^t V_{k2}^2(D_{13}+D_{23})] \\
&(m_b^2, m_W^2, m_{H^+}^2, m_b^2, \hat{u}, \hat{s}, m_{\tilde{\chi}_k^+}^2, m_{\tilde{t}_i}^2, m_{\tilde{b}_l}^2, m_{\tilde{t}_j}^2) \\
&+\sum_{i,j} \frac{g h_b \alpha_{2i}\varphi_{ij}}{16\sqrt{2}\pi^2}\{h_t^2\beta_{11}\beta_{1j}C_2(m_b^2, m_{H^+}^2, \hat{t}, m_{H_i}^2, m_b^2, m_t^2)+[-h_b^2 m_b^2\beta_{12}\beta_{2j}(D_{23} \\
&+2D_3+2D_{33})-h_b h_t m_b m_t \beta_{11}\beta_{2j}D_{33}+h_b h_t m_b m_t \beta_{12}\beta_{1j}(D_{23}+2D_3) \\
&+h_t^2\beta_{11}\beta_{1j}(m_b^2(D_{23}+D_{33})+m_W^2 D_{13}+\hat{u}D_{23} \\
&+m_{H_j^+}^2 D_3)](m_W^2, m_b^2, m_{H^+}^2, m_b^2, \hat{u}, \hat{t}, m_{H_j^+}^2, m_{H_i} m_b^2, m_t^2)\}
\end{aligned}
$$

$$
\begin{aligned}
& -\sum_i \frac{g h_b \beta_{2i}}{16\sqrt{2}\pi^2}\{h_t^2\beta_{11}\beta_{1i}(C_0+C_1+C_2)(m_{H^+}^2, m_b^2, \hat{t}, m_t^2, m_b^2, m_{A_i}^2) \\
& +[h_t^2\beta_{11}\beta_{1i}(m_b^2(D_{12}-D_{11})+m_W^2 D_{13}-\hat{u}D_{12}-m_{H_i^+}^2 D_1) \\
& +h_b h_t m_b m_t(\beta_{11}\beta_{2i}D_{11}-\beta_{21}\beta_{1i}D_{12})+h_b^2\beta_{21}\beta_{2i}D_{12}] \\
& (m_b^2, m_{H^+}^2, m_b^2, m_W^2, \hat{u}, \hat{t}, m_{H_i^+}^2, m_t^2, m_b^2, m_{A_i}^2)\} \\
& +\sum_{i,j,k,l}\sum_{k',l'}\frac{g h_b \theta_{kk'}^b \theta_{ll'}^t}{8\pi^2}(h_b\Theta_{k'l'1}^5+h_t\Theta_{k'l'1}^6)[h_t\theta_{k2}^b\theta_{l2}^t V_{j2}(m_b N_{i3}O_{ij}^{L*}D_{23} \\
& +m_{\tilde{\chi}_j^+}N_{i3}^* O_{ij}^{R*}D_3)+h_b m_b\theta_{k1}^b\theta_{l1}^t N_{i3}^* U_{j2}O_{ij}^{R*}D_{33}] \\
& (m_W^2, m_b^2, m_{H^+}^2, m_b^2, \hat{u}, \hat{t}, m_{\tilde{\chi}_j^+}^2, m_{\tilde{\chi}_i^0}^2, m_{\tilde{b}_k}^2, m_{\tilde{t}_l}^2),
\end{aligned}
$$

$$
\begin{aligned}
f_3^{(b)} = & \sum_i \frac{g h_b^2 \alpha_{2i}^2}{16\sqrt{2}\pi^2}\{-h_b m_b^2\beta_{21}C_2(m_{H^+}^2, m_W^2, \hat{s}, m_b^2, m_t^2, m_b^2)+[h_t m_b m_t\beta_{11}(2D_3 \\
& +D_{33})-2h_b m_b^2\beta_{21}D_{33}+h_b m_W^2\beta_{21}D_{13}-h_b\hat{t}\beta_{21}(D_{13}+D_{23}) \\
& -h_b m_{H_i}^2\beta_{21}D_3](m_b^2, m_{H^+}^2, m_W^2, m_b^2, \hat{t}, \hat{s}, m_{H_i}^2, m_b^2, m_t^2, m_b^2)\} \\
& +\sum_i \frac{g h_b^2\beta_{2i}^2}{16\sqrt{2}\pi^2}\{h_b\beta_{21}C_2(m_{H^+}^2, m_W^2, \hat{s}, m_b^2, m_t^2, m_b^2) \\
& +[h_t m_b m_t\beta_{11}D_{33}-h_b m_W^2\beta_{21}D_{13}+h_b\hat{t}\beta_{21}(D_{13}+D_{23}) \\
& +h_b m_{A_i}^2\beta_{21}D_3](m_b^2, m_{H^+}^2, m_W^2, m_b^2, \hat{t}, \hat{s}, m_{A_i}^2, m_b^2, m_t^2, m_b^2)\} \\
& +\sum_i \frac{g\beta_{2i}}{8\sqrt{2}\pi^2}[h_t^3 m_b m_t\beta_{11}\beta_{1i}(D_0+D_1+D_2+D_3)-h_b h_t^2 m_b^2\beta_{11}\beta_{1i}(D_0+D_1 \\
& +D_{12}+D_{13}+2D_2+D_{22}+2D_{23}+2D_3+D_{33})-h_b h_t^2 m_t^2\beta_{11}\beta_{1i}(D_0+D_2 \\
& +D_3)+h_b^2 h_t m_b m_t\beta_{1i}\beta_{21}(D_2+D_3)+h_b^2 h_t m_b m_t\beta_{11}\beta_{2i}(D_1+2D_2+D_{22} \\
& +2D_{23}+2D_3+D_{33})-h_b^3 m_b^2\beta_{21}\beta_{2i}(D_2+D_{22}+2D_{23}+D_3+D_{33})] \\
& (m_b^2, m_W^2, m_{H^+}^2, m_b^2, \hat{u}, \hat{s}, m_{H_i^+}^2, m_t^2, m_b^2, m_t^2) \\
& +\sum_{i,j,k,l}\sum_{i',k'}\frac{-\sqrt{2}g h_b^2}{16\pi^2}N_{l3}\theta_{ii'}^b\theta_{j1}^b\theta_{k1}^t\theta_{kk'}^t(h_b\Theta_{i'k'1}^5+h_t\Theta_{i'k'1}^6)[m_b\theta_{i1}^b\theta_{j1}^b N_{l3}^* D_{33} \\
& -m_{\tilde{\chi}_l^0}N_{l3}\theta_{i2}^b\theta_{j1}^b D_3+m_b\theta_{i2}^b\theta_{j2}^b N_{l3}^*(D_{13}+D_{23})] \\
& (m_b^2, m_{H^+}^2, m_W^2, m_b^2, \hat{t}, \hat{s}, m_{\tilde{\chi}_l^0}^2, m_{\tilde{b}_i}^2, m_{\tilde{t}_k}^2, m_{\tilde{b}_j}^2) \\
& +\sum_{i,j,k,l}\sum_{j',l'}\frac{g\theta_{l1}^b\theta_{ll'}^b\theta_{i1}^t\theta_{jj'}^t}{8\sqrt{2}\pi^2}(h_b\Theta_{l'j'1}^5+h_t\Theta_{l'j'1}^6)[h_b h_t m_{\tilde{\chi}_k^+}\theta_{i2}^t\theta_{j1}^t U_{k2}V_{k2}(D_0+D_1+D_2) \\
& -h_t^2 m_b\theta_{i2}^t\theta_{j2}^t V_{k2}^2(D_{13}+D_{33}+D_3)-h_b^2 m_b\theta_{i1}^t\theta_{j1}^t U_{k2}^2(D_1+D_{11}+2D_{12}+D_2 \\
& +D_{22})](m_b^2, m_W^2, m_{H^+}^2, m_b^2, \hat{u}, \hat{s}, m_{\tilde{\chi}_k^+}^2, m_{\tilde{t}_i}^2, m_{\tilde{b}_l}^2, m_{\tilde{t}_j}^2) \\
& +\sum_{i,j}\frac{g h_b\alpha_{2i}\varphi_{ij}}{16\sqrt{2}\pi^2}\{h_b^2\beta_{12}\beta_{2j}C_1(m_b^2, m_{H^+}^2, \hat{t}, m_{H_i}^2, m_b^2, m_t^2)+[-h_t^2 m_b^2\beta_{11}\beta_{1j}(2D_2 \\
& +D_{22}+2D_{23})+h_b h_t m_b m_t\beta_{11}\beta_{2j}(D_{22}+2D_2)-h_b h_t m_b m_t\beta_{12}\beta_{1j}D_{23} \\
& +h_b^2\beta_{12}\beta_{2j}(m_b^2(D_{22}+D_{23})+m_W^2 D_{12}+\hat{u}D_{22}+m_{H_j^+}^2 D_2)]
\end{aligned}
$$

$$
\begin{aligned}
&(m_W^2, m_b^2, m_{H^+}^2, m_b^2, \hat{u}, \hat{t}, m_{H_j^+}^2, m_{H_i}^2 m_b^2, m_t^2)\}\\
&+\sum_i \frac{g h_b \beta_{2i}}{16\sqrt{2}\pi^2}\{h_b^2\beta_{21}\beta_{2i}C_1(m_{H^+}^2, m_b^2, \hat{t}, m_t^2, m_b^2, m_{A_i}^2) + [h_b^2\beta_{21}\beta_{2i}(m_b^2(D_{12}\\
&-D_{22}) + m_W^2 D_{23} + \hat{u}D_{22} + m_{H_i^+}^2 D_2) - h_b h_t m_b m_t(\beta_{11}\beta_{2i}D_{12} - \beta_{21}\beta_{1i}D_{22})\\
&-h_t^2 m_b^2 \beta_{11}\beta_{1i}D_{22}](m_b^2, m_{H^+}^2, m_b^2, m_W^2, \hat{u}, \hat{t}, m_{H_i^+}^2, m_t^2, m_b^2, m_{A_i}^2)\}\\
&+\sum_{i,j,k,l}\sum_{k',l'} \frac{g h_b \theta_{kk'}^b \theta_{ll'}^t}{8\pi^2}(h_b\Theta_{k'l'1}^5 + h_t\Theta_{k'l'1}^6)[h_b\theta_{k1}^b\theta_{l1}^t U_{j2}O_{ij}^{R*}(-m_b N_{i3}^* D_{22}\\
&+m_{\tilde{\chi}_i^0}N_{i3}D_2) - h_t m_b \theta_{k2}^b\theta_{l2}^t N_{i3}V_{j2}O_{ij}^{L*}D_{23}]\\
&(m_W^2, m_b^2, m_{H^+}^2, m_b^2, \hat{u}, \hat{t}, m_{\tilde{\chi}_j^+}^2, m_{\tilde{\chi}_i^0}^2, m_{\tilde{b}_k}^2, m_{\tilde{t}_l}^2),
\end{aligned}
$$

$$
\begin{aligned}
f_4^{(b)} =& \sum_i \frac{g h_b^2 \alpha_{2i}^2}{16\sqrt{2}\pi^2}[h_t m_b m_t \beta_{11}(D_{13} + D_{23}) - h_b m_b^2 \beta_{21}(2D_{13} + 2D_{23}\\
&+2D_3 + D_{33})](m_b^2, m_{H^+}^2, m_W^2, m_b^2, \hat{t}, \hat{s}, m_{H_i}^2, m_b^2, m_t^2, m_b^2)\\
&+\sum_i \frac{g h_b^2 \beta_{2i}^2}{16\sqrt{2}\pi^2}[h_t m_b m_t \beta_{11}(D_{13} + D_{23}) + h_b m_b^2 \beta_{21}D_{33}]\\
&(m_b^2, m_{H^+}^2, m_W^2, m_b^2, \hat{t}, \hat{s}, m_{A_i}^2, m_b^2, m_t^2, m_b^2)\\
&+\sum_i \frac{g h_b \beta_{2i}}{8\sqrt{2}\pi^2}\{-h_t^2\beta_{11}\beta_{1i}C_0(m_W^2, m_{H^+}^2, \hat{s}, m_t^2, m_b^2, m_t^2) + [h_b h_t m_b m_t \beta_{11}\beta_{2i}(D_1\\
&+D_{12} + D_{13}) - h_b^2 m_b^2 \beta_{21}\beta_{2i}(D_{12} + D_{13}) - h_t^2\beta_{11}\beta_{1i}(-2D_{00} + m_b^2(D_1 - D_{23}\\
&-D_{33}) + m_{H^+}^2(D_{12} + D_{13}) - \hat{u}(D_{12} + D_{13} + D_{22} + D_{23})\\
&+m_{H_i^+}^2 D_0)](m_b^2, m_W^2, m_{H^+}^2, m_b^2, \hat{u}, \hat{s}, m_{H_i^+}^2, m_t^2, m_b^2, m_t^2)\}\\
&+\sum_{i,j,k,l}\sum_{i',k'} \frac{-\sqrt{2}g h_b^2}{16\pi^2}N_{l3}^*\theta_{ii'}^b\theta_{j1}^b\theta_{k1}^t\theta_{kk'}^t(h_b\Theta_{i'k'1}^5 + h_t\Theta_{i'k'1}^6)[m_b\theta_{i2}^b\theta_{j2}^b N_{l3}D_{33}\\
&-m_{\tilde{\chi}_l^0}N_{l3}^*\theta_{i1}^b\theta_{j2}^b D_3 + m_b\theta_{i1}^b\theta_{j1}^b N_{l3}(D_{13} + D_{23})]\\
&(m_b^2, m_{H^+}^2, m_W^2, m_b^2, \hat{t}, \hat{s}, m_{\tilde{\chi}_l^0}^2, m_{\tilde{b}_i}^2, m_{\tilde{t}_k}^2, m_{\tilde{b}_j}^2)\\
&+\sum_{i,j,k,l}\sum_{j',l'} \frac{g\theta_{l1}^b\theta_{ll'}^b\theta_{i1}^t\theta_{jj'}^t}{8\sqrt{2}\pi^2}(h_b\Theta_{l'j'1}^5 + h_t\Theta_{l'j'1}^6)[-h_b^2 m_b\theta_{i1}^t\theta_{j1}^t U_{k2}^2(D_{13} + D_{23} + D_3)\\
&+h_b h_t m_{\tilde{\chi}_k^+}\theta_{i1}^t\theta_{j2}^t U_{k2}V_{k2}(D_0 + D_1 + D_2) - h_t^2 m_b\theta_{i2}^t\theta_{j2}^t V_{k2}^2(D_1 + D_2 + D_{11}\\
&+2D_{12} + D_{22})](m_b^2, m_W^2, m_{H^+}^2, m_b^2, \hat{u}, \hat{s}, m_{\tilde{\chi}_k^+}^2, m_{\tilde{t}_i}^2, m_{\tilde{b}_l}^2, m_{\tilde{t}_j}^2)\\
&+\sum_{i,j} \frac{g h_b \alpha_{2i}\varphi_{ij}}{16\sqrt{2}\pi^2}\{-h_t^2\beta_{11}\beta_{1j}C_1(m_b^2, m_{H^+}^2, \hat{t}, m_{H_i}^2, m_b^2, m_t^2) + [h_b^2 m_b^2\beta_{12}\beta_{2j}(2D_2\\
&+D_{22} + 2D_{23}) + h_b h_t m_b m_t(\beta_{11}\beta_{2j}D_{23} + \beta_{12}\beta_{1j}(D_{22} + 2D_2))\\
&-h_t^2\beta_{11}\beta_{1j}(m_b^2(D_{22} + D_{23}) + m_W^2 D_{12} + \hat{u}D_{22} + m_{H_j^+}^2 D_2)]\\
&(m_W^2, m_b^2, m_{H^+}^2, m_b^2, \hat{u}, \hat{t}, m_{H_j^+}^2, m_{H_i}^2 m_b^2, m_t^2)\}
\end{aligned}
$$

$$
\begin{aligned}
& -\sum_i \frac{g h_b \beta_{2i}}{16\sqrt{2}\pi^2}\{h_t^2\beta_{11}\beta_{1i}C_1(m_{H^+}^2, m_b^2, \hat{t}, m_t^2, m_b^2, m_{A_i}^2) + [h_t^2\beta_{11}\beta_{1i}(m_b^2(D_{12} \\
& -D_{22}) + m_W^2 D_{23} + \hat{u}D_{22} + m_{H_i^+}^2 D_2) - h_b h_t m_b m_t(\beta_{21}\beta_{1i}D_{12} - \beta_{11}\beta_{2i}D_{22}) \\
& -h_b^2 m_b^2 \beta_{21}\beta_{2i}D_{22}](m_b^2, m_{H^+}^2, m_b^2, m_W^2, \hat{u}, \hat{t}, m_{H_i^+}^2, m_t^2, m_b^2, m_{A_i}^2)\} \\
& + \sum_{i,j,k,l}\sum_{k',l'} \frac{g h_b \theta_{kk'}^b \theta_{ll'}^t}{8\pi^2}(h_b\Theta_{k'l'1}^5 + h_t\Theta_{k'l'1}^6)[h_t\theta_{k2}^b\theta_{l2}^t V_{j2}O_{ij}^{L*}(-m_b N_{i3}D_{22} \\
& +m_{\tilde{\chi}_i^0}N_{i3}^* D_2) - h_b m_b \theta_{k1}^b\theta_{l1}^t N_{i3}^* U_{j2}O_{ij}^{R*}D_{23}] \\
& (m_W^2, m_b^2, m_{H^+}^2, m_b^2, \hat{u}, \hat{t}, m_{\tilde{\chi}_j^+}^2, m_{\tilde{\chi}_i^0}^2, m_{\tilde{b}_k}^2, m_{\tilde{t}_l}^2), \\
f_5^{(b)} = & \sum_i \frac{g h_b^2 \alpha_{2i}^2}{32\sqrt{2}\pi^2}\{[h_t m_t \beta_{11}C_0 - h_b m_b \beta_{21}(2C_0 + C_2)](m_{H^+}^2, m_W^2, \hat{s}, m_b^2, m_t^2, m_b^2) \\
& +[2h_t m_b^2 m_t \beta_{11}(D_1 + D_2 + D_3) + 4h_b m_b \beta_{21}D_{00} - 2h_t m_t \beta_{11}D_{00} \\
& -h_b m_b^3 \beta_{21}(4D_0 + 6D_1 + D_{13} + 4D_2 + 4D_3 + D_{33}) + h_b m_b m_{H^+}^2 \beta_{21}(2D_3 \\
& +D_{33}) + h_b m_b m_W^2 \beta_{21}D_{13} - h_b m_b \hat{t}\beta_{21}(D_{13} + 2D_2 + 2D_{23} + 2D_3 + D_{33}) \\
& +h_t m_t m_{H_i}^2 \beta_{11}D_0 - h_b m_b m_{H_i}^2 \beta_{21}(2D_0 + D_3)] \\
& (m_b^2, m_{H^+}^2, m_W^2, m_b^2, \hat{t}, \hat{s}, m_{H_i}^2, m_b^2, m_t^2, m_b^2)\} \\
& + \sum_i \frac{g h_b^2 \beta_{2i}^2}{32\sqrt{2}\pi^2}\{(h_t m_t \beta_{11}C_0 + h_b m_b \beta_{21}C_2)(m_{H^+}^2, m_W^2, \hat{s}, m_b^2, m_t^2, m_b^2) \\
& +[h_b m_b^3 \beta_{21}(D_{13} + D_{33}) - 2h_t m_t \beta_{11}D_{00} - h_b m_b m_{H^+}^2 \beta_{21}D_{33} \\
& -h_b m_b m_W^2 \beta_{21}D_{13} + h_b m_b \hat{t}\beta_{21}(D_{13} + 2D_{23} + D_{33}) + h_t m_t m_{A_i}^2 \beta_{11}D_0 \\
& +h_b m_b m_{A_i}^2 \beta_{21}D_3](m_b^2, m_{H^+}^2, m_W^2, m_b^2, \hat{t}, \hat{s}, m_{A_i}^2, m_b^2, m_t^2, m_b^2)\} \\
& + \sum_i \frac{g}{16\sqrt{2}\pi^2}\{h_b\beta_{2i}[-h_b^2 m_b \beta_{21}\beta_{2i}C_0 + h_b h_t m_t \beta_{11}\beta_{2i}C_0 + h_t^2 m_b \beta_{11}\beta_{1i}(C_1 \\
& +C_2)](m_W^2, m_{H^+}^2, \hat{s}, m_t^2, m_b^2, m_t^2) + [h_t^3 m_b^2 m_t \beta_{11}\beta_{1i}^2(D_0 + D_1 + D_2 + D_3) \\
& +h_b^2 h_t m_b^2 m_t \beta_{1i}\beta_{21}\beta_{2i}(D_1 + D_2 + D_3) - h_b^3 m_b \beta_{21}\beta_{2i}^2(-2D_{00} + m_b^2(D_1 + D_2 \\
& +D_3) + m_{H_i^+}^2 D_0) + h_b^2 h_t m_t \beta_{11}\beta_{2i}^2(-2D_{00} + m_b^2(D_0 + D_2 + 2D_3) - m_{H^+}^2 D_1 \\
& +\hat{u}(D_1 + D_2) + m_{H_i^+}^2 D_0) + h_b h_t^2 m_b \beta_{11}\beta_{1i}\beta_{2i}(2D_{00} + m_{H^+}^2(D_1 + D_{11}) \\
& -m_t^2(D_0 + D_2 + D_3) + m_W^2 D_{13} - m_{H_i^+}^2(D_0 + D_1) - m_b^2(2D_1 + D_{11} \\
& +D_2 + 2D_3) - \hat{u}(D_1 + D_{11} + 2D_{12} + D_{13} + D_2))] \\
& (m_b^2, m_W^2, m_{H^+}^2, m_b^2, \hat{u}, \hat{s}, m_{H_i^+}^2, m_t^2, m_b^2, m_t^2)\} \\
& + \sum_{i,j,k}\sum_{i',k'} \frac{\sqrt{2}g h_b^2}{16\pi^2}|N_{l3}|^2 \theta_{ii'}^b \theta_{i1}^b (\theta_{j1}^b)^2 \theta_{k1}^t \theta_{kk'}^t (h_b\Theta_{i'k'1}^5 + h_t\Theta_{i'k'1}^6)D_{00} \\
& (m_b^2, m_{H^+}^2, m_W^2, m_b^2, \hat{t}, \hat{s}, m_{\tilde{\chi}_l^0}^2, m_{\tilde{b}_i}^2, m_{\tilde{t}_k}^2, m_{\tilde{b}_j}^2) \\
& + \sum_{i,j,k,l}\sum_{j',l'} \frac{g h_b^2 \theta_{l1}^b \theta_{ll'}^b (\theta_{i1}^t)^2 \theta_{j1}^t \theta_{jj'}^t U_{k2}^2}{8\sqrt{2}\pi^2}(h_b\Theta_{l'j'1}^5 + h_t\Theta_{l'j'1}^6)D_{00} \\
& (m_b^2, m_W^2, m_{H^+}^2, m_b^2, \hat{u}, \hat{s}, m_{\tilde{\chi}_k^+}^2, m_{\tilde{t}_i}^2, m_{\tilde{b}_l}^2, m_{\tilde{t}_j}^2)
\end{aligned}
$$

$$
\begin{aligned}
&+\sum_{i,j}\frac{gh_b\alpha_{2i}\varphi_{ij}}{16\sqrt{2}\pi^2}(h_t^2m_b\beta_{11}\beta_{1j}-h_bh_t\beta_{11}\beta_{2j}-2h_b^2m_b\beta_{12}\beta_{2j})D_{00}\\
&(m_W^2,m_b^2,m_{H^+}^2,m_b^2,\hat{u},\hat{t},m_{H_j^+}^2,m_{H_i}^2m_b^2,m_t^2)\\
&+\sum_{i}\frac{gh_bh_t\beta_{11}\beta_{2i}}{16\sqrt{2}\pi^2}(h_tm_b\beta_{1i}-h_bm_t\beta_{2i})D_{00}(m_b^2,m_{H^+}^2,m_b^2,m_W^2,\hat{u},\hat{t},m_{H_i^+}^2,m_t^2,m_b^2,m_{A_i}^2)\\
&+\sum_{i,j,k,l}\sum_{k',l'}\frac{gh_b\theta^b_{kk'}\theta^t_{ll'}}{16\pi^2}(h_b\Theta^5_{k'l'1}+h_t\Theta^6_{k'l'1})\{-h_b\theta^b_{k1}\theta^t_{l1}N^*_{i3}U_{j2}O^{R*}_{ij}\\
&C_0(m_b^2,m_{H^+}^2,\hat{t},m_{\tilde{\chi}_i^0}^2,m_{\tilde{b}_k}^2,m_{\tilde{t}_l}^2)+[h_bm_{\tilde{\chi}_i^0}m_{\tilde{\chi}_j^+}\theta^b_{k1}\theta^t_{l1}N^*_{i3}U_{j2}O^{L*}_{ij}D_0\\
&+h_b\theta^b_{k1}\theta^t_{l1}N^*_{i3}U_{j2}O^{R*}_{ij}(2D_{00}+m_b^2D_2-m_W^2D_1-\hat{u}D_2-m_{\tilde{\chi}_j^+}^2D_0)\\
&+h_bm_b\theta^b_{k2}\theta^t_{l1}N_{i3}U_{j2}(-m_{\tilde{\chi}_j^+}O^{L*}_{ij}+m_{\tilde{\chi}_i^0}O^{R*}_{ij})D_2+h_tm_b\theta^b_{k1}\theta^t_{l2}N^*_{i3}V_{j2}(m_{\tilde{\chi}_j^+}O^{R*}_{ij}\\
&-m_{\tilde{\chi}_i^0}O^{L*}_{ij})D_3](m_W^2,m_b^2,m_{H^+}^2,m_b^2,\hat{u},\hat{t},m_{\tilde{\chi}_j^+}^2,m_{\tilde{\chi}_i^0}^2,m_{\tilde{b}_k}^2,m_{\tilde{t}_l}^2)\},
\end{aligned}
$$

$$
\begin{aligned}
f_6^{(b)}=&\sum_{i}\frac{gh_b^2\alpha_{2i}^2}{32\sqrt{2}\pi^2}\{-h_bm_b\beta_{21}C_2(m_{H^+}^2,m_W^2,\hat{s},m_b^2,m_t^2,m_b^2)+[-2h_tm_b^2m_t\beta_{11}(2D_0\\
&+D_1+D_2+D_3)+4h_bm_b\beta_{21}D_{00}+h_bm_b^3\beta_{21}(D_{11}+D_{12}+D_{13}+D_{23}+2D_3)\\
&-h_bm_bm_{H^+}^2\beta_{21}(D_{13}+D_{23})-h_bm_bm_W^2\beta_{21}(2D_1+D_{11}+D_{12})\\
&+h_bm_b\hat{t}\beta_{21}(2D_1+D_{11}+3D_{12}+D_{13}+2D_2+2D_{22}+D_{33})\\
&+h_bm_bm_{H_i}^2\beta_{21}(D_0+D_1+D_2)](m_b^2,m_{H^+}^2,m_W^2,m_b^2,\hat{t},\hat{s},m_{H_i}^2,m_b^2,m_t^2,m_b^2)\}\\
&+\sum_{i}\frac{gh_b^3m_b\beta_{21}\beta_{2i}^2}{32\sqrt{2}\pi^2}\{(2C_0+C_2)(m_{H^+}^2,m_W^2,\hat{s},m_b^2,m_t^2,m_b^2)+[-4D_{00}-m_b^2(D_{11}\\
&+D_{12}+D_{13}+D_{23})+m_{H^+}^2(D_{13}+D_{23})+m_W^2(D_{11}+D_{12})-\hat{t}(D_{11}+3D_{12}\\
&+D_{13}+2D_{22}+D_{23})+m_{A_i}^2(D_0-D_1-D_2)]\\
&(m_b^2,m_{H^+}^2,m_W^2,m_b^2,\hat{t},\hat{s},m_{A_i}^2,m_b^2,m_t^2,m_b^2)\}\\
&+\sum_{i}\frac{g}{16\sqrt{2}\pi^2}\{h_t^2\beta_{11}\beta_{1i}[h_bm_b\beta_{2i}(C_1+C_2)-h_tm_t\beta_{1i}C_0]\\
&(m_W^2,m_{H^+}^2,\hat{s},m_t^2,m_b^2,m_t^2)+[h_bh_t^2m_bm_t^2\beta_{1i}^2\beta_{21}D_0-h_b^2h_tm_b^2m_t\beta_{1i}\beta_{21}\beta_{2i}(2D_0\\
&+D_1+D_2+D_3)+h_b^3m_b^3\beta_{21}\beta_{2i}^2(D_0+D_1+D_2+D_3)-h_t^3m_t\beta_{11}\beta_{1i}^2(m_b^2D_1\\
&-m_W^2D_3+\hat{u}(D_2+D_3)+m_{H_i^+}^2D_0)+h_bh_t^2m_b\beta_{11}\beta_{1i}\beta_{2i}(4D_{00}+m_b^2(D_{12}\\
&+D_{13}+D_{23}+D_{33})-m_{H^+}^2D_{13}+m_t^2D_1-m_W^2(D_{23}+D_3-D_{33})\\
&+\hat{u}(D_{12}+D_{13}+D_2+2D_{22}+3D_{23}+D_3+D_{33})+m_{H_i^+}^2(D_2+D_3))]\\
&(m_b^2,m_W^2,m_{H^+}^2,m_b^2,\hat{u},\hat{s},m_{H_i^+}^2,m_t^2,m_b^2,m_t^2)\}\\
&+\sum_{i,j,k,l}\sum_{i',k'}\frac{\sqrt{2}gh_b^2}{16\pi^2}|N_{l3}|^2\theta^b_{ii'}\theta^b_{i2}\theta^b_{j1}\theta^b_{j2}\theta^t_{k1}\theta^t_{kk'}(h_b\Theta^5_{i'k'1}+h_t\Theta^6_{i'k'1})D_{00}\\
&(m_b^2,m_{H^+}^2,m_W^2,m_b^2,\hat{t},\hat{s},m_{\tilde{\chi}_l^0}^2,m_{\tilde{b}_i}^2,m_{\tilde{t}_k}^2,m_{\tilde{b}_j}^2)
\end{aligned}
$$

$$
\begin{aligned}
&+\sum_{i,j,k,l}\sum_{j',l'}\frac{gh_t^2\theta^b_{l1}\theta^b_{ll'}(\theta^t_{i2})^2\theta^t_{j1}\theta^t_{jj'}V^2_{k2}}{8\sqrt{2}\pi^2}(h_b\Theta^5_{l'j'1}+h_t\Theta^6_{l'j'1})D_{00}\\
&(m_b^2,m_W^2,m_{H^+}^2,m_b^2,\hat{u},\hat{s},m^2_{\tilde{\chi}^+_k},m^2_{\tilde{t}_i},m^2_{\tilde{b}_l},m^2_{\tilde{t}_j})\\
&+\sum_{i,j}\frac{gh_b\alpha_{2i}\varphi_{ij}}{16\sqrt{2}\pi^2}(2h_t^2m_b\beta_{11}\beta_{1j}+h_bh_t\beta_{12}\beta_{1j}-h_b^2m_b\beta_{12}\beta_{2j})D_{00}\\
&(m_W^2,m_b^2,m_{H^+}^2,m_b^2,\hat{u},\hat{t},m^2_{H^+_j},m^2_{H_i}m_b^2,m_t^2)\\
&-\sum_{i}\frac{gh_bh_t\beta_{21}\beta_{2i}}{16\sqrt{2}\pi^2}(h_bm_b\beta_{2i}-h_tm_t\beta_{1i})D_{00}(m_b^2,m_{H^+}^2,m_b^2,m_W^2,\hat{u},\hat{t},m^2_{H^+_i},m_t^2,m_b^2,m^2_{A_i})\\
&+\sum_{i,j,k,l}\sum_{k',l'}\frac{gh_b\theta^b_{kk'}\theta^t_{ll'}}{16\pi^2}(h_b\Theta^5_{k'l'1}+h_t\Theta^6_{k'l'1})\{-h_t\theta^b_{k2}\theta^t_{l2}N_{i3}V_{j2}O^{L*}_{ij}\\
&C_0(m_b^2,m_{H^+}^2,\hat{t},m^2_{\tilde{\chi}^0_i},m^2_{\tilde{b}_k},m^2_{\tilde{t}_l})+[h_tm_{\tilde{\chi}^0_i}m_{\tilde{\chi}^+_j}\theta^b_{k2}\theta^t_{l2}N_{i3}V_{j2}O^{R*}_{ij}D_0\\
&+h_t\theta^b_{k2}\theta^t_{l2}N_{i3}V_{j2}O^{L*}_{ij}(2D_{00}+m_b^2D_2-m_W^2D_1-\hat{u}D_2-m^2_{\tilde{\chi}^+_j}D_0)\\
&+h_tm_b\theta^b_{k1}\theta^t_{l2}N^*_{i3}V_{j2}(-m_{\tilde{\chi}^+_j}O^{R*}_{ij}+m_{\tilde{\chi}^0_i}O^{L*}_{ij})D_2+h_bm_b\theta^b_{k2}\theta^t_{l1}N_{i3}U_{j2}(m_{\tilde{\chi}^+_j}O^{L*}_{ij}\\
&-m_{\tilde{\chi}^0_i}O^{R*}_{ij})D_3](m_W^2,m_b^2,m_{H^+}^2,m_b^2,\hat{u},\hat{t},m^2_{\tilde{\chi}^+_j},m^2_{\tilde{\chi}^0_i},m^2_{\tilde{b}_k},m^2_{\tilde{t}_l})\},
\end{aligned}
$$

$$
\begin{aligned}
f_7^{(b)}=&\sum_i\frac{gh_b^2\alpha^2_{2i}}{16\sqrt{2}\pi^2}[h_tm_t\beta_{11}(D_{12}+D_{22})-h_bm_b\beta_{21}(2D_{12}+D_{13}+2D_2+2D_{22}\\
&+D_{23})](m_b^2,m_{H^+}^2,m_W^2,m_b^2,\hat{t},\hat{s},m^2_{H_i},m_b^2,m_t^2,m_b^2)\\
&+\sum_i\frac{gh_b^2\beta^2_{2i}}{16\sqrt{2}\pi^2}[h_tm_t\beta_{11}(D_{12}+D_{22})+h_bm_b\beta_{21}(D_{13}+D_{23})]\\
&(m_b^2,m_{H^+}^2,m_W^2,m_b^2,\hat{t},\hat{s},m^2_{A_i},m_b^2,m_t^2,m_b^2)\\
&+\sum_i\frac{gh_b\beta^2_{2i}}{8\sqrt{2}\pi^2}[h_t^2m_b\beta_{11}\beta_{1i}(D_1+D_{11}+D_{12})-h_bh_tm_t\beta_{11}\beta_{2i}(D_1+D_{12})\\
&+h_b^2m_b\beta_{21}\beta_{2i}D_{12}](m_b^2,m_W^2,m_{H^+}^2,m_b^2,\hat{u},\hat{s},m^2_{H^+_i},m_t^2,m_b^2,m_t^2)\\
&+\sum_{i,j,k,l}\sum_{i',k'}\frac{\sqrt{2}gh_b^2}{16\pi^2}|N_{l3}|^2\theta^b_{ii'}\theta^b_{i1}(\theta^b_{j1})^2\theta^t_{k1}\theta^t_{kk'}(h_b\Theta^5_{i'k'1}+h_t\Theta^6_{i'k'1})(D_{12}+D_2+D_{22})\\
&(m_b^2,m_{H^+}^2,m_W^2,m_b^2,\hat{t},\hat{s},m^2_{\tilde{\chi}^0_l},m^2_{\tilde{b}_i},m^2_{\tilde{t}_k},m^2_{\tilde{b}_j})\\
&+\sum_{i,j,k,l}\sum_{j',l'}\frac{gh_b^2\theta^b_{l1}\theta^b_{ll'}(\theta^t_{i1})^2\theta^t_{j1}\theta^t_{jj'}U^2_{k2}}{8\sqrt{2}\pi^2}(h_b\Theta^5_{l'j'1}+h_t\Theta^6_{l'j'1})D_{23}\\
&(m_b^2,m_W^2,m_{H^+}^2,m_b^2,\hat{u},\hat{s},m^2_{\tilde{\chi}^+_k},m^2_{\tilde{t}_i},m^2_{\tilde{b}_l},m^2_{\tilde{t}_j})\\
&+\sum_{i,j}\frac{gh_b\alpha_{2i}\varphi_{ij}}{16\sqrt{2}\pi^2}[h_t^2m_b\beta_{11}\beta_{1j}(D_{13}+D_{23}+D_3+D_{33})-h_bh_tm_t\beta_{11}\beta_{2j}(D_{13}\\
&+D_{23}+D_3)-h_b^2m_b\beta_{12}\beta_{2j}(2D_{13}+D_{23})]\\
&(m_W^2,m_b^2,m_{H^+}^2,m_b^2,\hat{u},\hat{t},m^2_{H^+_j},m^2_{H_i}m_b^2,m_t^2)
\end{aligned}
$$

$$
\begin{aligned}
&+\sum_i \frac{g h_b \beta_{2i}}{16\sqrt{2}\pi^2}[h_b^2 m_b \beta_{21}\beta_{2i} D_{12} - h_b h_t m_t(\beta_{11}\beta_{2i} D_1 + \beta_{21}\beta_{1i} D_{12}) \\
&+h_t^2 m_b \beta_{11}\beta_{1i}(D_1 + D_{11} + D_{12} + D_{13})](m_b^2, m_{H^+}^2, m_b^2, m_W^2, \hat{u}, \hat{t}, m_{H_i^+}^2, m_t^2, m_b^2, m_{A_i}^2) \\
&+\sum_{i,j,k,l}\sum_{k',l'} \frac{g h_b^2}{8\pi^2}\theta_{k1}^b \theta_{kk'}^b \theta_{l1}^t \theta_{ll'}^t (h_b \Theta_{k'l'1}^5 + h_t \Theta_{k'l'1}^6) N_{i3}^* U_{j2} O_{ij}^{R*}(D_{13} \\
&+D_{23})(m_W^2, m_b^2, m_{H^+}^2, m_b^2, \hat{u}, \hat{t}, m_{\tilde{\chi}_j^+}^2, m_{\tilde{\chi}_i^0}^2, m_{\tilde{b}_k}^2, m_{\tilde{t}_l}^2),
\end{aligned}
$$

$$
\begin{aligned}
f_8^{(b)} &= \sum_i \frac{g h_b^3 m_b \alpha_{2i}^2 \beta_{21}}{16\sqrt{2}\pi^2}(2D_1 + D_{11} + D_{12}) \\
&(m_b^2, m_{H^+}^2, m_W^2, m_b^2, \hat{t}, \hat{s}, m_{H_i}^2, m_b^2, m_t^2, m_b^2) \\
&+\sum_i \frac{-g h_b^3 m_b \beta_{2i}^2 \beta_{21}}{16\sqrt{2}\pi^2}(D_{11} + D_{12})(m_b^2, m_{H^+}^2, m_W^2, m_b^2, \hat{t}, \hat{s}, m_{A_i}^2, m_b^2, m_t^2, m_b^2) \\
&+\sum_i \frac{-g h_b h_t^2 m_b}{8\sqrt{2}\pi^2}\beta_{11}\beta_{1i}\beta_{2i} D_{13}(m_b^2, m_W^2, m_{H^+}^2, m_b^2, \hat{u}, \hat{s}, m_{H_i^+}^2, m_t^2, m_b^2, m_t^2) \\
&+\sum_{i,j,k,l}\sum_{i',k'} \frac{\sqrt{2} g h_b^2}{16\pi^2}|N_{l3}|^2 \theta_{ii'}^b \theta_{i2}^b \theta_{j1}^b \theta_{j2}^b \theta_{k1}^t \theta_{kk'}^t (h_b \Theta_{i'k'1}^5 + h_t \Theta_{i'k'1}^6)(D_{12} + D_2 + D_{22}) \\
&(m_b^2, m_{H^+}^2, m_W^2, m_b^2, \hat{t}, \hat{s}, m_{\tilde{\chi}_l^0}^2, m_{\tilde{b}_i}^2, m_{\tilde{t}_k}^2, m_{\tilde{b}_j}^2) \\
&+\sum_{i,j,k,l}\sum_{j',l'} \frac{g h_t^2 \theta_{l1}^b \theta_{ll'}^b (\theta_{i2}^t)^2 \theta_{j1}^t \theta_{jj'}^t V_{k2}}{8\sqrt{2}\pi^2}(h_b \Theta_{l'j'1}^5 + h_t \Theta_{l'j'1}^6) D_{23} \\
&(m_b^2, m_W^2, m_{H^+}^2, m_b^2, \hat{u}, \hat{s}, m_{\tilde{\chi}_k^+}^2, m_{\tilde{t}_i}^2, m_{\tilde{b}_l}^2, m_{\tilde{t}_j}^2) \\
&+\sum_{i,j} \frac{g h_b \alpha_{2i}\varphi_{ij}}{16\sqrt{2}\pi^2}[h_t^2 m_b \beta_{11}\beta_{1j}(2D_{13} + D_{23}) + h_b h_t m_t \beta_{11}\beta_{2j}(D_{13} + D_{23} \\
&+D_3) - h_b^2 m_b \beta_{12}\beta_{2j}(D_{13} + D_{23} + D_{33})] \\
&(m_W^2, m_b^2, m_{H^+}^2, m_b^2, \hat{u}, \hat{t}, m_{H_j^+}^2, m_{H_i}^2 m_b^2, m_t^2) \\
&-\sum_i \frac{g h_b \beta_{2i}}{16\sqrt{2}\pi^2}[h_t^2 m_b \beta_{11}\beta_{1i} D_{12} - h_b h_t m_t(\beta_{21}\beta_{1i} D_1 + \beta_{11}\beta_{2i} D_{12}) \\
&+h_b^2 m_b \beta_{21}\beta_{2i}(D_1 + D_{11} + D_{12} + D_{13})](m_b^2, m_{H^+}^2, m_b^2, m_W^2, \hat{u}, \hat{t}, m_{H_i^+}^2, m_t^2, m_b^2, m_{A_i}^2) \\
&+\sum_{i,j,k,l}\sum_{k',l'} \frac{g h_b h_t}{8\pi^2}\theta_{k2}^b \theta_{kk'}^b \theta_{l2}^t \theta_{ll'}^t (h_b \Theta_{k'l'1}^5 + h_t \Theta_{k'l'1}^6) N_{i3} V_{j2} O_{ij}^{L*}(D_{13} \\
&+D_{23})(m_W^2, m_b^2, m_{H^+}^2, m_b^2, \hat{u}, \hat{t}, m_{\tilde{\chi}_j^+}^2, m_{\tilde{\chi}_i^0}^2, m_{\tilde{b}_k}^2, m_{\tilde{t}_l}^2),
\end{aligned}
$$

$$
\begin{aligned}
f_9^{(b)} &= \sum_i \frac{g h_b^2 \alpha_{2i}^2}{16\sqrt{2}\pi^2}[-h_t m_t \beta_{11} D_{23} + h_b m_b \beta_{21}(2D_{23} + 2D_3 + D_{33})] \\
&(m_b^2, m_{H^+}^2, m_W^2, m_b^2, \hat{t}, \hat{s}, m_{H_i}^2, m_b^2, m_t^2, m_b^2) \\
&+\sum_i \frac{-g h_b^2 \beta_{2i}^2}{16\sqrt{2}\pi^2}(h_t m_t \beta_{11} D_{23} + h_b m_b \beta_{21} D_{33}) \\
&(m_b^2, m_{H^+}^2, m_W^2, m_b^2, \hat{t}, \hat{s}, m_{A_i}^2, m_b^2, m_t^2, m_b^2)
\end{aligned}
$$

$$
\begin{aligned}
&+\sum_i \frac{g h_b \beta_{2i}}{8\sqrt{2}\pi^2}[-h_t^2 m_b \beta_{11}\beta_{1i}(D_{12}+D_{13}+D_2+D_{22}+D_{23}) \\
&+h_b h_t m_t \beta_{11}\beta_{2i}(D_2+D_{22}+D_{23}) - h_b^2 m_b \beta_{11}\beta_{2i}(D_{22} \\
&+D_{23})](m_b^2, m_W^2, m_{H^+}^2, m_b^2, \hat{u}, \hat{s}, m_{H_i^+}^2, m_t^2, m_b^2, m_t^2) \\
&+\sum_{i,j,k,l}\sum_{i',k'} \frac{\sqrt{2} g h_b^2}{16\pi^2}|N_{l3}|^2 \theta^b_{ii'}\theta^b_{i1}(\theta^b_{j1})^2\theta^t_{k1}\theta^t_{kk'}(h_b\Theta^5_{i'k'1}+h_t\Theta^6_{i'k'1})D_{23} \\
&(m_b^2, m_{H^+}^2, m_W^2, m_b^2, \hat{t}, \hat{s}, m^2_{\tilde{\chi}^0_l}, m^2_{\tilde{b}_i}, m^2_{\tilde{t}_k}, m^2_{\tilde{b}_j}) \\
&-\sum_{i,j,k,l}\sum_{j',l'} \frac{g h_b^2}{8\sqrt{2}\pi^2}\theta^b_{l1}\theta^b_{ll'}(\theta^t_{i1})^2\theta^t_{j1}\theta^t_{jj'}U^2_{k2}(h_b\Theta^5_{l'j'1}+h_t\Theta^6_{l'j'1})(D_2+D_{12}+D_{22}) \\
&(m_b^2, m_W^2, m_{H^+}^2, m_b^2, \hat{u}, \hat{s}, m^2_{\tilde{\chi}^+_k}, m^2_{\tilde{t}_i}, m^2_{\tilde{b}_l}, m^2_{\tilde{t}_j}) \\
&+\sum_{i,j} \frac{g h_b \alpha_{2i}\varphi_{ij}}{16\sqrt{2}\pi^2}[-h_t^2 m_b \beta_{11}\beta_{1j}(D_{12}+D_2+D_{22}+D_{23}) \\
&+h_b h_t m_t \beta_{11}\beta_{2j}(D_{12}+D_2+D_{22}) + h_b^2 m_b \beta_{12}\beta_{2j}(2D_{12}+D_{22})] \\
&(m_W^2, m_b^2, m_{H^+}^2, m_b^2, \hat{u}, \hat{t}, m^2_{H_j^+}, m^2_{H_i} m_b^2, m_t^2) \\
&+\sum_i \frac{g h_b \beta_{2i}}{16\sqrt{2}\pi^2}[-h_b^2 m_b \beta_{21}\beta_{2i}D_{22} + h_b h_t m_t \beta_{11}\beta_{2i}(D_2+D_{22}+D_{23}) \\
&-h_t^2 m_b \beta_{11}\beta_{1i}(D_{12}+D_2+D_{22}+D_{23})](m_b^2, m_{H^+}^2, m_b^2, m_W^2, \hat{u}, \hat{t}, m^2_{H_i^+}, m_t^2, m_b^2, m^2_{A_i}) \\
&-\sum_{i,j,k,l}\sum_{k',l'} \frac{g h_b^2}{8\pi^2}\theta^b_{k1}\theta^b_{kk'}\theta^t_{l1}\theta^t_{ll'}(h_b\Theta^5_{k'l'1}+h_t\Theta^6_{k'l'1})N^*_{i3}U_{j2}O^{R*}_{ij}(D_{12}+D_2 \\
&+D_{22})(m_W^2, m_b^2, m_{H^+}^2, m_b^2, \hat{u}, \hat{t}, m^2_{\tilde{\chi}^+_j}, m^2_{\tilde{\chi}^0_i}, m^2_{\tilde{b}_k}, m^2_{\tilde{t}_l}),
\end{aligned}
$$

$$
\begin{aligned}
f_{10}^{(b)} =& \sum_i \frac{-g h_b^3 m_b \alpha_{2i}^2 \beta_{21}}{16\sqrt{2}\pi^2} D_{13}(m_b^2, m_{H^+}^2, m_W^2, m_b^2, \hat{t}, \hat{s}, m^2_{H_i}, m_b^2, m_t^2, m_b^2) \\
&+\sum_i \frac{g h_b^3 m_b \beta_{2i}^2 \beta_{21}}{16\sqrt{2}\pi^2} D_{13}(m_b^2, m_{H^+}^2, m_W^2, m_b^2, \hat{t}, \hat{s}, m^2_{A_i}, m_b^2, m_t^2, m_b^2) \\
&+\sum_i \frac{g h_t^2 \beta_{11}\beta_{1i}}{8\sqrt{2}\pi^2}[h_t m_t \beta_{1i} D_3 + h_b m_b \beta_{2i}(D_{23}+D_3+D_{33})] \\
&(m_b^2, m_W^2, m_{H^+}^2, m_b^2, \hat{u}, \hat{s}, m^2_{H_i^+}, m_t^2, m_b^2, m_t^2) \\
&+\sum_{i,j,k,l}\sum_{i',k'} \frac{\sqrt{2} g h_b^2}{16\pi^2}|N_{l3}|^2 \theta^b_{ii'}\theta^b_{i2}\theta^b_{j1}\theta^b_{j2}\theta^t_{k1}\theta^t_{kk'}(h_b\Theta^5_{i'k'1}+h_t\Theta^6_{i'k'1})D_{23} \\
&(m_b^2, m_{H^+}^2, m_W^2, m_b^2, \hat{t}, \hat{s}, m^2_{\tilde{\chi}^0_l}, m^2_{\tilde{b}_i}, m^2_{\tilde{t}_k}, m^2_{\tilde{b}_j}) \\
&-\sum_{i,j,k,l}\sum_{j',l'} \frac{g h_t^2}{8\sqrt{2}\pi^2}\theta^b_{l1}\theta^b_{ll'}(\theta^t_{i2})^2\theta^t_{j1}\theta^t_{jj'}V^2_{k2}(h_b\Theta^5_{l'j'1}+h_t\Theta^6_{l'j'1})(D_2+D_{12}+D_{22}) \\
&(m_b^2, m_W^2, m_{H^+}^2, m_b^2, \hat{u}, \hat{s}, m^2_{\tilde{\chi}^+_k}, m^2_{\tilde{t}_i}, m^2_{\tilde{b}_l}, m^2_{\tilde{t}_j})
\end{aligned}
$$

$$
\begin{aligned}
&+\sum_{i,j}\frac{gh_b\alpha_{2i}\varphi_{ij}}{16\sqrt{2}\pi^2}[-h_t^2m_b\beta_{11}\beta_{1j}(D_{12}+D_{22})-h_bh_tm_t\beta_{12}\beta_{1j}(D_{12}+D_2+D_{22})\\
&+h_b^2m_b\beta_{12}\beta_{2j}(2D_{12}+D_{22})](m_W^2,m_b^2,m_{H^+}^2,m_b^2,\hat{u},\hat{t},m_{H_j^+}^2,m_{H_i}^2m_b^2,m_t^2)\\
&-\sum_{i}\frac{gh_b\beta_{2i}}{16\sqrt{2}\pi^2}[-h_t^2m_b\beta_{11}\beta_{1i}D_{22}+h_bh_tm_t\beta_{21}\beta_{1i}(D_2+D_{22}+D_{23})\\
&-h_b^2m_b\beta_{21}\beta_{2i}(D_{12}+D_2+D_{22}+D_{23})](m_b^2,m_{H^+}^2,m_b^2,m_W^2,\hat{u},\hat{t},m_{H_i^+}^2,m_t^2,m_b^2,m_{A_i}^2)\\
&-\sum_{i,j,k,l}\sum_{k',l'}\frac{gh_bh_t}{8\pi^2}\theta_{k2}^b\theta_{kk'}^b\theta_{l2}^t\theta_{ll'}^t(h_b\Theta_{k'l'1}^5+h_t\Theta_{k'l'1}^6)N_{i3}V_{j2}O_{ij}^{L*}(D_{12}+D_2\\
&+D_{22})(m_W^2,m_b^2,m_{H^+}^2,m_b^2,\hat{u},\hat{t},m_{\tilde{\chi}_j^+}^2,m_{\tilde{\chi}_i^0}^2,m_{\tilde{b}_k}^2,m_{\tilde{t}_l}^2),
\end{aligned}
$$

$$
\begin{aligned}
f_{11}^{(b)}=&\sum_{i}\frac{gh_b^2\alpha_{2i}^2}{32\sqrt{2}\pi^2}\{-h_b\beta_{21}(C_0-C_1)(m_{H^+}^2,m_W^2,\hat{s},m_b^2,m_t^2,m_b^2)\\
&+[h_b\beta_{21}D_{00}-2h_tm_bm_t\beta_{11}D_2-h_bm_b^2\beta_{21}(2D_1-D_{12}-D_{23}+2D_3)\\
&-h_bm_{H^+}^2\beta_{21}D_{23}-h_bm_W^2\beta_{21}D_{12}+h_b\hat{t}\beta_{21}(D_{12}+2D_{22}+D_{23})\\
&-h_bm_{H_i}^2(D_0-D_2)](m_b^2,m_{H^+}^2,m_W^2,m_b^2,\hat{t},\hat{s},m_{H_i}^2,m_b^2,m_t^2,m_b^2)\}\\
&+\sum_{i}\frac{gh_b^3\beta_{21}\beta_{2i}^2}{32\sqrt{2}\pi_2}\{(C_0-C_1)(m_{H^+}^2,m_W^2,\hat{s},m_b^2,m_t^2,m_b^2)+[-4D_{00}-m_b^2(D_{12}\\
&+D_{23})+m_{H^+}^2D_{23}+m_W^2D_{12}-\hat{t}(D_{12}+2D_{22}+D_{23})+m_{A_i}^2(D_0\\
&-D_2)](m_b^2,m_{H^+}^2,m_W^2,m_b^2,\hat{t},\hat{s},m_{A_i}^2,m_b^2,m_t^2,m_b^2)\}\\
&+\sum_{i}\frac{g}{16\sqrt{2}\pi^2}\{h_t^3m_bm_t\beta_{11}\beta_{1i}^2(D_0+D_1+D_2)-h_bh_t^2\beta_{11}\beta_{1i}\beta_{2i}[m_b^2(D_0+D_1\\
&+D_2+D_3)+m_t^2(D_0+D_2)]+h_b^2h_tm_bm_t\beta_{2i}[\beta_{1i}\beta_{21}D_2+\beta_{11}\beta_{2i}(D_0+D_2\\
&+D_3)]-h_b^3m_b^2\beta_{21}\beta_{2i}^2D_2\}(m_b^2,m_W^2,m_{H^+}^2,m_b^2,\hat{u},\hat{s},m_{H_i^+}^2,m_t^2,m_b^2,m_t^2)\\
&-\sum_{i,j}\frac{gh_b^3\alpha_{2i}\beta_{12}\beta_{2j}\varphi_{ij}}{16\sqrt{2}\pi^2}D_{00}(m_W^2,m_b^2,m_{H^+}^2,m_b^2,\hat{u},\hat{t},m_{H_j^+}^2,m_{H_i}^2m_b^2,m_t^2)\\
&-\sum_{i}\frac{gh_b^3\beta_{21}\beta_{2i}^2}{16\sqrt{2}\pi^2}D_{00}(m_b^2,m_{H^+}^2,m_b^2,m_W^2,\hat{u},\hat{t},m_{H_i^+}^2,m_t^2,m_b^2,m_{A_i}^2)\\
&+\sum_{i,j,k,l}\sum_{k',l'}\frac{gh_b\theta_{kk'}^b\theta_{ll'}^t}{16\pi^2}(h_b\Theta_{k'l'1}^5+h_t\Theta_{k'l'1}^6)\{h_bm_b\theta_{k1}^b\theta_{l1}^tN_{i3}^*U_{j2}D_2\\
&+h_b\theta_{k2}^b\theta_{l1}^tN_{i3}U_{j2}[-m_{\tilde{\chi}_j^+}O_{ij}^{L*}(D_0+D_1+D_2)+m_{\tilde{\chi}_i^0}O_{ij}^{R*}(D_1+D_2)]\\
&+h_tm_b\theta_{k2}^b\theta_{l2}^tN_{i3}V_{j2}O_{ij}^{L*}D_3\}(m_W^2,m_b^2,m_{H^+}^2,m_b^2,\hat{u},\hat{t},m_{\tilde{\chi}_j^+}^2,m_{\tilde{\chi}_i^0}^2,m_{\tilde{b}_k}^2,m_{\tilde{t}_l}^2),
\end{aligned}
$$

$$
\begin{aligned}
f_{12}^{(b)}=&\sum_{i}\frac{gh_b^2\alpha_{2i}^2}{16\sqrt{2}\pi^2}[h_tm_bm_t\beta_{11}D_2-h_bm_b^2\beta_{21}(2D_0-D_1-2D_2-D_3)]\\
&(m_b^2,m_{H^+}^2,m_W^2,m_b^2,\hat{t},\hat{s},m_{H_i}^2,m_b^2,m_t^2,m_b^2)\\
&+\sum_{i}\frac{g}{16\sqrt{2}\pi^2}\{-h_bh_t^2\beta_{11}\beta_{1i}\beta_{2i}(C_0-C_1)(m_W^2,m_{H^+}^2,\hat{s},m_t^2,m_b^2,m_t^2)\\
&+[h_t^3m_bm_t\beta_{11}\beta_{1i}^2D_3-h_b^2h_tm_bm_t\beta_{2i}(\beta_{1i}\beta_{21}D_2-\beta_{11}\beta_{2i}D_1)
\end{aligned}
$$

$$+h_b^3 m_b^2 \beta_{21}\beta_{2i}^2 D_2 - h_b h_t^2 \beta_{11}\beta_{1i}\beta_{2i}(-4D_{00} + m_b^2(D_1 - D_{12} - D_{23}$$
$$+D_3) + m_{H^+}^2 D_{12} + m_W^2 D_{23} - \hat{u}(D_{12} + D_{22} + D_{23}) + m_{H_i^+}^2(D_0 - D_2))]$$
$$(m_b^2, m_W^2, m_{H^+}^2, m_b^2, \hat{u}, \hat{s}, m_{H_i^+}^2, m_t^2, m_b^2, m_t^2)\}$$
$$+\sum_{i,j} \frac{g h_b^3 \alpha_{2i}\beta_{11}\beta_{1j}\varphi_{ij}}{16\sqrt{2}\pi^2} D_{00}(m_W^2, m_b^2, m_{H^+}^2, m_b^2, \hat{u}, \hat{t}, m_{H_j^+}^2, m_{H_i}^2 m_b^2, m_t^2)$$
$$+\sum_{i} \frac{g h_b h_t^2 \beta_{11}\beta_{1i}\beta_{2i}}{16\sqrt{2}\pi^2} D_{00}(m_b^2, m_{H^+}^2, m_b^2, m_W^2, \hat{u}, \hat{t}, m_{H_i^+}^2, m_t^2, m_b^2, m_{A_i}^2)$$
$$+\sum_{i,j,k,l}\sum_{k',l'} \frac{g h_b \theta^b_{kk'}\theta^t_{ll'}}{16\pi^2}(h_b\Theta^5_{k'l'1} + h_t\Theta^6_{k'l'1})\{h_t m_b \theta^b_{k2}\theta^t_{l2} N_{i3} V_{j2} D_2$$
$$+h_t \theta^b_{k1}\theta^t_{l2} N^*_{i3} V_{j2}[-m_{\tilde{\chi}^+_j} O^{R*}_{ij}(D_0 + D_1 + D_2) + m_{\tilde{\chi}^0_i} O^{L*}_{ij}(D_1 + D_2)]$$
$$+h_b m_b \theta^b_{k1}\theta^t_{l1} N^*_{i3} U_{j2} O^{R*}_{ij} D_3\}(m_W^2, m_b^2, m_{H^+}^2, m_b^2, \hat{u}, \hat{t}, m^2_{\tilde{\chi}^+_j}, m^2_{\tilde{\chi}^0_i}, m^2_{\tilde{b}_k}, m^2_{\tilde{t}_l});$$

All other form factors f_i not listed above vanish.

Here A_0, C_i, D_i and D_{ij} are the one-, three- and four-point Feynman integrals[20]. The definitions of U_{ij}, V_{ij}, N_{ij}, O^L_{ij} and O^R_{ij} can be found in Ref.[2].

References

[1] For a review, see J.Gunion, H. Haber, G. Kane, and S.Dawson, The Higgs Hunter's Guide(Addison-Wesley, New York,1990).

[2] H.E. Haber and G.L. Kane, Phys. Rep. 117, 75(1985); J.F. Gunion and H.E. Haber, Nucl. Phys. **B272**, 1(1986).

[3] CMS Technical Proposal. CERN/LHC94-43 LHCC/P1, December 1994.

[4] CDF Collaboration, Phys. Rev. Lett. 79, 35(1997); D0 Collaboration, Phys. Rev.Lett. 82, 4975(1999).

[5] Z.Kunszt and F. Zwirner, Nucl. Phys. **B385**, 3(1992), and references cited therein.

[6] J.F. Gunion, H.E. Haber, F.E. Paige, W.-K. Tung, and S. Willenbrock, Nucl. Phys. **B294**,621(1987); R.M. Barnett, H.E. Haber, and D.E. Soper, ibid. B306, 697(1988); F.I. Olness and W.-K. Tung, ibid. **B308**, 813(1988).

[7] V. Barger, R.J.N. Phillips, and D.P. Roy, Phys. Lett. **B324**, 236(1994).

[8] C.S. Huang and S.H. Zhu, Phys. Rev. **D60**, 075012(1999). L.G. Jin, C.S.Li, R.J. Oakes, and S.H. Zhu, to appear in Eur.Phys.J.C. L.G. Jin, C.S.Li, R.J. Oakes, and S.H. Zhu, hep-ph/0003159.

[9] D.A. Dicus, J.L.Hewett, C. Kao, and T.G. Rizzo, Phys. Rev. **D40**,789(1989).

[10] A.A.Barrientos Bendezu and B.A. Kniehl, Phys. Rev. **D59**, 015009(1998).

[11] S. Moretti and K. Odagiri, Phys. Rev. **D59**, 055008(1999).

[12] K. Odagiri, hep-ph/9901432; Phys. Lett. **B452**, 327(1999).

[13] D.P. Roy, Phys. Lett. **B459**, 607(1999).

[14] S. Raychaudhuri and D.P.Roy, Phys. Rev. **D53**, 4902(1996).

[15] S. Sirlin, Phys. Rev. **D22**, 971 (1980); W. J. Marciano and A. Sirlin,*ibid.* **22**, 2695(1980); **31**, 213(E) (1985); A. Sirlin and W.J. Marciano, Nucl. Phys. **B189**, 442(1981); K.I. Aoki et.al., Prog. Theor. Phys. Suppl. **73**, 1(1982).

[16] A. Mendez and A. Pomarol, Phys.Lett.**B279**, 98(1992).

[17] Particle Data Group, C.Caso *et al*, Eur.Phys.J.C 3, 1(1998).

[18] H.L. Lai, et al.(CTEQ collaboration), hep-ph/9903282.

[19] J.Gunion, A.Turski, Phys. Rev. **D39**, 2701(1989); **D40**, 2333(1990); J.R.Espinosa, M.Quiros, Phys. Lett. **B266**, 389(1991); M.Carena, M.Quiros, C.E.M.Wagner, Nucl. Phys. **B461**, 407(1996).

[20] G.Passarino and M.Veltman, Nucl. Phys. **B160**, 151(1979); A.Axelrod, *ibid.* **B209**, 349 (1982); M.Clements *et al.*, Phys. Rev. **D27**, 570 (1983); A.Denner, Fortschr. Phys. **41**, 4 (1993); R. Mertig *et al.*, Comput. Phys. Commun. **64**, 345 (1991).

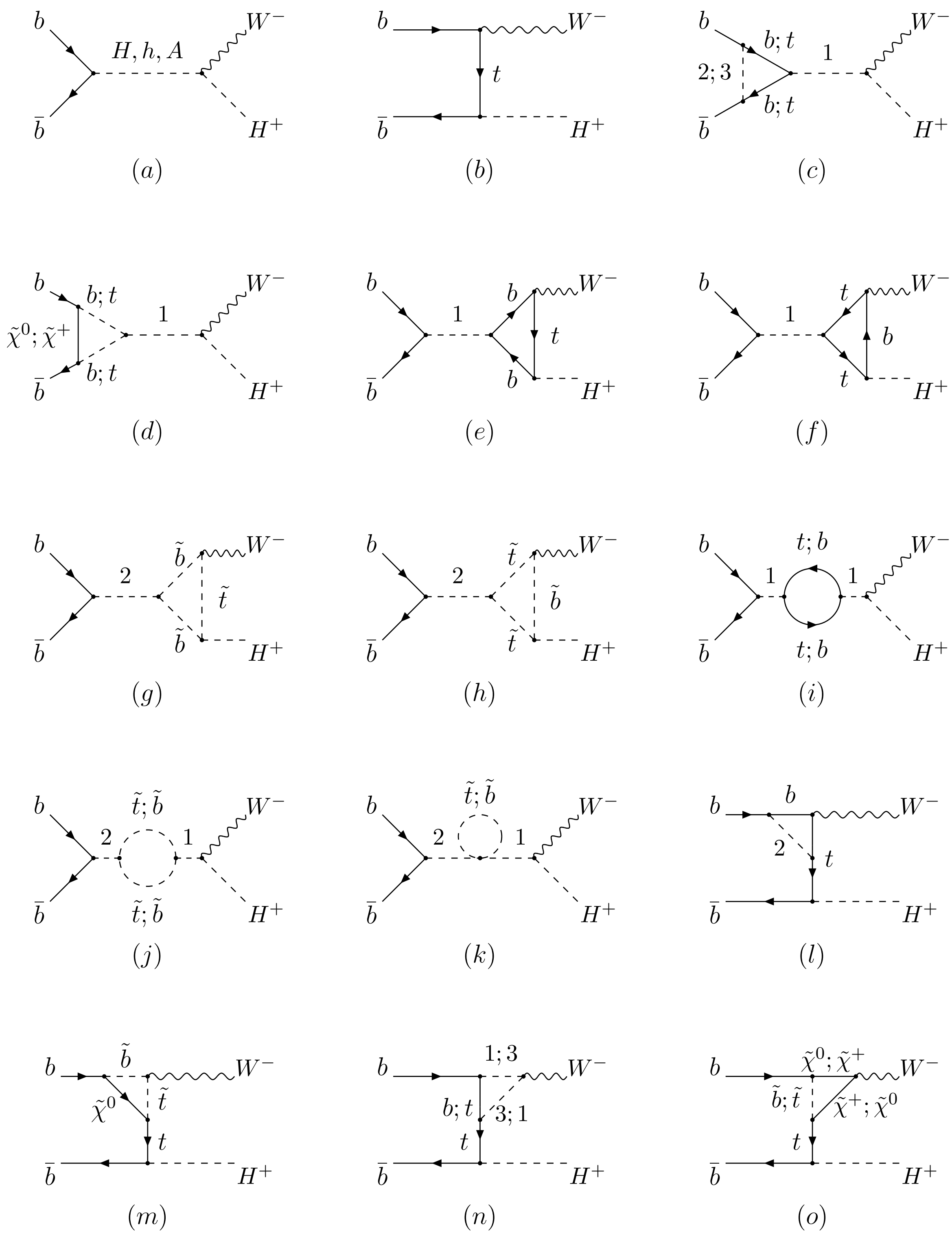
b $\bar{b}$ H, h, A W^- H^+
(a)
b $\bar{b}$ t W^- H^+
(b)
b $\bar{b}$ $b; t$ $2; 3$ $b; t$ 1 W^- H^+
(c)
b $\bar{b}$ $b; t$ $\tilde{\chi}^0; \tilde{\chi}^+$ $b; t$ 1 W^- H^+
(d)
b $\bar{b}$ 1 b t b W^- H^+
(e)
b $\bar{b}$ 1 t b t W^- H^+
(f)
b $\bar{b}$ 2 $\tilde{b}$ $\tilde{t}$ $\tilde{b}$ W^- H^+
(g)
b $\bar{b}$ 2 $\tilde{t}$ $\tilde{b}$ $\tilde{t}$ W^- H^+
(h)
b $\bar{b}$ 1 $t; b$ $t; b$ 1 W^- H^+
(i)
b $\bar{b}$ 2 $\tilde{t}; \tilde{b}$ $\tilde{t}; \tilde{b}$ 1 W^- H^+
(j)
b $\bar{b}$ 2 $\tilde{t}; \tilde{b}$ 1 W^- H^+
(k)
b $\bar{b}$ b 2 t W^- H^+
(l)
b $\bar{b}$ $\tilde{b}$ $\tilde{\chi}^0$ $\tilde{t}$ t W^- H^+
(m)
b $\bar{b}$ $1; 3$ $b; t$ $3; 1$ t W^- H^+
(n)
b $\bar{b}$ $\tilde{\chi}^0; \tilde{\chi}^+$ $\tilde{b}; \tilde{t}$ $\tilde{\chi}^+; \tilde{\chi}^0$ t W^- H^+
(o)

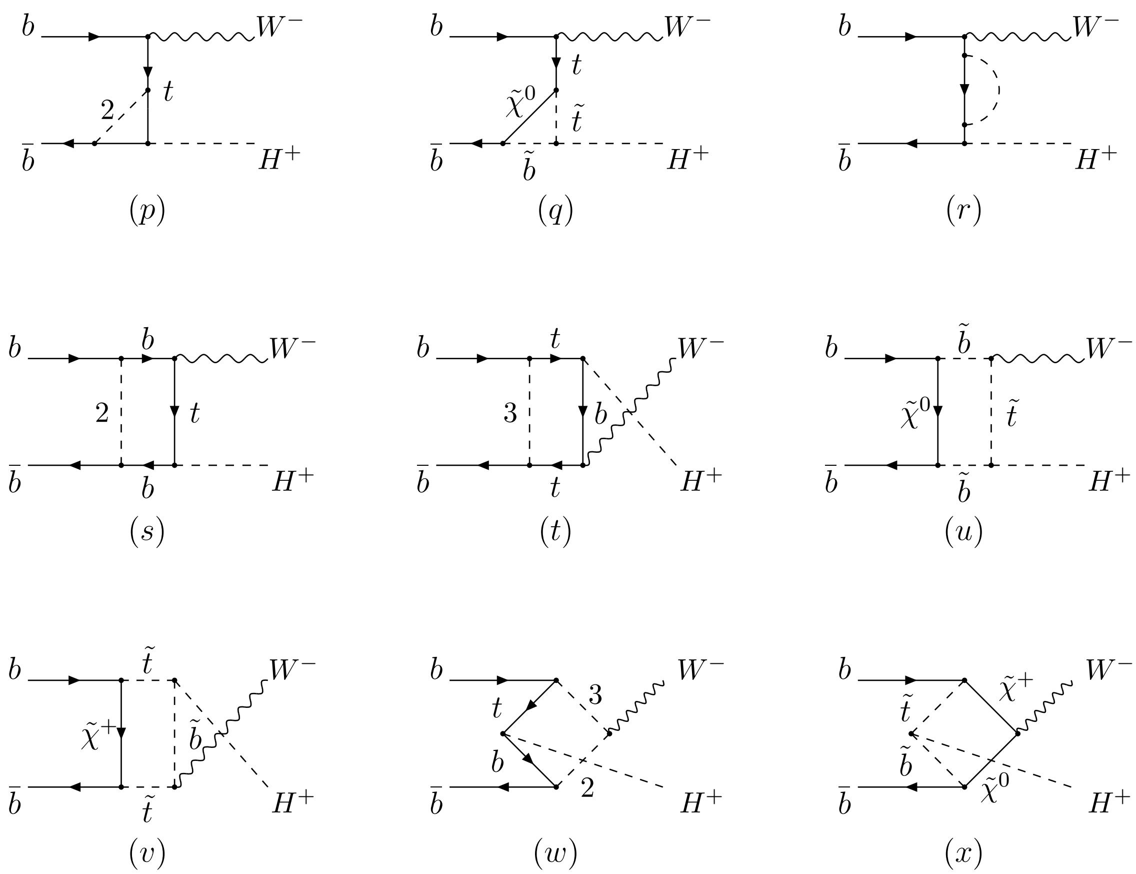

Figure 1: Feynman diagrams contributing to supersymmetric electroweak corrections to $b\bar{b} \to W^-H^+$: (a) and (b) are tree level diagrams; $(c)-(x)$ are one-loop corrections. The dashed line 1 represents H, h, A; the dashed line 2 represents H, h, A, G^0; the dashed line 3 represents H^+, G^+. For diagram (r), the dashed line in the loop represents $H, h, A, G^0, H^+, G^+, \tilde{t}, \tilde{b}$.

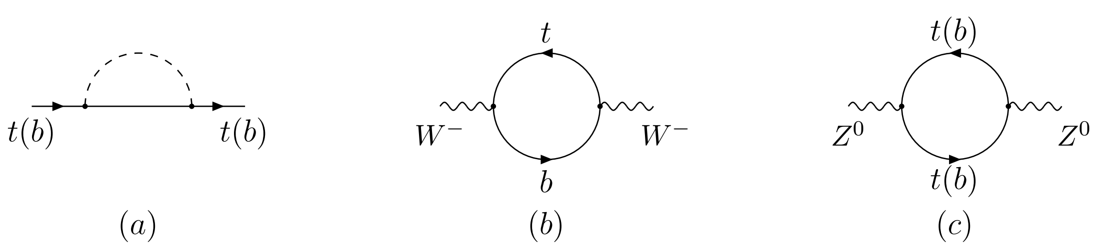

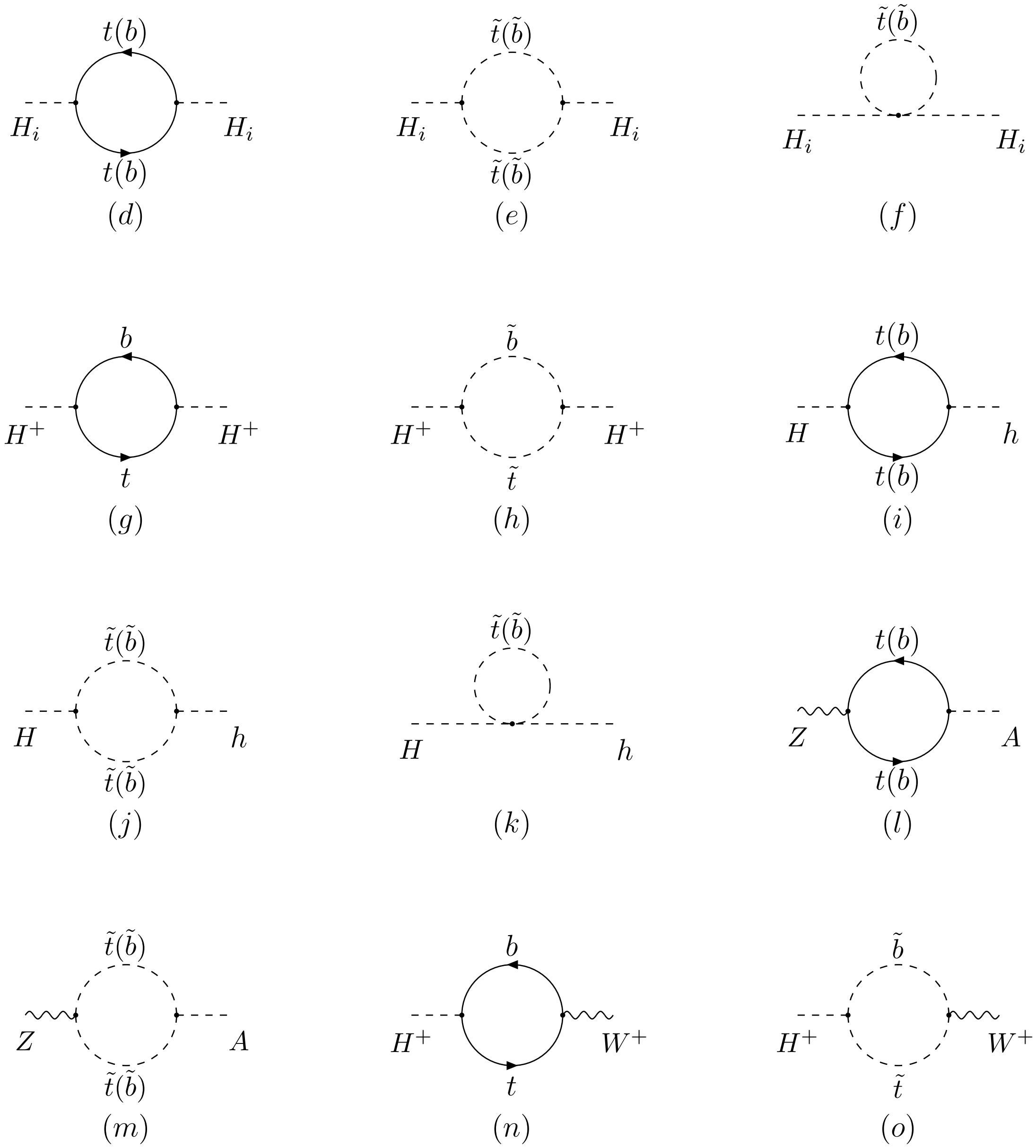

Figure 2: Feynman diagrams contributing to renormalization constants: The dashed line represents $H, h, A, G^0, H^+, G^+, \tilde{t}, \tilde{b}$ for diagram (a), and H_i in diagrams $(d)-(f)$ represents H, h, A.

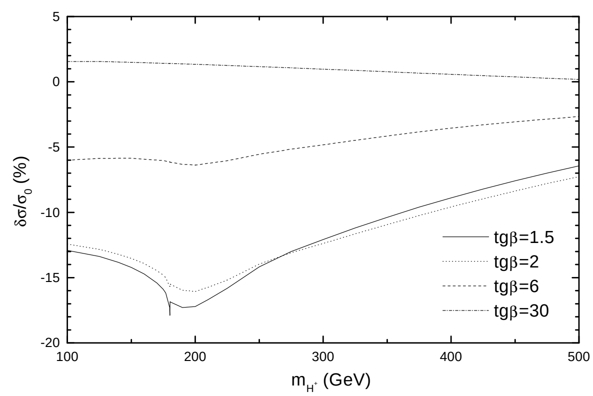

Figure 3: The Yukawa corrections versus m_{H^+} for $\tan\beta = 1.5$, 2, 6 and 30, respectively.

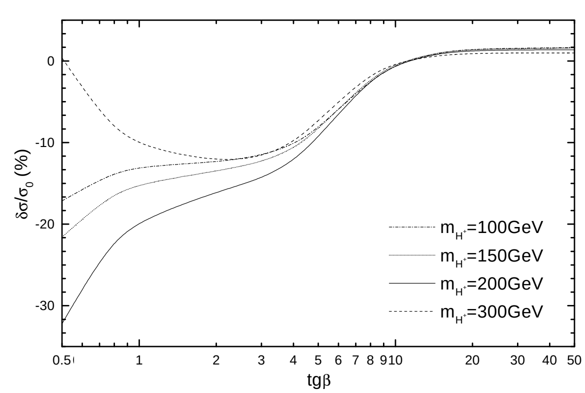

Figure 4: The Yukawa corrections versus $\tan\beta$ for $m_{H^+} = 100$, 150, 200 and 300GeV, respectively.

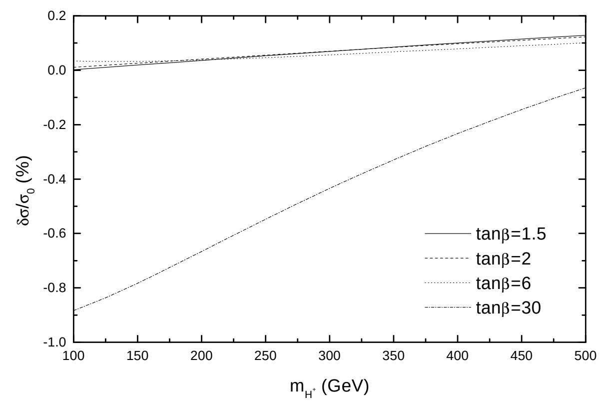

Figure 5: The genuine SUSY EW corrections versus m_{H^+} for $\tan\beta = 1.5$, 2, 6 and 30, respectively, assuming $M_2 = 300\text{GeV}$, $\mu = -100\text{GeV}$, $A_t = A_b = 200\text{GeV}$ and $M_{\tilde{Q}} = M_{\tilde{U}} = M_{\tilde{D}} = 500\text{GeV}$.

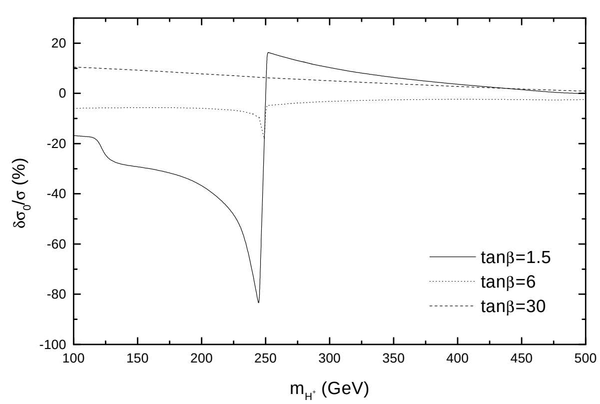

Figure 6: The genuine SUSY EW corrections versus m_{H^+} for $\tan\beta = 1.5$, 6 and 30, respectively, assuming $M_2 = 200\text{GeV}$, $\mu = 100\text{GeV}$, $A_t = A_b = 1\text{TeV}$, $M_{\tilde{Q}} = M_{\tilde{U}}$, $m_{\tilde{t}_1} = 100\text{GeV}$ and $m_{\tilde{b}_1} = 150\text{GeV}$.

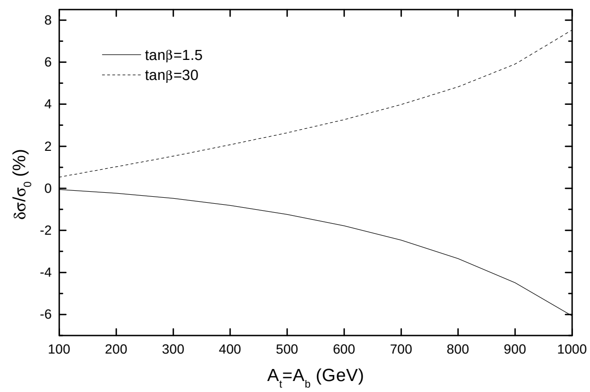

Figure 7: The genuine SUSY EW corrections versus $A_t = A_b$ for $\tan\beta = 1.5$ and 30, respectively, assuming $m_{H^+} = 200$GeV, $M_2 = 300$GeV, $\mu = 100$GeV, and $M_{\tilde{Q}} = M_{\tilde{U}} = M_{\tilde{D}} = 400$GeV.

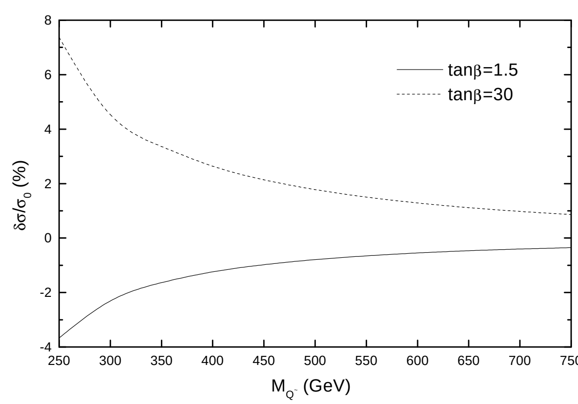

Figure 8: The genuine SUSY EW corrections versus $M_{\tilde{Q}} = M_{\tilde{U}} = M_{\tilde{D}}$ for $\tan\beta = 1.5$ and 30, respectively, assuming $m_{H^+} = 200$GeV, $M_2 = 300$GeV, $\mu = 100$GeV, and $A_t = A_b = 500$GeV.

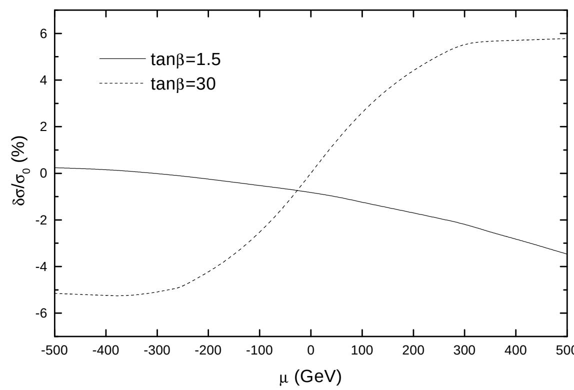

Figure 9: The genuine SUSY EW corrections versus μ for $\tan\beta = 1.5$ and 30, respectively, assuming $m_{H^+} = 200$GeV, $M_2 = 300$GeV, $A_t = A_b = 500$GeV and $M_{\tilde{Q}} = M_{\tilde{U}} = M_{\tilde{D}} = 400$GeV.

Part II
FCNC Physics

4 Preface

In this part, I will present some works on flavor changing neutral current (FCNC) processes. As already emphasized, the FCNC processes are forbidden at tree level in the SM, so it acts as the ground to test the quantum structure of the SM; at the same time, it is also the ideal place in searching new physics beyond the SM.

In the first section of this part, $t\bar{c}$ associated production in the SM at linear colliders is presented, which corrects some mistakes in literature; the second section is the $t\bar{c}$ production in supersymmetrical models, the FCNC process is mediated by gluino; the third section is $b\bar{s}$ production in the SM at linear colliders; the fourth section is about inclusive process of B meson decay in a CP-softly broken two-Higgs-doublet model; the last section is given to B exclusive decay to K and lepton pair in supersymmetrical models.

5 Top-Charm Associated Production at High Energy e^+e^- Colliders in Standard Model

ABSTRACT

The flavor changing neutral current tcV(V=γ,Z) couplings in the production vertex for the process $e^+e^- \to t\bar{c}$ or $\bar{t}c$ in the standard model are investigated. The precise calculations keeping all quark masses non-zero are carried out. The total production cross section is found to be 1.84×10^{-9} fb at $\sqrt{s}$=200 Gev and 0.572×10^{-9} fb at $\sqrt{s}$=500 Gev respectively. The result is much smaller than that given in ref. [6] by a factor of 10^{-5}.

Top quark physics has been extensively investigated [1]. The advantage of examining top quark physics than other quark physics is that one can directly determine the properties of top quark itself and does not need to worry about non-perturbative QCD effects which are difficult to attack because there exist no top-flavored hadron states at all. The properties of top quark could reveal information on flavor physics, electroweak symmetry breaking as well new physics beyond the standard model(SM).

One of important fields in top physics is to study flavor changing neutral current (FCNC) coupings. There are no flavor changing neutral currents at tree-level in the SM. FCNC appear at loop-levels and consequently offer a good place to test quantum effects of the fundamental quantum field theory on which SM based. Furthermore, they are very small at one loop-level due to the unitary of Cabbibo-Kobayashi-Maskawa (CKM) matrix. In models beyond SM new particles beyond the particles in SM may appear in the loop and have significant contributions to flavor changing transitions. Therefore, FCNC interactions give an ideal place to search for new physics. Any positive observation of FCNC couplings deviated from that in SM would unambiguously signal the presence of new physics. Searching for FCNC is clearly one of important goals of high energy colliders, in particular, e^+e^- colliders [2].

The flavor changing transitions involving external up-type quarks which are due to FCNC couplings are much more suppressed than those involving external down-type quarks in SM. The effects for external up-type quarks are derived by virtual exchanges of down-type quarks in a loop for which GIM mechanism [3] is much more effective because the mass splittings between down-type quarks are much less than those between up-type quarks. Therefore, the tc transition which is studied in the latter opens a good window to search for new physics.

The FCNC vertices tcV(V=γ, Z) can be probed either in rare decays of t quark or via top-charm associated production. A lot of works have been done in the former case [4]. And a number of papers on the latter case have also appeared [5, 6, 7]. In this letter we shall investigate the latter case in the process

$$e^+e^- \to t\bar{c} \text{ or } \bar{t}c. \tag{1}$$

Comparing t quark rare decays where the momentum transfer q^2 is limited, i. e., it should be less or equal to mass square of t quark m_t^2, the production process (1) allows

the large (time-like) momentum transfer, which is actually determined by the energies available at e^+e^- colliders. The reaction (1) has some advantages because of the ability to probe higher dimension operators at large momenta and striking kinematic signatures which are straightforward to detect in the clean environment of e^+e^- collisions. In particular, in some extensions of SM which induce FCNC there are large underlying mass scales and large momentum transfer so that these models are more naturally probed via t$\bar{c}$ associated production than t quark rare decays.

The production cross sections of the process (1) in SM have been calculated in refs. [6, 7]. In the early references [7] a top quark mass $m_t \leq m_Z$ is assumed and the on-shell Z boson dominance is adopted. The reference [6] considered a large top quark mass and abandoned the on-shell Z boson dominance. However, the "self energy" diagrams have been omitted in ref. [6]. This is not legal because the one-loop contribution for FC transitions is of the leading term of the FC transitions and must be finite, i.e., although there are some divergences for some diagrams they should cancel each other in the sum of contributions of all diagrams. Furthermore, the order of values of cross sections given in ref. [6] is not correct.

The order of values of cross sections for the process (1) in SM can easily be estimated. The differential cross section can be written as

$$\frac{d\sigma}{dcos\theta} = \frac{N_c}{32\pi s}(1 - \frac{m_t^2}{s})\frac{1}{4}\sum_{spins}|M|^2 \tag{2}$$

Where N_c is the color factor, θ is the the angle between incoming electron e^- and outgoing top quark t and M is the amplitude of the process. In eq.(2) the charm quark mass in kenetic factors has been omitted. Due to the GIM mechanism, one has

$$\begin{aligned}\sum_{spins}|M|^2 &= e^8|\sum_{j=d,s,b} V_{jt}^{\star}V_{jc}f(x_j, y_j)|^2 \\ &= e^8|V_{tb}^{\star}V_{cb}\frac{m_b^2 - m_s^2}{m_w^2}\frac{\partial f}{\partial x_j}|_{x_j,y_j=0} + ...|^2,\end{aligned} \tag{3}$$

where $x_j = m_j^2/m_w^2, y_j = m_j^2/s$, and "..." denote the less important terms for $\sqrt{s} \geq 200$ Gev. Assuming $\frac{\partial f}{\partial x_j}|_{x_j,y_j=0} = \mathrm{O}(1)$, one obtains from eqs. (2),(3)

$$\sigma \sim 10^{-8} - 10^{-9} fb$$

at $\sqrt{s} = 200$ Gev. However, the results given in ref. [6] are

$$\sigma = 0.71 \times 10^{-2} fb$$

for m_t=165 Gev and

$$\sigma = 4.1 \times 10^{-4} fb$$

for m_t=190 Gev, which are much larger than the above estimation by a factor of 10^5. In order to test SM and search for new physics from observations of some process one needs to know what are the precise results for the relevant observables of the process

in SM. Therefore, it is necessary to calculate precisely the cross sections in the SM. In this letter we calculate the differential and total cross sections of the process (1) in SM.

In SM for the process (1) there are three kinds of Feynman diagram at one loop, "self enengy" (actually it is a FC transition, not a usual self energy diagram), triangle and box diagram, which are shown in Fig.1. We carry out calculations in the Feynman-t'Hooft gauge. The contributions of the neutral Higgs H and Goldstone bosons $G^{0,\pm}$ which couple to electrons are neglected since they are proportional to the electron mass and we have put the mass of electron to zero.

We do the reduction using FeynCalc [8] and keep all masses non-zero except for the mass of electron. To control the ultraviolet divergence, the dimensional regularization is used. As a consistent check, we found that all divergences are canceled in the sum. The calculations are carried out in the frame of the centre of mass system (CMS) and Mandelstam variables have been employed:

$$s = (p_1 + p_2)^2 = (k_1 + k_2)^2 \qquad t = (p_1 - k_1)^2 \qquad u = (p_1 - k_2)^2, \tag{4}$$

where p_1, p_2 are the momenta of electron and positron respectively, and k_1, k_2 are the momenta of top quark t and anti-charm quark $\bar{c}$ respectively.

The amplitude of process $e^+e^- \to t\bar{c}$ can be expressed as

$$\begin{aligned} M \;=\; & \sum_{j=d,s,b} 16\pi^2\alpha^2 V^\star_{cj} V_{tj} [g_1 \bar{u}_t \gamma^\mu P_L v_c \bar{v}_e \gamma_\mu P_R u_e + g_2 \bar{u}_t \gamma^\mu P_L v_c \bar{v}_e \gamma_\mu P_L u_e + g_3 \bar{u}_t P_L v_c \bar{v}_e \not{k}_1 P_R u_e + \\ & g_4 \bar{u}_t P_L v_c \bar{v}_e \not{k}_1 P_L u_e + g_5 \bar{u}_t \not{p}_1 P_L v_c \bar{v}_e \not{k}_1 P_L u_e + g_6 \bar{v}_e \gamma^\mu P_L u_e \bar{u}_t \gamma_\mu \not{p}_1 P_L v_c + \\ & g_7 \bar{u}_t \gamma^\mu P_R v_c \bar{v}_e \gamma_\mu P_R u_e + g_8 \bar{u}_t \gamma^\mu P_R v_c \bar{v}_e \gamma_\mu P_L u_e + g_9 \bar{u}_t P_R v_c \bar{v}_e \not{k}_1 P_R u_e + \\ & g_{10} \bar{u}_t P_R v_c \bar{v}_e \not{k}_1 P_L u_e + g_{11} \bar{v}_e \gamma^\mu P_L u_e \bar{u}_t \gamma_\mu \not{p}_1 P_R v_c] \end{aligned} \tag{5}$$

where α is fine structure constant, V_{ij} is CKM matrix element, P_L is defined as $(1-\gamma^5)/2$, and P_R is defined as $(1+\gamma^5)/2$. The exact expressions of the coefficients $g_j (j = 1, 2, ...11)$ are too long to be given. Instead, in order to show the essential points, we give them in the limit of m_i/m (i=d,s,c, m=m_w, m_t, s) approach to zero. In the limit $g_j (j = 7, 8, 9, 10, 11)$ is zero, and the others are given as follows.

$$\begin{aligned} g_1 \;=\; & a_3 m_j^2 - 2a_4 m_j^2 s_w^4 + 6a_4 C_2^c m_j^2 m_t^2 s_w^2 + 6m_w^2(2C_{11}^d m_t^2 + 2C_{22}^d s + 2C_{12}^d(m_t^2 + s))(a_3 + 2a_4 c_w^2 s_w^2) + \\ & 12m_w^2 C_2^d(a_3(m_t^2 + s) + a_4(2sc_w^2 s_w^2 + m_t^2 c_w^2 s_w^2 - m_t^2 s_w^4)) - B_0^b(m_j^4 - m_j^2 m_t^2 + m_j^2 m_w^2 + \\ & 2m_t^2 m_w^2 - 2m_w^4)(a_1 + 2a_2 s_w^2(3 - 4s_w^2)) + 12C_{00}^d(a_3(m_j^2 + 6m_w^2) + a_4 s_w^2(c_w^2 m_j^2 + 12c_w^2 m_w^2 - \\ & m_j^2 s_w^2)) + 6C_1^d m_w^2(2a_3(m_t^2 + s) + 2a_4 s_w^2(c_w^2 m_t^2 + 2c_w^2 s - m_t^2 s_w^2)) - 6C_0^d m_w^2(2a_3(m_j^2 - s) - \\ & 2a_4 s_w^2(2c_w^2 m_t^2 + 2c_w^2 s + 2m_j^2 s_w^2 - m_t^2 s_w^2 - 3m_t^2 c_w^2)) + 2C_0^c m_j^2(a_3(m_j^2 + 2m_w^2 - m_t^2) + \\ & a_4 s_w^2(3m_j^2 - 2m_j^2 s_w^2 - 4m_w^2 s_w^2 + 2m_t^2 s_w^2)) - 2(2C_{00}^c + C_{11}^c m_t^2 + C_{22}^c s + C_2^c s + \\ & C_{12}^c(m_t^2 + s))(a_3(m_j^2 + 2m_w^2) + 2a_4 s_w^2(3m_w^2 - m_j^2 s_w^2 - 2m_w^2 s_w^2)) + \\ & B_0^a(a_1(m_j^2 - m_w^2)(m_j^2 + 2m_w^2) - 2a_1 m_t^2 m_j^2 + 2a_2 s_w^2(3m_j^4 - 6m_j^2 m_t^2 + 3m_j^2 m_w^2 - 6m_w^4 - \\ & 4m_j^4 s_w^2 - 4m_j^2 m_w^2 s_w^2 + 8m_w^4 s_w^2 + 8m_t^2 m_j^2 s_w^2)) - 2C_1^c(a_3(2m_w^2 s + m_t^2 m_j^2) - \\ & a_4 s_w^2(3m_j^2 m_t^2 + 2m_t^2 m_j^2 s_w^2 - 6m_w^2 s + 4m_w^2 s s_w^2)) \end{aligned} \tag{6}$$

$$
\begin{aligned}
g_2 \;=\;& a_3 m_j^2 + a_4 m_j^2(1-2s_w^2)(s_w^2 - 3C_2^c m_t^2) + a_5(8D_{00}^e + u(D_1^e + D_2^e + 2D_3^e + 2D_{12}^e + 4D_{13}^e + \\
& 2D_{23}^e + 2D_{33}^e) + (2m_t^2 D_3^e + 2sD_{13}^e + 2D_{33}^e m_t^2)) + 6m_w^2(2C_{11}^d m_t^2 + 2C_{22}^d s + \\
& 2C_{12}^d(m_t^2+s))(a_3 - a_4 c_w^2(1-2s_w^2)) + 6m_w^2 C_2^d(2a_3(m_t^2+s) - a_4(1-2s_w^2)(m_t^2 c_w^2 - m_t^2 s_w^2 + \\
& 2sc_w^2)) - B_0^b(m_j^4 - m_j^2 m_t^2 + m_j^2 m_w^2 + 2m_t^2 m_w^2 - 2m_w^4)(a_1 - a_2(3-4s_w^2)(1-2s_w^2)) + \\
& 6C_{00}^d(2a_3(m_j^2+6m_w^2) - a_4(1-2s_w^2)(c_w^2 m_j^2 + 12c_w^2 m_w^2 - m_j^2 s_w^2)) + 6C_1^d m_w^2(2a_3(m_t^2+s) - \\
& a_4(1-2s_w^2)(c_w^2 m_t^2 + 2c_w^2 s - m_t^2 s_w^2)) - 6C_0^d m_w^2(2a_3(m_j^2 - s) + a_4(1-2s_w^2)(-c_w^2 m_t^2 + 2c_w^2 s + \\
& 2m_j^2 s_w^2 - m_t^2 s_w^2)) + C_0^c m_j^2(2a_3(m_j^2 + 2m_w^2 - m_t^2) - a_4(1-2s_w^2)(3m_j^2 - 2m_j^2 s_w^2 - 4m_w^2 s_w^2 + \\
& 2m_t^2 s_w^2)) - 2(2C_{00}^c + C_{11}^c m_t^2 + C_{22}^c s + C_2^c s + C_{12}^c(m_t^2+s))(a_3(m_j^2+2m_w^2) - \\
& a_4(1-2s_w^2)(3m_w^2 - m_j^2 s_w^2 - 2m_w^2 s_w^2)) + B_0^a(a_1(m_j^2 - m_w^2)(m_j^2+2m_w^2) - 2a_1 m_t^2 m_j^2 - \\
& a_2(1-2s_w^2)(3m_j^4 - 6m_j^2 m_t^2 + 3m_j^2 m_w^2 - 6m_w^4 - 4m_j^4 s_w^2 - 4m_j^2 m_w^2 s_w^2 + 8m_w^4 s_w^2 + 8m_t^2 m_j^2 s_w^2)) - \\
& C_1^c(2a_3(m_t^2 m_j^2 + 2sm_w^2) + a_4(1-2s_w^2)(3m_j^2 m_t^2 - 6sm_w^2 + 4sm_w^2 s_w^2 + 2m_t^2 m_j^2 s_w^2)) \qquad (7)
\end{aligned}
$$

$$
\begin{aligned}
g_3 \;=\;& 12a_4 s_w^2 m_t(2C_2^d m_w^2 - C_2^c m_j^2) + 4m_t C_0^c m_j^2(a_3 - 2a_4 s_w^4) + 24m_t m_w^2(2C_1^d + C_0^d)(a_3 + 2a_4 c_w^2 s_w^2) + \\
& 8C_1^c m_t(a_3 m_j^2 - 2a_4 s_w^4 m_j^2) + 12m_t(C_{11}^d + C_{12}^d)(a_3(m_j^2+2m_w^2) + a_4 s_w^2(c_w^2 m_j^2 + 4c_w^2 m_w^2 - m_j^2 s_w^2)) + \\
& 4m_t(C_{11}^c + C_{12}^c)(a_3(m_j^2+2m_w^2) + 2a_4 s_w^2(3m_w^2 - m_j^2 s_w^2 - 2m_w^2 s_w^2)) \qquad (8)
\end{aligned}
$$

$$
\begin{aligned}
g_4 \;=\;& -2a_5 m_t(2D_{23}^e + D_2^e + 2D_{33}^e + 2D_3^e) + 6a_4 m_t(C_2^c m_j^2 - 2C_2^d m_w^2)(1-2s_w^2) + 4C_0^c m_t m_j^2(a_3 + \\
& a_4 s_w^2(1-2s_w^2)) + 24m_t m_w^2(2C_1^d + C_0^d)(a_3 - a_4 c_w^2(1-2s_w^2)) + 8C_1^c m_t(a_3 m_j^2 + \\
& a_4 s_w^2 m_j^2(1-2s_w^2)) + 6(C_{11}^d + C_{12}^d)m_t(2a_3(m_j^2+2m_w^2) - a_4(1-2s_w^2)(c_w^2 m_j^2 + 4c_w^2 m_w^2 - \\
& m_j^2 s_w^2)) + 4m_t(C_{11}^c + C_{12}^c)(a_3(m_j^2+2m_w^2) - a_4(1-2s_w^2)(3m_w^2 - m_j^2 s_w^2 - 2m_w^2 s_w^2)) \qquad (9) \\
g_5 \;=\;& -4a_5(D_{12}^e + D_{13}^e) \qquad (10) \\
g_6 \;=\;& a_5 m_t(2D_{12}^e + 2D_{13}^e + 2D_{23}^e + D_2^e + 2D_{33}^e + 2D_3^e) \qquad (11)
\end{aligned}
$$

with $m_j^2 = m_b^2$(since m_s, m_d have been omitted in the above expressions of g's), where $a_i(i=1,2,...,5)$ are defined by

$$
a_1 = \frac{1}{96s\pi^2 s_w^2 m_t^2 m_w^2}, \quad a_2 = \frac{1}{768\pi^2 c_w^2 s_w^4 m_t^2 m_w^2(m_z^2 - im_z\Gamma z - s)}, \quad a_3 = \frac{1}{192s\pi^2 s_w^2 m_w^2}
$$

$$
a_4 = \frac{1}{384\pi^2 c_w^2 s_w^4 m_w^2(m_z^2 - im_z\Gamma z - s)}, \quad a_5 = \frac{1}{32\pi^2 s_w^4}
$$

with $c_w = cos\theta_w$ and $s_w = sin\theta_w$. In the presentation of g_j above, we have used the definition of scalar integrals Bs, Cs,and Ds[8], and these functions, Bs, Cs,and Ds, with superscripts a,b,...,e have the arguments
$(0, m_j^2, m_w^2)$, (m_t^2, m_j^2, m_w^2), $(m_t^2, 0, s, m_j^2, m_w^2, m_j^2)$, $(m_t^2, 0, s, m_w^2, m_j^2, m_w^2)$
$(0, s, m_t^2, u, 0, 0, 0, m_w^2, m_w^2, m_j^2)$
respectively. Here m_j denotes the mass of down-type quark b.

In the numerical calculations the following values of the parameters have been used [9]:

$$
m_e = 0, \quad m_c = 1.4Gev, \quad m_t = 175Gev, \quad m_d = 0.005Gev, \quad m_s = 0.17Gev,
$$

$$
m_b = 4.4Gev, \quad m_w = 80.41Gev, \quad m_z = 91.187Gev, \quad \Gamma_z = 2.5Gev, \quad \alpha = \frac{1}{128}
$$

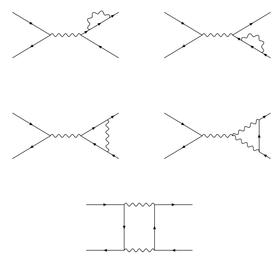

Figure 1: Feynman diagrams of prosess $e^+e^- \to t\bar{c}$

In order to keep the unitary condition of CKM matrix exactly, we employ the standard parametrization and take the values [9, 10]

$$s_{12} = 0.220, \qquad s_{23} = 0.039, \qquad s_{13} = 0.0031, \qquad \delta_{13} = 70^\circ.$$

Numerical results are shown in Figs. 2, 3. In Fig.2, we show the total cross section σ_{tot} of the process $e^+e^- \to t\bar{c}$ as a function of the centre of mass energy $\sqrt{s}$. One can see from the figure that the total cross section is the order of $10^{-10} \sim 10^{-9}$ fb, as expected, and decreases when center-of-mass energy increases and is large enough ($\geq$ 250 Gev). We fixed the centre of mass energy $\sqrt{s}$ at $200Gev$. Differential cross section of the process at the energy as a function of $\cos\theta$ is shown in Fig.3.

To summarize, we have calculated the production cross sections of the process $e^+e^- \to t\bar{c}$ in SM. We found that the total cross section is $1.84 \times 10^{-9} fb$ at $\sqrt{s} =$ 200 Gev and 0.572×10^{-9} fb at $\sqrt{s} = 500$ Gev. It is too small to be of experimental relevance. Therefore, this is a remarkable situation that allows for a precise test of the SM and, in particular, of the GIM mechanism in SM. Even a small number of $t\bar{c}$ events, detected at LEP II or a NLC running with a yearly integrated luminosity of $\mathcal{L} \geq 10^2 [fb]^{-1}$, will unambiguously indicate new FCNC dynamics beyond SM.

References

[1] For recent reviews, see e.g., R. Frey et al., hep-ph/9704243; F. Larios, E. Malkawi, and C.-P. Yuan, hep-ph/9704288; S. Willenbrock, hep-ph/9709355; C. Quigg, hep-ph/9802320.

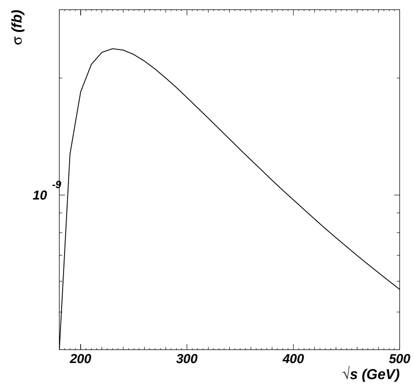

Figure 2: Cross section of the process $e^+e^- \rightarrow t\bar{c}$ as a function of $\sqrt{s}$.

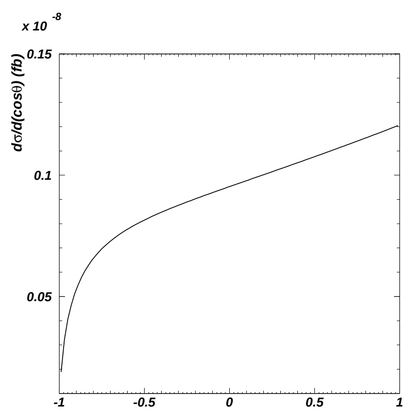

Figure 3: Differential cross section of the process $e^+e^- \rightarrow t\bar{c}$, where $\sqrt{s} = 200$ GeV.

[2] Proceedings of the Workshop on Physics and Experiments with Linear e^+e^- Colliders, eds. A. Miyamoto and Y. Fujii, World Scientific, Singapore, 1996.

[3] S. L. Glashow, J. Iliopoulos, and L. Maiani, Phys. Rev. **D2** (1970) 1285.

[4] G. Eilam, J.L. Hewett and A. Soni, Phys. Rev. **D44**, 1473 (1991); Erratum, to appear in Phys. Rev. **D**; W. Buchmüller and M. Gronau, Phys. Lett. **220B**, 641 (1989); H. Fritzsch, Phys. Lett. **224B**, 423 (1989); J.L. Diaz-Cruz, R. Martinez, M.A. Perez and A. Rosado, Phys. Rev. **D41**, 891 (1990); B. Dutta-Roy *et al.*, Phys. Rev. Lett. **65**, 827 (1990); J.L. Diaz-Cruz and G. Lopez Castro, Phys. Lett. **301B**, 405 (1993); B. Mele, S. Petrarca and and A. Soddu, Phys. Lett. **435B**, 401 (1998); M. Luke and M.J. Savage, Phys. Lett. **307B**, 387 (1993); D. Atwood, L. Reina and A. Soni, Phys. Rev. **D55**, 3156 (1997); C.S. Li, R.J. Oakes and J.M. Yang, Phys. Rev. **D49**, 293 (1994), Erratum-*ibid.* **D56**, 3156 (1997); G. Couture, C. Hamzaoui and H. König, Phys. Rev. **D52**, 1713 (1995); J.L. Lopez, D.V. Nanopoulos and R. Rangarajan, Phys. Rev. **D56**, 3100 (1997); G. Couture, M. Frank and H. König, Phys. Rev. **D56**, 4213 (1997); G.M. de Divitiis, R. Petronzio and L. Silvestrini, Nucl. Phys. **B504**, 45 (1997); J.M. Yang, B.-L. Young and X. Zhang, Phys. Rev. **D58**, 5001 (1998); J.-M. Yang and C.-S. Li, Phys. Rev. **D49**, 3412 (1994), Erratum-*ibid.* **D51**, 3974 (1995); W.-S. Hou, Phys. Lett. **296B**, 179 (1992); S. Bar-Shalom, G. Eilam, A. Soni and J. Wudka, Phys. Rev. Lett. **79**, 1217 (1997), Phys. Rev. **D57**, 2957 (1998); S. Bar-Shalom, G. Eilam, and A. Soni, hep-ph/9812518.

[5] T. Han and J. Hewett, hep-ph/9811237; U. Mahanta and A. Ghosal, Phys. Rev. **D57** (1998) 1735; Y. Koide, hep-ph/9701261; D. Atwood, L. Reina, and A. Soni, Phys. Rev. **D53** (1996) 1199, hep-ph/9612388.

[6] C-.H. Chang, X-.Q. Li, J-.X., Wang, and M-.Z. Yang, Phys. Lett. **B313** (1993) 389.

[7] V. Barger and K. Hagiwara, Phys. Rev. **D37** (1988) 3320; M. J. Duncan, Phys. Rev. **D31** (1985) 1139; K. Hikasa, Phys. Lett. **B149** (1984) 221; G. Mann and T. Rumann, Ann. Phys. **40** (1983)334; G. Eliam, Phys. Rev. **D28** (1983) 1202; V. Ganapathi et al., Phys. Rev. **D 27** (1983) 579; M. Clements et al., Phys. Rev. **D 27** (1983) 570; A. Axelrod, Nucl. Phys. **B 209** (1982) 349.

[8] G.Passarino and M.Veltman, Nucl. Phys, B160(1979) 151 ; R.Mertig, M. Bohm, and A.Denner, Comp. Phys. Comm. 64(1991)345.

[9] Particle Data Group, Eur.Phys.J. C3,1-794(1998).

[10] A. J. Buras, hep-ph/9711217, hep-ph/9806473.

6 SUSY-QCD Effect on Top-Charm Associated Production at Linear Collider

ABSTRACT

We evaluate the contribution of SUSY-QCD to top-charm associated production at next generation linear colliders. Our results show that the production cross section of the process $e^+e^- \to t\bar{c}$ or $\bar{t}c$ could be as large as 0.1 fb, which is larger than the prediction of the SM by a factor of 10^8.

One of the most important physics in top quark sector is to probe anomalous flavor changing neutral current (FCNC) couplings. In the Standard Model (SM), FCNC couplings are forbidden at the tree level and much suppressed in loops by the GIM mechanism. Any signals on FCNC couplings in the processes of top quark decay and productions or indirectly in loops will indicate the existence of new physics beyond the SM. Recently in the framework of effective lagrangian, Han and Hewett[1] have examined carefully the possibility of exploring the FCNC couplings $tcZ/tc\gamma$ in the production vertex for the reaction $e^+e^- \to t\bar{c}+\bar{t}c$ and concluded that at higher energy colliders with $0.5-1$ TeV center-of-mass energy, the resulting sensitivity to FCNC couplings will be better than the present constraints [2]. In this paper, in the minimal supersymmetric standard model (MSSM) we study the process $e^+e^- \to t\bar{c}+\bar{t}c$ and perform an detail calculation of the contribution from the FCNC couplings in the vertex of gluino-squark-quark to the production cross section. We will point out that at higher energy e^+e^- colliders the cross section could be as large as 0.1 fb which is at least eight order of magnitude larger than the prediction of the SM $\sim 10^{-10}-10^{-9}$ fb [3].

The MSSM is arguably the most promising candidate for physics beyond the SM. Beside many attractive features of supersymmetry in understanding the mass hierarchy, gauge coupling unification, the weak scale SUSY models in generally lead to a rich flavor physics. In fact, SUSY models often have arbitrary flavor mixings and mass parameters in the squark and slepton sectors and these mass matrices after diagonalization induce FCNC couplings at tree level in the vertex of gluino-squark-quark *etc*. Phenomenologically one would have to assume certain symmetries or dynamical mechanisms to prevent large FCNC among the first and second generations. On the other hand the flavor structure, especially among the second and third generations in the SUSY sector motivates us to seek for new physics and any experimental observation on the FCNC processes beyond the SM would undoubtedly shed light on our understanding for flavor physics. In this paper we take model of Ref. [4, 5] where the FCNC couplings relevant to our calculation is given by:

$$\mathcal{L}_{\mathcal{FC}} = -\sqrt{2} g_s T^a K \bar{\tilde{g}} P_L q \tilde{q}_L + h.c. \tag{1}$$

In (1), K is the supersymmetric version of the Kobayashi–Maskawa matrix, which is

explicitly expressed as:

$$K_{ij} = \begin{pmatrix} 1 & \varepsilon & \varepsilon^2 \\ -\varepsilon & 1 & \varepsilon \\ -\varepsilon^2 & -\varepsilon & 1 \end{pmatrix} \tag{2}$$

where ϵ parameterizes the strength of flavor mixing and is shown to be as large as 1/2 without contradicting with the low energy experimental data [5].

In Fig.(1) we give the Feynman diagrams for the process $e^+(p_1)e^-(p_2) \to t(k_1)\bar{c}(k_2)$. In calculations, we have neglected the scalar u-quark contribution since it is highly suppressed by $K_{12}K_{13}$; and we use the dimensional regularization to control the ultraviolet divergence. We have checked that all divergences cancel out in the final result with the summing up of all of the diagrams. The calculations are carried out in the frame of the center of mass system (CMS) and Mandelstam variables have been employed:

$$s = (p_1+p_2)^2 = (k_1+k_2)^2 \qquad t = (p_1-k_1)^2 \qquad u = (p_1-k_2)^2. \tag{3}$$

After a straightforward calculations, one obtains for the amplitudes

$$\begin{aligned} M &= \frac{e}{S}\bar{v}(p_1)\gamma_\mu u(p_2)\bar{u}(k_1)V^\mu(tc\gamma)v(k_2) \\ &+ \frac{g}{2\cos\theta_W(S-M_Z^2)}\bar{v}(p_1)\gamma_\mu(g_V^e - g_A^e\gamma_5)u(p_2)\bar{u}(k_1)V^\mu(tcZ)v(k_2) \end{aligned} \tag{4}$$

where, $g_V^e = 1/2 - 2\sin^2\theta_W$, $g_A^e = 1/2$, and $V^\mu(tc\gamma)$ and $V^\mu(tcZ)$ are the on-shell quarks effective vertices given by [1]

$$\begin{aligned} V^\mu(tc\gamma;Z) &= f_1^{\gamma;Z}\gamma_\mu P_R + f_2^{\gamma;Z}\gamma_\mu P_L + f_3^{\gamma;Z}k_{1\mu}P_R + f_4^{\gamma;Z}k_{1\mu}P_L \\ &\quad + f_5^{\gamma;Z}k_{2\mu}P_R + f_6^{\gamma;Z}k_{2\mu}P_L. \end{aligned} \tag{5}$$

The form factors, $f_i^{\gamma;Z}$ are

$$\begin{aligned} f_1^\gamma &= \sum_{\tilde{q}=\tilde{c},\tilde{t}} \frac{(\pm 1)\epsilon e g_s^2 \cos(\theta_{\tilde{q}})\sin(\theta_{\tilde{q}})m_{\tilde{g}}}{12 m_t \pi^2}[B_0(0,m_{\tilde{g}}^2,m_{\tilde{q}_2}^2) - B_0(m_t^2,m_{\tilde{g}}^2,m_{\tilde{q}_2}^2)] + R.R. \\ f_2^\gamma &= \sum_{\tilde{q}=\tilde{c},\tilde{t}} \frac{(\pm 1)\epsilon e g_s^2 \sin^2(\theta_{\tilde{q}})}{24 m_t^2 \pi^2}[(m_{\tilde{g}}^2 - m_{\tilde{q}_2}^2)B_0(0,m_{\tilde{g}}^2,m_{\tilde{q}_2}^2) - (m_{\tilde{g}}^2 - m_{\tilde{q}_2}^2 + m_t^2)B_0(m_t^2,m_{\tilde{g}}^2,m_{\tilde{q}_2}^2) \\ &\quad + 4m_t^2 C_{00}] + R.R \\ f_3^\gamma &= \sum_{\tilde{q}=\tilde{c},\tilde{t}} \frac{(\mp 1)\epsilon e g_s^2 \sin(\theta_{\tilde{q}})\cos(\theta_{\tilde{q}})m_{\tilde{g}}}{12\pi^2}[C_0 + 2C_1] + R.R. \\ f_4^\gamma &= \sum_{\tilde{q}=\tilde{c},\tilde{t}} \frac{(\pm 1)\epsilon e g_s^2 \sin(\theta_{\tilde{q}})\cos(\theta_{\tilde{q}})m_{\tilde{g}}}{12\pi^2}[C_0 + 2C_2] + R.R. \end{aligned}$$

[1]For simplicity, we only give the results in the limit of $m_c = 0$. However in our numerical calculations, we use the full formulas.

$$
\begin{aligned}
f_5^{\gamma} &= \sum_{\tilde{q}=\tilde{c},\tilde{t}} \frac{(\pm 1)\epsilon e g_s^2 \sin^2(\theta_{\tilde{q}}) m_t}{12\pi^2}[C_0 + 2C_{11}] + R.R. \\
f_6^{\gamma} &= \sum_{\tilde{q}=\tilde{c},\tilde{t}} \frac{(\mp 1)\epsilon e g_s^2 \sin^2(\theta_{\tilde{q}}) m_t}{12\pi^2}[C_0 + 2C_{12}] + R.R.
\end{aligned} \tag{6}
$$

$$
\begin{aligned}
f_1^{Z} &= \sum_{\tilde{q}=\tilde{c},\tilde{t}} \frac{(\mp 1)\epsilon g g_s^2 \sin^2(\theta_w)\cos(\theta_{\tilde{q}})\sin(\theta_{\tilde{q}})}{12 m_t \cos(\theta_w)\pi^2}[B_0(0, m_{\tilde{g}}^2, m_{\tilde{q}_2}^2) - B_0(m_t^2, m_{\tilde{g}}^2, m_{\tilde{q}_2}^2)] + R.R. \\
f_2^{Z} &= \sum_{\tilde{q}=\tilde{c},\tilde{t}} \frac{(\mp 1)\epsilon g g_s^2 \sin^2(\theta_{\tilde{q}})}{96 m_t^2 \cos(\theta_w)\pi^2}\{(-3 + 4\sin^2(\theta_w))[(m_{\tilde{g}}^2 - m_{\tilde{q}_2}^2)B_0(0, m_{\tilde{g}}^2, m_{\tilde{q}_2}^2) \\
&\quad -(m_{\tilde{g}}^2 - m_{\tilde{q}_2}^2 + m_t^2)B_0(m_t^2, m_{\tilde{g}}^2, m_{\tilde{q}_2}^2)] + 4m_t^2(-3\sin^2(\theta_{\tilde{q}}) + 4\sin^2(\theta_w))C_{00} \\
&\quad -12 m_t^2 \cos^2(\theta_{\tilde{q}})\hat{C}_{00}\} + R.R \\
f_3^{Z} &= \sum_{\tilde{q}=\tilde{c},\tilde{t}} \frac{(\pm 1)\epsilon g g_s^2 \sin(\theta_{\tilde{q}})\cos(\theta_{\tilde{q}}) m_{\tilde{g}}}{48\cos(\theta_w)\pi^2}[(4\sin^2(\theta_w) - 3\sin^2(\theta_{\tilde{q}}))(C_0 + 2C_1) \\
&\quad +3\sin^2(\theta_{\tilde{q}})(\hat{C}_0 + 2\hat{C}_1)] + R.R. \\
f_4^{Z} &= \sum_{\tilde{q}=\tilde{c},\tilde{t}} \frac{(\mp 1)\epsilon g g_s^2 \sin(\theta_{\tilde{q}})\cos(\theta_{\tilde{q}}) m_{\tilde{g}}}{48\cos(\theta_w)\pi^2}[(4\sin^2(\theta_w) - 3\sin^2(\theta_{\tilde{q}}))(C_0 + 2C_2) \\
&\quad +3\sin^2(\theta_{\tilde{q}})(\hat{C}_0 + 2\hat{C}_2)] + R.R. \\
f_5^{Z} &= \sum_{\tilde{q}=\tilde{c},\tilde{t}} \frac{(\mp 1)\epsilon g g_s^2 \sin^2(\theta_{\tilde{q}}) m_t}{48\cos(\theta_w)\pi^2}[(4\sin^2(\theta_w) - 3\sin^2(\theta_{\tilde{q}}))(C_0 + 2C_{11}) \\
&\quad -3\cos^2(\theta_{\tilde{q}})(\hat{C}_0 + 2\hat{C}_{11})] + R.R. \\
f_6^{Z} &= \sum_{\tilde{q}=\tilde{c},\tilde{t}} \frac{(\pm 1)\epsilon g g_s^2 \sin^2(\theta_{\tilde{q}}) m_t}{48\cos(\theta_w)\pi^2}[(4\sin^2(\theta_w) - 3\sin^2(\theta_{\tilde{q}}))(C_0 + 2C_{12}) \\
&\quad -3\cos^2(\theta_{\tilde{q}})(\hat{C}_0 + 2\hat{C}_{12})] + R.R.
\end{aligned} \tag{7}
$$

where $R.R.$ represents the replacement of $\theta_{\tilde{q}} \to \pi/2 + \theta_{\tilde{q}}$ and $m_{\tilde{q}_1} \leftrightarrow m_{\tilde{q}_2}$. The variables of three point functions C_i, C_{ij} [6] and $\hat{C}_i$, $\hat{C}_{ij}$ are $(m_t^2, S, 0, m_{\tilde{g}}^2, m_{\tilde{q}_2}^2, m_{\tilde{q}_2}^2)$ and $(m_t^2, S, 0, m_{\tilde{g}}^2, m_{\tilde{q}_2}^2, m_{\tilde{q}_1}^2)$, respectively.

In the MSSM the mass eigenstates of the squarks $\tilde{q}_1$ and $\tilde{q}_2$ are related to the weak eigenstates $\tilde{q}_L$ and $\tilde{q}_R$ by [7]

$$
\begin{pmatrix} \tilde{q}_1 \\ \tilde{q}_2 \end{pmatrix} = R^{\tilde{q}} \begin{pmatrix} \tilde{q}_L \\ \tilde{q}_R \end{pmatrix} \quad \text{with} \quad R^{\tilde{q}} = \begin{pmatrix} \cos\theta_{\tilde{q}} & \sin\theta_{\tilde{q}} \\ -\sin\theta_{\tilde{q}} & \cos\theta_{\tilde{q}} \end{pmatrix}. \tag{8}
$$

For the squarks, the mixing angle $\theta_{\tilde{q}}$ and the masses $m_{\tilde{q}_{1,2}}$ can be calculated by diagonalizing the following mass matrices

$$
M_{\tilde{q}}^2 = \begin{pmatrix} M_{LL}^2 & m_q M_{LR} \\ m_q M_{RL} & M_{RR}^2 \end{pmatrix},
$$

$$
\begin{aligned}
M_{LL}^2 &= m_{\tilde{Q}}^2 + m_q^2 + m_z^2 \cos 2\beta (I_q^{3L} - e_q \sin^2\theta_w), \\
M_{RR}^2 &= m_{\tilde{U},\tilde{D}}^2 + m_q^2 + m_z^2 \cos 2\beta e_q \sin^2\theta_w, \\
M_{LR} = M_{RL} &= \begin{cases} A_t - \mu\cot\beta & (\tilde{q} = \tilde{t}) \\ A_b - \mu\tan\beta & (\tilde{q} = \tilde{b}), \end{cases}
\end{aligned}
\tag{9}
$$

where $m_{\tilde{Q}}^2$, $m_{\tilde{U},\tilde{D}}^2$ are soft SUSY breaking mass terms of the left- and right-handed squark, respectively; μ is the coefficient of the H_1H_2 term in the superpotential; A_t and A_b are the coefficient of the dimension-three tri-linear soft SUSY-breaking terms; I_q^{3L}, e_q are the weak isospin and electric charge of the squark $\tilde{q}$. From Eqs. 8 and 9, we have

$$
\begin{aligned}
m_{\tilde{t}_{1,2}}^2 &= \frac{1}{2}\left[M_{LL}^2 + M_{RR}^2 \mp \sqrt{(M_{LL}^2 - M_{RR}^2)^2 + 4m_t^2 M_{LR}^2}\right] \\
\tan\theta_{\tilde{t}} &= \frac{m_{\tilde{t}_1}^2 - M_{LL}^2}{m_t M_{LR}}.
\end{aligned}
\tag{10}
$$

Now we present the numerical results. For the SM parameters, we take

$$
\begin{aligned}
m_Z = 91.187GeV, \quad m_W = 80.33GeV \quad &, \quad m_t = 176.0GeV, \quad m_c = 1.4GeV \\
\alpha = 1/128 \quad &, \quad \alpha_S = 0.118
\end{aligned}
\tag{11}
$$

For the MSSM parameters, we choose $\mu = -100GeV$ and $\epsilon^2 = 1/4$. To simplify the calculation we have taken that $m_{\tilde{U}} = m_{\tilde{D}} = m_{\tilde{Q}} = A_t = m_S$ (global SUSY). In Figs. 2-5, we show the cross sections of the process $e^+e^- \to t\bar{c}$ as functions of m_S, $m_{\tilde{g}}$, $\sqrt{s}$ and $\tan\beta$. One can see that the production cross section increases as squarks and gluino masses decrease, and it could reach 0.1 fb for favorable parameters. This is an enhancement by a factor of 10^8 relative to the SM prediction. Such enhancement could be easily understood as following:

$$
\frac{\sigma_{SUSY}}{\sigma_{SM}} \sim \left(\frac{\alpha_s \Delta m_{\tilde{q}}^2}{\alpha m_b^2}\right)^2,
\tag{12}
$$

where $\Delta m_{\tilde{q}}^2$ represents the possible mass square difference among squarks. If $\Delta m_{\tilde{q}}^2$ varies from $100^2 - 200^2 (GeV)^2$, $\frac{\sigma_{SUSY}}{\sigma_{SM}} = 10^7 \sim 10^8$. At the same time, this kind of enhancement could also be observed in FCNC decay process of top quark [8]. Due to the rather clean experimental environment and well-constrained kinematics, the signal of $\bar{t}c$ or $t\bar{c}$ would be spectacular [1]. We expect the SUSY-QCD effects studied in this paper be observed at higher energy e^+e^- colliders.

References

[1] T. Han and J. Hewett, hep-ph/9811237.

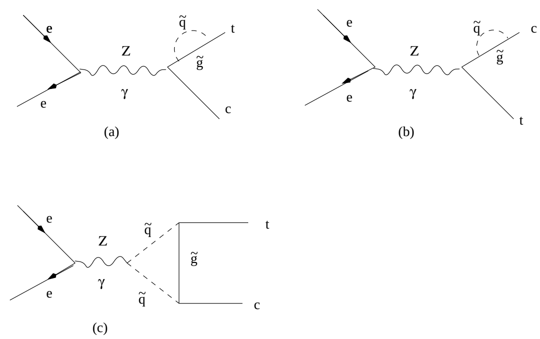

Figure 1: The Feynmann diagrams for the process $e^+e^- \to t\bar{c}$.

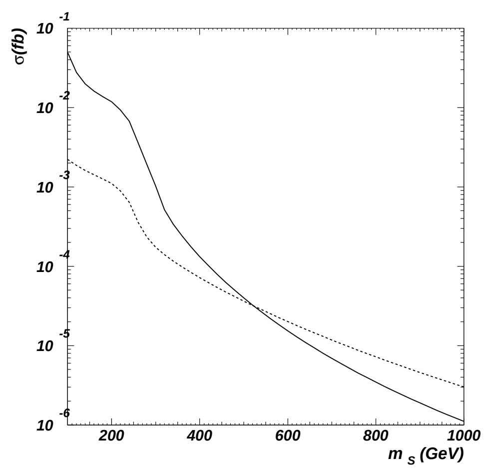

Figure 2: The cross section for the process $e^+e^- \to t\bar{c}$ as a function of m_S, where $\sqrt{S} = 500GeV$, $\tan\beta = 2$, $\epsilon^2 = 1/4$ and $\mu = -100GeV$. The solid and dashed lines represent $m_{\tilde{g}} = 100GeV$ and $500GeV$, respectively.

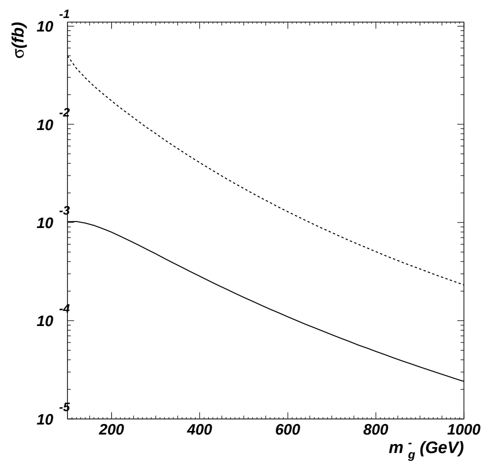

Figure 3: The cross section for the process $e^+e^- \to t\bar{c}$ as a function of $m_{\tilde{g}}$, where $\sqrt{S} = 500GeV$, $\tan\beta = 2$, $\epsilon^2 = 1/4$ and $\mu = -100GeV$. The solid and dashed lines represent $m_S = 300GeV$ and $100GeV$, respectively.

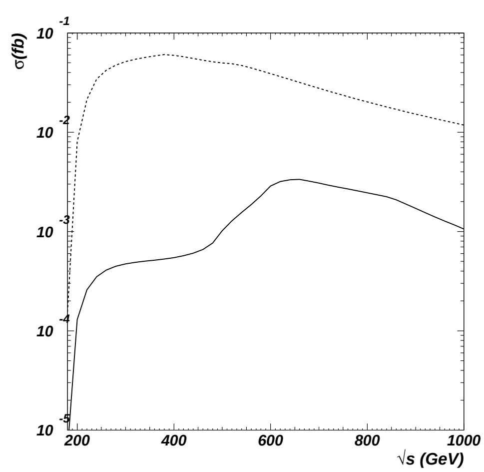

Figure 4: The cross section for the process $e^+e^- \to t\bar{c}$ as a function of $\sqrt{S}$, where $m_{\tilde{g}} = 100GeV$, $\tan\beta = 2$, $\epsilon^2 = 1/4$ and $\mu = -100GeV$. The solid and dashed lines represent $m_S = 300GeV$ and $100GeV$, respectively.

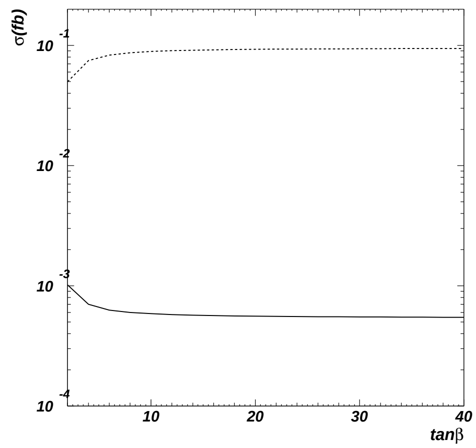

Figure 5: The cross section for the process $e^+e^- \to t\bar{c}$ as a function of $\tan\beta$, where $\sqrt{S} = 500GeV$, $m_{\tilde{g}} = 100GeV$, $\epsilon^2 = 1/4$ and $\mu = -100GeV$. The solid and dashed lines represent $m_S = 300GeV$ and $100GeV$, respectively.

[2] R.D. Peccei, S. Peris and X. Zhang, Nucl. Phys. B349, 305 (1991); T. Han, R.D. Peccei and X. Zhang, Nucl. Phys. B454, 527 (1995); T. Han et al, Phys. Rev. D55, 7241 (1997).

[3] C.S. Huang, X.H. Wu and S.H. Zhu, Phys. Lett. B452 (1999) 143 and references there-in.

[4] J. Ellis and D.V. Nanopoulos, Phys.Lett **110B**(1982)44; R. Barbieri and R. Gatto, Phys.Lett**110B** (1982)211; T. Inami and C.S. Lim, Nucl.Phys.**B207** (1982)533; B.A. Campbell, Phys. Rev.**D28**(1983)209; M.J. Duncan, Nucl.Phys.**B221**(1983)221; J.F. Donoghue, H.P. Nilles and D. Wyler, Phys.Lett.**128 B**(1983)55.

[5] M.J. Duncan, Phys.Rev.**D31**(1985)1139.

[6] G. Passarino and M. Veltman, Nucl. Phys. B 33, 151 (1979); R. Mertig, M. Bohm and A. Denner, Comp. Phys. Comm. 64, 345 (1991); A. Denner, Fortschr. Phys. 41, 307 (1993).

[7] H.E. Haber and G.L. Kane, Phys.Rep. **117**, 75(1985); J.F. Gunion and H.E. Haber, Nucl. Phys. **B272**, 1(1986) For a review see, e.g. J.F. Gunion et.al., Higgs Hunter's Guide (Addison-Wesley, MA,1990).

[8] To see for examples, C.S. Li, R.J. Oakes and J.M. Yang, Phys. Rev. **D49**, 293 (1994), Erratum-*ibid.* **D56**, 3156 (1997); J.M. Yang, B.-L. Young and X. Zhang, Phys. Rev. **D58**, 055001 (1998); J.-M. Yang and C.-S. Li, Phys. Rev. **D49**, 3412

(1994), Erratum-*ibid.* **D51**, 3974 (1995); G. Eilam, J.L. Hewett and A. Soni, Phys. Rev. **D44**, 1473 (1991); Erratum-ibid.D59:039901,1999.

7 Bottom-Strange Associated Production at High Energy e^+e^- Colliders in Standard Model

Abstract

We investigate the flavor changing neutral current bsV(V=γ,Z) couplings in the production vertex for the process $e^+e^- \to b\bar{s}$ or $\bar{b}s$ in the standard model. The precise calculations keeping all quark masses non-zero are carried out. Production cross sections are found to be the order of 10^{-3} fb at LEP II and the order of 10^{-1} fb when center-of-mass energy is near the mass of neutral gauge boson Z.

7.1 Introduction

There are no flavor changing neutral currents (FCNC) at tree-level in the standard model (SM). FCNC appear at loop-levels and consequently offer a good place to test quantum effects of the fundamental quantum field theory on which SM based. Furthermore, they are very small at one loop-level due to the unitarity of Cabbibo-Kobayashi-Maskawa (CKM) matrix. In models beyond SM new particles beyond the particles in SM may appear in the loop and have significant contributions to flavor changing transitions. Therefore, FCNC interactions give an ideal place to search for new physics. Any positive observation of FCNC couplings deviated from that in SM would unambiguously signal the presence of new physics. Searching for FCNC is clearly one of important goals of the next generation of high energy colliders [1].

The flavor changing transitions involving external up-type quarks which are due to FCNC couplings are much more suppressed than those involving external down-type quarks in SM. The effects for external up-type quarks are derived by virtual exchanges of down-type quarks in a loop for which GIM mechanism [2] is much more effective because the mass splitting between down-type quarks are much less than those between up-type quarks. Therefore, for example, the bs transition which is studied in the paper has larger probability to be observed than that for the tc transition.

The b-hadron system promises to give a fertile ground to test the SM and probe new physics. The FCNC vertices bsV(V=γ, Z) have been extensively examined in rare decays of b-hadron system [3, 4, 5]. The observation of FCNC processes in both the exclusive $B \to K^\star\gamma$ and inclusive $B \to X_s\gamma$ channels has placed the rare B decays on a new footing and has put a stringent constraint on classes of models [6]. Analyses of the inclusive decay $B \to X_s l^+l^-$ show that in the minimal supergravity model(SUGRA) there are regions in the parameter space where the branching ratio of $b \to sl^+l^- (l = e, \mu)$ is enhanced by about 50% compared to the SM [7] and the first distinct signals of SUSY could come from the observation of $B \to X_s\mu^+\mu^-$ if tanβ is large (≥ 30) and the mass of the lightest neutral Higgs boson m$_h$ is not too large (say, less than 150 Gev) [3]. The B factories presently under construction will collect some 10^7—10^8 B mesons per year which can be used to obtain good precision on low branching fraction modes.

The FCNC vertices bsV(V=γ, Z) can also be investigated via bottom-strange associated production. In the paper we shall investigate the process

$$e^+e^- \to b\bar{s} \text{ or } \bar{b}s. \tag{1}$$

Comparing b quark rare decays where the momentum transfer q^2 is limited, i. e., it should be less or equal to mass square of b quark m_b^2, the production process (1) allows the large (time-like) momentum transfer, which is actually determined by the energies available at e^+e^- colliders. The reaction (1) has some advantages because of the ability to probe higher dimension operators at large momenta and striking kinematic signatures which are straightforward to detect in the clean environment of e^+e^- collisions. In particular, in some extensions of SM which induce FCNC there are large underlying mass scales and large momentum transfer so that these models are more naturally probed via b$\bar{s}$ associated production than b quark rare decays.

It has been shown that the cross sections of $e^+e^- \to t\bar{c}$ in SM are too small to be observed at LEP or NLC [8]. As pointed above, in SM the cross sections of $e^+e^- \to b\bar{s}$ should be much larger than those of tc final states. Are they large enough to be seen at LEP or NLC? In the paper we would like to address the problem by calculating cross sections and backward-forward asymmetry of the process (1) in SM.

7.2 Analytic calculations

In SM for the process (1) there are three kinds of Feynman diagram at one loop, self energy-type, triangle and box diagram, which are shown in Fig.1. We carry out calculations in the Feynman-t'Hooft gauge. The contributions of the neutral Higgs H and Goldstone bosons $G^{0,\pm}$ which couple to electrons are neglected since they are proportional to the electron mass and we have put the mass of electron to zero.

We do the reduction using FeynCalc [13] and keep all masses non-zero except for the mass of electron. To control the ultraviolet divergence, the dimensional regularization is used. As a consistent check, we found that all divergences are canceled in the sum of contributions of all Feynman diagrams. The calculations are carried out in the frame of the center of mass system (CMS) and Mandelstam variables have been employed:

$$s = (p_1 + p_2)^2 = (k_1 + k_2)^2 \qquad t = (p_1 - k_1)^2 \qquad u = (p_1 - k_2)^2, \tag{2}$$

where p_1, p_2 are the momentum of electron and positron respectively, and k_1, k_2 are the momentum of bottom quark b, and anti-strange quark $\bar{s}$ respectively.

The amplitude of process $e^+e^- \to \bar{b}s$ can be expressed as

$$\begin{aligned} M \;=\; \sum_{j=u,c,t} & 16\pi^2\alpha^2 V_{jb}^{\star}V_{js}[g_1\bar{u}_b\gamma^\mu P_R v_s\bar{v}_e\gamma_\mu P_R u_e + g_2\bar{u}_b\gamma^\mu P_L v_s\bar{v}_e\gamma_\mu P_R u_e + g_3\bar{u}_b\gamma^\mu P_R v_s\bar{v}_e\gamma_\mu P_L u_e + \\ & g_4\bar{u}_b\gamma^\mu P_L v_s\bar{v}_e\gamma_\mu P_L u_e + g_5\bar{u}_b P_R v_s\bar{v}_e \not{k}_1 P_R u_e + g_6\bar{u}_b P_L v_s\bar{v}_e \not{k}_1 P_R u_e + g_7\bar{u}_b P_R v_s\bar{v}_e \not{k}_1 P_L u_e + \\ & g_8\bar{u}_b P_L v_s\bar{v}_e \not{k}_1 P_L u_e + g_9\bar{u}_b \not{p}_1 P_L v_s\bar{v}_e \not{k}_1 P_L u_e + g_{10}\bar{v}_e\gamma^\mu P_L u_e\bar{u}_b\gamma_\mu \not{p}_1 P_R v_s + \\ & g_{11}\bar{v}_e\gamma^\mu P_L u_e\bar{u}_b\gamma_\mu \not{p}_1 P_L v_s] \end{aligned} \tag{3}$$

where α is fine structure constant, V_{ij} is CKM matrix element, P_L is defined as $(1-\gamma^5)/2$, and P_R is defined as $(1+\gamma^5)/2$. The expressions of the coefficients $g_j (j = 1, 2, ...11)$ can be found in Appendix.

Having the amplitude M, it is straightforward to obtain the differential cross section by

$$\frac{d\sigma}{dcos\theta} = \frac{N_c}{16\pi}\frac{|\vec{k_1}|}{s^{\frac{3}{2}}}\frac{1}{4}\sum_{spins}|M|^2 \tag{4}$$

Where N_c is the color factor and θ is the angle between incoming electron e^- and outgoing bottom quark b.

7.3 Numerical results

In the numerical calculations the following values of the parameters have been used [11]:

$$\begin{array}{l} m_e = 0, \quad m_u = 0.005Gev, \quad m_c = 1.4Gev, \quad m_t = 175Gev, \quad m_s = 0.17Gev, \\ m_b = 4.4Gev, \quad m_w = 80.41Gev, \quad m_z = 91.187Gev, \quad \Gamma_z = 2.5Gev, \quad \alpha = \frac{1}{128} \end{array}$$

In order to keep the unitary condition of CKM matrix exactly, we employ the standard parameterization and took the values [11, 12]

$$s_{12} = 0.220, \qquad s_{23} = 0.039, \qquad s_{13} = 0.0031, \qquad \delta_{13} = 70^\circ$$

Numerical results are shown in Figs. 2, 3, 4.

In Fig.2, we show the total cross section σ_{tot} of the process $e^+e^- \to b\bar{s}$ as a function of the center-of-mass energy $\sqrt{s}$. There are three peaks, corresponding to the pole of neutral gauge boson Z^0, a pair of charged gauge boson W threshold, and a pair of top quark $t\bar{t}$ threshold respectively. In most of high energy region, total cross section is the order of 10^{-3} fb, which is too small to be seen at LEP II or planning NLC colliders. Therefore, even a small number of bs events, detected at LEP II or NLC, will unambiguously indicate new FCNC couplings beyond SM. Smallness of the total cross section can easily be understood. One has

$$\begin{aligned} \sum_{spins}|M|^2 &= e^8|\sum_{j=u,c,t}V^\star_{jt}V_{jc}f(x_j,y_j)|^2 \\ &= e^8|V^\star_{tb}V_{ts}\frac{m_t^2-m_c^2}{m_w^2}\frac{\partial f}{\partial x_j}|_{x_j,y_j=0}+...|^2, \end{aligned} \tag{5}$$

due to GIM mechanism, where $x_j = m_j^2/m_w^2$, $y_j = m_j^2/s$, and "..." denote the less important terms for $\sqrt{s} \geq 200$ Gev. Assuming $\frac{\partial f}{\partial x_j}|_{x_j,y_j=0} = $ O(1), one obtains from eqs. (4), (5)

$$\sigma \sim 10^{-3} fb$$

at $\sqrt{s} = 200$ Gev.

We fixed the center-of-mass energy $\sqrt{s}$ at 200 Gev. Differential cross section of the process at the energy as a function of $\cos\theta$ is shown in Fig.3.

The Fig.4 is devoted to the backward-forward asymmetry

$$A_{FB} = \frac{\int_0^{\pi/2} \frac{d\sigma}{d\theta} d\theta - \int_{\pi/2}^{\pi} \frac{d\sigma}{d\theta} d\theta}{\int_0^{\pi/2} \frac{d\sigma}{d\theta} d\theta + \int_{\pi/2}^{\pi} \frac{d\sigma}{d\theta} d\theta} \tag{6}$$

as a function of $\sqrt{s}$.

To summarize, we have calculated the process $e^+e^- \to b\bar{s}$ in SM. We found that the total cross section is of the order of $10^{-3} fb$ in the high energy region which is still too small to be seen at LEP II or planning NLC. However, it is worth to note that the total cross section at Z resonance may reach as large as 10^{-1} fb. Therefore, it is possible to see the process if a luminosity reaches 100-1000 fb^{-1}. In addition to that, the process is of a good place to search for new physics.

7.4 Appendix

$$\begin{aligned} g_1 &= m_s(B_0^a(m_b^2 - m_s^2)(m_j^2 - m_w^2)(m_j^2 + 2m_w^2) + B_0^b m_s^2(m_b^4 - 2m_b^2 m_j^2 + m_j^4 + m_b^2 m_w^2 + m_j^2 m_w^2 - \\ &\quad 2m_w^4) - B_0^c m_b^2(m_s^4 - 2m_s^2 m_j^2 + m_j^4 + m_s^2 m_w^2 + m_j^2 m_w^2 - 2m_w^4))(a_1 - 4a_2 s_w^4) + \\ &\quad 2m_b m_s(2C_{00}^e + C_{11}^e m_b^2 + C_0^e m_j^2 + C_1^e(m_b^2 + m_j^2 - 2m_w^2) + C_{22}^e s + C_2^e s + \\ &\quad C_{12}^e(m_b^2 - m_s^2 + s))(a_3 + 6a_4 s_w^2 - 8a_4 s_w^4) - 6C_{00}^d m_b m_s(a_3 + 4a_4 s_w^2(c_w^2 - s_w^2)) + \\ &\quad 12 m_b m_s m_w^2(C_0^d + C_1^d)(a_3 + 6a_4 c_w^2 s_w^2 - 2a_4 s_w^4) \end{aligned} \tag{7}$$

$$\begin{aligned} g_2 &= -a_3 m_j^2 + 8a_4 m_j^2 s_w^4 - 6m_w^2(C_{11}^d m_b^2 + C_{22}^d s + C_{12}^d(m_b^2 - m_s^2 + s))(a_3 + 8a_4 c_w^2 s_w^2) + \\ &\quad m_b m_s^2(B_0^a(m_b^2 - m_s^2)(m_j^2 - m_w^2) + (m_b^2 m_s^2 - m_b^2 m_j^2 - m_s^2 m_j^2 + m_j^4 + m_j^2 m_w^2 - \\ &\quad 2m_w^4)(B_0^b - B_0^c) + m_w^2(B_0^b(2m_b^2 - m_s^2) - B_0^c(2m_s^2 - m_b^2)))(a_1 + 6a_2 s_w^2 - 4a_2 s_w^4) - \\ &\quad 6C_2^d m_w^2(a_3(m_b^2 - m_s^2 + s) + 4a_4 s_w^2((m_b^2 - m_s^2)(c_w^2 - s_w^2) + 2sc_w^2)) - 6C_{00}^d(a_3(m_j^2 + 6m_w^2) + \\ &\quad 4a_4 s_w^2(c_w^2 m_j^2 + 12c_w^2 m_w^2 - m_j^2 s_w^2)) + 2(2C_{00}^e + C_{11}^e m_b^2 + C_{22}^e s + C_{12}^e(m_b^2 - m_s^2 + s)) \\ &\quad (a_3(m_j^2 + 2m_w^2) + 4a_4 s_w^2(3m_w^2 - 2m_j^2 s_w^2 - 4m_w^2 s_w^2)) + 2C_0^e m_j^2(a_3(m_b^2 + m_s^2 - m_j^2 - 2m_w^2) + \\ &\quad 2a_4 s_w^2(3m_s^2 - 3m_j^2 - 4m_b^2 s_w^2 - 4m_s^2 s_w^2 + 4m_j^2 s_w^2 + 8m_w^2 s_w^2)) + 2C_2^e(a_3 s(m_j^2 + 2m_w^2) - \\ &\quad 2a_4 s_w^2(3m_b^2 m_j^2 - 3m_s^2 m_j^2 - 6m_w^2 s + 4m_j^2 s s_w^2 + 8m_w^2 s s_w^2)) - 6C_1^d m_w^2(a_3(m_b^2 - m_s^2 + s) + \\ &\quad 4a_4 s_w^2(m_b^2 c_w^2 - m_b^2 s_w^2 - 2c_w^2 m_s^2 + 2c_w^2 s)) - 6C_0^d m_w^2(a_3(s - m_s^2 - m_j^2) + \\ &\quad 4a_4 s_w^2(2sc_w^2 - m_b^2 + 2m_j^2 s_w^2 - 2c_w^2 m_s^2)) + 2C_1^e(a_3(2sm_w^2 + m_b^2 m_s^2 + m_b^2 m_j^2 - 2m_w^2 m_s^2) + \\ &\quad 2a_4 s_w^2(3m_b^2 m_s^2 - 3m_b^2 m_j^2 + 6sm_w^2 - 4m_b^2 m_s^2 s_w^2 - 4m_b^2 m_j^2 s_w^2 - 8sm_w^2 s_w^2 - \\ &\quad 6m_w^2 m_s^2 + 8m_w^2 m_s^2 s_w^2)) \end{aligned} \tag{8}$$

$$g_3 = -a_5 m_b m_s(2D_{23}^f + D_3^f) + m_s(B_0^a(m_b^2 - m_s^2)(m_j^2 - m_w^2)(m_j^2 + 2m_w^2) + B_0^b m_s^2(m_b^4 - 2m_b^2 m_j^2 +$$

$$
\begin{aligned}
& m_j^4+m_b^2m_w^2+m_j^2m_w^2-2m_w^4)-B_0^cm_b^2(m_s^4-2m_s^2m_j^2+m_j^4+m_s^2m_w^2+m_j^2m_w^2-2m_w^4))(a_1+\\
& 2a_2s_w^2-4a_2s_w^4)+2m_bm_s(2C_{00}^e+C_{11}^em_b^2+C_0^em_j^2+C_1^e(m_b^2+m_j^2-2m_w^2)+C_{22}^es+C_2^es+\\
& C_{12}^e(m_b^2-m_s^2+s))(a_3-3a_4+10a_4s_w^2-8a_4s_w^4)-6C_{00}^dm_bm_s(a_3-2a_4(1-2s_w^2)^2)+\\
& 12m_bm_sm_w^2(C_0^d+C_1^d)(a_3-a_4(3-4s_w^2)(1-2s_w^2)) \qquad (9)
\end{aligned}
$$

$$
\begin{aligned}
g_4 \;=\;& -a_5(2D_{00}^f-(2D_{13}^f+D_1^f)(m_b^2-t)+2D_{23}^ft+D_3^ft)-a_3m_j^2-4a_4m_j^2s_w^2(1-2s_w^2)-\\
& 6m_w^2(C_{11}^dm_b^2+C_{22}^ds+C_{12}^d(m_b^2-m_s^2+s))(a_3-4a_4c_w^2(1-2s_w^2))+\\
& m_bm_s^2(B_0^a(m_b^2-m_s^2)(m_j^2-m_w^2)+B_0^b(m_b^2m_s^2-m_b^2m_j^2-m_s^2m_j^2+m_j^4+2m_b^2m_w^2-m_s^2m_w^2+\\
& m_j^2m_w^2-2m_w^4)-B_0^c(m_b^2m_s^2-m_b^2m_j^2-m_s^2m_j^2+m_j^4-m_b^2m_w^2+2m_s^2m_w^2+m_j^2m_w^2-2m_w^4))\times\\
& (a_1-3a_2+8a_2s_w^2-4a_2s_w^4)-6C_2^dm_w^2(a_3(m_b^2-m_s^2+s)+2a_4(c_w^2m_s^2-c_w^2m_b^2-2c_w^2s+\\
& m_b^2s_w^2+2c_w^2m_b^2s_w^2-m_s^2s_w^2-2c_w^2m_s^2s_w^2+4c_w^2ss_w^2-2m_b^2s_w^4+2m_s^2s_w^4))-6C_{00}^d(a_3(m_j^2+6m_w^2)+\\
& 2a_4(m_j^2s_w^2-c_w^2m_j^2-12c_w^2m_w^2+2c_w^2m_j^2s_w^2+24c_w^2m_w^2s_w^2-2m_j^2s_w^4))+\\
& 2(2C_{00}^e+C_{11}^em_b^2+C_{22}^es)(a_3(m_j^2+2m_w^2)+2a_4(2m_j^2s_w^2-3m_w^2+10m_w^2s_w^2-4m_j^2s_w^4-8m_w^2s_w^4))+\\
& 2C_0^em_j^2(a_3(m_b^2+m_s^2-m_j^2-2m_w^2)+a_4(3m_j^2-3m_s^2+4m_b^2s_w^2+10m_s^2s_w^2-10m_j^2s_w^2-8m_w^2s_w^2-\\
& 8m_b^2s_w^4-8m_s^2s_w^4+8m_j^2s_w^4+16m_w^2s_w^4))+2C_2^e(a_3s(m_j^2+2m_w^2)+a_4(3m_b^2m_j^2-3m_s^2m_j^2-\\
& 6m_w^2s-6m_b^2m_j^2s_w^2+6m_s^2m_j^2s_w^2+4m_j^2ss_w^2+20m_w^2ss_w^2-8m_j^2ss_w^4-16m_w^2ss_w^4))+\\
& 2C_{12}^e(m_b^2-m_s^2+s)(a_3(m_j^2+2m_w^2)-2a_4(3m_w^2-2m_j^2s_w^2-10m_w^2s_w^2+4m_j^2s_w^4+8m_w^2s_w^4))-\\
& 6C_1^dm_w^2(a_3(m_b^2-m_s^2+s)+2a_4(m_b^2s_w^2-3c_w^2m_b^2+6c_w^2m_b^2s_w^2-2m_b^2s_w^4+2c_w^2t-4c_w^2s_w^2t+\\
& 2c_w^2u-4c_w^2s_w^2u))-6C_0^dm_w^2(a_3(s-m_s^2-m_j^2)+2a_4(m_b^2s_w^2+c_w^2m_b^2-2c_w^2m_b^2s_w^2-2m_j^2s_w^2-\\
& 2m_b^2s_w^4+4m_j^2s_w^4+2m_s^2c_w^2-4m_s^2c_w^2s_w^2-2sc_w^2+4sc_w^2s_w^2))+2C_1^e(a_3(m_b^2m_s^2+m_b^2m_j^2+\\
& 2m_b^2m_w^2-2m_w^2t-2m_w^2u)+a_4(3m_b^2m_j^2-3m_b^2m_s^2+6m_s^2m_w^2+10m_b^2m_s^2s_w^2-2m_b^2m_j^2s_w^2-\\
& 20m_s^2m_w^2s_w^2-8m_b^2m_s^2s_w^4-8m_b^2m_j^2s_w^4+16m_s^2m_w^2s_w^4-6sm_w^2+20sm_w^2s_w^2-16sm_w^2s_w^4)) \qquad (10)
\end{aligned}
$$

$$
\begin{aligned}
g_5 \;=\;& -24a_4m_ss_w^2(C_2^em_j^2-2C_2^dm_w^2)-4m_s(C_{11}^em_b^2+C_0^em_j^2+C_1^e(m_b^2+m_j^2-2m_w^2))(a_3+6a_4s_w^2-\\
& 8a_4s_w^4)-6m_s(C_{11}^dm_b^2+2C_0^dm_w^2+C_1^d(m_b^2-m_j^2+2m_w^2))(a_3+4a_4c_w^2s_w^2-4a_4s_w^4)-\\
& 6C_{12}^dm_s(a_3(m_b^2-m_j^2-2m_w^2)+4a_4s_w^2(m_b^2c_w^2-c_w^2m_j^2-4c_w^2m_w^2-m_b^2s_w^2+m_j^2s_w^2))-\\
& 4C_{12}^em_s(a_3(m_b^2-m_j^2-2m_w^2)+2a_4s_w^2(3m_b^2-6m_w^2-4m_b^2s_w^2+4m_j^2s_w^2+8m_w^2s_w^2)) \qquad (11)
\end{aligned}
$$

$$
\begin{aligned}
g_6 \;=\;& 24a_4m_bs_w^2(C_2^em_j^2-2C_2^dm_w^2)-12m_bm_w^2(C_0^d+2C_1^d)(a_3+8a_4c_w^2s_w^2)-\\
& 4m_bm_j^2(C_0^e+2C_1^e)(a_3-8a_4s_w^4)-6C_{11}^dm_b(a_3(m_j^2+2m_w^2)+4a_4s_w^2(c_w^2m_j^2+4c_w^2m_w^2-m_j^2s_w^2))+\\
& 6C_{12}^dm_b(a_3(m_s^2-m_j^2-2m_w^2)+4a_4s_w^2(c_w^2m_s^2-c_w^2m_j^2-4c_w^2m_w^2-m_s^2s_w^2+m_j^2s_w^2))-\\
& 4C_{11}^em_b(a_3(m_j^2+2m_w^2)+4a_4s_w^2(3m_w^2-2m_j^2s_w^2-4m_w^2s_w^2))+4C_{12}^em_b(a_3(m_s^2-m_j^2-2m_w^2)+\\
& 2a_4s_w^2(3m_s^2-6m_w^2-4m_s^2s_w^2+4m_j^2s_w^2+8m_w^2s_w^2)) \qquad (12)
\end{aligned}
$$

$$
g_7 \;=\; 2a_5m_s(D_{23}^f+D_3^f)+12a_4m_s(C_2^em_j^2-2C_2^dm_w^2)(1-2s_w^2)-4m_s(C_{11}^em_b^2+C_0^em_j^2+C_1^e(m_b^2+
$$

$$m_j^2 - 2m_w^2))(a_3 - 3a_4 + 10a_4 s_w^2 - 8a_4 s_w^4) - 6m_s(C_{11}^d m_b^2 + 2C_0^d m_w^2 +$$
$$C_1^d(m_b^2 - m_j^2 + 2m_w^2))(a_3 - 2a_4(s_w^2 - c_w^2)^2) - 6C_{12}^d m_s(a_3(m_b^2 - m_j^2 - 2m_w^2) + 2a_4(c_w^2 m_j^2 -$$
$$c_w^2 m_b^2 + 4c_w^2 m_w^2 + m_b^2 s_w^2 + 2c_w^2 m_b^2 s_w^2 - m_j^2 s_w^2 - 2c_w^2 m_j^2 s_w^2 - 8c_w^2 m_w^2 s_w^2 - 2m_b^2 s_w^4 + 2m_j^2 s_w^4)) -$$
$$4C_{12}^e m_s(a_3(m_b^2 - m_j^2 - 2m_w^2) + a_4(6m_w^2 - 3m_b^2 + 10m_b^2 s_w^2 - 4m_j^2 s_w^2 - 20m_w^2 s_w^2 - 8m_b^2 s_w^4 +$$
$$8m_j^2 s_w^4 + 16m_w^2 s_w^4)) \qquad (13)$$

$$\begin{aligned} g_8 = & -2a_5 m_b(D_{22}^f - D_{23}^f + D_2^f) - 12a_4 m_b(C_2^e m_j^2 - 2C_2^d m_w^2)(1 - 2s_w^2) - 12m_b m_w^2(C_0^d + 2C_1^d)(a_3 - \\ & 4a_4 c_w^2(1 - 2s_w^2)) - 4m_b m_j^2(C_0^e + 2C_1^e)(a_3 + 4a_4 s_w^2(1 - 2s_w^2)) - 6C_{11}^d m_b(a_3(m_j^2 + 2m_w^2) - \\ & 2a_4(c_w^2 m_j^2 + 4c_w^2 m_w^2 - m_j^2 s_w^2 - 2c_w^2 m_j^2 s_w^2 - 8c_w^2 m_w^2 s_w^2 + 2m_j^2 s_w^4)) + 6C_{12}^d m_b(a_3(m_s^2 - m_j^2 - \\ & 2m_w^2) - 2a_4(c_w^2 m_s^2 - c_w^2 m_j^2 - 4c_w^2 m_w^2 - m_s^2 s_w^2 - 2c_w^2 m_s^2 s_w^2 + m_j^2 s_w^2 + 2c_w^2 m_j^2 s_w^2 + 8c_w^2 m_w^2 s_w^2 + \\ & 2m_s^2 s_w^4 - 2m_j^2 s_w^4)) - 4C_{11}^e m_b(a_3(m_j^2 + 2m_w^2) + 2a_4(2m_j^2 s_w^2 - 3m_w^2 + 10m_w^2 s_w^2 - 4m_j^2 s_w^4 - \\ & 8m_w^2 s_w^4)) + 4C_{12}^e m_b(a_3(m_s^2 - m_j^2 - 2m_w^2) + a_4(6m_w^2 - 3m_s^2 + 10m_s^2 s_w^2 - 4m_j^2 s_w^2 - \\ & 20m_w^2 s_w^2 - 8m_s^2 s_w^4 + 8m_j^2 s_w^4 + 16m_w^2 s_w^4)) \qquad (14) \\ g_9 = & \ 2a_5(D_{12}^f - 2D_{13}^f + D_{22}^f - D_{23}^f + D_2^f) \qquad (15) \\ g_{10} = & -a_5 m_s(2D_{13}^f + 2D_{23}^f + D_3^f) \qquad (16) \\ g_{11} = & \ a_5 m_b(2D_{13}^f + D_1^f) \qquad (17) \end{aligned}$$

where a_i is defined as

$$a_1 = \frac{1}{192\pi^2 s m_b m_s^2 m_w^2 (m_b^2 - m_s^2) s_w^2}, \quad a_2 = \frac{1}{768\pi^2 m_b m_s^2 m_w^2 (m_b^2 - m_s^2)(m_z^2 - i m_z \Gamma z - s) c_w^2 s_w^4}$$
$$a_3 = \frac{1}{96\pi^2 s m_w^2 s_w^2}, \quad a_4 = \frac{1}{768\pi^2 m_w^2 (m_z^2 - i m_z \Gamma z - s) c_w^2 s_w^4}, \quad a_5 = \frac{1}{32\pi^2 s_w^4}$$

where $c_w = cos\theta_w$ and $s_w = sin\theta_w$. In the presentation of g_j above, we have used the definition of scalar integrals Bs, Cs,and Ds[13],and these functions, Bs, Cs,and Ds, with superscripts a,b,...,f have the arguments
$(0, m_j^2, m_w^2)$, (m_b^2, m_j^2, m_w^2), (m_s^2, m_j^2, m_w^2), $(m_b^2, m_s^2, s, m_w^2, m_j^2, m_w^2)$
$(m_b^2, m_s^2, s, m_j^2, m_w^2, m_j^2)$, $(0, m_b^2, m_s^2, 0, t, s, 0, m_w^2, m_j^2, m_w^2)$
respectively. Here m_j denotes the mass of up-type quark u, c, t.

References

[1] Proceedings of the Workshop on Physics and Experiments with Linear e^+e^- Colliders, eds. A. Miyamoto and Y. Fujii, World Scientific, Singapore, 1996.

[2] S. L. Glashow, J. Iliopoulos, and L. Maiani, Phys. rev. **D2** (1970) 1285.

[3] Y.B. Dai, C.S. Huang and H.W. Huang, Phys. Lett. B 390 (1997) 257; Chao-shang Huang, Wei Liao, and Qi-shu Yan, Phys. Rev. **D59** (1998) 011701; Chao-shang Huang and Qi-shu Yan, Phys. Lett. **B442** (1998) 209.

[4] S. Bertolini, F. borzumati, A. Masieso and G. Ridolfi, Nucl. Phys. **B353** (1991) 591; A. Ali, G. Gindice and T. Mannel, Z. Phys. **C67** (1995) 417; P. Cho, M. Misiak and D. Wlyer, Phys. Rev. **D54** (1996) 3329; A. Masiero and L. Silvestrini, hep-ph/9711401; J. L. Hewett and J. D. Wells, Phys. Rev. **D55** (1997) 5549; M. Ciuchini et al., hep-ph/9806308; A. L. Kagan and M. Neubert, hep-ph/9805303; M. Neubert, hep-ph/9809377; C. S. Huang, T. Li, W. Liao, Q. S. Yan and S. H. Zhu, hep-ph/9810412; M. Brhlik, hep-ph/9807309; H. Baer, M. Brhlik, C-H. Chen and X. Tata, Phys. Rev. **D55** (1997) 4463; J.L. Lopez, D.V. Nanopoulos, X. Wang and A. Zichichi, Phys. Rev. **D51**(1995) 147; R. Barbieri and G.F. Giudice, Phys Lett **B309**(1993)86; M.A. Diaz, Phys. Lett. **B322** (1994) 591; T. Goto and Y. Okada, Prog. of Theor. Phys. **94** (1995) 407; R. Garisto and J. N. Ng Phys. Lett. **B315** (1993) 372; B. Grinstein, M.J. Savage and M.B. Wise, Nucl. Phys. B 319 (1989) 271; For a recent discussion of the $b \to s\gamma$ see C. Greub and T. Hurth, hep-ph/9809468.

[5] For reviews see, for example, A. Ali, hep-ph/9709507; A. J. Buras, hep-ph/9806471; M. Misiak, S. Pokorski and J. Rosiek, hep-ph/9703442; G. Burdman, hep-ph/9811457; J. L. Hewett, hep-ph/9803370.

[6] J. L. Hewett, hep-ph/9406302.

[7] T. Goto, Y. Okada, Y. Shimizu and M. Tanaka, Phys. Rev. D 55 (1997) 4273.

[8] Chao-shang Huang, Xiao-hong Wu and Shou-hua Zhu, hep-ph/9901369.

[9] A. Axelrod, Nucl. Phys. B209,(1982)349

[10] J.Kublbeck, M.Bohm and A. Denner, Comp. Phys. Comm, 60 (1990)165

[11] Particle Data Group, Eur.Phys.J. C3,1-794(1998)

[12] A. J. Buras, hep-ph/9711217, hep-ph/9806473.

[13] G.Passarino and M.Veltman, Nucl. Phys, B160(1979) 151 ; R.Mertig, M. Bohm, and A.Denner, Comp. Phys. Comm. 64(1991)345

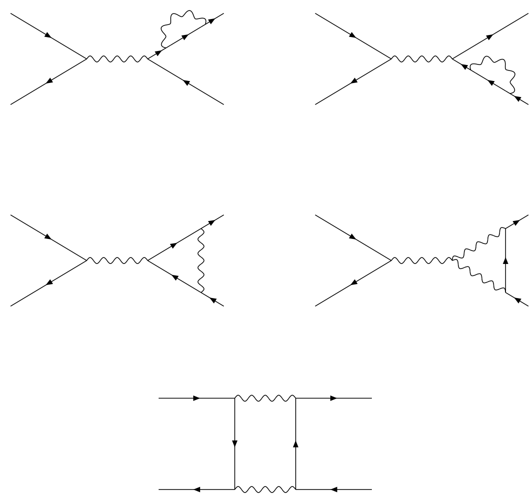

Figure 1: Typical Feynman diagram of prosess $e^+e^- \to b\bar{s}$

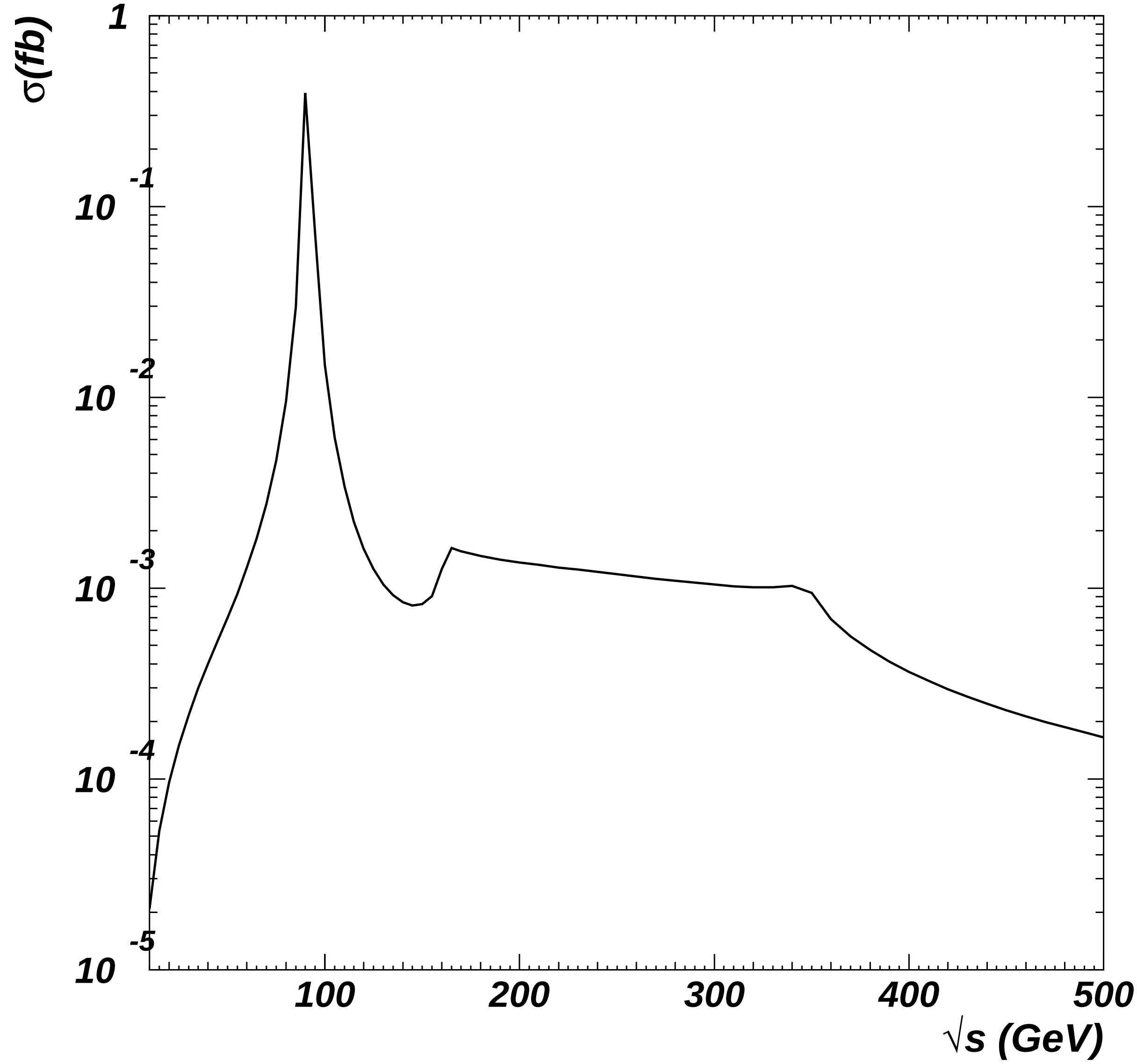

Figure 2: Cross section of the process $e^+e^- \to b\bar{s}$ as a function of $\sqrt{s}$.

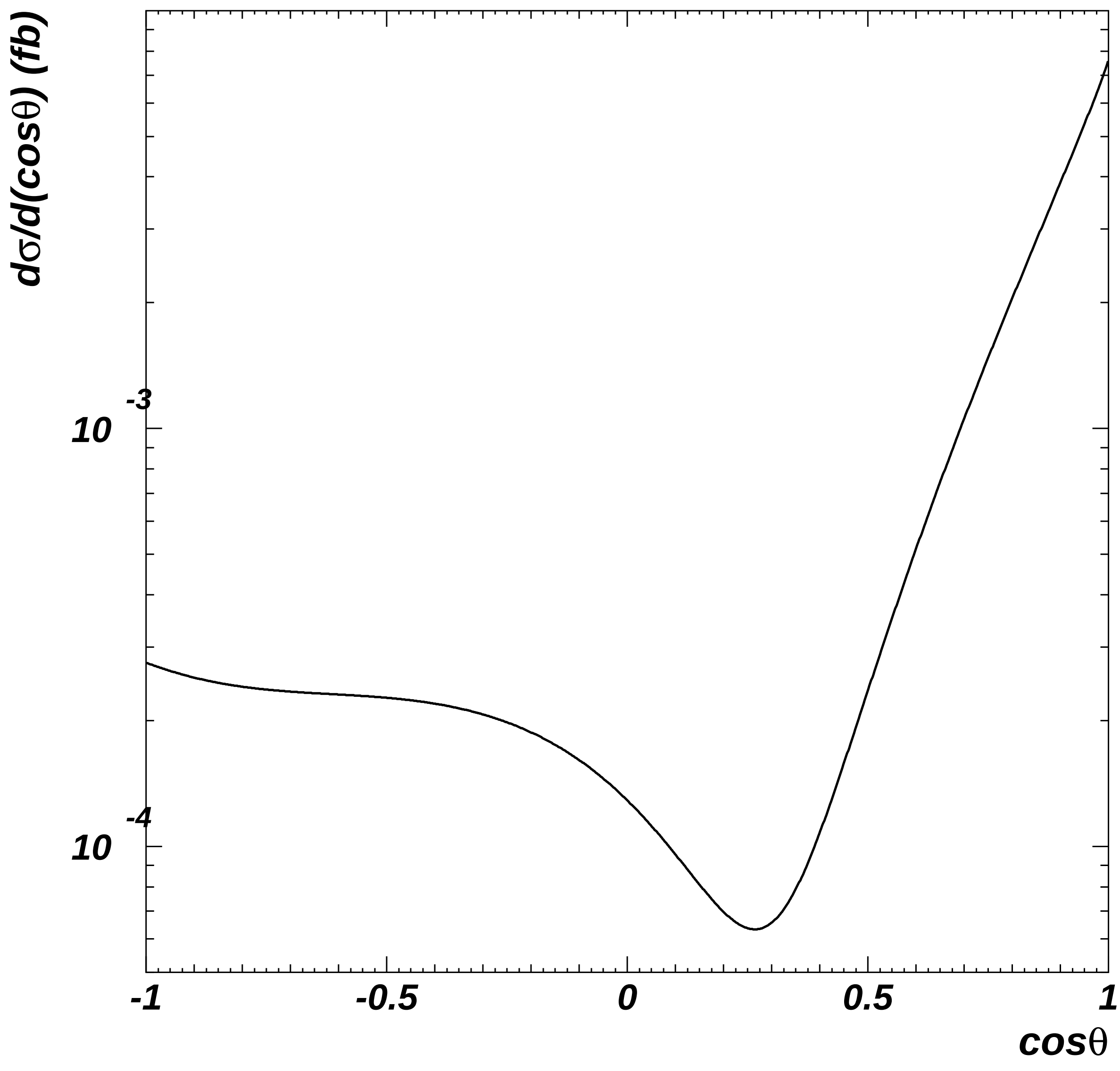

Figure 3: Differential cross section of the process $e^+e^- \rightarrow b\bar{s}$, where $\sqrt{s} = 200$ GeV.

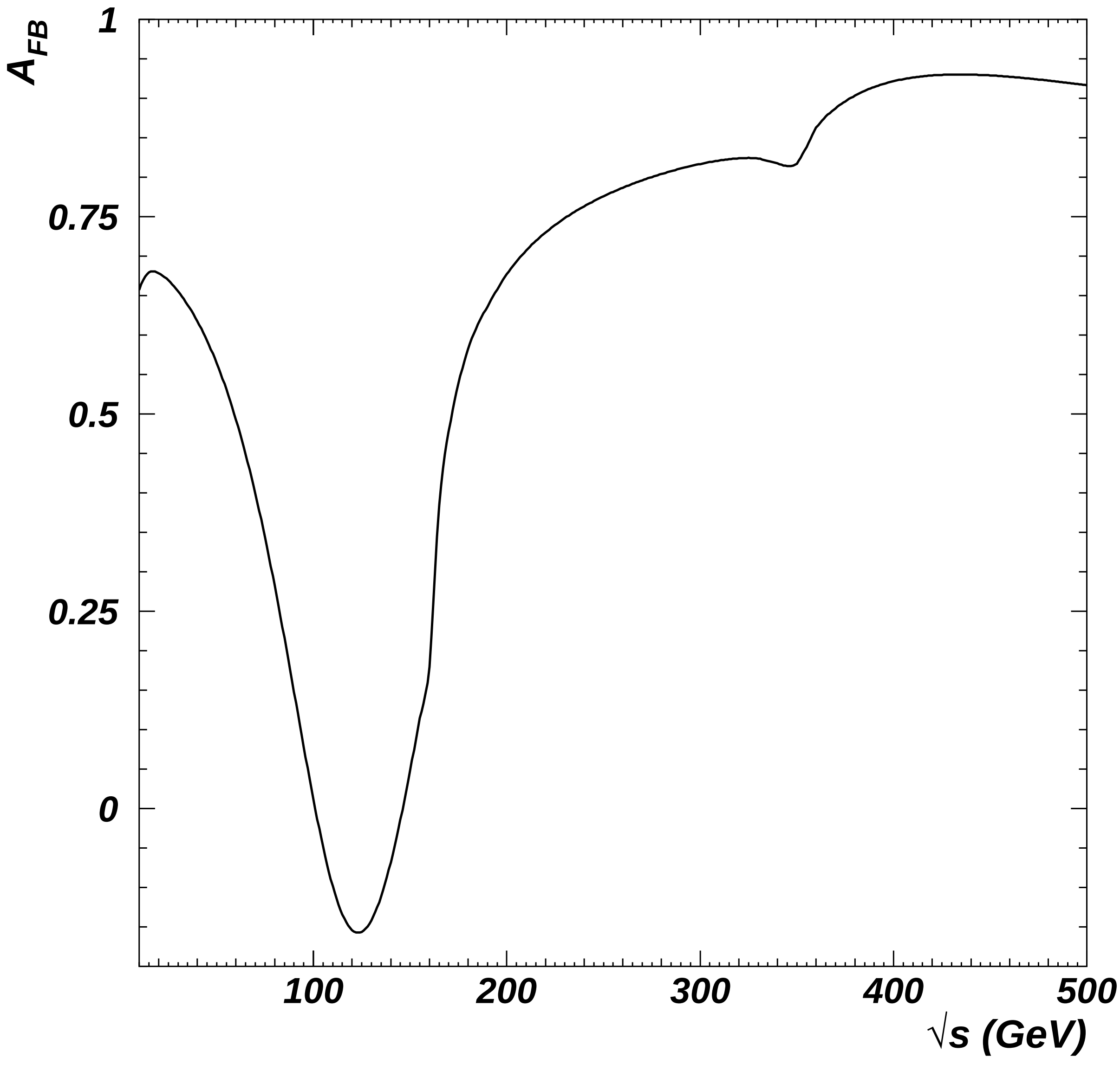

Figure 4: A_{FB} of the process $e^+e^- \to b\bar{s}$ as a function of $\sqrt{s}$.

8 $B \to X_s\tau^+\tau^-$ in a CP softly broken two Higgs doublet model

ABSTRACT

The differential branching ratio, forward-backward asymmetry, CP asymmetry and lepton polarization for a B-meson to decay to strange hadronic final states and a $\tau^+\tau^-$ pair in a CP softly broken two Higgs doublet model are computed. It is shown that contributions of neutral Higgs bosons to the decay are quite significant when $\tan\beta$ is large. And it is proposed to measure the direct CP asymmetry in back-forward asymmetry.

8.1 Introduction

The origin of the CP violation has been one of main issues in high energy physics since the discovery of the CP violation in the $K_0-\overline{K}_0$ systerm in 1964 [1]. The measurements of electric dipole moments of the neutron and electron and the matter-antimatter asymmetry in the universe indicate that one needs new sources of CP violation in addition to the CP violation come from CKM matrix, which has been one of motivations to search new theoretical models beyond the standard model (SM).

The minimal extension of the SM is to enlarge the Higgs sectors of the SM [2]. It has been shown that if one adheres to the natural flavor conservation (NFC) in the Higgs sector, then a minimum of three Higgs doublets are necessary in order to have spontaneous CP violations [3]. However, the constraint can be evaded if one allows the real and image parts of $\phi_1^+\phi_2$ have different self-couplings and adds a linear term of $\mathrm{Re}(\phi_1^+\phi_2)$ in the Higgs potential (see below Eq. (2) with $m_4^2 = 0$). Then, one can construct a CP spontaneously broken two Higgs doublet (2HDM), which is the minimal and the most "economical" one [2] among the extensions of the SM that provide new source of CP violation. Furthermore, in addition to the above terms, if one adds a linear term of $\mathrm{Im}(\phi_1^+\phi_2)$, then one has a CP softly broken 2HDM [4].

Flavor changing neutral current (FCNC) transitions $B \to X_s\gamma$ and $B \to X_s l^+l^-$ provide testing grounds for the SM at the loop level and sensitivity to new physics. Rare decays $B \to X_s l^+l^-(l = e, \mu)$ have been extensively investigated in both SM and the beyond [6, 7]. In these processes contributions from exchanging neutral Higgs bosons (NHB) can be safely neglected because of smallness of $\frac{m_l}{m_W}(l = e, \mu)$. The inclusive decay $B \to X_s\tau^+\tau^-$ has also been investigated in the SM, the model II 2HDM and SUSY models with and without including the contributions of NHB [8, 9, 10, 11]. In this note we investigate the inclusive decay $B \to X_s\tau^+\tau^-$ with emphasis on CP violation effect in a CP softly broken 2HDM, which we shall call Model IV hereafter for the sake of simplisity. We consider the Model IV in which the up-type quarks get masses from Yukawa couplings to the one Higgs doublet H_2 and down-type quarks and leptons

[2] Comparing the Model III 2HDM [5], in which CP is explicitly violated, the CP spontaneously broken 2HDM has only two new parameters besides the masses of the Higgs bosons in the large $\tan\beta$ limit (see below). In this sense it is the most "economical".

get masses from Yukawa couplings to the another Higgs doublet H_1. The Higgs boson couplings to down-type quarks and leptons depend on only the CP violated phase ξ which comes from the expectation value of Higgs and the ratio $tg\beta = \frac{v_2}{v_1}$ in the large $tg\beta$ limit (see next subsection), which are the free parameters in the model. Because the couplings of the charged Higgs to fermions in Model IV are the same as those in the model II, the constraints on $\tan\beta$ due to effects arising from the charged Higgs are the same as those in the model II. Constraints on $tg\beta$ from $K-\bar{K}$ and $B-\bar{B}$ mixing, $\Gamma(b\to s\gamma)$,$\Gamma(b\to c\tau\bar{\nu}_\tau)$ and R_b have been given [12]

$$0.7 \le tg\beta \le 0.52(\frac{m_{H^\pm}}{1Gev}) \tag{1}$$

(and the lower limit $m_{H^\pm} \ge 200Gev$ has also been given in the ref. [12]). It is obvious that the contributions from exchanging neutral Higgs bosons now is enhanced roughly by a factor of $tg^2\beta$ and can compete with those from exchanging $\gamma,\ Z$ when $tg\beta$ is large enough. Because the CP violation effects in $B\to X_s\tau^+\tau^-$ come from the couplings of NHB to leptons and quarks, we shall be interested in the large $\tan\beta$ limit in this note. The constraints on ξ can be obtained from the electric dipole moments (EDM) of the neutron and electron, which will be analysed in the next subsection.

8.2 Model description

Consider two complex $y=1$, $SU(2)_w$ doublet scalar fields, ϕ_1 and ϕ_2. The Higgs potential which spontaneously breaks $SU(2)\times U(1)$ down to $U(1)_{EM}$ can be written in the following form [4]:

$$\begin{aligned} V(\phi_1,\phi_2) &= \sum_{i=1,2}[m_i^2\phi_i^+\phi_i + \lambda_i(\phi_i^+\phi_i)^2] \\ &\quad +m_3^2 Re(\phi_1^+\phi_2) + m_4^2 Im(\phi_1^+\phi_2) \\ &\quad +\lambda_3[(\phi_1^+\phi_1)(\phi_2^+\phi_2)] + \lambda_4[(\phi_1^+\phi_2)(\phi_2^+\phi_1)] \\ &\quad +\lambda_5[\mathrm{Re}(\phi_1^+\phi_2)]^2 + \lambda_6[\mathrm{Im}(\phi_1^+\phi_2)]^2 \end{aligned} \tag{2}$$

Hermiticity requires that all parameters are real. The potential is CP softly broken due to the presence of the term $m_4^2 Im(\phi_1^+\phi_2)$. It is easy to see that the minimum of the potential is at

$$<\phi_1>=\begin{pmatrix}0\\ v_1\end{pmatrix}, \quad <\phi_2>=\begin{pmatrix}0\\ v_2e^{i\xi}\end{pmatrix}, \tag{3}$$

thus breaking $SU(2)\times U(1)$ down to $U(1)_{EM}$ and simutaneously breaking CP, as desired. It should be noticed that only for $\lambda_5 \neq \lambda_6$, the phase ξ can't rotated away as usual, which breaks the CP-conservation. If m_4^2=0 in (2) then the potential is CP invarint. It has been shown that the CP spontaneously breaking happens at (3) [13]. We limit ourself to the case of $m_4^2 \neq 0$ in the paper and shall investigate the m_4^2=0 case in a separate paper [14].

In the following we will work out the mass spectrum of the Higgs boson. For charged components, the mass-squared matrix for negtive states is

$$\lambda_4 \begin{pmatrix} v_1^2 & -v_1 v_2 e^{i\xi} \\ -v_1 v_2 e^{-i\xi} & v_2^2 \end{pmatrix}, \tag{4}$$

Diagonalizing the mass-squared matrix results in one zero-mass Goldstone state:

$$G^- = e^{i\xi} \sin\beta \phi_2^- + \cos\beta \phi_1^-, \tag{5}$$

and one massive charged Higgs boson state:

$$H^- = e^{i\xi} \cos\beta \phi_2^- - \sin\beta \phi_1^-, \tag{6}$$

$$m_{H^-} = |\lambda_4|(v_1^2 + v_2^2), \tag{7}$$

where $\tan\beta = v_2/v_1$. Correspondingly we could also get the positive states G^+ and H^+ with the same masses zero and $|\lambda_4|(v_1^2 + v_2^2)$, respectively.

For neutral Higgs components, because CP-conservation is breaking, the mass-squared matrix is 4×4, which could not be simply separated into two 2×2 matrices as usual. However, in the case of large $\tan\beta$ which is we intrested in, the neutral parts can be written as separately two 2×2 matrices and one of them is

$$v_2^2 \begin{pmatrix} \frac{\lambda_5+\lambda_6+(\lambda_6-\lambda_5)\cos(2\xi)}{2} & -\frac{(\lambda_6-\lambda_5)\sin(2\xi)}{2} \\ -\frac{(\lambda_6-\lambda_5)\sin(2\xi)}{2} & \frac{\lambda_5+\lambda_6+(\lambda_5-\lambda_6)\cos(2\xi)}{2} \end{pmatrix}. \tag{8}$$

Diagonalizing the Higgs boson mass-squared matrix results in two eigenstates:

$$\begin{pmatrix} H_1^0 \\ H_2^0 \end{pmatrix} = \sqrt{2} \begin{pmatrix} c_\xi & -s_\xi \\ s_\xi & c_\xi \end{pmatrix} \begin{pmatrix} \mathrm{Im}\phi_1^0 \\ \mathrm{Re}\phi_1^0 \end{pmatrix} \tag{9}$$

with masses

$$\begin{aligned} m_{H_1^0}^2 &= \lambda_5 v_2^2 \\ m_{H_2^0}^2 &= \lambda_6 v_2^2, \end{aligned} \tag{10}$$

where $c_\xi = \cos\xi$ and $s_\xi = \sin\xi$. The diagonalizing of the 4×4 neutral Higgs mass-squared matrix has been analytically carried out under some assumptions in Ref. [15] and the results reduce to Eq. (9) and (10) in the case of large $\tan\beta$.

The another 2×2 matrix can be similarly deal with. Because the couplings of the third physical neutral Higgs boson and neutral Goldstone to down-type quarks and leptons are not enhanced for large $\tan\beta$ case in which we are interested, we do not show the explicit results.

Now, we turn to the discussion of the Higgs-fermion-fermion couplings. After completing the transformation from the weak states to the mass states, the couplings of neutral Higgs to fermions which are relevant to our analysis are

$$\begin{aligned} H_1^0 \bar{f} f : &\qquad \frac{i g m_f}{2 m_w \cos\beta}(s_\xi - i c_\xi \gamma_5) \\ H_2^0 \bar{f} f : &\qquad -\frac{i g m_f}{2 m_w \cos\beta}(c_\xi + i s_\xi \gamma_5) \end{aligned} \tag{11}$$

where f represents down-type quarks and leptons. And the couplings of the charged Higgs bosons to fermions are the same as those in the CP-conservative 2HDM (model II, for examples see Ref. [16]). This is in contrary with the model III in which the couplings of the charged Higgs to fermions are quite different from model II. It is easy to see from Eq. (11) that the contributions come from exchanging NHB is proportional to $\sqrt{2}G_F s_\xi c_\xi m_f^2/\cos^2\beta$, so that the constaints due to EDM translate into the constraints on $\sin 2\xi \tan^2\beta$ ($1/\cos\beta \sim \tan\beta$ in the large $\tan\beta$ limit). According to the analysis in Ref. [17], we have the constraint

$$\sqrt{|\sin 2\xi|}\tan\beta < 50 \tag{12}$$

from the neutron EDM. And the constraint from the electron EDM is not stronger than Eq. (12). It is obvious from Eq. (12) that there is a constraint on ξ only if $\tan\beta > 50$ and the stringent constraint on $\tan\beta$ comes out and is $\tan\beta < 50$ when $\xi = \pi/4$.

8.3 Formula for $B \to X_s\tau^+\tau^-$

Inclusive decay rates of heavy hadrons can be calculated in heavy quark effective theory (HQET) [18] and it has been shown that the leading terms in $1/m_Q$ expansion turn out to be the decay of a free (heavy) quark and corrections stem from the order $1/m_Q^2$ [19]. In what follows we shall calculate the leading term. The transition rate for $b \to s\tau^+\tau^-$ can be computed in the framework of the QCD corrected effective weak hamiltonian, obtained by integrating out the top quark, Higgs bosons and $W^\pm, Z$ bosons

$$H_{eff} = \frac{4G_F}{\sqrt{2}}V_{tb}V_{ts}^*(\sum_{i=1}^{10}C_i(\mu)O_i(\mu) + \sum_{i=1}^{10}C_{Q_i}(\mu)Q_i(\mu)) \tag{13}$$

where $O_i (i = 1, \cdots, 10)$ is the same as that given in the ref.[6], Q_i's come from exchanging the neutral Higgs bosons and are defined in Ref. [10]. The explicit expressions of the operators governing $B \to X_s\tau^+\tau^-$ are given as follows:

$$\begin{aligned}
O_7 &= (e/16\pi^2)m_b(\bar{s}_{L\alpha}\sigma^{\mu\nu}b_{R\alpha})F_{\mu\nu},\\
O_8 &= (e/16\pi^2)(\bar{s}_{L\alpha}\gamma^\mu b_{L\alpha})\bar{\tau}\gamma_\mu\tau,\\
O_9 &= (e/16\pi^2)(\bar{s}_{L\alpha}\gamma^\mu b_{L\alpha})\bar{\tau}\gamma_\mu\gamma_5\tau,\\
Q_1 &= (e^2/16\pi^2)(\bar{s}_{L\alpha}b_{R\alpha})(\bar{\tau}\tau),\\
Q_2 &= (e^2/16\pi^2)(\bar{s}_{L\alpha}b_{R\alpha})(\bar{\tau}\gamma_5\tau).
\end{aligned} \tag{14}$$

At the renormalization point $\mu = m_W$ the coefficients C_i's in the effective hamiltonian have been given in the ref.[6] and C_{Q_i}'s are (neglecting the $O(tg\beta)$ term)

$$\begin{aligned}
C_{Q_1}(m_W) &= \frac{m_b m_\tau tg^2\beta x_t}{2sin^2\theta_W}\{\sum_{i=H_1,H_2}\frac{A_i}{m_i^2}(f_1B_i + f_2E_i)\},\\
C_{Q_2}(m_W) &= \frac{m_b m_\tau tg^2\beta x_t}{2sin^2\theta_W}\{\sum_{i=H_1,H_2}\frac{D_i}{m_i^2}(f_1B_i + f_2E_i)\},
\end{aligned}$$

$$
\begin{aligned}
C_{Q_3}(m_W) &= \frac{m_b e^2}{m_\tau g_s^2}(C_{Q_1}(m_W)+C_{Q_2}(m_W)),\\
C_{Q_4}(m_W) &= \frac{m_b e^2}{m_\tau g_s^2}(C_{Q_1}(m_W)-C_{Q_2}(m_W)),\\
C_{Q_i}(m_W) &= 0, \quad i=5,\cdots,10
\end{aligned}
\tag{15}
$$

where

$$
\begin{aligned}
A_{H_1} &= -s_\xi, \; D_{H_1} = ic_\xi,\\
A_{H_2} &= c_\xi, \; D_{H_2} = is_\xi,\\
B_{H_1} &= \tfrac{ic_\xi - s_\xi}{2}, \; B_{H_2} = \frac{c_\xi + is_\xi}{2},
\end{aligned}
$$

$$
\begin{aligned}
f_1 &= \frac{x_t ln x_t}{x_t-1} - \frac{x_{H^\pm} ln x_{H^\pm} - x_t ln x_t}{x_{H^\pm}-x_t},\\
f_2 &= \frac{x_t ln x_t}{(x_t-1)(x_{H^\pm}-1)} - \frac{x_{H^\pm} ln x_{H^\pm}}{(x_{H^\pm}-x_t)(x_{H^\pm}-1)}
\end{aligned}
\tag{16}
$$

with $x_i = m_i^2/m_w^2$. In Eq. (15), E_i are given by

$$
\begin{aligned}
E_{H_1} &= \frac{1}{2}(-s_\xi c_1 + c_\xi c_2),\\
E_{H_2} &= \frac{1}{2}(c_\xi c_1 + s_\xi c_2),\\
c_1 &= -x_{H^\pm} + c_\xi x_{H_1}(c_\xi + is_\xi) + s_\xi x_{H_2}(s_\xi - ic_\xi),\\
c_2 &= i\left(-x_{H^\pm} + s_\xi x_{H_1}(s_\xi - ic_\xi) + c_\xi x_{H_2}(c_\xi + is_\xi)\right).
\end{aligned}
\tag{17}
$$

Neglecting the strange quark mass, the effective hamiltonian (13) leads to the following matrix element for $b \to s\tau^+\tau^-$

$$
\begin{aligned}
M &= \frac{G_F\alpha}{\sqrt{2}\pi} V_{tb}V_{ts}^*[C_8^{eff}\bar{s}_L\gamma_\mu b_L\bar{\tau}\gamma^\mu\tau + C_9\bar{s}_L\gamma_\mu b_L\bar{\tau}\gamma^\mu\gamma^5\tau\\
&+ 2C_7 m_b\bar{s}_L i\sigma^{\mu\nu}\frac{q^\nu}{q^2}b_R\bar{\tau}\gamma^\mu\tau + C_{Q_1}\bar{s}_L b_R\bar{\tau}\tau + C_{Q_2}\bar{s}_L b_R\bar{\tau}\gamma^5\tau],
\end{aligned}
\tag{18}
$$

where [6, 8, 20]

$$
\begin{aligned}
C_8^{eff} &= C_8 + \{g(\frac{m_c}{m_b},\hat{s})\\
&+ \frac{3}{\alpha^2}k\sum_{V_i=\psi',\psi''\ldots}\frac{\pi M_{V_i}\Gamma(V_i\to\tau^+\tau^-)}{M_{V_i}^2 - q^2 - iM_{V_i}\Gamma_{V_i}}\}(3C_1+C_2),
\end{aligned}
\tag{19}
$$

with $\hat{s} = q^2/m_b^2$, $q = (p_{\tau^+} + p_{\tau^-})^2$. In (19) $g(\frac{m_c}{m_b},\hat{s})$ arises from the one-loop matrix element of the four-quark operators and can be found in Refs. [6, 21]. The second

term in braces in (19) estimates the long-distance contribution from the intermediate, ψ', ψ'' ... [6, 20]. In our numerical calculations, we choose $k(3C_1 + C_2) = -0.875$ [22].

The QCD corrections to coefficients C_i and C_{Q_i} can be incooperated in the standard way by using the renormalization group equations. Although the C_i at the scale $\mu = O(m_b)$ have been given in the next-to-leading order approximation (NLO) and without including mixing with Q_i, we use the values of C_i only in the leading order approximation (LO) since no C_{Q_i} have been calculated in NLO. The C_i and C_{Q_i} with LO QCD corrections have been given in Ref. [10].

$$\begin{aligned} C_7(m_b) &= \eta^{-16/23}\Big[C_7(m_W) - [\frac{58}{135}(\eta^{10/23}-1) + \frac{29}{189}(\eta^{28/23}-1)]C_2(m_W) \\ &\quad -0.012 C_{Q_3}(m_W)\Big], \end{aligned} \tag{20}$$

$$C_8(m_b) = C_8(m_W) + \frac{4\pi}{\alpha_s(m_W)}[-\frac{4}{33}(1-\eta^{-11/23}) + \frac{8}{87}(1-\eta^{-29/23})]C_2(m_W), \tag{21}$$

$$C_9(m_b) = C_9(m_W), \tag{22}$$

$$C_{Q_i}(m_b) = \eta^{-\gamma_Q/\beta_0} C_{Q_i}(m_W), \quad i = 1, 2, \tag{23}$$

where $\gamma_Q = -4$ [23] is the anomalous dimension of $\bar{s}_L b_R$, $\beta_0 = 11 - 2n_f/3$, and $\eta = \alpha_s(m_b)/\alpha_s(m_W)$.

After a straightforward calculation, we obtain the invariant dilepton mass distribution [10]

$$\begin{aligned} \frac{\mathrm{d}\Gamma(B \to X_s\tau^+\tau^-)}{\mathrm{d}s} &= B(B \to X_c l\bar{\nu})\frac{\alpha^2}{4\pi^2 f(m_c/m_b)}(1-s)^2(1-\frac{4t^2}{s})^{1/2}\frac{|V_{tb}V_{ts}^*|^2}{|V_{cb}|^2}D(s) \\ D(s) &= |C_8^{eff}|^2(1+\frac{2t^2}{s})(1+2s) + 4|C_7|^2(1+\frac{2t^2}{s})(1+\frac{2}{s}) \\ &\quad +|C_9|^2[(1+2s) + \frac{2t^2}{s}(1-4s)] + 12\mathrm{Re}(C_7 C_8^{eff*})(1+\frac{2t^2}{s}) \\ &\quad +\frac{3}{2}|C_{Q_1}|^2(s-4t^2) + \frac{3}{2}|C_{Q_2}|^2 s + 6\mathrm{Re}(C_9 C_{Q_2}^*)t \end{aligned} \tag{24}$$

where s=q^2/m_b^2, t=m_τ/m_b, $B(B \to X_c l\bar{\nu})$ is the branching ratio, f is the phase-space factor and f(x)=$1 - 8x^2 + 8x^6 - x^8 - 24x^4 \ln\ x$.

The CP asymmetry for the $B \to X_s l^+l^-$ and $\overline{B} \to \overline{X}_s l^+l^-$ is defined as

$$A^1_{CP}(s) = \frac{\mathrm{d}\Gamma/\mathrm{d}s - \mathrm{d}\overline{\Gamma}/\mathrm{d}s}{\mathrm{d}\Gamma/\mathrm{d}s + \mathrm{d}\overline{\Gamma}/\mathrm{d}s}. \tag{25}$$

We also give the forward-backward asymmetry

$$A(s) = \frac{\int_0^1 dz \frac{d^2\Gamma}{dsdz} - \int_{-1}^0 dz \frac{d^2\Gamma}{dsdz}}{\int_0^1 dz \frac{d^2\Gamma}{dsdz} + \int_{-1}^0 dz \frac{d^2\Gamma}{dsdz}} = \frac{E(s)}{D(s)} \tag{26}$$

where $z = \cos\theta$ and θ is the angle between the momentum of the B-meson and that of l^+ in the center of mass frame of the dileptons $\tau^+\tau^-$. Here,

$$E(s) = \mathrm{Re}(C_8^{eff} C_9^* s + 2C_7 C_9^* + C_8^{eff} C_{Q1}^* t + 2C_7 C_{Q2}^* t). \tag{27}$$

The CP asymmetry in the forward-backward asymmetry for $B \to X_s\tau^+\tau^-$ and $\overline{B} \to \overline{X}_s\tau^+\tau^-$ is defined as

$$A_{CP}^2(s) = \frac{A(s) - \overline{A}(s)}{A(s) + \overline{A}(s)}. \tag{28}$$

It is easy to see from Eq. (24) that the CP asymmetry A_{CP}^1 is very small because the weak phase difference in $C_7 C_8^{eff}$ arises from the small mixing of O_7 with Q_3 (see Eq. (20)). In contrast with it, A_{CP}^2 can reach a large value when $\tan\beta$ is large, as can be seen from Eq. (27) and (15). Therefore, we propose to measure A_{CP}^2 in order to search for new CP violation sources.

Let us now discuss the lepton polarization effects. We define three orthogonal unit vectors:

$$\begin{aligned}
\vec{e}_L &= \frac{\vec{p}_1}{|\vec{p}_1|}\ , \\
\vec{e}_N &= \frac{\vec{p}_s \times \vec{p}_1}{|\vec{p}_s \times \vec{p}_1|}\ , \\
\vec{e}_T &= \vec{e}_N \times \vec{e}_L\ ,
\end{aligned}$$

where $\vec{p}_1$ and $\vec{p}_s$ are the three momenta of the ℓ^- lepton and the s quark, respectively, in the center of mass of the $\ell^+\ \ell^-$ system. The differential decay rate for any given spin direction $\vec{n}$ of the ℓ^- lepton, where $\vec{n}$ is a unit vector in the ℓ^- lepton rest frame, can be written as

$$\frac{d\Gamma\,(\vec{n})}{\mathrm{d}s} = \frac{1}{2}\left(\frac{d\Gamma}{\mathrm{d}s}\right)_0 \Big[1 + (P_L\,\vec{e}_L + P_N\,\vec{e}_N + P_T\,\vec{e}_T)\cdot\vec{n}\Big]\ , \tag{29}$$

where the subscript "0" corresponds to the unpolarized case, and P_L, P_T, and P_N, which correspond to the longitudinal, transverse and normal projections of the lepton spin, respectively, are functions of s. From Eq. (29), one has

$$P_i(s) = \frac{\dfrac{d\Gamma}{ds}(\vec{n} = \vec{e}_i) - \dfrac{d\Gamma}{ds}(\vec{n} = -\vec{e}_i)}{\dfrac{d\Gamma}{ds}(\vec{n} = \vec{e}_i) + \dfrac{d\Gamma}{ds}(\vec{n} = -\vec{e}_i)}\ . \tag{30}$$

The calculations for the P_i's (i = $L,\ T,\ N$) lead to the following results:

$$\begin{aligned}
P_L &= (1 - \frac{4t^2}{s})^{1/2}\frac{D_L(s)}{D(s)}, \\
P_N &= \frac{3\pi}{4s^{1/2}}(1 - \frac{4t^2}{s})^{1/2}\frac{D_N(s)}{D(s)}, \\
P_T &= -\frac{3\pi t}{2s^{1/2}}\frac{D_T(s)}{D(s)},
\end{aligned} \tag{31}$$

where

$$\begin{aligned}
D_L(s) &= \mathrm{Re}\left(2(1+2s)C_8^{eff}C_9^* + 12C_7C_9^* - 6tC_{Q_1}C_9^* - 3sC_{Q_1}C_{Q_2}^*\right), \\
D_N(s) &= \mathrm{Im}\left(2sC_{Q_1}C_7^* + sC_{Q_1}C_8^{eff*} + sC_{Q_2}C_9^* + 4tC_9C_7^* + 2tsC_8^{eff\ *}C_9\right), \\
D_T(s) &= \mathrm{Re}\left(-2C_7C_9^* + 4C_8^{eff}C_7^* + \frac{4}{s}|C_7|^2 - C_8^{eff}C_9^* \right. \\
&\quad \left. +s|C_8^{eff}|^2 - \frac{s-4t^2}{2t}C_{Q_1}C_9^* - \frac{s}{t}C_{Q_2}C_7^* - \frac{s}{2t}C_8^{eff}C_{Q_2}^*\right).
\end{aligned} \tag{32}$$

P_i (i=L, T, N) have been given in the ref. [9], where there are some errors in P_T and they gave only two terms in D_N, the numerator of P_N. We remind that P_N is the CP-violating projection of the lepton spin onto the normal of the decay plane. Because P_N in $B \to X_s l^+ l^-$ comes from both the quark and lepton sectors, purely hadronic and leptonic CP-violating observables, such as d_n or d_e, do not necessarily strongly constrain P_N [24]. So it is advantageous to use P_N to investigate CP violation effects in some extensions of SM [25]. In the model IV 2HDM, as pointed out above, d_n and d_e constrain $\sqrt{|\sin 2\xi|}\tan\beta$ and consequently P_N through C_{Q_i} $(i = 1, 2)$ (see Eq. (32)).

8.4 Numerical results

The following parameters have been used in the numerical calculations:

$$m_t = 175Gev,\ m_b = 5.0Gev,\ m_c = 1.6Gev,\ m_\tau = 1.77Gev,\ \eta = 1.724,$$

$$m_{H_1} = 100Gev,\ m_{H_2} = m_{H^\pm} = 200Gev.$$

Numerical results are shown in Figs. 1-9. From Figs. 1 and 2, we can see that the contributions of NHB to the differential branching ratio $d\Gamma/ds$ are significant when $\tan\beta$ is not smaller than 30 and the masses of NHB are in the reasonable region, and the forward-backward asymmetry $A(s)$ is more sensitive to $\tan\beta$ than $d\Gamma/ds$, which is similar to the case of the normal 2HDM without CP violation [10].

The direct CP violation A_{CP}^i $(i = 1, 2)$ and CP-violating polarization P_N of $B \to X_s\tau^+\tau^-$ are presented in Figs. 3-7, respectively. As expected, A_{CP}^1 is about 0.1% and hard to be measured. However, A_{CP}^2 can reach about 10%. A_{CP}^2 is strongly dependent of the CP violation phase ξ and comes mainly from exchanging NHBs as expected. From Figs. 6 and 7, one can see that P_N is also strongly dependent of the CP violation phase ξ and can be as large as 5% for some values of ξ, which should be within the luminosity reach of coming B factories, and comes mainly from NHB contributions in the most of range of ξ.

Figs. 8 and 9 show the longitudinal and transverse polarizations respectively. It is obviously that the contributions of NHB can change the polarization greatly, especially when $\tan\beta$ is large, and the dependence of P_L on CP violation phase ξ is not significant in the most of range of ξ. The longitudinal polarization of $B \to X_s\tau^+\tau^-$ has

been calculated in SM and several new physics scenarios [8]. Switching off the NHB contributions, our results are in agreement with those in Ref. [8].

In summary, we have calculated the differential braching ratio, back-forward asymmetry, lepton polarizations and some CP violated observables for $B \to X_s \tau^+\tau^-$ in the model IV 2HDM. As the main features of the model, NHB play an important role in inducing CP violations, in particular, for large $\tan\beta$. We propose to measure A_{CP}^2, the direct CP asymmetry in back-forward asymmetry, in stead of A_{CP}^1, the usual direct CP violation in branching ratio, because the former could be observed if $\tan\beta$ is large enough (say, ≥ 30) and the latter is too small to be observed. It is possible to discriminate the model IV from the other 2HDMs by measuring the CP-violated observables such as A_{CP}^2, P_N if the nature chooses large $\tan\beta$.

References

[1] Christensen et al., Phys. Rev. Lett. **13** (1964) 138.

[2] T. D. Lee, Phys. Rev. **D8** (1973) 1226; Phys. Rep. **9c** (1974) 143; P. Sikivie, Phys. Lett. **B65** (1976) 141.

[3] S. Weinberg, Phys. Rev. Lett. **37** (1976) 657; G. C. Branco, Phys. Rev. **D22** (1980) 2901; K. Shizuya and S.-H. H. Tye, Phys. Rev. **D23** (1981) 1613.

[4] H. Georgi, Hadronic Jour. 1 (1978) 155.

[5] see, for example, D. Bowser-Chao, K. Cheung and W. Y. Keung, hep-ph/9811235, and references therein.

[6] B.Grinstein, M.J.Savage and M.B.Wise, *Nucl.Phys.***B319** (1989)271.

[7] C.S. Huang, W. Liao and Q.S. Yan, Phys. Rev. **D59** (1999) 011701; T. Goto et.al., hep-ph/9812369; S. Baek and P. Ko, hep-ph/9904283; Y.G. Kim, P. Ko and J.S. Lee, Nucl. Phys. **B544** (1999) 64, and references therein. For the earlier references, see, for example, the references in ref. [9].

[8] J. L. Hewett, Phys. Rev. **D53** (1996) 4964.

[9] Y. Grossman, Z. Ligeti and E. Nardi, Phys. Rev. **D55** (1997) 2768.

[10] Y.B. Dai, C.S. Huang and H.W. Huang, Phys. Lett. **B390** (1997) 257; C.S. Huang and Q.S. Yan, Phys. Lett. **B442** (1998) 209.

[11] S. Choudhury et.al., hep-ph/9902355. P_i (i=L, T, N) have been given in the paper, where there are some errors in P_T and they gave only two terms in P_N.

[12] ALEPH Collaboration (D. Buskulic et al.), Phys. Lett. B343 (1995)444; J.Kalinowski,*Phys.Lett.***B245**(1990)201; A.K.Grant,*Phys.Rev.***D51**(1995)207.

[13] O. Lebedev, Eur. Phys. J. **C4** (1998) 363.

[14] C.-S. Huang and S.-H. Zhu, in preparation.

[15] I. Vendramin, Nuovo. Cim. **106A** (1993) 79.

[16] J.F.Gunion,H.E.Haber,G.Kane and S.Dawson, *The Higgs hunter's guide* (Addison-Wesley, MA, 1990).

[17] N. G. Deshpande and E. Ma, Phys. Rev. **D16** (1977) 1583; A. A. Anselm et al., Phys. Lett. **B152** (1985) 116; T. P. Cheng and L. F. Li, Phys. Lett. **B234** (1990) 165; S. Weinberg, Phys. Rev. Lett. **63** (1989) 2333; X. -G. He and B. H. J. McKellar, Phys. Rev. **D42** (1990) 3221; Erratum-ibid **D50** (1994) 4719.

[18] For a comprehensive review, see: M.Neubert,*Phys.Rep.* **245**(1994)396.

[19] I.I.Bigi, M.Shifman, N.G.Vraltsev and A.I.Vainshtein, *Phys. Rev.Lett.***71**(1993)496; B.Blok, L.Kozrakh, M.Shifman and A.I.Vainshtein, *Phys.Rev.***D49**(1994)3356; A.V.Manohar and M.B.Wise, *Phys.Rev.* **D49**(1994)1310; S.Balk, T.G.Körner, D.Pirjol and K.Schilcher, *Z.Phys.* **C64**(1994)37; A.F.Falk, Z.Ligeti, M.Neubert and Y.Nir, *Phys.Lett.***B326**(1994)145.

[20] N. G. Deshpande, J. Trampetic and K. Ponose, *Phys. Lett.* **B214** (1988) 467, *Phys. Rev.* **D39** (1989) 1461; C.S.Lim, T.Morozumi and A.I.Sanda, *Phys.Lett.***B218** (1989)343; A. Ali, T. Mannel and T. Morozumi, *Phys. Lett.* **B273** (1991) 505; P. J. O'Donnell and H. K. Tung, Phys. Rev. **D43** (1991) R2067; G. Buchalla, A. Buras, M. Lautenbacher, Rev. Mod. Phys. 68, (1996) 1125; C. S. Kim, T. Morozumi and A. I. Sanda, *Phys. Rev.* **D56** (1997) 7240.

[21] N. G. Deshpande and J. Trampetic, *Phys. Rev.* **D60** (1988) 2583; A. J. Buras and M. Münz, *Phys. Rev.* **D52** (1995) 186; A. Ali, G. F. Giudice, and T. Mannel, *Z. Phys.* **C67** (1995) 417.

[22] Prticle Data Group, C. Caso et. al., Eur. Phys. J. **C3** (1998)1.

[23] C.S.Huang, *Commun. Theor. Phys.* **2**(1983)1265.

[24] R. Garisto, Phys. Rev. **D51** (1995) 1107.

[25] R. Garisto and G. Kane, Phys. Rev. **D44** (1991) 2038.

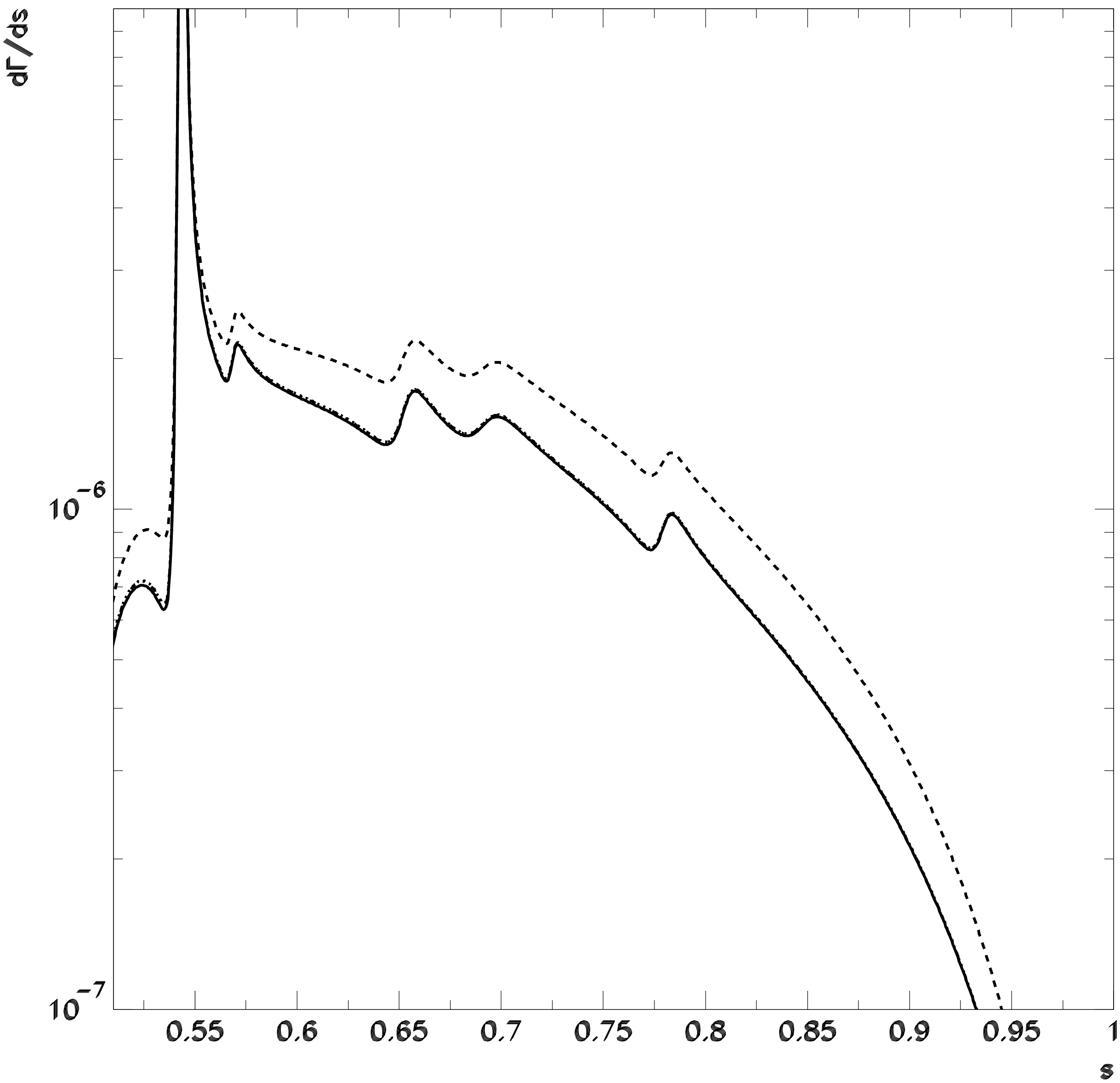

Figure 1: Differential branching ratio as function of s, where $\xi = \pi/4$, solid and dashed lines represent $\tan\beta = 10$ and 30, dot-dashed line represents the case of switching off C_{Q_i} contributions.

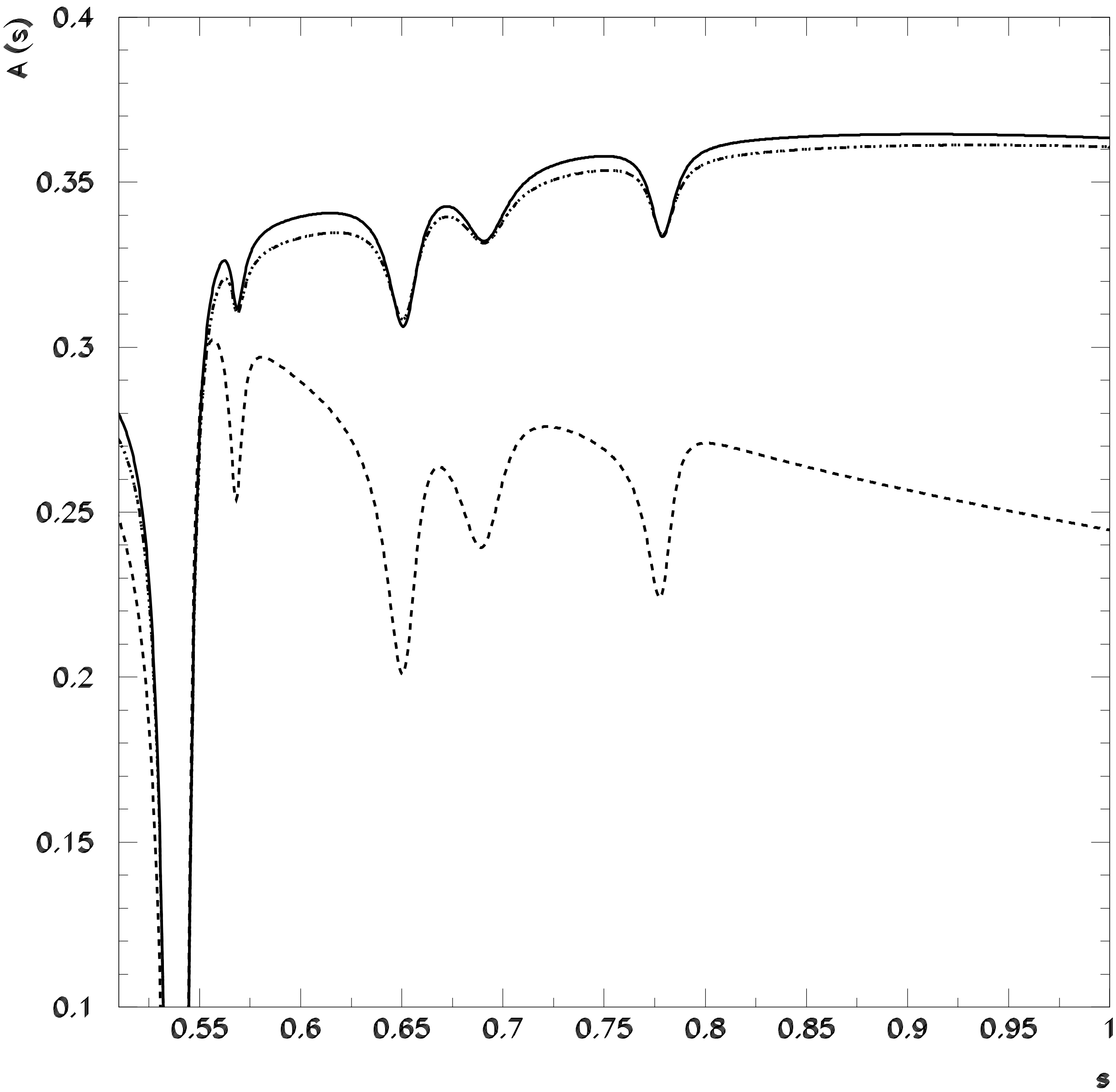

Figure 2: Backward-forward asymmetry as function of s, where $\xi = \pi/4$, solid and dashed lines represent $\tan\beta = 10$ and 30, dot-dashed line represents the case of switching off C_{Q_i} contributions.

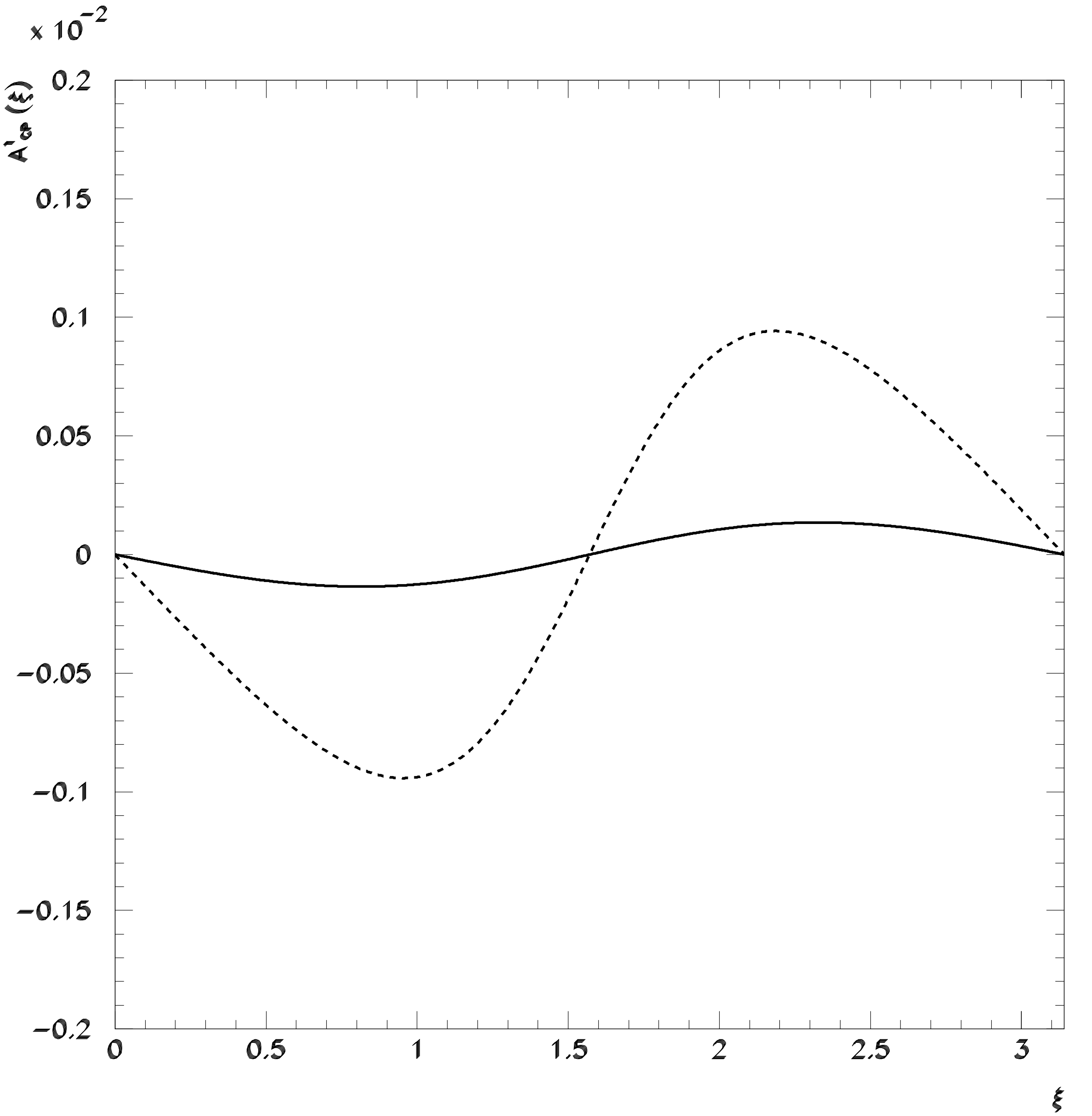

Figure 3: A^1_{CP} as function of ξ, where $s = 0.8$, solid and dashed lines represent $\tan\beta = 10$ and 30.

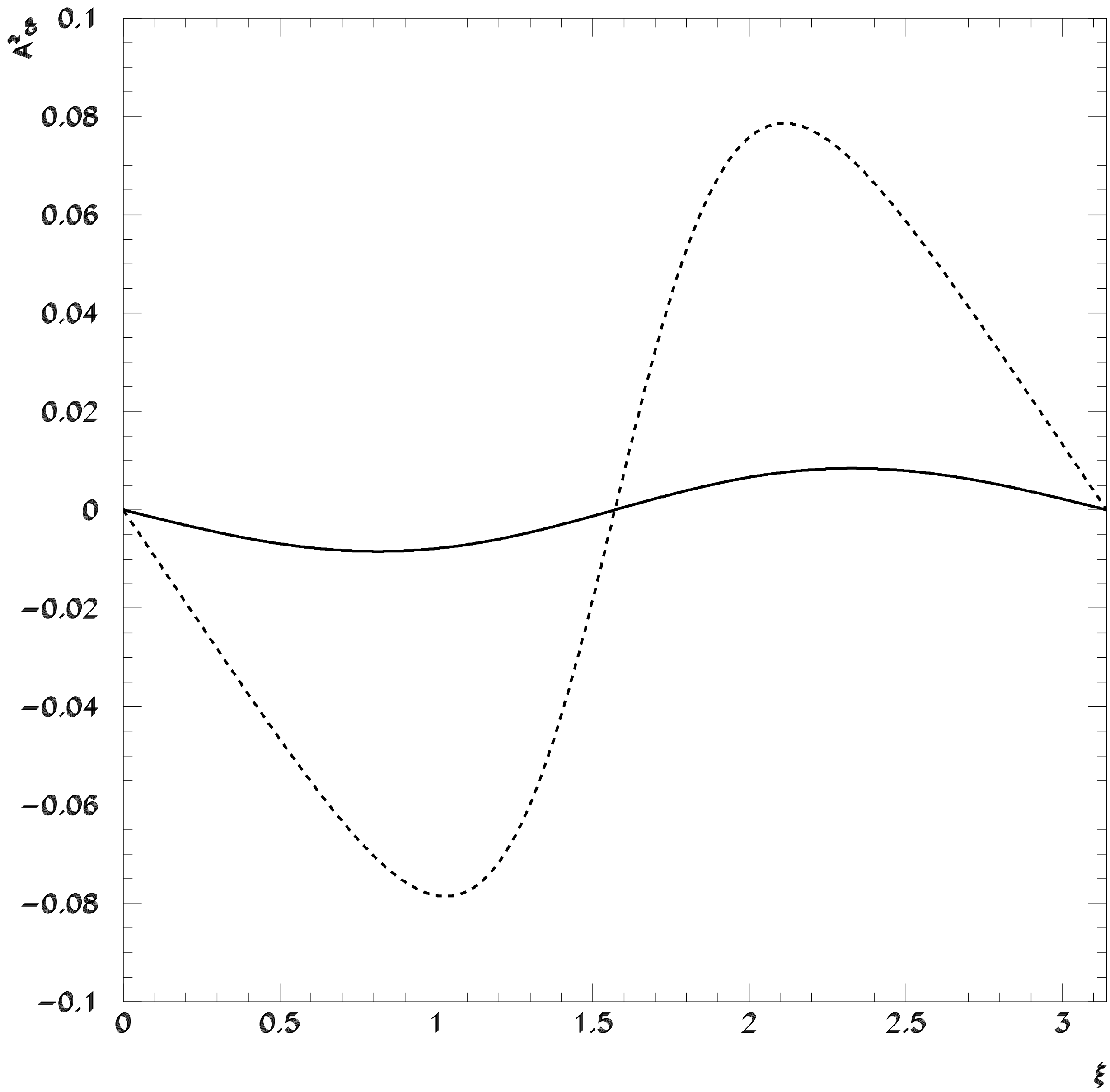

Figure 4: A^2_{CP} as function of ξ, where $s = 0.8$, solid and dashed lines represent $\tan\beta = 10$ and 30.

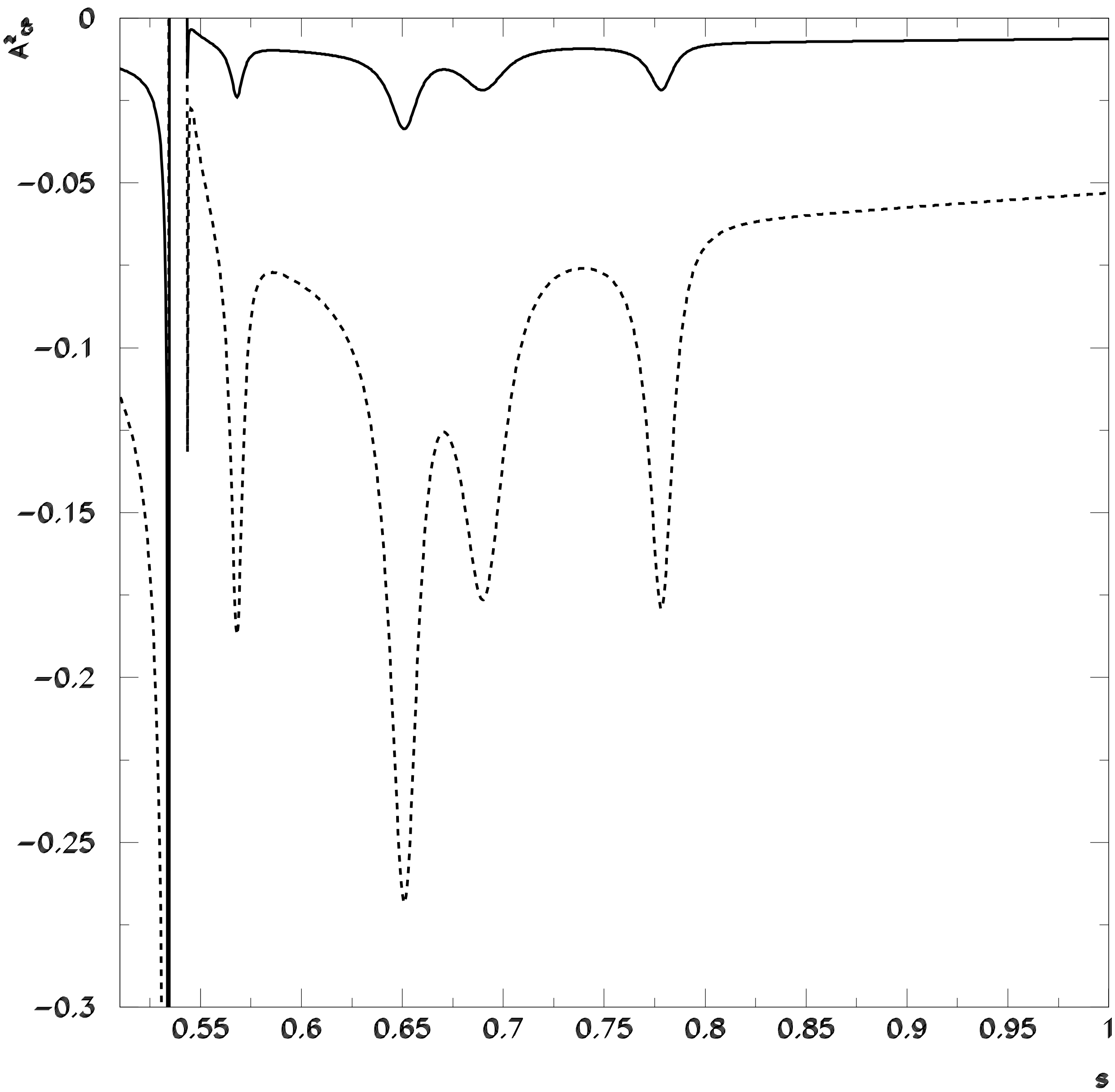

Figure 5: A^2_{CP} as function of s, where $\xi = \pi/4$, solid and dashed lines represent $\tan\beta = 10$ and 30.

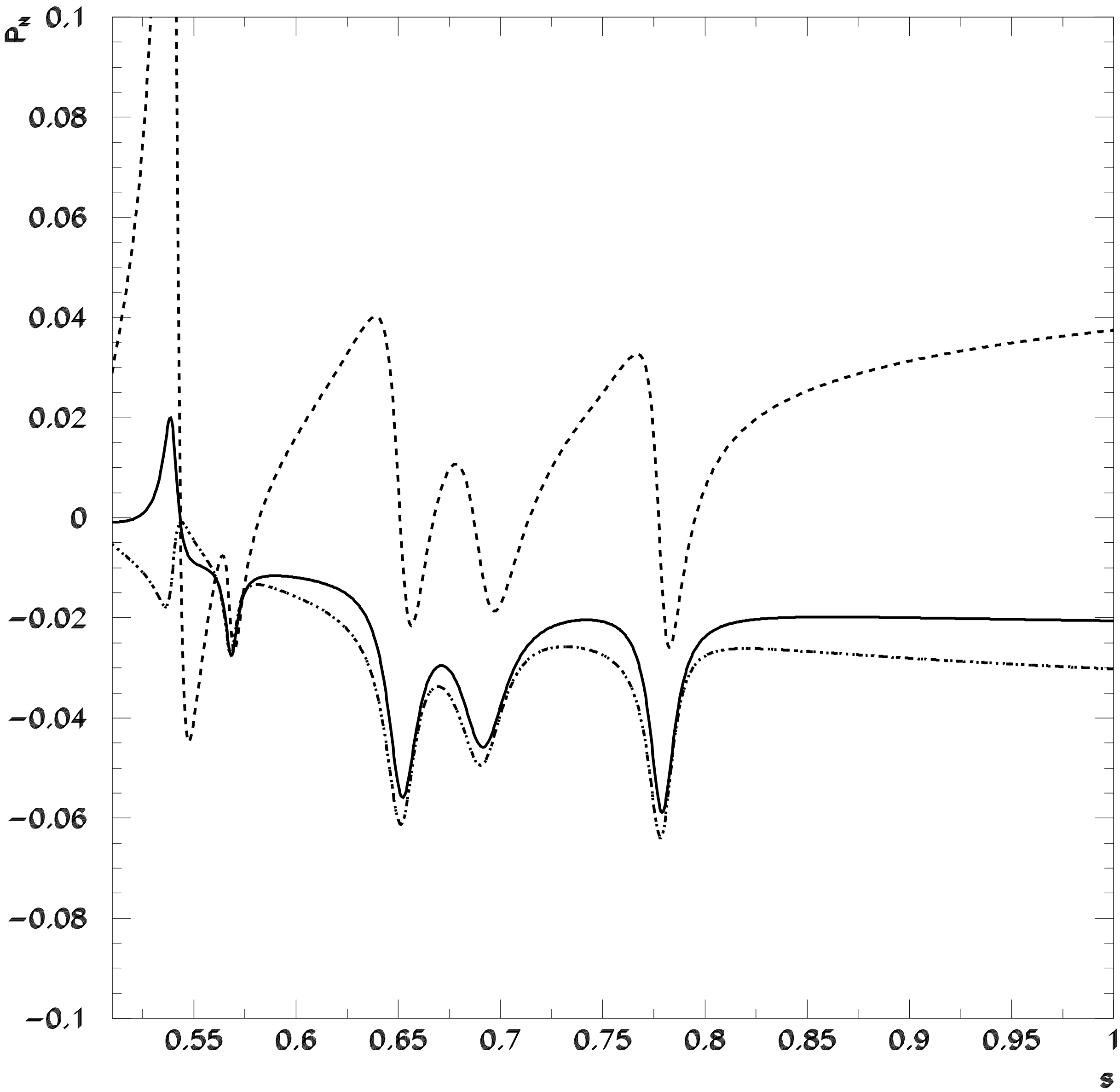

Figure 6: P_N as function of s, where $\xi = \pi/4$, solid and dashed lines represent $\tan\beta =$ 10 and 30, dot-dashed line represents the case of switching off C_{Q_i} contributions.

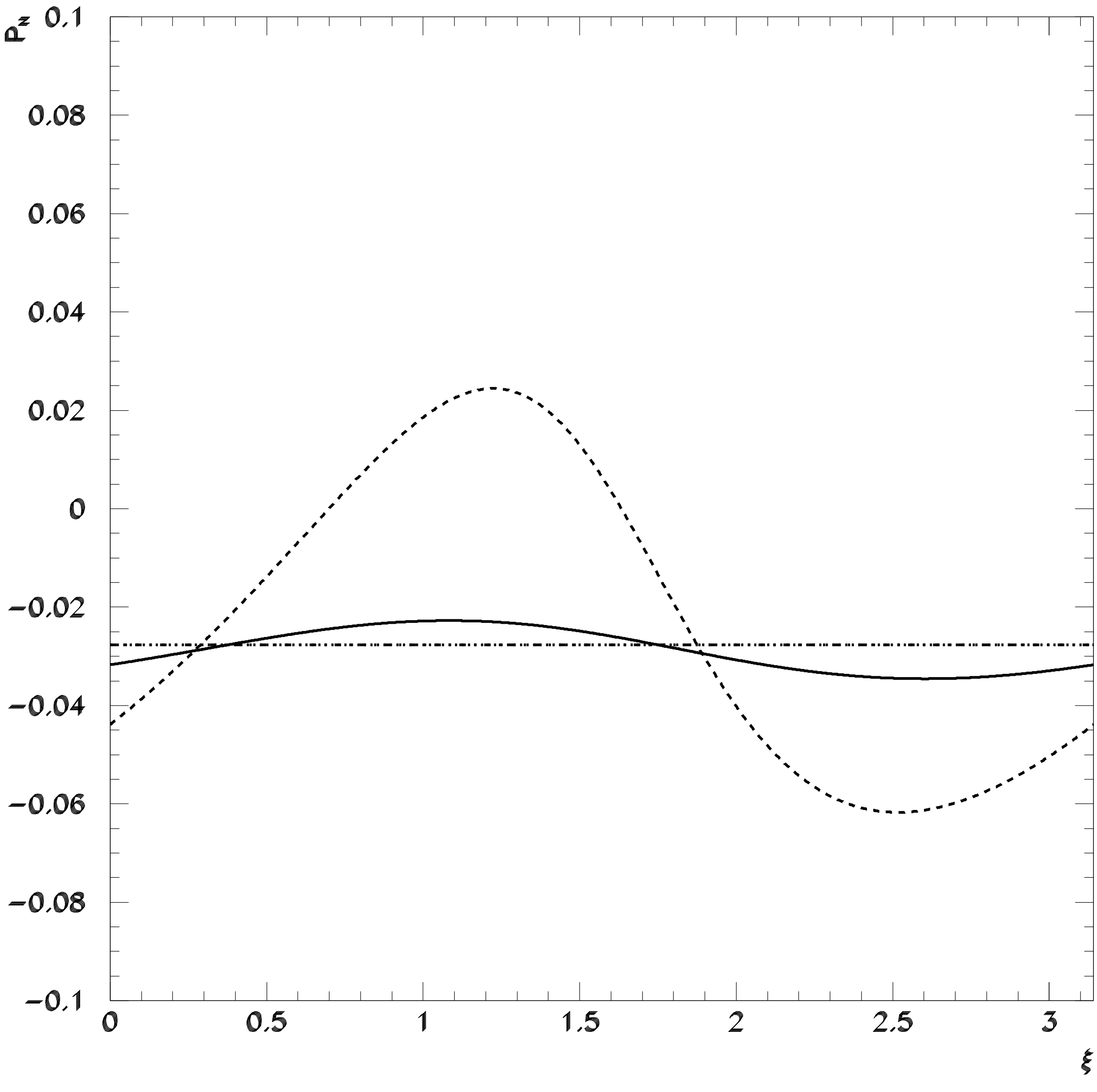

Figure 7: P_N as function of ξ, where $s = 0.8$, solid and dashed lines represent $\tan\beta =$ 10 and 30, dot-dashed line represents the case of switching off C_{Q_i} contributions.

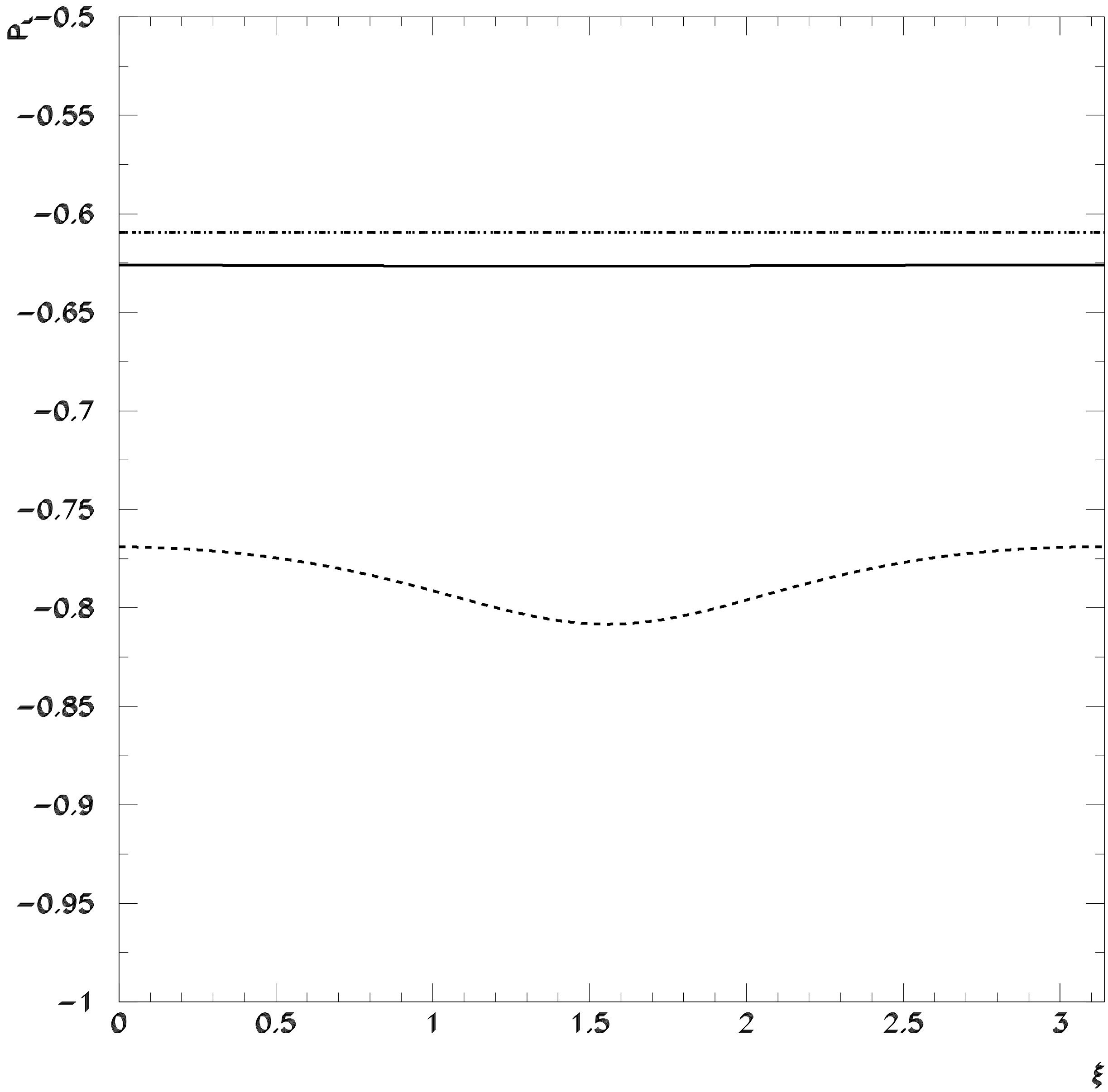

Figure 8: P_L as function of ξ, where $s = 0.8$, solid and dashed lines represent $\tan\beta =$ 10 and 30, dot-dashed line represents the case of switching off C_{Q_i} contributions.

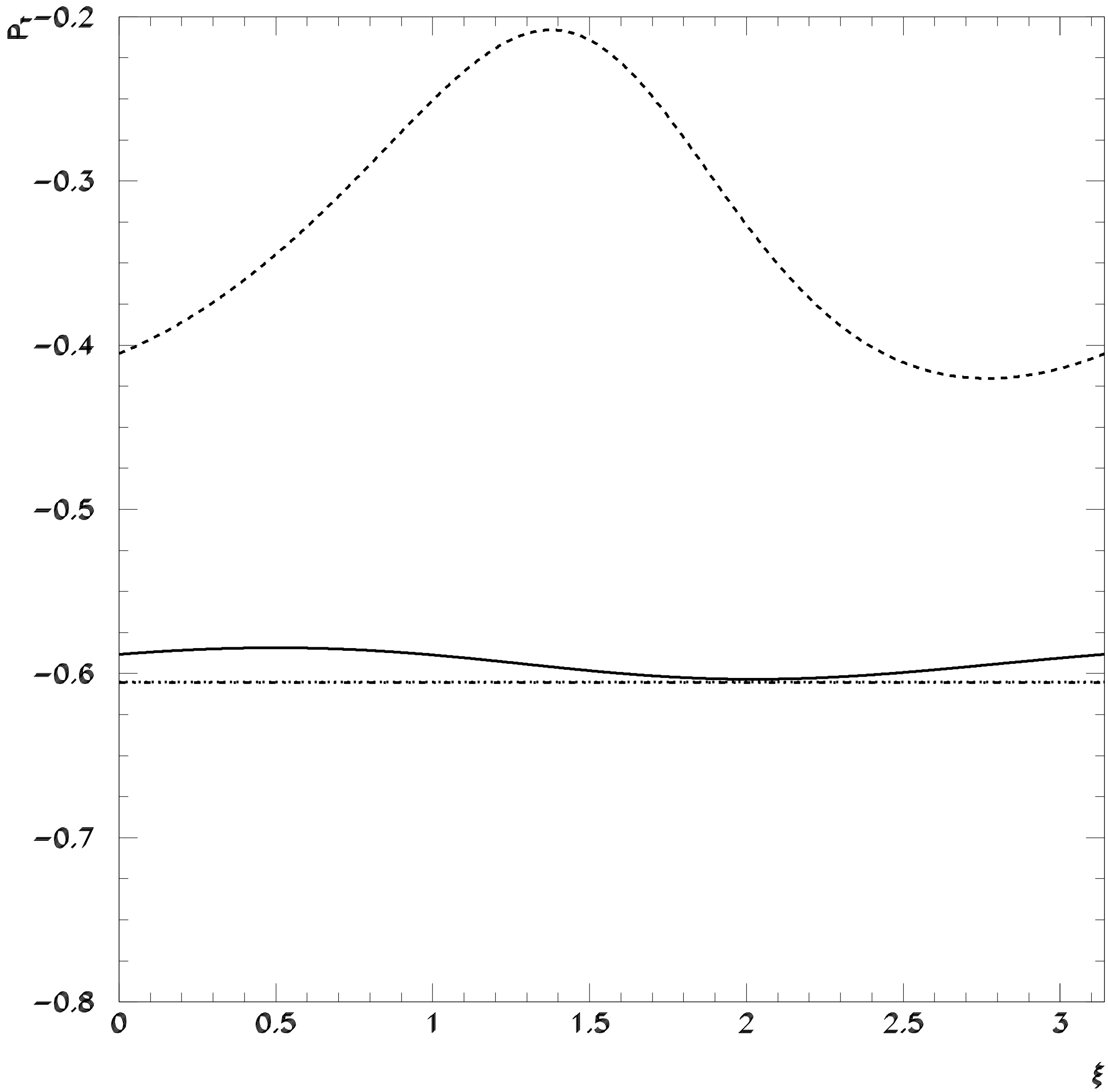

Figure 9: P_T as function of ξ, where $s = 0.8$, solid and dashed lines represent $\tan\beta =$ 10 and 30, dot-dashed line represents the case of switching off C_{Q_i} contributions.

9 Exclusive Semileptonic Rare Decays $B \to (K, K^*)\ell^+\ell^-$ in Supersymmetric Theories

ABSTRACT

The invariant mass spectrum, forward-backward asymmetry, and lepton polarizations of the exclusive processes $B \to K(K^*)\ell^+\ell^-, \ell = \mu,\ \tau$ are analyzed under supersymmetric context. Special attention is paid to the effects of neutral Higgs bosons (NHBs). Our analysis shows that the branching ratio of the process $B \to K\mu^+\mu^-$ can be quite largely modified by the effects of neutral Higgs bosons and the forward-backward asymmetry would not vanish. For the process $B \to K^*\mu^+\mu^-$, the lepton transverse polarization is quite sensitive to the effects of NHBs, while the invariant mass spectrum, forward- backward asymmetry, and lepton longitudinal polarization are not. For both $B \to K\tau^+\tau^-$ and $B \to K^*\tau^+\tau^-$, the effects of NHBs are quite significant. The partial decay widths of these processes are also analyzed, and our analysis manifest that even taking into account the theoretical uncertainties in calculating weak form factors, the effects of NHBs could make SUSY shown up.

9.1 Introduction

The inclusive rare processes $b \to X_s\ell^+\ell^-, \ell = e,\ \mu,\ \tau$ have been intensively studied in literatures[1, 2, 3, 4, 5, 6, 7, 8, 9, 10, 11, 12]. As one of flavor changing neutral current processes, it is sensitive to fine structure of the standard model and to the possible new physics as well, and is expected to shed light on the existence of new physics before the possible new particles are produced at colliders.

It is well known that invariant mass spectrum, forward-backward asymmetries, and lepton polarizations are important observables to probe new physics, while the first two observables are mostly analyzed. About lepton polarizations, it is known that due to the smallness of the mass of it, therefore electron polarizations are very difficult to be measured experimentally. So only the lepton polarizations of muon and tau are considered in literatures [10, 12, 13, 14]. The longitudinal polarization of tau in $B \to X_s\tau^+\tau^-$ has been calculated in standard model (SM) and several new physics scenarios [10]. For $B \to X_s l^+l^-$ $(l = \mu, \tau)$, the polarizations of lepton in SM are analyzed in [12] and it is pointed out that for the μ channel, the only significant component is P_L, while all three components are sizable in the τ channel.The analysis has been extended to supersymmetric models (SUSY) and a CP softly broken two Higgs doublet model in refs. [13] and [14] respectively. The reference [5] also gives a general model-independent analysis of the lepton polarization asymmetries in the process $B \to X_s\tau^+\tau^-$ and it is found that the contribution from $C_{LRLR} + C_{LRRL}$ is much larger than other scalar-type interactions.

Compared with the inclusive processes $b \to X_s\ell^+\ell^-, \ell = e,\ \mu,\ \tau$, the theoretical study of the exclusive processes $B \to K(K^*)\ell^+\ell^-$ is relatively hard. For inclusive semileptonic decays of B, the decay rates can be calculated in heavy quark effective theory (HQET) [15]. However, for exclusive semileptonic decays of B, to make theoret-

ical predictions, additional knowledge of decay form factors is needed, which is related with the calculation of hadronic transition matrix elements. Hadronic transition matrix elements depend on the non-perturbative properties of QCD, and can only be reliably calculated by using a nonperturbative method. The form factors for B decay into $K^{(*)}$ have been computed with different methods such as quark models [16], SVZ QCD sum rules [17], light cone sum rules (LCSRs) [18, 19, 20, 21, 22]. Compared to the lattice approach which mainly deal with the form factors at small recoil, the QCD sum rules on the light-cone can complementarily provide information of the form factors at smaller values of $\hat{s}$. And they are consistent with perturbative QCD and the heavy quark limit. In this work, we will use the weak decay form factors calculated by using the technique of the light cone QCD sum rules and given in [23].

A upper limit on the branching ratio of $B^0 \to K^{0*}\mu^+\mu^-$ has been recently given by CLEO [24]:

$$BR(B^o \to K^{0*}\mu^+\mu^-) < 4.0 \times 10^{-6}, \tag{1.1}$$

and they will be precisely measured at B factories, these exclusive processes are quite worthy of intensive study and have attracted many attentions [23, 25, 26, 27, 28, 29, 30, 31, 32, 33, 34, 35]. In reference [23], by using improved theoretical calculations of the decay dorm factors in the light cone QCD sum rule approach, dilepton invariant mass spectra and the forward-backward asymmetry of these exclusive decays are analyzed in the standard model and a number of popular variants of the supersymmetric models. However, as the author claimed, the effects of neutral Higgs exchanges are neglected. For exclusive processes, as pointed out in [35], the polarization asymmetries of μ and τ for $B \to K^{(}*)\mu^+\mu^-$ and $B \to K^{(}*)\tau^+\tau^-$ are also accessible at the B-factories under construction. In reference [33], the lepton polarizations and CP violating effects in $B \to K^*\tau^+\tau^-$ are analyzed in SM and two Higgs doublet models.

As pointed in refs. [3, 4], in two-Higgs-doublet models and SUSY models, neutral Higgs boson could contribute largely to the inclusive processes $b \to X_s\ell^+\ell^-, \ell = \mu, \tau$ and greatly modify the branching ratio and forward-backward asymmetry in the large tanβ case. The effects of neutral Higgs in the 2HDM to polarizations of τ in $B \to K\tau^+\tau^-$ are analyzed in [34], and it was found that polarizations of the charged final lepton are very sensitive to the tanβ.

In this paper, we will investigate the exclusive decay $B \to K(K^*)\ell^+\ell^-, \ell = \mu, \tau$ in SUSY models. We shall evaluate branching ratios and forward-backward asymmetries (FBA) with emphasis on the effects of neutral Higgs and analyze lepton polarizations in MSSM. According to the analysis of [28], different sources of the vector current could manifest themselves in different regions of phase space, for the very low $\hat{s}$ the photonic penguin dominates, while the Z penguin and W box becomes important towards high $\hat{s}$. In order to search the regions of $\hat{s}$ where neutral Higgs bosons could contribute large, we analyze the partial decay widths of these two processes. Beside that they are accessible to B factories, our motivation also bases on the fact that to the inclusive processes $B \to X_s\ell^+\ell^-, \ell = \mu, \tau$, neutral Higgs could make quite a large contributions at certain large tanβ regions of parameter space in SUSY models, since part of supersymmetric contributions is proportional to $\tan^3\beta$ [4]. Such regions considerably exist in SUGRA

and M-theory inspired models [36]. We also analyze the effects of neutral Higgs to the position of the zero value of the forward-backward asymmetry. Our results show that the branching ratio of the process $B \to K\mu^+\mu^-$ can be quite largely modified by the effects of neutral Higgs bosons and the forward-backward asymmetry would not vanish. Because the FBA for $B \to K\,\ell^+\,\ell^-(\ell = \mu,\ \tau)$ vanishes if there are no the contributions of NHBs and the contributionsof NHBs can be large enough to be observed only in SUSY and/or 2HDM with large tanβ, a non-zero FBA for $B \to K\,\ell^+\,\ell^-$ would signal the existance of new physics. For the process $B \to K^*\mu^+\mu^-$, the lepton transverse polarization is quite sensitive to the effects of NHBs, while the invariant mass spectrum, forward- backward asymmetry, and lepton longitudinal polarization are not. For both $B \to K\tau^+\tau^-$ and $B \to K^*\tau^+\tau^-$, the effects of NHBs are quite significant. Our analysis manifest that even taking into account the theoretical uncertainties in calculating weak form factors, the effects of NHBs could show SUSY up. In a word, our analysis manifest that effects of NHBs is quite remarkable in some regions of parameter space of SUSY, even for the process $B \to K\mu^+\mu^-$.

The paper is organized as follows. In the subsection 2, the effective Hamiltonian is presented and the form factors given by using light cone sum rule method are briefly discussed. Basic formula of observables are introduced in subsection 3. Section 4 is devoted to the numerical analysis. In subsection 5 we make discussions and conclusions.

9.2 Effective Hamiltonian and Form Factors

By integrating out the degrees of heavy freedom from the full theory, MSSM, at electroweak(EW) scale, we can get the effective Hamiltonian describing the rare semileptonic decay $b \to s\ell^+\ell^-$:

$$\mathcal{H}_{\rm eff} = -\frac{4G_F}{\sqrt{2}} V_{tb}V_{ts}^*\left(\sum_{i=1}^{10} C_i(\mu)O_i(\mu) + \sum_{i=1}^{10} C_{Q_i}(\mu)Q_i(\mu)\right) , \tag{2.1}$$

where the first ten operators and Wilson coefficients (WC) at EW scale can be found in [8, 37][1], and last ten operators and WC which represent the contributions of neutral Higgs can be found in [4].

With the renormalization group equations to resum the QCD corrections, WCs at energy scale $\mu = m_b$ are evaluated. Theoretical uncertainties related to renormalization-scale can be substantially reduced when the next-leading-logarithm corrections are included [38].

The above Hamiltonian leads to the following free quark decay amplitude:

$$\begin{aligned}\mathcal{M}(b \to s\ell^+\ell^-) \;\;=\;\; & \frac{G_F\alpha}{\sqrt{2}\pi} V_{ts}^* V_{tb} \left\{ C_9^{\rm eff}\left[\bar{s}\gamma_\mu L b\right]\left[\bar{\ell}\gamma^\mu\ell\right] + C_{10}\left[\bar{s}\gamma_\mu L b\right]\left[\bar{\ell}\gamma^\mu\gamma_5\ell\right]\right. \\ & \left. -2\hat{m}_b C_7^{\rm eff}\left[\bar{s}i\sigma_{\mu\nu}\frac{\hat{q}^\nu}{\hat{s}}Rb\right]\left[\bar{\ell}\gamma^\mu\ell\right] + C_{Q1}\left[\bar{s}Rb\right]\left[\bar{\ell}\ell\right] + C_{Q2}\left[\bar{s}Rb\right]\left[\bar{\ell}\gamma_5\ell\right]\right\}\end{aligned} \tag{2.2}$$

[1] In our previous papers, e.g., [3, 4], we follow the convention of ref. [1] for the indices of operators as well as Wilson coefificients. In this paper. we use more popular conventions (see, e.g., [38]). That is, $O_8 \to O_9$ and $O_9 \to O_{10}$.

where C_9^{eff} is defined as [39, 40]

$$C_9^{\rm eff}(\mu, \hat{s}) = C_9(\mu) + Y(\mu, \hat{s}) + \frac{3\pi}{\alpha^2} C(\mu) \sum_{V_i=\psi(1s),\dots,\psi(6s)} \kappa_i \frac{\Gamma(V_i \to \ell^+\ell^-)\, m_{V_i}}{{m_{V_i}}^2 - \hat{s}\, {m_B}^2 - i m_{V_i}\Gamma_{V_i}} \quad (2.3)$$

where $\hat{s} = s/m_b^2$,s=q^2, $C(\mu) = (3\,C_1 + C_2 + 3\,C_3 + C_4 + 3\,C_5 + C_6)$, and

$$\begin{aligned} Y(\mu, \hat{s}) \;&=\; g(\hat{m_c}, \hat{s}) C(\mu) \\ &\quad -\frac{1}{2} g(1, \hat{s})\,(4\,C_3 + 4\,C_4 + 3\,C_5 + C_6) - \frac{1}{2} g(0, \hat{s})\,(C_3 + 3\,C_4) \\ &\quad -\frac{2}{9}\,(3\,C_3 + C_4 + 3\,C_5 + C_6)\;. \end{aligned} \quad (2.4)$$

where the function $g(\hat{m_c}, \hat{s})$ comes from one loop contributions of four-quark operators and is defined by

$$g(z, \hat{s}) = -\frac{4}{9} ln z^2 + \frac{8}{27} + \frac{16}{9}\frac{z^2}{\hat{s}} - \begin{cases} \frac{2}{9}\sqrt{1 - \frac{4z^2}{\hat{s}}}(2 + \frac{4z^2}{\hat{s}})\left[ln(\frac{1+\sqrt{1-4z^2/\hat{s}}}{1-\sqrt{1-4z^2/\hat{s}}}) + i\pi\right], & 4z^2 < \hat{s} \\ \frac{4}{9}\sqrt{\frac{4z^2}{\hat{s}} - 1}(2 + \frac{4z^2}{\hat{s}}) arctan\left(\frac{1}{\sqrt{4z^2/\hat{s}-1}}\right), & 4z^2 > \hat{s} \end{cases} \quad (2.5)$$

The last terms in (2.3) are nonperturbative effects from $(\bar{c}c)$ resonance contributions, while the phenomenological factors κ_i can be fixed from the processes [23] $B \to K^{(*)} V_i \to K^{(*)}\ell^+\ell^-$ and as given in the Table. 1.

Exclusive decays $B \to (K, K^*)\ell^+\ell^-$ are described in terms of matrix elements of the quark operators in Eq. (2.2) over meson states, which can be parametrized in terms of form factors.

For the process $B \to K\ell^+\ell^-$, the non-vanishing matrix elements are $(q = p_B - p)$

$$\langle K(p)|\bar{s}\gamma_\mu b|B(p_B)\rangle = f_+(s)\left\{(p_B + p)_\mu - \frac{m_B^2 - m_K^2}{s}\, q_\mu\right\} + \frac{m_B^2 - m_K^2}{s}\, f_0(s)\, q_\mu, \quad (2.6)$$

and

$$\begin{aligned} \langle K(p)|\bar{s}\sigma_{\mu\nu}q^\nu(1+\gamma_5)b|B(p_B)\rangle \;&=\; \langle K(p)|\bar{s}\sigma_{\mu\nu}q^\nu b|B(p_B)\rangle \\ &=\; i\left\{(p_B + p)_\mu s - q_\mu(m_B^2 - m_K^2)\right\}\, \frac{f_T(s)}{m_B + m_K} \end{aligned} \quad (2.7)$$

κ	J/Ψ	Ψ'
K	2.70	3.51
K^*	1.65	2.36

Table 1: *Fudge factors in $B \to K^{(*)} J/\Psi, \Psi' \to K^{(*)}\ell^+\ell^-$ decays calculated using the LCSR form factors.*

While for $B \to K^*\ell^+\ell^-$, related transition matrix elements are

$$\begin{aligned} \langle K^*(p)|(V-A)_\mu|B(p_B)\rangle &= -i\epsilon^*_\mu(m_B+m_{K^*})A_1(s) + i(p_B+p)_\mu(\epsilon^* p_B)\,\frac{A_2(s)}{m_B+m_{K^*}} \\ &\quad + iq_\mu(\epsilon^* p_B)\,\frac{2m_{K^*}}{s}\,(A_3(s)-A_0(s)) + \epsilon_{\mu\nu\rho\sigma}\epsilon^{*\nu}p_B^\rho p^\sigma\,\frac{2V(s)}{m_B+m_{K^*}}\,. \end{aligned} \tag{2.8}$$

and

$$\begin{aligned} \langle K^*|\bar s\sigma_{\mu\nu}q^\nu(1+\gamma_5)b|B(p_B)\rangle &= i\epsilon_{\mu\nu\rho\sigma}\epsilon^{*\nu}p_B^\rho p^\sigma\, 2T_1(s) \\ &\quad + T_2(s)\left\{\epsilon^*_\mu(m_B^2-m_{K^*}^2) - (\epsilon^* p_B)\,(p_B+p)_\mu\right\} \\ &\quad + T_3(s)(\epsilon^* p_B)\left\{q_\mu - \frac{s}{m_B^2-m_{K^*}^2}\,(p_B+p)_\mu\right\} \end{aligned} \tag{2.9}$$

Where ϵ_μ is polarization vector of the vector meson K^*. By means of the equation of motion, one obtains several relations between form factors

$$\begin{aligned} A_3(s) &= \frac{m_B+m_{K^*}}{2m_{K^*}}\,A_1(s) - \frac{m_B-m_{K^*}}{2m_{K^*}}\,A_2(s), \\ A_0(0) &= A_3(0), \\ \langle K^*|\partial_\mu A^\mu|B\rangle &= 2m_{K^*}(\epsilon^* p_B)A_0(s), \\ T_1(0) &= T_2(0). \end{aligned} \tag{2.10}$$

All signs are defined in such a way as to render the form factors real and positive. The physical range in $\hat s$ extends from $\hat s_{\rm min} = 4\hat m_\ell^2$ to $\hat s_{\rm max} = (1-\hat m_{K,K^*})^2$.

The calculation of the form factors given above is a real task, and one has to rely on certain approximate methods. We use the results calculated by using technique of LCSRs and given in [23]. And form factors can be parametrized as

$$F(\hat s) = F(0)\exp(c_1\hat s + c_2\hat s^2 + c_3\hat s^3). \tag{2.11}$$

The parameterization formula works within 1% accuracy for $s < 15\,\mathrm{GeV}^2$ and can avoid the spurious singularities at $s = m_B^2$. Related parameters is given in the Table. 4 of [23]

9.3 Formula of Observables

In this subsection we provide formula of experimental observables, which include dilepton invariant mass spectrum, forward-backward asymmetry, and lepton polarizations.

¿From eqs. (2.2 - 2.8), it is straightforward to obtain the matrix element of $B \to K(K^*)l^+l^-$ as follows.

$$\mathcal{M} = \frac{G_F\alpha}{2\sqrt{2}\pi}\,V_{ts}^*V_{tb}m_B\,\left[\mathcal{T}^1_\mu\,\left(\bar\ell\,\gamma^\mu\,\ell\right) + \mathcal{T}^2_\mu\,\left(\bar\ell\,\gamma^\mu\,\gamma_5\,\ell\right) + \mathcal{S}\left(\bar\ell\ell\right)\right]\,, \tag{3.1}$$

where for $B \to K\ell^+\ell^-$,

$$\mathcal{T}^1_\mu = A'(\hat{s})\,\hat{p}_\mu, \tag{3.2}$$
$$\mathcal{T}^2_\mu = C'(\hat{s})\,\hat{p}_\mu + D'(\hat{s})\,\hat{q}_\mu\ , \tag{3.3}$$
$$\mathcal{S} = \mathcal{S}_1(\hat{s}) \tag{3.4}$$

and for $B \to K^*\ell^+\ell^-$,

$$\mathcal{T}^1_\mu = A(\hat{s})\,\epsilon_{\mu\rho\alpha\beta}\epsilon^{*\rho}\hat{p}_B^\alpha\hat{p}_{K^*}^\beta - iB(\hat{s})\,\epsilon^*{}_\mu + iC(\hat{s})\,(\epsilon^*\cdot\hat{p}_B)\hat{p}_\mu\ , \tag{3.5}$$
$$\mathcal{T}^2_\mu = E(\hat{s})\,\epsilon_{\mu\rho\alpha\beta}\epsilon^{*\rho}\hat{p}_B^\alpha\hat{p}_{K^*}^\beta - iF(\hat{s})\,\epsilon^*{}_\mu + iG(\hat{s})\,(\epsilon^*\cdot\hat{p}_B)\hat{p}_\mu + iH(\hat{s})\,(\epsilon^*\cdot\hat{p}_B)\hat{q}_\mu\ , \tag{3.6}$$
$$\mathcal{S} = i2\hat{m}_{K^*}(\epsilon^*\cdot\hat{p}_B)\mathcal{S}_2(\hat{s}) \tag{3.7}$$

with $p \equiv p_B + p_{K,K^*}$. Note that, using the equation of motion for lepton fields, the terms in $\hat{q}_\mu$ in $\mathcal{T}^1_\mu$ vanish.

The auxiliary functions above are defined as

$$A'(\hat{s}) = C_9^{\text{eff}}(\hat{s})\,f_+(\hat{s}) + \frac{2\hat{m}_b}{1+\hat{m}_K}C_7^{\text{eff}}f_T(\hat{s})\ , \tag{3.8}$$
$$C'(\hat{s}) = C_{10}\,f_+(\hat{s})\ , \tag{3.9}$$
$$D'(\hat{s}) = C_{10}\,f_-(\hat{s}) - \frac{1-\hat{m}_K^2}{2\hat{m}_\ell(\hat{m}_b-\hat{m}_s)}C_{Q2}f_0(\hat{s})\ , \tag{3.10}$$
$$\mathcal{S}_1(\hat{s}) = \frac{1-\hat{m}_K^2}{(\hat{m}_b-\hat{m}_s)}C_{Q1}f_0(\hat{s})\ , \tag{3.11}$$
$$A(\hat{s}) = \frac{2}{1+\hat{m}_{K^*}}C_9^{\text{eff}}(\hat{s})V(\hat{s}) + \frac{4\hat{m}_b}{\hat{s}}C_7^{\text{eff}}T_1(\hat{s})\ , \tag{3.12}$$
$$B(\hat{s}) = (1+\hat{m}_{K^*})\left[C_9^{\text{eff}}(\hat{s})A_1(\hat{s}) + \frac{2\hat{m}_b}{\hat{s}}(1-\hat{m}_{K^*})C_7^{\text{eff}}T_2(\hat{s})\right]\ , \tag{3.13}$$
$$C(\hat{s}) = \frac{1}{1-\hat{m}_{K^*}^2}\left[(1-\hat{m}_{K^*})C_9^{\text{eff}}(\hat{s})A_2(\hat{s}) + 2\hat{m}_bC_7^{\text{eff}}\left(T_3(\hat{s}) + \frac{1-\hat{m}_{K^*}^2}{\hat{s}}T_2(\hat{s})\right)\right], \tag{3.14}$$
$$E(\hat{s}) = \frac{2}{1+\hat{m}_{K^*}}C_{10}V(\hat{s})\ , \tag{3.15}$$
$$F(\hat{s}) = (1+\hat{m}_{K^*})C_{10}A_1(\hat{s})\ , \tag{3.16}$$
$$G(\hat{s}) = \frac{1}{1+\hat{m}_{K^*}}C_{10}A_2(\hat{s})\ , \tag{3.17}$$
$$\begin{aligned} H(\hat{s}) &= \frac{C_{10}}{\hat{s}}\left[(1+\hat{m}_{K^*})A_1(\hat{s}) - (1-\hat{m}_{K^*})A_2(\hat{s}) - 2\hat{m}_{K^*}A_0(\hat{s})\right] \\ &\quad + \frac{\hat{m}_{K^*}}{\hat{m}_\ell(\hat{m}_b+\hat{m}_s)}A_0(\hat{s})C_{Q2}\ , \end{aligned} \tag{3.18}$$
$$\mathcal{S}_2(\hat{s}) = -\frac{1}{(\hat{m}_b+\hat{m}_s)}A_0(\hat{s})C_{Q1}\ . \tag{3.19}$$

where

$$f_0(\hat{s}) = \frac{1}{1-\hat{m}_K^2}\left[\hat{s}f_-(\hat{s}) + (1-\hat{m}_K^2)f_+(\hat{s})\right] \tag{3.20}$$

and to get the auxiliary functions given above, we have used equations of motion

$$q^\mu(\bar{\psi}_1\gamma_\mu\psi_2) = (m_1 - m_2)\bar{\psi}_1\psi_2, \tag{3.21}$$
$$q^\mu(\bar{\psi}_1\gamma_\mu\gamma_5\psi_2) = -(m_1 + m_2)\bar{\psi}_1\gamma_5\psi_2. \tag{3.22}$$

The contributions of NHBs have been incorporated in the terms of $\mathcal{S}_1(\hat{s})$, $D'(\hat{s})$, $H(\hat{s})$ and $\mathcal{S}_2(\hat{s})$. It is remarkable that the contributions of NHBs in $D'(\hat{s})$ and $H(\hat{s})$ are proportional to the inverse mass of the lepton, and for the case $l = \mu$, the effects of NHBs can be manifested through these terms.

A phenomenological effective Hamiltonian is recently given in [29]. If ignoring tensor type interactions in the phenomenological Hamiltonian (it is shown that physical observables are not sensitive to the presence of tensor type interactions [6]), it is easy to verify that the matrix element of $B \to K^{(*)}\ell^+\ell^-$ can always be expressed as the form of the equation (3.1) with the auxiliary functions defined as

$$A'(\hat{s}) = w_{c_1}\, f_+(\hat{s}) - \frac{w_{c_9} + w_{c_{10}}}{1 + \hat{m}_K} f_T(\hat{s}) \,, \tag{3.23}$$
$$C'(\hat{s}) = w_{c_2}\, f_+(\hat{s}) \,, \tag{3.24}$$
$$D'(\hat{s}) = w_{c_2}\, f_-(\hat{s}) - \frac{1 - \hat{m}_K^2}{2\hat{m}_\ell(\hat{m}_b - \hat{m}_s)} w_{c_6} f_0(\hat{s}) \,, \tag{3.25}$$
$$\mathcal{S}_1(\hat{s}) = \frac{1 - \hat{m}_K^2}{(\hat{m}_b - \hat{m}_s)} w_{c_5} f_0(\hat{s}) \,, \tag{3.26}$$
$$A(\hat{s}) = \frac{2}{1 + \hat{m}_{K^*}} w_{c_1} V(\hat{s}) - \frac{2)}{\hat{s}}(w_{c_9} + w_{c_{10}})T_1(\hat{s}) \,, \tag{3.27}$$
$$B(\hat{s}) = -(1 + \hat{m}_{K^*}) \left[w_{c_3} A_1(\hat{s}) + \frac{1}{\hat{s}}(1 - \hat{m}_{K^*})(w_{c_9} + w_{c_{10}})T_2(\hat{s}) \right] \,, \tag{3.28}$$
$$\begin{aligned} C(\hat{s}) = & -\frac{1}{1 - \hat{m}_{K^*}^2} \left[(1 - \hat{m}_{K^*})w_{c_3}(\hat{s})A_2(\hat{s}) \right. \\ & \left. +(w_{c_9} - w_{c_{10}}) \left((1 + \hat{m}_{K^*})T_3(\hat{s}) + \frac{1 - \hat{m}_{K^*}^2}{\hat{s}} T_2(\hat{s}) \right) \right] \,, \end{aligned} \tag{3.29}$$
$$E(\hat{s}) = \frac{2}{1 + \hat{m}_{K^*}} w_{c_2} V(\hat{s}) \,, \tag{3.30}$$
$$F(\hat{s}) = -(1 + \hat{m}_{K^*}) w_{c_4} A_1(\hat{s}) \,, \tag{3.31}$$
$$G(\hat{s}) = -\frac{1}{1 + \hat{m}_{K^*}} w_{c_4} A_2(\hat{s}) \,, \tag{3.32}$$
$$H(\hat{s}) = -\frac{2\hat{m}_{K^*}}{\hat{s}}\, w_{c_4}\, (A_3(\hat{s}) - A_0(\hat{s})) + \frac{\hat{m}_{K^*}}{\hat{m}_\ell(\hat{m}_b + \hat{m}_s)} w_{c_8} A_0(\hat{s}) \,, \tag{3.33}$$
$$\mathcal{S}_2(\hat{s}) = -\frac{1}{(\hat{m}_b + \hat{m}_s)} w_{c_7} A_0(\hat{s}) \,, \tag{3.34}$$

where

$$w_{c_1} = \frac{1}{4}(C_{LL} + C_{LR} + C_{RL} + C_{RR}) \,, \tag{3.35}$$

$$w_{c_2} = \frac{1}{4}(-C_{LL} + C_{LR} - C_{RL} + C_{RR}) \ , \tag{3.36}$$
$$w_{c_3} = \frac{1}{4}(-C_{LL} - C_{LR} + C_{RL} + C_{RR}) \ , \tag{3.37}$$
$$w_{c_4} = \frac{1}{4}(C_{LL} - C_{LR} - C_{RL} + C_{RR}) \ , \tag{3.38}$$
$$w_{c_5} = \frac{1}{4}(C_{LRLR} + C_{RLLR} + C_{LRRL} + C_{RLRL}) \ , \tag{3.39}$$
$$w_{c_6} = \frac{1}{4}(C_{LRLR} + C_{RLLR} - C_{LRRL} - C_{RLRL}) \ , \tag{3.40}$$
$$w_{c_7} = \frac{1}{4}(C_{LRLR} - C_{RLLR} + C_{LRRL} - C_{RLRL}) \ , \tag{3.41}$$
$$w_{c_8} = \frac{1}{4}(C_{LRLR} - C_{RLLR} - C_{LRRL} + C_{RLRL}) \ , \tag{3.42}$$
$$w_{c_9} = m_b C_{BR} \ , \tag{3.43}$$
$$w_{c_{10}} = m_s C_{SL} \ , \tag{3.44}$$
$$. \tag{3.45}$$

In the above equations C_{LL}, C_{LR} etc. are defined in ref. [6]. Therefore our formula given below can also be used to make model independent phenomenological analysis, if using Eqs. ((3.23)-(3.34)) in stead of Eqs. ((3.8)-(3.19)).

Keeping the lepton mass, we find the double differential decay widths Γ^K and Γ^{K^*} for the decays $B \to K\ell^+\ell^-$ and $B \to K^*\ell^+\ell^-$, respectively, as

$$\begin{aligned}
\frac{\mathrm{d}^2\Gamma^K}{\mathrm{d}\hat{s}\mathrm{d}\hat{u}} &= \frac{G_F^2\alpha^2 m_B^5}{2^{11}\pi^5} |V_{ts}^* V_{tb}|^2 \\
&\times \Big\{ (|A'|^2 + |C'|^2)(\lambda - \hat{u}^2) + |\mathcal{S}_1|^2(\hat{s} - 4\hat{m}_\ell^2) + Re(\mathcal{S}_1 A'^*) 4\hat{m}_\ell \hat{u} \\
&+ |C'|^2 4\hat{m}_\ell{}^2 (2 + 2\hat{m}_K^2 - \hat{s}) + Re(C'D'^*) 8\hat{m}_\ell{}^2 (1 - \hat{m}_K^2) + |D'|^2 4\hat{m}_\ell{}^2 \hat{s} \Big\} \ , \quad (3.46) \\
\frac{\mathrm{d}^2\Gamma^{K^*}}{\mathrm{d}\hat{s}\mathrm{d}\hat{u}} &= \frac{G_F^2\,\alpha^2\,m_B^5}{2^{11}\pi^5} |V_{ts}^*\,V_{tb}|^2 \\
&\times \Bigg\{ \frac{|A|^2}{4}\left(\hat{s}(\lambda + \hat{u}^2) + 4\hat{m}_\ell^2\lambda\right) + \frac{|E|^2}{4}\left(\hat{s}(\lambda + \hat{u}^2) - 4\hat{m}_\ell^2\lambda\right) + |\mathcal{S}_2|^2(\hat{s} - 4\hat{m}_\ell^2)\lambda \\
&+ \frac{1}{4\hat{m}_{K^*}^2}\left[|B|^2\left(\lambda - \hat{u}^2 + 8\hat{m}_{K^*}^2(\hat{s} + 2\hat{m}_\ell^2)\right) + |F|^2\left(\lambda - \hat{u}^2 + 8\hat{m}_{K^*}^2(\hat{s} - 4\hat{m}_\ell^2)\right)\right] \\
&- 2\hat{s}\hat{u}\left[\mathrm{Re}(BE^*) + \mathrm{Re}(AF^*)\right] + \frac{2\hat{m}_\ell\hat{u}}{\hat{m}_{K^*}}\left[\mathrm{Re}(\mathcal{S}_2 B^*)(\hat{s} + \hat{m}_{K^*}^2 - 1) + \mathrm{Re}(\mathcal{S}_2 C^*)\lambda\right] \\
&+ \frac{\lambda}{4\hat{m}_{K^*}^2}\left[|C|^2(\lambda - \hat{u}^2) + |G|^2\left(\lambda - \hat{u}^2 + 4\hat{m}_\ell^2(2 + 2\hat{m}_{K^*}^2 - \hat{s})\right)\right] \\
&- \frac{1}{2\hat{m}_{K^*}^2}\Big[\mathrm{Re}(BC^*)(1 - \hat{m}_{K^*}^2 - \hat{s})(\lambda - \hat{u}^2) \\
&\qquad + \mathrm{Re}(FG^*)\left((1 - \hat{m}_{K^*}^2 - \hat{s})(\lambda - \hat{u}^2) + 4\hat{m}_\ell^2\lambda\right)\Big]
\end{aligned}$$

$$- 2\frac{\hat{m}_\ell^2}{\hat{m}_{K^*}^2}\lambda \left[\mathrm{Re}(FH^*) - \mathrm{Re}(GH^*)(1-\hat{m}_{K^*}^2)\right] + |H|^2\frac{\hat{m}_\ell^2}{\hat{m}_{K^*}^2}\hat{s}\lambda\Big\} . \quad (3.47)$$

Here the kinematic variables $(\hat{s}, \hat{u})$ are defined as

$$\hat{s} = \hat{q}^2 = (\hat{p}_+ + \hat{p}_-)^2 , \quad (3.48)$$
$$\hat{u} = (\hat{p}_B - \hat{p}_-)^2 - (\hat{p}_B - \hat{p}_+)^2 \quad (3.49)$$

which are bounded as

$$(2\hat{m}_\ell)^2 \le \hat{s} \le (1 - \hat{m}_{K,K^*})^2 , \quad (3.50)$$
$$-\hat{u}(\hat{s}) \le \hat{u} \le \hat{u}(\hat{s}) , \quad (3.51)$$

with $\hat{m_\ell} = m_\ell/m_B$ and

$$\hat{u}(\hat{s}) = \sqrt{\lambda(1 - 4\frac{\hat{m}_\ell^2}{\hat{s}})} , \quad (3.52)$$
$$\lambda = 1 + \hat{m}_{K,K*}^4 + \hat{s}^2 - 2\hat{s} - 2\hat{m}_{K,K*}^2(1+\hat{s}) , \quad (3.53)$$
$$\mathcal{D} = \sqrt{1 - \frac{4\hat{m}_\ell^2}{s}} . \quad (3.54)$$

Note that the variable $\hat{u}$ corresponds to θ, the angle between the momentum of the B-meson and the positively charged lepton ℓ^+ in the dilepton CMS frame, through the relation $\hat{u} = -\hat{u}(\hat{s})\cos\theta$ [41].

Integrating over $\hat{u}$ in the kinematic region given in Eq. (3.51) we get the formula of dilepton invariant mass spectra (IMS)

$$\frac{\mathrm{d}\Gamma^K}{\mathrm{d}\hat{s}} = \frac{G_F^2\alpha^2 m_B^5}{2^{10}\pi^5}|V_{ts}^*V_{tb}|^2\,\hat{u}(\hat{s})D^K \quad (3.55)$$

$$D^K = (|A'|^2 + |C'|^2)(\lambda - \frac{\hat{u}(\hat{s})^2}{3}) + |\mathcal{S}_1|^2(\hat{s} - 4\hat{m}_\ell^2)$$
$$+|C'|^2 4\hat{m_\ell}^2(2 + 2\hat{m}_K^2 - \hat{s}) + Re(C'D'^*)8\hat{m_\ell}^2(1 - \hat{m}_K^2) + |D'|^2 4\hat{m_\ell}^2\hat{s} , \quad (3.56)$$

$$\frac{\mathrm{d}\Gamma^{K^*}}{\mathrm{d}\hat{s}} = \frac{G_F^2\,\alpha^2\, m_B^5}{2^{10}\pi^5}|V_{ts}^*V_{tb}|^2\;\hat{u}(\hat{s})D^{K^*} \quad (3.57)$$

$$D^{K^*} = \frac{|A|^2}{3}\hat{s}\lambda(1 + 2\frac{\hat{m}_\ell^2}{\hat{s}}) + |E|^2\hat{s}\frac{\hat{u}(\hat{s})^2}{3} + |\mathcal{S}_2|^2(\hat{s} - 4\hat{m}_\ell^2)\lambda$$
$$+\frac{1}{4\hat{m}_{K^*}^2}\left[|B|^2(\lambda - \frac{\hat{u}(\hat{s})^2}{3} + 8\hat{m}_{K^*}^2(\hat{s} + 2\hat{m}_\ell^2)) + |F|^2(\lambda - \frac{\hat{u}(\hat{s})^2}{3} + 8\hat{m}_{K^*}^2(\hat{s} - 4\hat{m}_\ell^2))\right]$$
$$+\frac{\lambda}{4\hat{m}_{K^*}^2}\left[|C|^2(\lambda - \frac{\hat{u}(\hat{s})^2}{3}) + |G|^2\left(\lambda - \frac{\hat{u}(\hat{s})^2}{3} + 4\hat{m}_\ell^2(2 + 2\hat{m}_{K^*}^2 - \hat{s})\right)\right]$$
$$-\frac{1}{2\hat{m}_{K^*}^2}\Big[\mathrm{Re}(BC^*)(\lambda - \frac{\hat{u}(\hat{s})^2}{3})(1 - \hat{m}_{K^*}^2 - \hat{s})$$

$$+ \mathrm{Re}(FG^*)((\lambda - \frac{\hat{u}(\hat{s})^2}{3})(1 - \hat{m}_{K^*}^2 - \hat{s}) + 4\hat{m}_\ell^2\lambda)\Big]$$
$$-2\frac{\hat{m}_\ell^2}{\hat{m}_{K^*}^2}\lambda\left[\mathrm{Re}(FH^*) - \mathrm{Re}(GH^*)(1 - \hat{m}_{K^*}^2)\right] + \frac{\hat{m}_\ell^2}{\hat{m}_{K^*}^2}\hat{s}\lambda|H|^2 \,. \tag{3.58}$$

Both distributions agree with the ones obtained in [23, 35], if $C_{Q_{1,2}}$ are set to zero. The differential forward-backward-asymmetry (FBA) is defined as

$$A_{FB}(s) = \frac{-\int_0^{u(\hat{s})} dz \frac{d\Gamma}{dsdu} + \int_{-u(\hat{s})}^0 du \frac{d\Gamma}{dsdu}}{\int_0^{u(\hat{s})} dz \frac{d\Gamma}{dsdu} + \int_{-u(\hat{s})}^0 du \frac{d\Gamma}{dsdu}} \,.$$

For $B \to K\ell^+\ell^-$ decays it reads as follows

$$\frac{\mathrm{d}\mathcal{A}_{\mathrm{FB}}^K}{\mathrm{d}\hat{s}} D^K = -2\hat{m}_\ell \hat{u}(\hat{s}) \mathrm{Re}(\mathcal{S}_1 A'^*) \tag{3.59}$$

For $B \to K^*\ell^+\ell^-$ decays it reads as follows

$$\frac{\mathrm{d}\mathcal{A}_{\mathrm{FB}}^{K^*}}{\mathrm{d}\hat{s}} D^{K^*} = \hat{u}(\hat{s})\Big\{\hat{s}\left[\mathrm{Re}(BE^*) + \mathrm{Re}(AF^*)\right]$$
$$+ \frac{\hat{m}_\ell}{\hat{m}_{K^*}}\left[\mathrm{Re}(\mathcal{S}_2 B^*)(1 - \hat{s} - \hat{m}_{K^*}^2) - \mathrm{Re}(\mathcal{S}_2 C^*)\lambda\right]\Big\} \tag{3.60}$$

We can read from (3.59), the FB asymmetry of the process $B \to K\ell^+\ell^-$ does not vanish when the contributions of NHB are taken into account. With it, our analysis below also show the contributions of NHBs can even be accessible in B factories.

The lepton polarization can be defined as follows

$$\frac{d\Gamma(\vec{n})}{ds} = \frac{1}{2}(\frac{d\Gamma}{ds})_0\Big[1 + (P_L\,\vec{e}_L + P_N\,\vec{e}_N + P_T\,\vec{e}_T)\cdot\vec{n}\Big] \,, \tag{3.61}$$

where the subscript "0" corresponds to the unpolarized amplitude, and P_L, P_T, and P_N, correspond to the longitudinal, transverse and normal components of the polarization vector, respectively.

For the process $B \to K\ell^-\ell^+$, the P_L^K, P_T^K, and P_N^K, are derived respectively as

$$P_L^K D^K = \frac{4}{3}\mathcal{D}\Big\{\lambda\mathrm{Re}(A'C'^*) - 3\hat{m}_\ell(1 - \hat{m}_K^2)\mathrm{Re}(C'^*\mathcal{S}_1) - 3\hat{m}_\ell\hat{s}\mathrm{Re}(D'^*\mathcal{S}_1)\Big\}, \tag{3.62}$$

$$P_N^K D^K = \frac{\pi\sqrt{\hat{s}}\hat{u}(\hat{s})}{2}\Big\{ - \mathrm{Im}(A'\mathcal{S}_1^*) + 2\hat{m}_\ell\mathrm{Im}(C'D'^*)\Big\}, \tag{3.63}$$

$$P_T^K D^K = \frac{-\pi\sqrt{\lambda}}{\sqrt{\hat{s}}}\Big\{\hat{m}_\ell\Big[(1 - \hat{m}_K^2)\mathrm{Re}(A'C'^*)$$
$$+\hat{s}\mathrm{Re}(A'D'^*)\Big] + \frac{(\hat{s} - 4\hat{m}_\ell^2)}{2}\mathrm{Re}(C'\mathcal{S}_1^*)\Big\}. \tag{3.64}$$

D^K is defined in Eq. (3.56). For the process $B \to K^*\ell^-\ell^+$, the $P_L^{K^*}$, $P_T^{K^*}$, and $P_N^{K^*}$, are derived respectively as

$$\begin{aligned} P_L^{K^*}D^{K^*} &= \mathcal{D}\Bigg\{\frac{2\hat{s}\lambda}{3}\mathrm{Re}(AE^*) + \frac{(\lambda+12\hat{m}_{K^*}^2)}{3\hat{m}_{K^*}^2}\mathrm{Re}(BF^*) \\ &\quad - \frac{\lambda(1-\hat{m}_{K^*}^2-\hat{s})}{3\hat{m}_{K^*}^2}\mathrm{Re}(BG^*+CF^*) + \frac{\lambda^2}{3\hat{m}_{K^*}^2}\mathrm{Re}(CG^*) \\ &\quad + \frac{2\hat{m}_\ell\lambda}{\hat{m}_{K^*}}\Big[\mathrm{Re}(F\mathcal{S}_2^*) - \hat{s}\mathrm{Re}(H\mathcal{S}_2^*) - (1-\hat{m}_{K^*}^2)\mathrm{Re}(G\mathcal{S}_2^*)\Big]\Bigg\}, \end{aligned} \tag{3.65}$$

$$\begin{aligned} P_N^{K^*}D^{K^*} &= \frac{-\pi\sqrt{\hat{s}}\hat{u}(\hat{s})}{4\hat{m}_K}\Bigg\{\frac{\hat{m}_\ell}{\hat{m}_{K^*}}\Big[\mathrm{Im}(FG^*)(1+3\hat{m}_{K^*}^2-s) \\ &\quad + \mathrm{Im}(FH^*)(1-\hat{m}_{K^*}^2-s) - \mathrm{Im}(GH^*)\lambda\Big] \\ &\quad + 2\hat{m}_{K^*}\hat{m}_\ell\left[\mathrm{Im}(BE^*)+\mathrm{Im}(AF^*)\right] \\ &\quad - (1-\hat{m}_{K^*}^2-\hat{s})\mathrm{Im}(B\mathcal{S}_2^*) + \lambda\mathrm{Im}(C\mathcal{S}_2^*)\Bigg\}, \end{aligned} \tag{3.66}$$

$$\begin{aligned} P_T^{K^*}D^{K^*} &= \frac{\pi\sqrt{\lambda}\hat{m}_\ell}{4\sqrt{\hat{s}}}\Bigg\{4\hat{s}\mathrm{Re}(AB^*) \\ &\quad + \frac{(1-\hat{m}_{K^*}^2-\hat{s})}{\hat{m}_{K^*}^2}\Big[-\mathrm{Re}(BF^*) + (1-\hat{m}_{K^*}^2)\mathrm{Re}(BG^*) + \hat{s}\mathrm{Re}(BH^*)\Big] \\ &\quad + \frac{\lambda}{\hat{m}_{K^*}^2}\Big[\mathrm{Re}(CF^*) - (1-\hat{m}_{K^*}^2)\mathrm{Re}(CG^*) - \hat{s}\mathrm{Re}(CH^*)\Big] \\ &\quad + \frac{(\hat{s}-4\hat{m}_\ell^2)}{\hat{m}_{K^*}\hat{m}_\ell}\Big[(1-\hat{m}_{K^*}^2-\hat{s})\mathrm{Re}(F\mathcal{S}_2^*) - \lambda\mathrm{Re}(G\mathcal{S}_2^*)\Big]\Bigg\}. \end{aligned} \tag{3.67}$$

D^{K^*} is defined by Eq.(3.58).

9.4 Numerical analysis

Parameters used in our analysis are list in Table 2. Considering that the branching ratios of $B \to K\,\ell^+\,\ell^-$ and $B \to K^*\,\ell^+\,\ell^-$ are not very sensitive to the mass of m_b, we neglect the difference between the pole mass and running mass of b quark.

The Wilson coefficients in the SM used in the numerical analysis is given in the Table 3. C_7^{eff} is defined as

$$C_7^{eff} = C_7 - C_5/3 - C_6\ . \tag{4.68}$$

$C_{Q_{1,2}}$ come from exchanging NHBs and are proportional to $\tan^3\beta$ in some regions of the parameter space in SUSY models. According to the analysis in [4, 36], the necessary conditions for the large contributions of NHBs include: (i) the ratio of vacuum

m_b	4.8 GeV
m_c	1.4 GeV
m_s	0.2 GeV
m_{mu}	0.11 GeV
m_{tau}	1.78 GeV
M_B	5.28 GeV
M_K	0.49 GeV
M_{K^*}	0.89 GeV
$M_{J/psi}(M_{\psi'})$	3.10(3.69) GeV
Γ_B	4.22×10^{-13} GeV
$\Gamma_{J/\psi}(\Gamma_{\psi'})$	$8.70(27.70) \times 10^{-5}$ GeV
$\Gamma(J/psi \to \ell^+\ell^-)$	5.26×10^{-6} GeV
$\Gamma(\psi' \to \ell^+\ell^-)$	2.14×10^{-6} GeV
G_F	1.17×10^{-5} GeV^{-2}
α^{-1}	129
$\lvert V_{ts}^* V_{tb}\rvert$	0.0385

Table 2: *Values of the input parameters used in our numerical analysis.*

C_1	C_2	C_3	C_4	C_5	C_6	$C_7^{\rm eff}$	C_9	C_{10}	C
-0.248	$+1.107$	$+0.011$	-0.026	$+0.007$	-0.031	-0.313	$+4.344$	-4.669	$+0.362$

Table 3: *Wilson coefficients of the SM used in the numerical analysis.*

SUSY models	R_7	R_9	R_{10}	C_{Q_1}	C_{Q_2}
SUSY I	-1.2	1.1	0.8	0.0	0.0
SUSY II	-1.2	1.1	0.8	6.5(16.5)	$-6.5(-16.5)$
SUSY III	1.2	1.1	0.8	1.2(4.5)	$-1.2(-4.5)$

Table 4: *Wilson coefficients of the SUSY used in our numerical analysis. R_i means C_i/C_i^{SM}. SUSY I corresponds to the regions where SUSY can destructively contribute and can change the sign of C_7, but the contributions of NHBs are neglected. SUSY II corresponds to the regions where tanβ is large and the masses of superpartners are relatively small. SUSY III corresponds to the regions where tanβ is large but the masses of superpartners are relatively large. In the last two cases the effects of NHBs are taken into account. The contributions of NHBs are settled to be different for both the case $\ell = \mu$ and $\ell = \tau$, since $C_{Q_{1,2}}$ are proportional to the mass of lepton. The values in bracket are for the case $\ell = \tau$*

expectation value, tanβ, should be large, (*ii*) the mass values of the lighter chargino and the lighter stop should not be too large (say less than 120 GeV), (*iii*)mass splitting of charginos and stops should be large, which also indicate large mixing between stop sector and chargino sector. As the conditions are satisfied, the process $B \to X_s\gamma$ will impose a constraint on C_7. It is well known that this process puts a very stringent constraint on the possible new physics and that SUSY can contribute destructively when the signature of the Higgs mass term μ is minus. There exist considerable regions of SUSY parameter space in which NHBs can largely contribute to the process $b \to s\ell^+\ell^-$ while the constraint of $b \to s\gamma$ is respected (i.e., the signature of the Wilson coefficient C_7 is changed from positive to negative). When the masses of SUSY particle are relatively heavy (say, 450 Gev), there are still significant regions in the parameter space of SUSY models in which NHBs could contribute largely. However, at these cases C_7 does not change its sign, because contributions of charged Higgs and charginos cancel with each other. We will see it is hopeful to distinguish these two kinds of regions of SUSY parameter space through observing $B \to K^{(*)}\ell^+\ell^-$.

As pointed out in [3, 4], the contribution of NHBs is proportional to the lepton mass, therefore for $\ell = e$, contributions of NHBs can be safely neglected. While for cases $\ell = \mu$ and $\ell = \tau$, the contributions of NHBs can be considerably large. To investigate the effects of NHBs in SUSY models, we take typical values of $C_{7,9,10}$ and $C_{Q_{1,2}}$ as given in Table 4. The SUSY model without considering the effects of NHBs (SUSY I in Table 4) is given as a reference frame so that could the effects of NHBs be shown in high relief.

Numerical results are shown in Figs. 1-4. In Fig. 1(a), the IMS of $B \to K\mu^+\mu^-$ is depicted. We see that at the high $\hat{s}$ regions, NHBs greatly modify the spectrum. While at the low $\hat{s}$ region, the effects of NHBs become weak. In Fig. 1(b), the FB

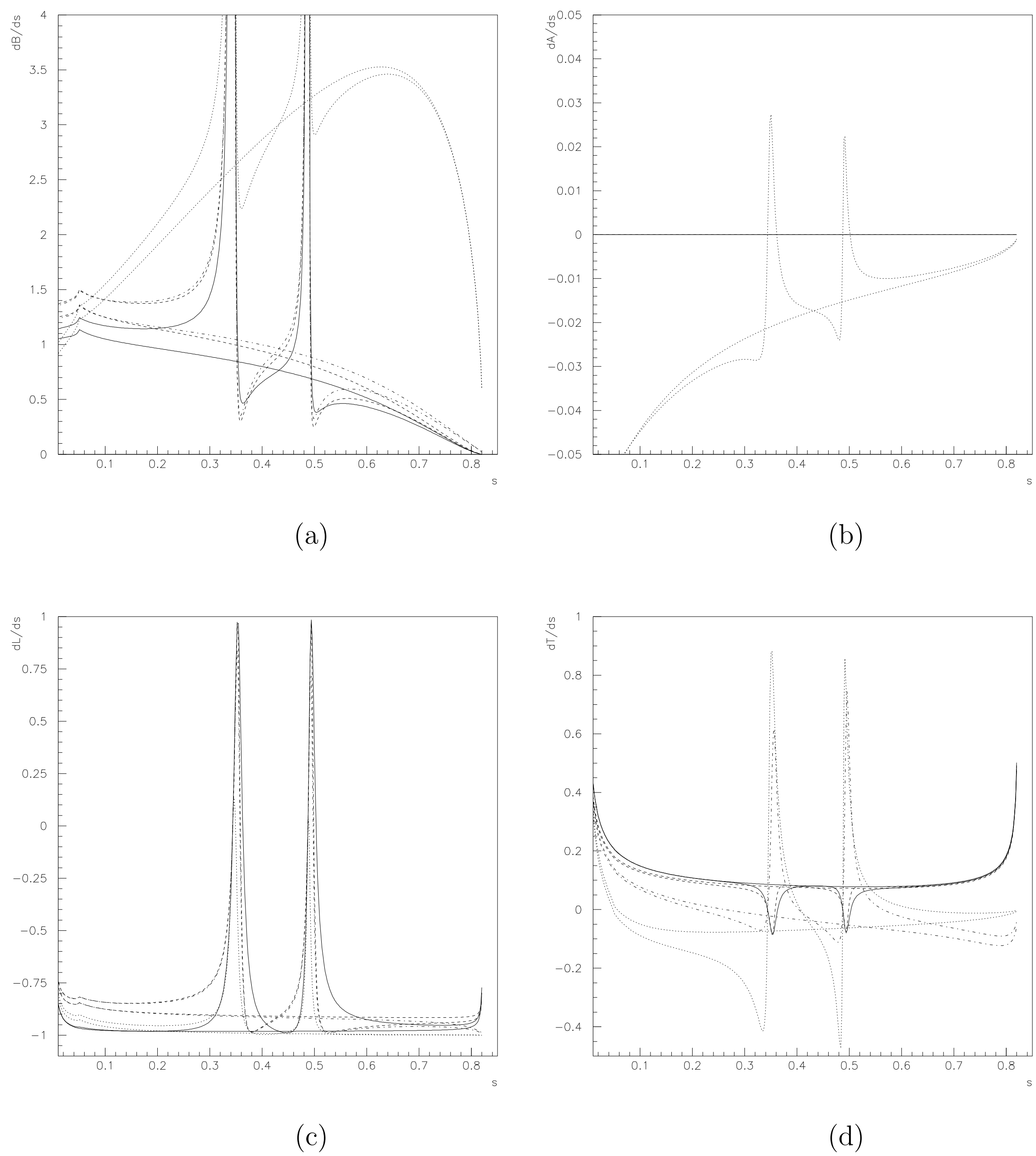

Figure 1: *The IMS(a), FBA(b), LP(c), and TP(d) of the process $B \to K\mu^+\mu^-$. The solid line, dashed line, dot line and dashed-dot line represent the SM, SUSY I, SUSY II, SUSY III respectively. Both the total (SD+LD) and the pure SD contributions are shown in order to compare.*

asymmetry of the $B \to K\mu^+\mu^-$ is presented. Fig. 1(b) shows that the average FB asymmetry in $B \to K\mu^+\mu^-$ 0.02. To measure an asymmetry A of a decay with the branching ratio Br at the $n\sigma$ level, the required number of events is $N = n^2/(BrA^2)$. For $B \to K\mu^+\mu^-$, the average FB asymmetry is 0.02 or so, the required number of events is 10^{-12} or so. Therefore it is hard to observe the derivation of FB asymmetry from the SM. In Fig. 1(c) and Fig. 1(d), the longitudinal and transverse polarizations are given. The effect of NHBs to the longitudinal polarization is weak but the effect to the transverse is remarkable.

In Fig. 2(a) and Fig. 2(b) the IMS and FB asymmetry of $B \to K\tau^+\tau^-$ are presented respectively. For SUSY II, the effects of NHBs to IMS is quite manifest, and the average FB asymmetry can reach 0.1. For SUSY III, the average FB asymmetry can reach 0.3. Therefore, in order to observe FBA, the required number of events should be 10^{-9} or so and 10^{-8}, respectively, so that in B factories, say LHCB, these two cases are accessible. In Fig. 2(c) and Fig. 2(d), the longitudinal and transverse polarizations are drawn respectively. The effects of NHBs are also very obvious.

Figs. 3 and 4 are devoted to the decay $B \to K^*l^+l^-$. In Fig. 3, the IMS, FB asymmetry, and polarizations of $B \to K^*\mu^+\mu^-$ are given. We see that this process is not as much as sensitive to the effect of NHB as $B \to K\mu^+\mu^-$. However, the contribution of NHBs will increase the part with positive FB asymmetry and will be helpful to determine the zero point of FB asymmetry. Fig. 3(d) depicts the transverse polarization of the $B \to K^*\mu^+\mu^-$, and the effect of NHBs is quite obvious. The zero point of the FB asymmetry can be slightly modified as shown in Figure 3(b) due to the contributions of NHBs.

In Fig. 4, the IMS, FB asymmetry, longitudinal and transverse polarizations of the $B \to K^*\tau^+\tau^-$ are depicted. The effect of NHBs does show in great relief. It is worth to note that IMS, FBA, and lepton polarizations for $B \to K^*\,\ell^+\,\ell^-$ in MSSM without including the contributions of NHBs are also significantly diffident from those in SM, while for $B \to K\,\ell^+\,\ell^-$ they have little differences from those in SM. Therefore, compared to the process $B \to K\,\ell^+\,\ell^-$, more precise measurements for $B \to K^*\,\ell^+\,\ell^-$ are needed in order to single out the contributions of NHBs.

Normal polarizations for both $B \to K\,\ell^+\,\ell^-$ and $B \to K^*\,\ell^+\,\ell^-$ are small and can be neglected because the imaginary parts of Wilson coefficients are small in SUSY models without CP violating phases which are implicitly assumed in the paper.

The behavior of IMS(a), FBA(b), LP(c), and TP(d) shown Figs 1-4 can be understood with the formula given in the Section 3. With Eqs. (3.56), (3.10) and (3.11), we see that the contributions of NHBs are contained in the terms of $\mathcal{S}_1$ and D'. At the high $\hat{s}$ regions, it is these two terms which are important. This explained the behavior of IMS given in (a) of Fig. 1 and Fig. 2. The Eq. (3.59) shows that the FBA is proportional to the mass of the lepton. For the case $B \to K\mu^+\mu^-$, due to

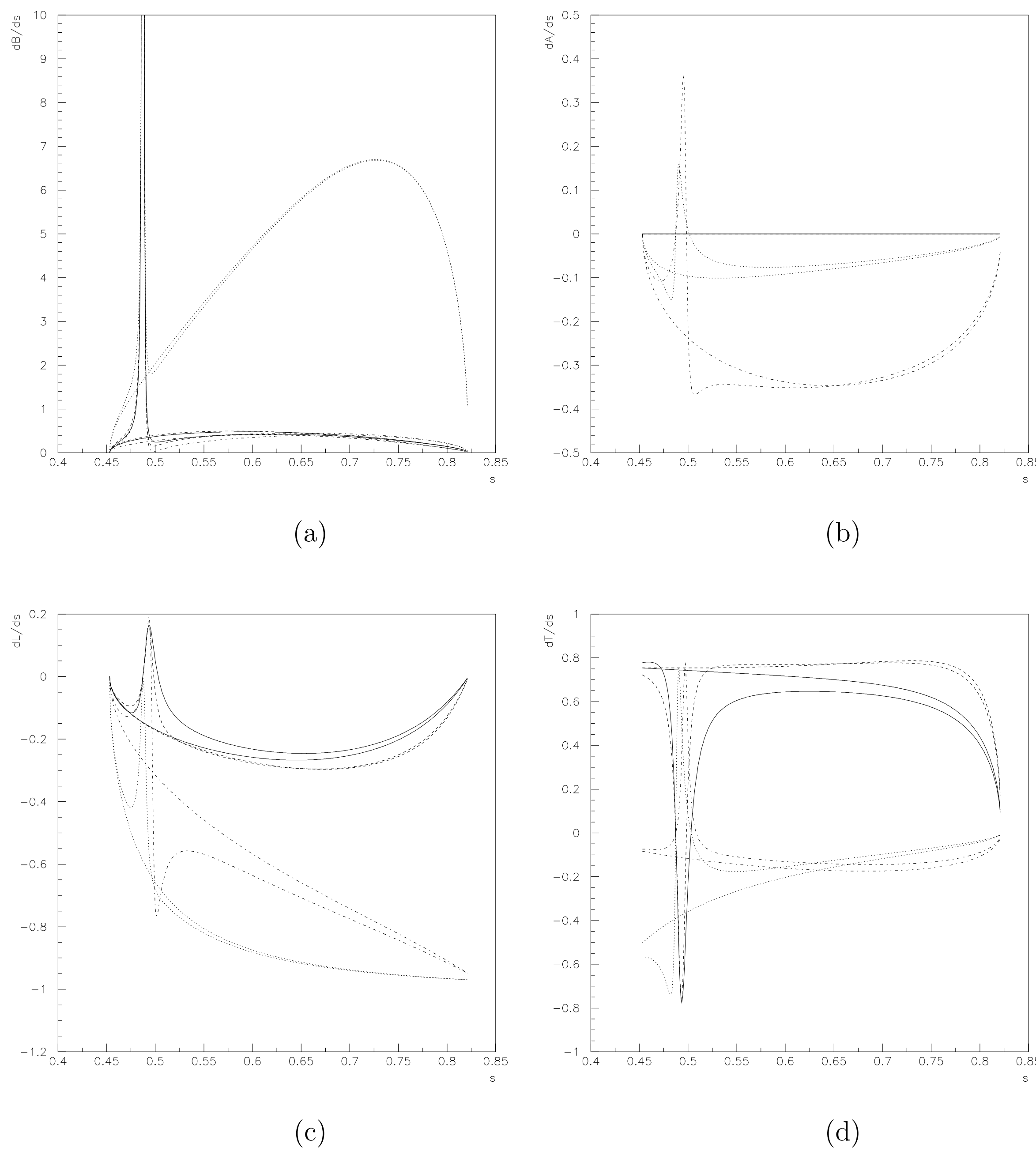

Figure 2: *The IMS(a), FBA(b), LP(c), and TP(d) of the process $B \to K\tau^+\tau^-$. The line conventions are the same as given in the legend of Fig 1.*

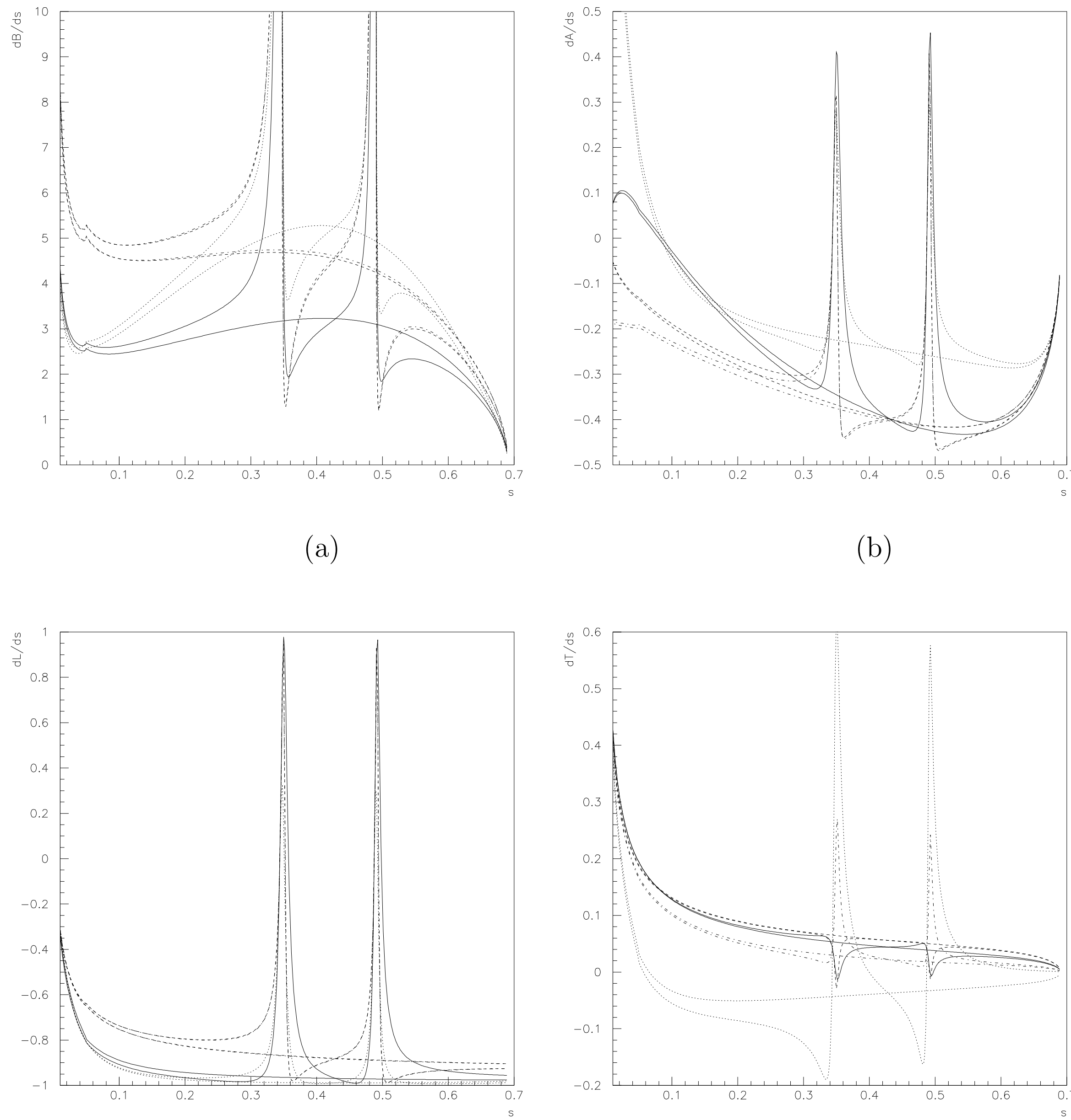

(a) (b)

(c) (d)

Figure 3: *The IMS(a), FBA(b), LP(c), and TP(d) of the process $B \to K^*\mu^+\mu^-$. The line conventions are the same as given in the legend of Fig 1.*

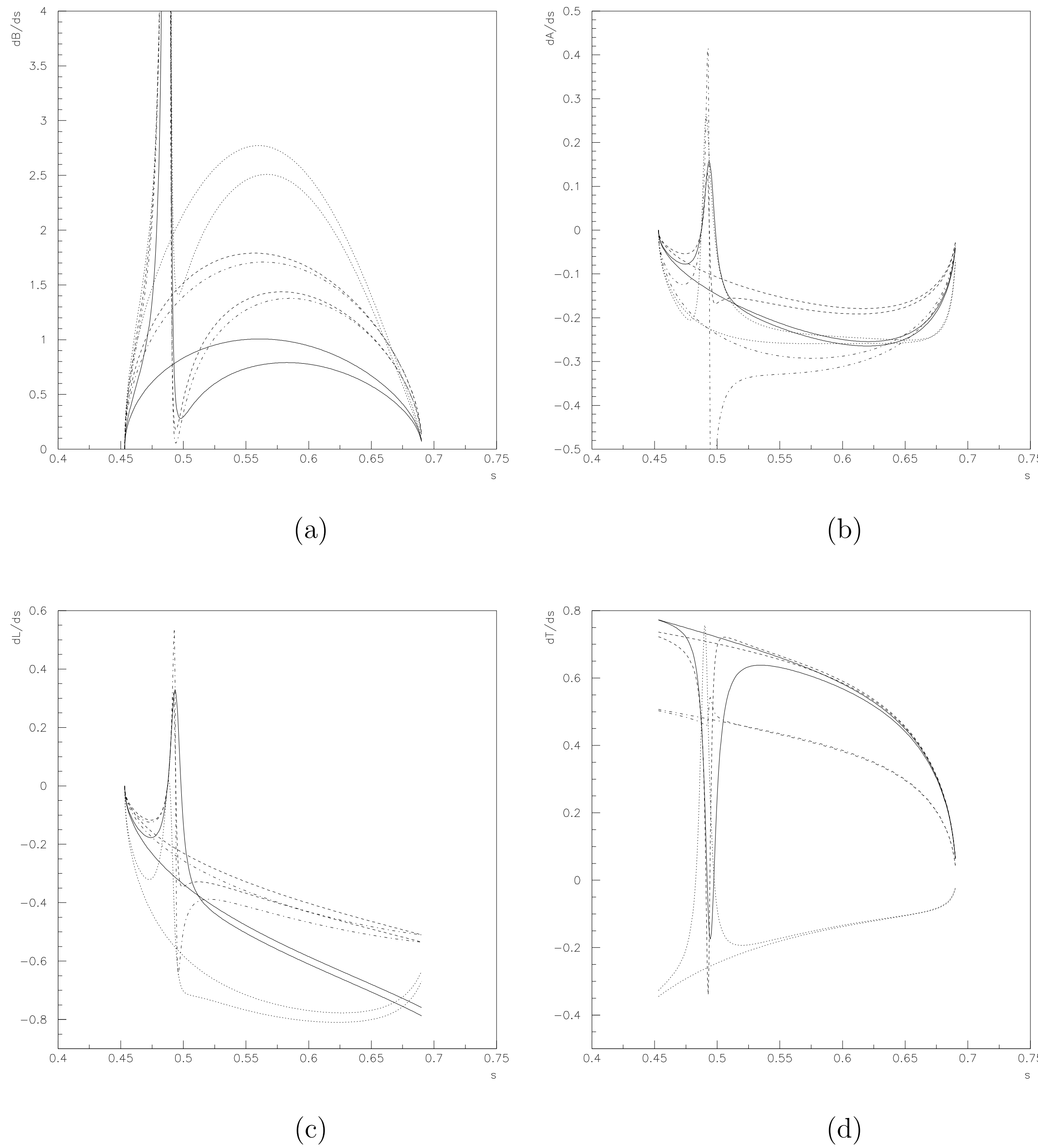

Figure 4: *The IMS(a), FBA(b), LP(c), and TP(d) of the process $B \to K^*\tau^+\tau^-$. The line conventions are the same as given in the legend of Fig 1.*

model		A	B	C	D	E	tot(SD)	tot(SD+LD)
SM	LCSR	0.353	54.707	0.032	4.566	0.076	0.573	59.736
	SVZ	0.215	22.918	0.015	1.593	0.026	0.299	24.767
SUSY I	LCSR	0.425	54.723	0.037	4.576	0.086	0.675	59.847
	SVZ	0.179	22.910	0.011	1.586	0.019	0.236	24.704
SUSY II	LCSR	0.556	54.865	0.131	4.833	0.849	2.067	61.233
	SVZ	0.348	23.009	0.068	1.726	0.321	1.002	25.473
SUSY III	LCSR	0.429	54.727	0.040	4.584	0.109	0.717	59.889
	SVZ	0.181	22.912	0.012	1.590	0.028	0.255	24.723

Table 5: Partial decay widths for $B \to K\mu^+\mu^-$. LCSR means the approach light-cone QCD sum rules, SVZ means the SVZ QCD sum rule [17]. Character A means the region $(\hat{s}_0, (\hat{m}_\psi - \hat{\delta})^2)$, B $((\hat{m}_\psi - \hat{\delta})^2, (\hat{m}_\psi + \hat{\delta})^2)$, C $((\hat{m}_\psi + \hat{\delta})^2, (\hat{m}_{\psi'} - \hat{\delta})^2)$, D$((\hat{m}_{\psi'} - \hat{\delta})^2, (\hat{m}_{\psi'} + \hat{\delta})^2)$ and E $((\hat{m}_{\psi'} + \hat{\delta})^2, \hat{s}^2_{\max})$. The unit is $\Gamma_B \times 10^{-6}$, which is 4.22×10^{-19} GeV. δ is selected to be 0.2 GeV. $\hat{\delta}$ is normalized with M_B

smallness of the mass μ, the FBA does not vanish but is hard to be measured. While for the case $B \to K\tau^+\tau^-$, the mass τ is quite large and observing FBA is relatively easy. For SUSY II, though the numerator of FBA is comparatively large, the large IMS suppresses the value of FBA; for SUSY III, the numerator is relatively small, but the FBA do demonstrate the effects of NHBs more manifestly, as shown in Fig. 2(b) due to smallness of IMS. The Eqs. (3.63) and (3.64) show that for the case $\ell = \mu$, the contributions of NHBs to P_N, P_T are suppressed by the mass of μ. But for the case $\ell = \tau$, the contributions of NHBs become quite manifest both for SUSY II and SUSY III. The term with D' in Eq. (3.64) will change its sign when there exists relatively not too small contributions of NHBs, the fact deduced from Eq. (3.10), that explains why the sign of TP is changed. The difference between the case SUSY II and SUSY III is small, the reason is just the same as stated in the analysis of FBA.

Since the terms incorporating the contributions of NHBs is proportional to λ as shown in Eq. (3.58), which approaches zero at high $\hat{s}$ regions; while at small $\hat{s}$ regions, the effects of NHBs are dwarfed by the other contributions. Therefore, only when C_{Q_i} are quite large could effects of NHBs be manifest, as shown in Fig. 3(a) and Fig. 4(a). According to the Eq. (3.60), at high $\hat{s}$ regions, the effects of NHBs would be suppressed by λ and $1-\hat{s}-\hat{m}^2_{K^*}$. The same suppression mechanism exists for LP. This suppression mechanism explains the fact that the processes $B \to K^*\,\ell^+\,\ell^-$ are not sensitive to the effects of NHBs. However, when there exist large contributions of NHBs, the sign of TP will be changed, as indicated in both Fig. 3(d) and Fig. 4(d).

The partial decay widths (PDW) are listed in Tables. 5,6,7,and 8. We see that at the high $\hat{s}$ region, for the process $B \to Kl^+l^-$, l=μ, τ, the contributions of NHBs do show up, as expected. For $B \to K^*l^+l^-$, the effects of NHBs in the high $\hat{s}$ region is signifiacnt when l=τ while they are small for l=μ. It can be read out from these four

model		A	B	C	D	E	tot(SD)	tot(SD+LD)
SM	LCSR	0.930	83.257	0.141	9.976	0.258	1.882	94.562
	SVZ	2.943	111.278	0.147	7.504	0.137	3.639	122.008
SUSY I	LCSR	1.627	83.402	0.198	10.085	0.330	2.915	95.64
	SVZ	4.517	111.423	0.183	7.552	0.149	5.291	123.825
SUSY II	LCSR	1.178	83.431	0.234	10.164	0.352	2.677	95.360
	SVZ	2.801	111.292	0.156	7.525	0.145	3.522	121.918
SUSY III	LCSR	1.631	83.407	0.201	10.092	0.334	2.938	95.664
	SVZ	4.518	111.425	0.184	7.553	0.150	5.296	123.830

Table 6: Partial decay widths for $B \to K^*\mu^+\mu^-$. Other conventions can be found in Table 5.

model		A'	B'	tot(SD)	tot(SD+LD)
SM	LCSR	1.884	0.094	0.132	1.978
	SVZ	0.659	0.036	0.054	0.695
SUSY I	LCSR	1.884	0.086	0.131	1.970
	SVZ	0.655	0.025	0.038	0.680
SUSY II	LCSR	2.022	1.496	1.674	3.519
	SVZ	0.726	0.552	0.637	1.278
SUSY III	LCSR	1.874	0.094	0.129	1.968
	SVZ	0.651	0.026	0.035	0.677

Table 7: Partial decay widths of $B \to K\tau^+\tau^-$. Character A' means $(\hat{s}_0, (\hat{m}_\psi - \hat{\delta})^2)$, B' means $((\hat{m}_{\psi'} + \hat{\delta})^2, \hat{s}_{\max})$. The unit is $\Gamma_B \times 10^{-6}$, which is 4.22×10^{-19} GeV.

model		A'	B'	tot(SD)	tot(SD+LD)
SM	LCSR	4.045	0.096	0.183	4.141
	SVZ	3.029	0.048	0.102	3.076
SUSY I	LCSR	4.088	0.173	0.327	4.261
	SVZ	3.052	0.072	0.159	3.124
SUSY II	LCSR	4.148	0.266	0.460	4.413
	SVZ	3.054	0.084	0.167	3.138
SUSY III	LCSR	4.078	0.168	0.312	4.246
	SVZ	3.050	0.071	0.156	3.121

Table 8: Partial decay widths of $B \to K^*\tau^+\tau^-$. Other conventions can be found at Table 7.

table that the results are consistent with the Fig. 1(a),2(a), 3(a), and 4(a). In order to estimate the theoretical uncertainty brought by the methods calculating the weak form factors, we use the form factors calculated with LCSR and SVZ QCD sum rules (SVZ) method [17]. For $B \to K\,\ell^+\,\ell^-$, PDWs calculated with form factors obtained by SVZ method is 50% of those by LCSR approach; while for $B \to K^*\,\ell^+\,\ell^-$, PDWs increase 100% or so. We see that at low $\hat{s}$ regions the theoretical uncertainty can reach from 100% to 200%. Another point worthy of mention is that the contribution of resonences domainate the integerated decay width, as had been pointed out in [28].

9.5 Conclusion

We have calculated invariant mass spectrum, back-forward asymmetry, and lepton polarizations for $B \to K\,\ell^+\,\ell^-$ and $B \to K^*\,\ell^+\,\ell^-$ l=μ, τ in SUSY theories. In particular, we have analyzed the effects of NHBs to these processes. It is shown that the effects of the NHBs to $B \to K\tau^+\tau^-$ and $B \to K^*\tau^+\tau^-$ in some regions of parameter space of SUSY models are considerable and remarkable. The reason lies in the mass of the τ, which can magnify the effects of NHBs and can be see through from the related formula. The numerical results imply that there still exist possiblities to observe the effects of NHB in $B \to K\mu^+\mu^-$ and $B \to K^*\mu^+\mu^-$ through IMS, FB asymmetry and lepton polarizations of these processes. In particular, for $B \to K\mu^+\mu^-$ in the case of SUSY II, the partial width in the high $\hat{s}$ where short distance physics dominants can be enhanced by a factor of 12 compared to SM. Our analysis also show that the theoretical uncertainties brought in calculating of weak form factors are quite large. But the effects of NHBs will not be washed out and can stand out in some regions of the parameter space in MSSM. If only partial widths are measured, it is difficult to observe the effects of NHBs except for the decay $B \to K\tau^+\tau^-$. However, the conbined analysis of IBS, FBA, and lepton polarizations can provide usefull knowledge to look for SUSY. Finally, we would like to point out that FBA for $B \to Kl^+l^-$ vanishes (or, more precisely, is neglegiblly small) in SM and it does not vanish in 2HDM and SUSY models with large tanβ due to the contributions of NHBs. However, only in SUSY models and for l=τ it is large enough to be observed in B factories in the near future.

References

[1] B.Grinstein, M.J.Savage and M.B.Wise, *Nucl. Phys.* **B 319** (1989) 271.

[2] T. Goto et.al., hep-ph/9812369; S. Baek and P. Ko, hep-ph/9904283; Y.G. Kim, P. Ko and J.S. Lee, *Nucl. Phys.* **B 544** (1999) 64, and references therein. For the earlier references, see, for example, the references in ref. [9].

[3] Y.B. Dai, C.S. Huang and H.W. Huang, *Phys. Lett.* **B 390** (1997) 257.

[4] C.S. Huang and Q.S. Yan, *Phys. Lett.* **B 442** (98) 209; C.S. Huang, W. Liao and Q.S. Yan, *Phys. Rev.* **D 59** (1999) 011701;

[5] S. Fukae, C.S. Kim and T. Yoshikawa, hep-ph/9908229.

[6] S. Fukae, C.S. Kim, T. Morozumi and T. Yoshikawa, *Phys. Rev.* **D 59** (1999) 074013

[7] Y.G. Kim, P.Ko, and J.S. Lee, *Nucl. Phys.* **B 544** (1999) 64.

[8] T. Goto *et.al.*,*Phys. Rev.* **D55** (1997) 4273; T. Goto, Y. Okada and Y. Shimizu, *Phys. Rev.* **D58** (1998) 094006.

[9] E. Lunghi *et.al.*, Preprint hep–ph/9906286.

[10] J. L. Hewett, *Phys. Rev.* **D 53** (1996) 4964.

[11] Y. Grossman, Z. Ligeti and E. Nardi, *Phys. Rev.* **D 55** (1997) 2768.

[12] K. Krüger and L.M. Sehgal, *Phys. Lett.* **B380** (1996) 199.

[13] S. Choudhury et.al., hep-ph/9902355.

[14] Chao-Shang Huang and Shou-Hua Zhu, *Phys. Rev.* **D 61** (2000) 015011.

[15] I.I. Bigi, M. Shifman, N.G. Vraltsev and A.I. Vainstein, *Phys. Rev. Lett.* **71** (1993) 496; B. Blok, L. Kozrakh, M. Shifman and A.I. Vainstein, *Phys. Rev.* **D 49** (1994) 3356; A.V. Manohar and M.B. Wise, *Phys. Rev.* **D 49** (1994) 1310; S. Balk, T.G. Körner, D. Pirjol and K. Schilcher, Z. Phys. C 64 (1994) 37; A.F. Falk, Z. Ligeti, M. Neubert and Y. Nir, *Phys. Lett.* **B 326** (1994) 145.

[16] W. Jaus and D. Wyler, *Phys. Rev.* **D 41** (1990) 3405; P. Colangelo et al., *Phys. Lett.* **B 317** (1993) 183; Ceng et al., *Phys. Rev.* **D 54** (1996) 3656.

[17] P. Colangelo et al., *Phys. Rev.* **D 53** (1996) 3672; Erratum, *ibid*, **D 57** (1998) 3186.

[18] I.I. Balitsky, V.M. Braun and A.V. Kolesnichenko,*Nucl. Phys.* **B312** (1989) 509.

[19] V.L. Chernyak and I.R. Zhitnitsky, *Nucl. Phys.* **B345** (1990) 137.

[20] V.M. Braun, Preprint NORDITA–98–1–P (hep–ph/9801222).

[21] A. Khodjamirian and R. Rückl, Preprint WUE–ITP–97–049 (hep–ph/9801443).

[22] P. Ball and V.M. Braun, *Phys. Rev.* **D58** (1998) 094016;*Nucl. Phys.* **B543** (1999) 201; P. Ball *et al.*, *Nucl. Phys.* **B529** (1998) 323; P. Ball, *JHEP* **09** (1998) 005;*JHEP* **01** (1999) 010.

[23] A. Ali, P. Ball, L.T. Handoko, G. Hiller,hep-ph/9910221.

[24] S. Glenn, *et.al.* (CLEO Collaboration), *Phys. Rev.* **D 60** (1999) 034017; T.Affolder, *et.al.* (CLEO Collaboration), hep-ex/9905004.

[25] N.G. Deshpande and J. Trampetić, *Phys. Rev. Lett.* **60** (1988) 2583.

[26] G. Burdman, hep-ph/9505352; W. Roberts, hep-ph/9512253.

[27] D.S. Du and C. Liu, Phys. Lett. **B317** (1993) 179.

[28] D.S. Liu hep-ph/9505314; M.R. Ahmady, D.S. Liu and A.H. Fariborz, hep-ph/9506235; M.R. Ahmady and D.S. Liu, hep-ph/9311335.

[29] T.M. Aliev, C.S. Kim and Y.G. Kim, hep-ph/9910501.

[30] M. Jezabek and P.Urban, hep-ph/9712440.

[31] D. Melikhov, N. Nikitin, and S. Simula, hep-ph/9807464.

[32] C. Greub, A.Ioannissian, and D.Wyler, *Phys. Lett.* **B 346** (1995) 149.

[33] T.M. Aliev and M. Savci, hep-ph/0003188.

[34] T. M. Aliev, M. Savci, A. Özpineci, and H. Koru; J. Phys. G24 (1998) 49

[35] C.Q. Geng and C.P Kao, *Phys. Rev.* **D54** (1996) 5636.

[36] C.S. Huang *et al*, hep-ph/9810412; *Commun. Theor. Phys.* **32** (1999) 499.

[37] S. Bertolini, F. Borzynatu, A. Masiero and G. Ridolfi, *Nucl. Phys.* **B 353** (91) 591;

[38] G. Buchalla, A.J. Buras, and M.E. Lauthenbache,*Rev. Mod. Phys.* **68** (96) 1125; A. Buras, *et al.*, Nucl. Phys.B 4009337; *Nucl. Phys.* **B 400** (93) 75; S. Bertonlini, *et al.*, *Nucl. Phys.* **B 353** (91) 591.

[39] A. Ali, G.F. Giudice, and T. Mannel, Z. Phys. **C67** (1995) 417.

[40] A.J. Buras and M. Münz, *Phys. Rev.* **D 52** (1995) 186.

[41] A. Ali, T. Mannel and T. Morozumi, *Phys. Lett.* **B273** (1991) 505.

Part III
Acknowledgement

It is my pleasure to thank Prof. C. S. Huang, Prof. C. S. Li, as well as their respectively group members. The closely collaboration and the stimulating discussions with them encourage me to live with High Energy Physics. Their name are Dr. Q.S. Yan, X.H. Wu, W. Liao, Y.S. Yang and L.G. Jin. Prof. R. Oakes and G. Eilam are also deserved special acknowledgement. The financial support of China Postdoctoral Foundation and K. C. Wong Education Foundation, Hong Kong are both gratefully acknowledged. Finally, I should give my special thanks to Alexander von Humboldt Foundation and Prof. W. Hollik, their kindly support make me to continue my research works smoothly.

Part IV
Publication List

1. Higgs Physics

   (a) Shou Hua Zhu, Chong Sheng Li and Chong Shou Gao, Lightest neutral Higgs boson pair production in photon-photon collisions in the minimal supersymmetric extension of standard model, Phys. Rev. **D58**, 015006 (1998) (22 pages).

   (b) Shou Hua Zhu, Chong Sheng Li and Chong Shou Gao, Squarks loop corrections to the charged Higgs boson pair production in photon-photon collisions, Phys. Rev. **D58**, 055007 (1998) (12 pages).

   (c) Shou Hua Zhu, Pseudoscalar Higgs boson pair production in photon-photon collisions, Journal of Physics G (nuclear and particle physics) 24, 1703-1721 (1998) (18 pages).

   (d) Chong Sheng Li, Shou Hua Zhu and Cong Feng Qiao, Radiative Higgs boson decay beyond the standard model, Phys. Rev. **D57**, 6928-6933 (1998) (6 pages).

   (e) Shou Hua Zhu, Chong Sheng Li and Chong Shou Gao, Single Higgs boson production in gamma-gamma collision in minimal supersymmetric extension of standard model, Chinese Physics Letters Vol 15, No. 2 (1998) 89 (4 pages).

   (f) Chong Sheng Li and Shou Hua Zhu, Top quark loop corrections to the neutral Higgs boson production at the Fermilab Tevatron, Phys. Lett. **B444**, 224(1998) (6 pages).

   (g) Qing Hong Cao, Chong Sheng Li and Shou Hua Zhu, Leading Electroweak Corrections to the Neutral Higgs Boson Production at the Fermilab Tevatron, Comm. Theor. Phys. 32, 275 (2000), hep-ph/9810458.

   (h) Chao-shang Huang and Shou Hua Zhu, Supersymmetrical Higgs bosons discovery potential at hadron collider through bg channel, Phys. Rev. D60, 075012 (1999) (4 pages).

   (i) Shou Hua Zhu, Charged Higgs associated production with W at linear collider, hep-ph/9901221.

   (j) Li Gang Jin, Chong Sheng Li, Robert J. Oakes, Shou Hua Zhu, Yukawa Corrections to Charged Higgs Boson Production in Association with a Top Quark at Hadron Colliders, Eur. Phys. J. C14, 91-101 (2000), hep-ph/9907482.

   (k) Li Gang Jin, Chong Sheng Li, Robert J. Oakes, Shou Hua Zhu, Supersymmetrical Electroweak Corrections to Charged Higgs Boson Production in Association with a Top Quark at Hadron Colliders, to appear in PRD (2000), hep-ph/0003159.

(l) Ya-sheng Yang, Li Gang Jin, Chong Sheng Li, Shou Hua Zhu, Supersymmetrical Electroweak Corrections to Charged Higgs Boson Production in Association with W through $b\bar{b}$ channel, submitted to PRD, hep-ph/0004248.

2. FCNC

   (a) Chao-shang Huang, Xiao-hong Wu and Shou Hua Zhu, Top-charm Associated production at high energy e^+e^-colliders in standard model, Phys. Lett. **B452**, 143 (1999) (7 pages).

   (b) Chao-shang Huang, Xiao-hong Wu and Shou Hua Zhu, Bottom stange associated production at high energy e^+e^- colliders in standard model, J. Phys. **G 25**, 2215-2223 (1999) (9 pages).

   (c) Chong Sheng Li, Xin-min Zhang, Shou Hua Zhu, SUSY QCD effect on top charm associated production at linear colliders, Phys. Rev. D60, 077702 (1999) (4 pages).

3. B Physics

   (a) Qi-shu Yan, Chao-shang Huang, Wei Liao and Shou Hua Zhu, Exclusive semileptonic rare decays $B \to (K, K^*)l^+l^-$ in supersymmetric theories, hep-ph/0004262, submitted to PRD.

   (b) Chao-shang Huang, Shou-Hua Zhu, $B \to X(S)\tau^+\tau^-$ in a cp spontaneous broken two higgs doublet model, Phys. Rev. **D61**, 015011 (2000), hep-ph/9905463.

4. M-theory phenomenology

   (a) Chao-shang Huang, Tian-jun Li, Wei Liao, Qi-shu Yan and Shou Hua Zhu, Scales, Couplings Revisited and Low Energy Phenomenology in M-theory on $S^1/Z(2)$, submitted to EPJC, hep-ph/9810412.

   (b) Chao-shang Huang, Tian-jun Li, Wei Liao, Qi-shu Yan and Shou Hua Zhu, M-theory Low Energy Phenomenology, Commun. Theor. Phys., **32**, 499-506 (1999).

5. Top physics

   (a) Cong Feng Qiao and Shou Hua Zhu, Supersymmetric QCD corrections to top quark semi-leptonic decay, Phys. Lett. **B451**, 93 (1999) (5 pages).

   (b) Lian-you Shan and Shou Hua Zhu, Top decays into light stop and gluino, to appear in PRD (2000), hep-ph/9811430.